UNIVERSITY OF BIRMINGHAM

STABILIZATION OF SAND FOR ROAD CONSTRUCTION

By

OMAR E A ABUBAKER

A thesis submitted to
the University of Birmingham
for the degree of
DOCTOR OF PHILOSOPHY

College of Civil Engineering and Physical Science
School of Civil Engineering
The University of Birmingham
April 2019

ABSTRACT

In a desert where suitable granular materials which can be used for the construction of roads are not easily available. Desert sands tend to be single sized and therefore it is not essay to use them for construction as pavement materials. This research aimed at investigating techniques for stabilizing uniform sand for using in a road.

An extensive literature review on stabilisation of desert sand showed that little research had been undertaken on the subject. Nonetheless, extensive literature study was used to inform the development of an experimental programme, which included the following sand reinforced with fibre, fly ash and vitrified slag and a combination of fly ash with fibre reinforced sand and fibre with slag reinforced sand. In addition to the standard characterisation tests, resilient modulus, permanent deformation, shear strength, and unconfined compressive strength compacted at a range of water contents were also determined. Tests also included freeze-thaw durability tests as minimum desert temperatures can drop below zero. The optimum materials contents were a 0.5% polypropylene fibre content which 19mm long, 35% fly ash content and 40% slag content of the dry weight of sand. For the analytical pavement design, traffic data from an existing road in was used. Thereafter, pavement responses of different pavement materials were obtained using the KENLAYER program to determine the road section. Results showed that the fibre reinforced sand, fibre with fly ash reinforced sand, slag stabilized sand and slag with fibre reinforced sand were appropriate materials for to improve the uniform sand to a level where it could be used as subgrade.

ACKNOWLEDGEMENT

I would like to acknowledge gratefully for the assistance received from supervisors Dr. Gurmel Ghataora and Dr. Michael Burrow for their constant supervision, guidance, and encouragement throughout the research.

I am very much grateful to Libyan Ministry of Higher Education for granting the scholarship for this research.

I would specially like to thank all the technicians at civil engineering laboratories for their help.

Finally, I thank my family for their patience and understanding to make this piece work possible.

LIST OF CONTENTS

LIST OF FIGURES

LIST OF TABLES

LIST OF SYMBOLS AND ABREVIATIONS

NCHRP	the National Cooperative Highway Research Program
CBR	California Bearing Ratio
MEPDG	Mechanistic-Empirical Pavement Design Guide
ASTM	American Society for Testing and Materials
AASHTO	American Association of State Highway and Transportation Officials
AASHO	American Association of State Highway Officials
PD	Permanent Deformation
UCS	Unconfined Compressive Strength
UU	Unconsolidated Undrained triaxial test
BS	British Standard
MDD	Maximum Dry Density
OMC	Optimum Water Content
D10	Grain Diameter at 10% Passing
D30	Grain Diameter at 30% Passing
D50	Grain Diameter at 50% Passing
D60	Grain Diameter at 60% Passing
Cc	Coefficient of Curvature
Cu	Coefficient of Uniformity
e_{max}	Maximum Void Ratio
e_{min}	Minimum Void Ratio
RD	Relative density
Sr	Degree of Saturation
PP	Polypropylene

FL	Fibre Length
FC	Fibre Content
HMA	Hot Mix Asphalt
SSRLT	Single Stage Repeated Load Triaxial Test
MSRLT	Multi Stage Repeated Load Triaxial Test
F-T	Freezing and Thawing Durability
F_{env}	Adjustment Factor
M_{Ropt}	Resilient Modulus at Optimum Condition and any Stress Level
M_R	Resilient Modulus
$M_{R\ (F\text{-}T)\ min}$	Minimum Resilient Modulus after F-T Cycles
K_1, K_2, K_3, K_4	Constant Parameters
Z	Depth of Required Resilient Modulus
K_o	Coefficient of Earth Pressure at Rest
E	Modulus of Elasticity
σ_d	Deviatoric Stress
σ_1	Vertical Stress
σ_3	Confining Stress
Θ	Bulk Stress
SSR	Shear Stress Ratio
τ_f	Applied Shear Stress
τ_{max}	Material Shear Stress at Failure
ADT	Average Daily Traffic
AADT	Annual Average Daily Traffic
T	Percentage of Truck in the ADT

G	Growth Factor
N	Number of Axle Load Application per Truck
D	Directional Distribution
L	Lane Factor
Y	Design Period in Year
GR	Total Growth Factor
R	Annual Growth Rate (%) of Vehicles
Y	Design Period, years
A	Contact Area
P	Tire Load
P	Tire Pressure
ESAL	Equivalent Single Axle Load
PSI	Present Serviceability Index
P_o	Initial Serviceability Index
P_t	Terminal Serviceability Index
SN	Structural Number
N_t	The Number of Load Repetitions in the Period of Time t,
ε_p^{3000}	Cumulative Permanent Strain at the 3000th in the RLT
ε_p^{5000}	Cumulative Permanent Strain at the 5000th in the RLT
N_f	Allowable Number of Load Repetition
ε_t	Tensile Strain at the Bottom of the Asphalt Layer
f_1, f_2 & f_3	Coefficients of Fatigue Criterion
N_d	Allowable Number of Load Repetition
ε_c	Vertical Strain on the Surface of the Subgrade

f_4 & f_5	Coefficients of Permanent Deformation Criterion
Fe_2O_3	Ferric Oxide
MgO	Magnesium Oxide
CaO	Calcium Oxide
Al_2O_3	Aluminium Oxide
SiO_2	Silicon Dioxide
SO_3	Sulfur Trioxide
NaOH	Sodium Hydroxide
LOI	Loss of Ignition
XRF	X-Ray Fluorescence
XRD	X-Ray Diffraction
s	Matrix Suction
u_a	Pore Air Pressure
u_w	Pore Water Pressure
p	Total Mean Normal Stress
p'	Effective Stress
$\varepsilon_{1,p}$	Permanent Deformation after the First 100 cycles.
q_{max}	Maximum Deviator Stress
p_{max}	Maximum Mean Normal Stress
m	Slope of The Static Failure Line
p^*	Stress Parameter
ε_r	Resilient Strain
$\varepsilon_{1,p}$	Accumulated Permanent after N_{ref}
N_{ref}	Any Given Number of Load Cycles Greater Than 100

L	Length of Stress Path
p_o	Reference Stress
β_1	Laboratory to Field Correlation Factor
ε_v	Vertical Resilient Strain
h	Thickness of Layer
N_0	Reference Number of Load
β_1	Laboratory to Field Correlation Factor
C and b	Materials Parameters
δ_{sg}	Permanent Deformation in the Lower Part of Subgrade
ε_0	Materials Constant
εv_1 and εv_2	Vertical Strain at the Surface of Subgrade
Z	Required Depth of the Subgrade
U_f	Relative Damage Factor
W_{tx}	Number of x-axle Load Applications Applied over the Design Period
W_{t18}	Number of Equivalent 80kN Single Axle Loads over the Design Period
p_i	Percentage of Repetitions for i^{th} Load Group
A	Average Number of Axles per Truck
SN	Structural Number
$a_{1, 2, 3}$	Layer Coefficient
$D_{1, 2, 3}$	Layers Thickness
μ	Poisson's Ratio

CHAPTER 1 INTRODUCTION

1.1 Introduction

Road pavements were first constructed in Libya sometime before the Second World War. After the war, road pavements were constructed using crushed stone road bases and subbases with dense bituminous surfacing as shown in Figure 1.1. This construction method is still being practiced nowadays. To ensure the smooth operation of the roadworks, the road pavement has been constantly maintained and upgraded. Due to the desert covers which cover a huge area of the country which is about 1,100,000km^2, it has become necessary to develop and discover new pavement procedure and materials.

Figure 1.1 Road in Libyan Desert.

Pavement design is a procedure to determine the layer thickness and types of materials for pavement construction which could be either rigid or flexible pavement. The pavement design methods were divided into two procedures which are the empirical pavement design method and Mechanistic-Empirical pavement design method. The empirical pavement design methods have been in use since 1920 and the soil classifications were updated (Huang, 2004). The Public Roads (PR) soil classification system published the first empirical methods without a strength test (Hogentogler & Terzaghi, 1929, after Huang, 2004). The California Bearing Ratio (CBR) strength test was developed by the California Highway Department and U.S. Corps of Engineers (USCE) in 1929; the method related the thickness of layers with the subgrade shear failure. Later in 1950, the data collection was used to establish regression models for pavement performance and design. The empirical method in (AASHTO, 1993) depends on the AASHO Road Test. Nowadays, the AASHTO pavement design method is been used for road construction. The AASHTO procedure depends on the pavement distresses. As mentioned earlier, the established models cannot be used for any condition except that similar to the condition they were developed for. The combination of mechanistic and empirical methods (M-E) was designed and used to evaluate the structural pavement as recommended by NCHRP 1-37A. The mechanistic responses are the stress, strain, and deflection which can be obtained by different software packages with taking the soil properties, traffic loading, and environmental conditions into account. Recently, the National Cooperative Highway Research Program 1-37A (NCHRP, 2004) provided a procedure of pavement design for the current Mechanistic-Empirical (M-E) design methods. The NCHRP 1-37A guide recommended that the traffic load distribution and vehicle class could be obtained based on the (AASHTO, 1993) procedure.

Generally, in the desert area, it is expensive to import good quality of imported materials as they tend to be remote from the construction site. Thus, desert sands have to be stabilized in the same manner to give the required performance for road construction. The stabilisation of sands could take many forms – importing different materials and mixing them with sand to achieve physical stability or using chemical stabilisation agents such as cement. Sometimes non-hydraulic binder such as asphalt may be used to stabilize the sand. Such techniques have been used for the construction of retaining walls, railway embankments, protection of slopes, foundation engineering, and earthquake engineering.

The use of hydraulic binder utilizes expensive cement and requires water which is a scarce commodity in the desert for hydration and thus, the costs can be high. In addition to this, hydraulically bound materials tend to be rigid and ground movements can cause cracking if the strength of the concrete or stabilized sand is not adequate.

Even though laboratory experiments and practice show the beneficial contribution of sand reinforcement under static and dynamic loading, there is no information in the literature on the resilient behaviour of either stabilized or reinforced sand. However, the AASHTO (1993) design procedure considers the resilient modulus for the determination of permanent deformation of pavement materials.

1.2 Problem Statement

Construction of roads in a desert is problematic not only because of migrating sand dunes but also because of the type of sand that is not easy to compact well enough to give a stable road structure.

The pavement layers are exposed to different cyclic deviator stress during the service life due to a combination of external traffic loads and environmental conditions. Also, they are susceptible to the variation of water content. Lee et al. (1995), Lekarp et al. (2000a) and Rahman et al. (2017) confirmed that the main parameters of pavement design for unbound granular materials (resilient modulus and permanent deformation) may be affected, with varying degrees of importance, by several factors such as stress, dry density, particles size distribution, soil type, moisture content, stress history, number of load cycles and load duration, frequency and load sequence. On the others hand, although these types of soils have high resilient modulus values, they may still experience high permanent deformation with repetition of applied loads as confirmed by (Lekarp et al., 2000a, Puppala et al., 2009). Therefore, NCHRP (2004) requires to replace the sand with better quality construction material.

In order to overcome these issues, it is generally better (i.e. cost-effective) to improve the sand properties rather than import sufficient materials to replace poor soils. In this way, additional materials are suggested to improve the sand instead of replacing it. Three materials were suggested for use in the sand to improve its properties and these are; polypropylene fibre, class C fly ash and vitrified slag.

The literature review shows that the synthetic fibre improves the interlock between the particles whatever the soil type (Al-Refeai and Al-Suhaibani, 1998). Also, the bonding between the sand particles needs to be improving. Therefore, cementitious materials should be used to improve the strength of the sands. Nevertheless, the advantages of using fly ash are that the particles size fills the voids between the sand grains, and use pozzolanic properties of the fly ash to improve the cohesion between the particles (Kumar and Singh, 2008). New

vitrified slag was investigated by (Keeley et al., 2017). A chemical investigation was carried out on the slag. It was confirmed that there is a good potential to increase the strength of the sand by activating the slag with an alkaline solution. The slag needed thereafter underwent an intensive experimental investigation.

In addition, to complete this research, durability was taken into account. The freeze-thaw cycles durability test was used to simulate the seasonal variations. The two main reasons for using freezing-thawing cycles instead of wetting-drying cycles were; the weather at night is dry and frosty, and cannot place the sand sample in the water bucket.

Finally, the empirical pavement design procedure was followed, which uses empirical relationships for pavement thickness design. However, these relationships are derived from other materials type, traffic load and environmental condition. Therefore, an analytical pavement design procedure can be used to consider the different materials, different loading and environmental conditions.

1.3 Research Aim and Objectives

The aim of this research is to evaluate the requirements for pavement design by using stabilizations and reinforcement materials into the sand with consideration for the environmental conditions.

To achieve the above aim, the following objectives were set:

1. Undertake a systematic review of stabilization of sand, particularly desert sand for road pavement construction. This review was involved in analytical pavement design.

2. Based on the finding in the systematic review, develop a test programme to undertake pilot tests to evaluate the envisaged methodology and for measuring properties of sand which were to be used in pavement design.
3. Undertake detailed tests program to evaluate/optimise suitable stabilization and reinforcement technique for road construction.
4. Evaluate the effect of environmental pavement conditions on the reinforced sand by assessing the resilient modulus and permanent deformation before and after the durability test at different water contents to determine deterioration of the reinforced subgrade layer.
5. Develop correlation models between the resilient modulus and unconfined compressive strength to be able to predict resilient modulus for reinforced sand, instead of conduct the resilient modulus test, which is not always practicable.
6. Explore a new design procedure for pavement design for reinforced and stabilized sand, by using the resilient modulus, deviator stress, performance criteria (the allowable number of load repetitions, the allowable number of load repetitions and deflection), and the permanent deformation.
7. Collect the traffic loading for use it in the developed analytical pavement design to simulate the existing traffic loading.
8. Based on the above findings, use analytical pavement design procedure to investigate different pavement section configurations, materials properties, and loading conditions as a case study.

1.4 Novelty and Contribution to Knowledge

The contribution of this research is to improve the properties of desert sand for use as subgrade layer of pavement. Many researchers have undertaken research into stabilizing sand for pavement construction, but very few have conducted detailed investigations. It's measuring properties that may be used in analytical pavement design. The novelties from this study are listed below.

- Stabilizing desert sand by different materials such as vitrified slag and class C fly ash and/or synthetic polypropylene fibre, for improving the strength and reduce the permanent deformation.
- Develop an iterative procedure rather than the existing procedure in the KENLAYER software, to reduce the number of trials to determine the appropriate resilient modulus for the stress of each layer (Chapter Seven).
- The national cooperative highway research program transportation research board (NCHRP 1-37A) does not include correlation between the resilient modulus and the unconfined compressive strength for the fly ash or fibre reinforced sand. Therefore, the development of a correlation between unconfined compressive strength and resilient modulus for reinforced sand, taking into account the water content will be developed. It will reduce the need to explore the carried laboratory test.
- Develop an analytical pavement design procedure that considers reinforced soils, traffic loading and environmental conditions which lead to deterioration of the subgrade layer. Current methods do not take account of soil reinforcement.

1.5 Methodology

The methodology in this adapted study consists of three tasks:

(1) A systematic review that includes the pavement design methods, reinforced materials and the behaviour of granular soil in the pavement.

(2) The laboratory investigation was undertaken to characterise sand and to determine design parameters such as resilient modulus and permanent deformation and durability.

(3) Undertake analytical design of pavement to evaluate the efficiency of the reinforced and stabilized materials in the context of a case study. These derived properties (Task 2) used together to explore the possibility of creating a more flexible pavement material using fibres and binders (fly ash and vitrified slag) such that, the use of imported (to site) materials is minimized.

The results of the previous investigations are represented in Chapters Four, Five and Six. The monotonic tests are carried out to obtain the threshold deviator stress values for stabilized and reinforced soil. Also, the variation of water contents was considered during the testing. The cyclic loading tests were conducted to obtain the required parameters for pavement design. NCHRP (2004) recommends the relationships used for Level 2 resilient modulus of lean concrete, cement stabilized, open graded cement stabilized, soil cement, lime-cement-fly ash and lime-treated materials. Thus, correlation models are developed between resilient modulus and unconfined compressive strength to obtain the resilient modulus with respect of the water contents. Thereafter, the results are used in analytical pavement design to assess the appropriateness of the materials for road construction.

1.6 Thesis Outline

The presented thesis includes; Chapter One which defines the aim, objectives, problem statement, and the outline of the thesis. This is followed by, Chapter Two which presents a rigorous literature review related to the pavement design procedures stabilized and synthetic fibre reinforced sand and the gap in knowledge. Chapter Three demonstrates the experimental work and materials which are used to obtain the requirements for Mechanistic-Empirical Design (1-37A) 2004 in terms of stress level (traffic loading), soil properties, and environmental conditions. Chapter Five presents the resilient modulus results for reinforced and stabilized sand under different conditions and stress levels and with interpretations. Chapter Six demonstrates the permanent deformations results for reinforced and stabilized sand under different conditions and stress levels likewise. Afterwards, Chapter Seven presents an analytical pavement design for subgrade layer with different reinforced and stabilized sand. The results presented in Chapter Four, Five and Six were used in the analytical design. The last chapter presents the conclusion and recommendations of the research while a reference is attached at the end of the thesis.

CHAPTER 2 LITERATURE REVIEW

2.1 Introduction

The methodology adopted for undertaking the literature review is designed in this chapter. It is followed by a review of the appropriate journal and capture paper (in the main) that cover the types of stabilization of desert sand, sand reinforcement and pavement design. Information gleaned from this study was used to inform the methodology adopted for this study.

2.1.1 Systematic literature review

The systematic literature review was conducted to collect and consider the available publications of pavement design procedures and reinforcement materials for subgrade layers. The data collection was collected the relevant investigation about the reinforced sand for road construction. The experimental works that have been used to assess the reinforced sand.

A systematic review of all the three subject areas was undertaken in stages described below.

Stage 1 was collecting all the publications related to reinforced and stabilized sand. The total number of publication those were reviewed about 400 of both journals and conference papers.

Stage 2 was parking the data. The data parking was to extract the data from the publication papers such the sand properties, stabilization, and reinforcement methods and the experimental works into excel sheet as demonstrated in Table 2-1, 2-2, and 2-3.

Stage 3 is a grouping of reinforcement types. In the grouping stage, the stabilizations and reinforcement methods were divided based on the reinforcement techniques. Figure 2.1 shows that most work has been conducted on synthetic fibres and conventional materials such as fly

ash, cement, and lime. Figure 2.2 demonstrates the number of publications for synthetic fibres while Figure 2.3 shows the number of publications for conventional materials. Figure 2.4 demonstrates the numbers of work for the combination of reinforcement and stabilization materials into the sand. The graph shows that the highest numbers of publications were carried out on the combination of synthetic fibres and conventional materials.

Stage 4 analyse information. For each group extract information data in terms of sand properties, reinforcement, and stabilizations materials from prepare and replot and analyse data. Develop a behaviour model between 2 relevant properties - repeat for all data. At the end of all do a multiracial analysis for suitable data sets. Within this stage also undertakes stabilized analyse to check the validity of data.

Table 2-1The sand characterization.

Name	Sand																			
	Wi	PSD	O.M.C (%)	ϒd Min	ϒd Max	In Situ Density	Sand	Grain Size			D10	D50	D60	Classification	Cc	Cu	Gs	emax	emin	Friction angle φ
								Fine	Medium	Coarse										
Al-Refeai, T.O. (1990)								x	x		x	x			x	x	x	x	x	x

Table 2-2 Stabilization and reinforcement methods

Name	Stabilization And Reinforcement Methods																							
	Mechanical																	Chemical					
	Randomly Distribution Fibres																Compaction	Hydraulic binders			Fly Ash	Polymeric Resins	Enzymes
	Natural fibres								Synthetic (Man-Made) fibres								Mineral							
	Coir	Sisal	Palm	Jute	Flax	Barely Straw	Bamboo	Cane	PP	PET	PE	Glass	Nylon	Steel	Waste	PVA		Cement	Lime	Bitumen			
AI-Refeai, T.O. (1990)											x	x												

Table 2-3 Conducted experimental works.

Name	Test																		
	Triaxial Compression Tests	Permeability	Unconfined Compression Test	Direct Shear Test	CBR Test	Three Point Bending Tests	Compaction Tests	Permanent Deformation Test	Resilient Modulus	Plane Strain Compression Tests	Permeability Test	Torsional Shear Test	Plate Load Test	Splitting Tensile Tests	Brazilian Tensile Strength Test	Plate Pullout Tests	Wet Sieving Method	Interface Shear Test	Load–Penetration Tests
AI-Refeai, T.O. (1990)	x																		

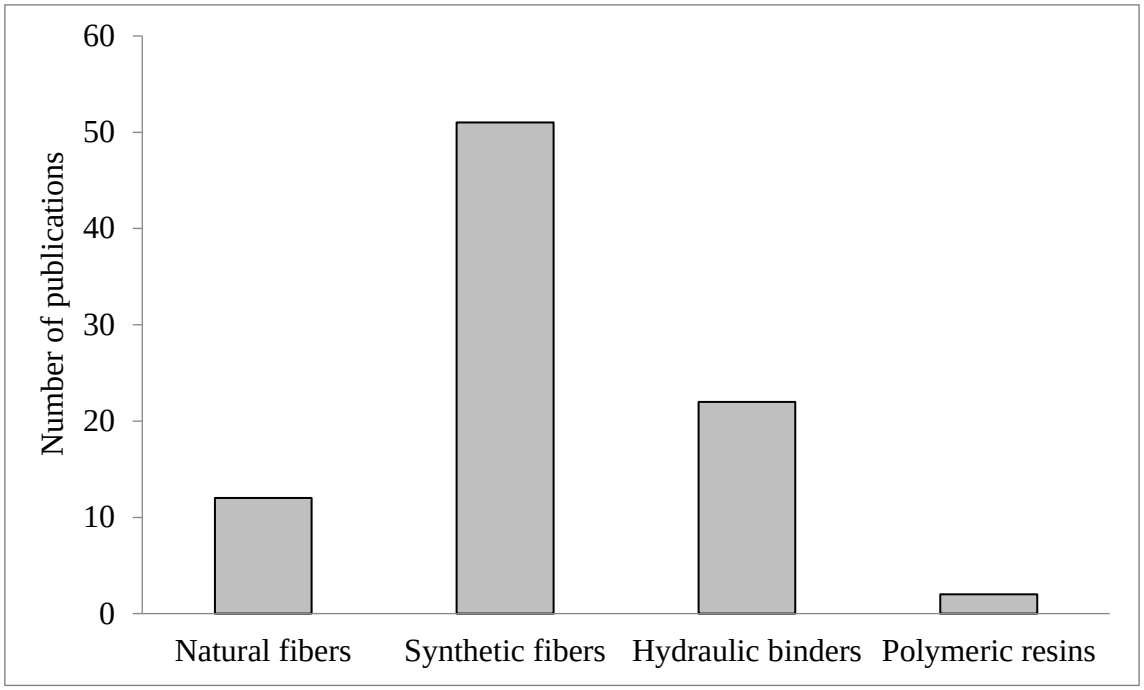

Figure 2.1 Number of publications on reinforcement and stabilizations techniques for sand.

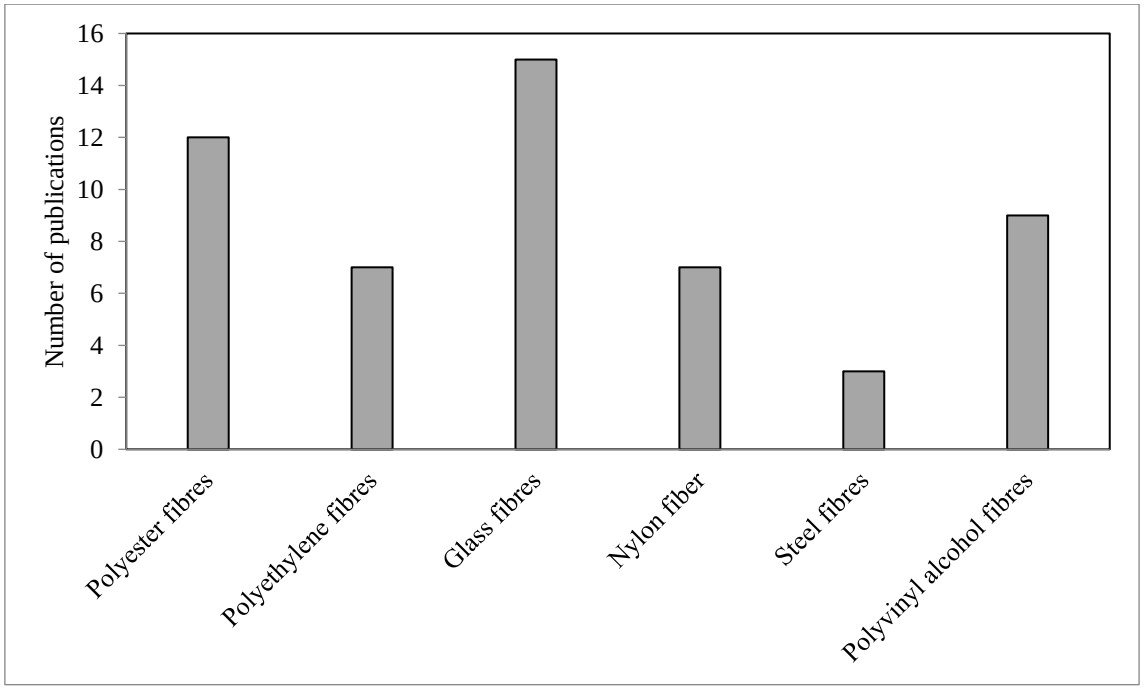

Figure 2.2 Number of publications on fibre reinforced sand.

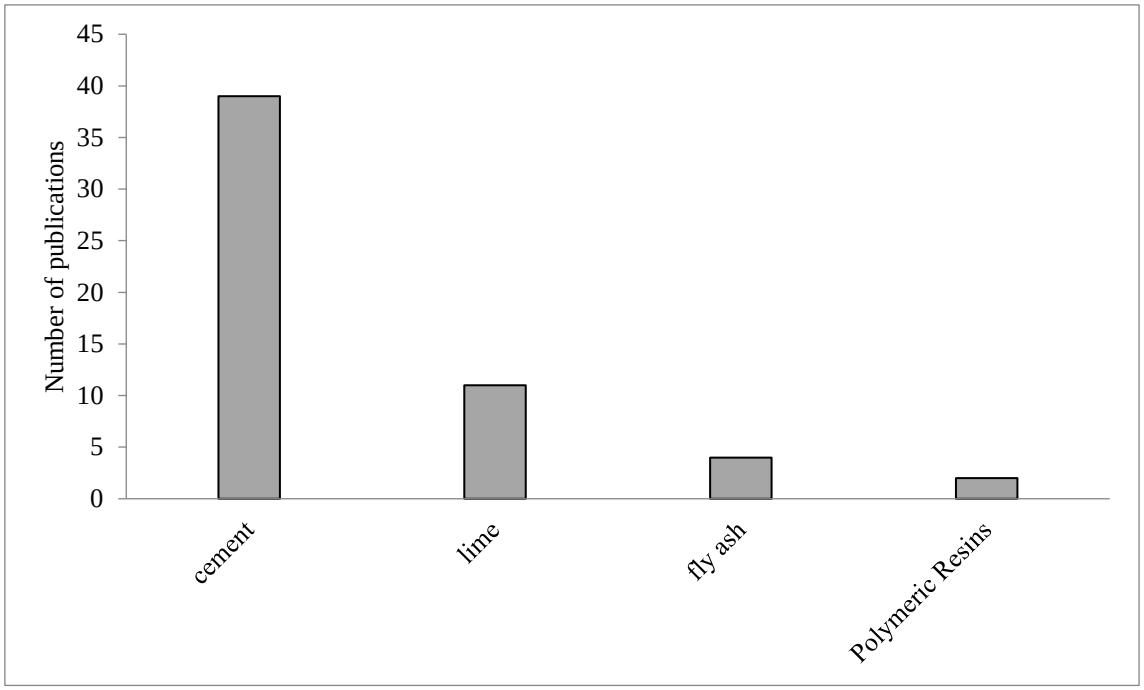

Figure 2.3 Publications on hydraulic binders.

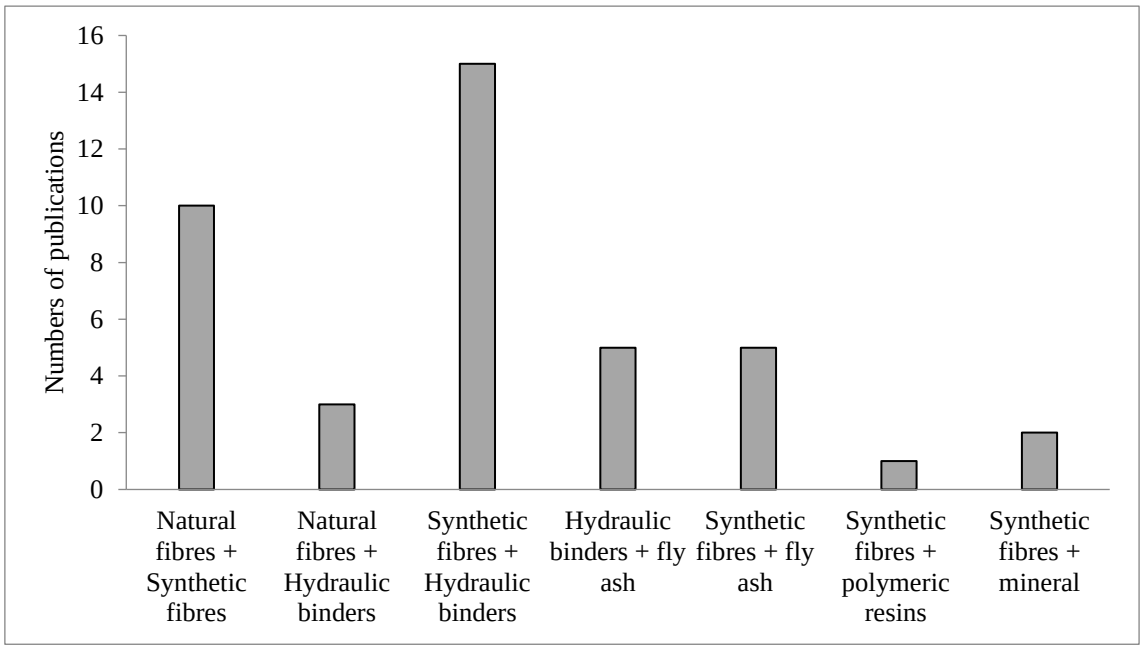

Figure 2.4 Number of papers on binary reinforcement of sand and fibre reinforced stabilized sand.

Table 2-4 Summary of researches published data on fly ash stabilized sand.

No	Sand					Sand, %	Clay, %	Silt, %	Synthetic fibres			Fly ash							Experimental test						Applications
	OMC, %	ϒd max, kN/m^3	Grain size						PP fibres	PP, %	Length, mm	Fly ash	Class	Fly ash, %	Gs	OMC, %	ϒd max, kN/m^3	LL	USC	UUT	Repeated triaxial test	CBR	M_R	Shear box	
			Fine, mm	Medium, mm	Course, mm																				
1						15	6	79	X	1	25	X	F		2.1	25.5	12								embankments
2	10	19							X	0.5,1, 1.5,2	20	X	F	10,15, 20,25, 30, 35	2.1	22	13.6	44	X	X	X	X	X	x	
3			0.28	0.43	0.08			0.03		0.5,1, 1.5	6,20	X	F	25,35, 50,75	2.2			27	X			X		X	
4			X			11	4	85	X	0,0.5, 1,1.5	6,12, 24	X		0,50, 100	2.1	30			X						
5			X			11	4	85	X	0,0.5, 1,1.6	6,12, 24	X	F	0,50, 100	2.1	30			X			X			
6									X	0,0.1, 0.2, .3, 0.4,0.5		X	F	75,85, 100					X	X	X	X			Road construction

1 Bhardwaj, D (2008), 2 Chauhan, M.S., (2008), 3 Chore, H.S., (2011), 4 Jadhao, P.D. (2008), 5 Jadhao, P.D. (2008),

6 Kumar, P. (2008)

Table 2-5 Summary of published data on fibre reinforced sand.

Paper	Sand			Fibre					Experimental tests					applications
	Classification	Cu	shape	Additive materials	Fibre type	Length (mm)	Diameter (mm)	Fibre content (%)	UUT	CBR	MR	Shear box test	Plate load test	
(Al-Refeai and Al-Suhaibani, 1998)	A-3	2.5	sub rounded,	--	PP	25	0.437	0, 0.2, 0.4, 0.6, 0.8, 1	X	X	X			Road construction
			sub-angular	--	PP	50	0.39	0, 0.2, 0.4, 0.6, 0.8, 1						
(Anagnostopoulos et al., 2013)	SP	5.90, 2.30, 8.40, 1.80, 2.86, 7.86	round	--	--	12	0.03	0.0, 0.1, 0.3, 0.5				X		
(Consoli et al., 2005)	SP	1.9	--	--	PP	24	0.023	0.5	X					
(Consoli et al., 2007a)	SP	1.9	--	--	PP	6, 12, 24	0.023	0.5				X		
(Consoli et al., 2003)			--	--	PP	24	0.023	0.5	X				X	
(Consoli et al., 2009a)	SP	2.1	--	--	PP	12, 24, 36, 50	0.023, 0.1	0.5	X					
(Consoli et al., 2007b)	--	2.1	--	--	PP	24	0.023	0.5	X			X		
(Consoli et al., 2004)	SP	1.9	--	--	Polyester	12&36	180	0; 0.5	X					
				--	PP	12&36	21	--						
				--	Glass	6.4&25.4	13	--						
(Consoli et al., 2012)	--	2.1	--	--	PP	50	0.1	0.5	X				X	
(Consoli et al., 2009b)	SP	2.1	--	--	PP	24	0.023	0.5	X					
(Diambra et al., 2010)	--		--	--	PP	35	0.1	0, 0.3, 0.6, 0.9	X					

Table 2-5 Summary of published data on fibre reinforced sand.
Continue…...

Paper	Sand			Fibre					Experimental tests			applications
	Classification	Cu	shape	Additive materials	Fibre type	Length, mm	Diameter, mm	Fibre content, %	UUT	Shear box test	Permeability Test	
(Diambra et al., 2013)	-	1.7	angular	--	Crimped fibres	35	0.1	0, 0.3, 0.6 0.9	x			
				--	PP	20	0.03	0, 0.3, 0.45, 0.6				
				--	Platy	40	0.12x1.45	0, 0.3, 0.6 0.9				
(Santos et al., 2010)	--	2.1	--	--	PP	24	0.023	0.5	x			
(Dos Santos et al., 2010)	SP	1.9	--	--	PP	24	0.023	--	x			
				Cement	--	--	--	--				
(Ghataora et al.)	--	--	--	--	PP	6, 12	--	--	x		x	
				--	PP, (crimped)	12	--	--				
				--	PP	6	--	0.1, 0.2				
				--	PP	12	--	--				
(Ibraim et al., 2010)	-	1.9	--	--	PP	35	0.1	0, 0.5, 1%	x			
(Ibraim et al., 2012)	--	1.62	angular to subangular	--	Crimped	35	0.1	0.05, 0.15, 0.25%	x			
				--	Platy	--	40x0.12x1.45	--				
(Liu et al., 2011)	--	2.29	subangular to angular	--	PP	12	0.034	0.15, 0.25, 0.50%		x		

Table 2-5 Summary of published data on fibre reinforced sand.
Continue…...

Reference	Sand				Fibre					Experimental tests		Applications
	Sand type	Classification	Cu	shape	Additive materials	Fibre type	Length (mm)	Diameter (mm)	Fibre content (%)	UUT	CBR	
(Santoni et al., 2001)	Vicksburg concrete sand	SP	2	--	--	Monofilaments (round)	13, 19, 25, 51	--	0, 0.5, 1.5, 3	x		
	CTD coarse sand	SP	4.44	--	--	Fibrillated	13, 25, 51, 76	--	--			
	New Orleans filter sand	SP	2.09	--	--	Tape (flat wide)	51, 76	--	--			
	Holland LZ sand	SM	6.98	--	--	Mesh	51x102	--	--			
	Tyndall AFB sand	SP	1.44	--	--	--	--	--	--			
	Yuma sand	SP-SM	1.63	--	--	--	--	--	--			
(Santoni and Webster, 2001)	Vicksburg	SP	2	--	--	PP	51	--	--	x		
(Tingle et al., 2002)	Coarse concrete sand	SP	2	--	--	PP	51	--	0.2, 0.5, 1.0, 1.5, 2.0	x		Road construction
	Yuma sand	SP-SM	1.63	--	--	PP	51 & 76	--	--			
	--	--	--	--	--	Tape	51 & 76	--	--			
	--	--	--	--	--	Netlon Mesh	50X100	--	--			
(Tiwari and Sharma, 2013)	--	SP	2.39	--	--	PP	--	0.3	--		x	Road construction
						Coir	--	0.2	--			
(Wasti and Butun, 1996)	--	--	3.995	angular to sub angular	--	PP mesh	--	--	--	x		

2.1.2 Discussion

Review of studies reinforcement and stabilization sand show that synthetic fibres were the work commonly used reinforcement material studies. It also shows that sand was mainly stabilized with hydraulic binders such as Portland cement, lime and fly ash, with Portland cement being the most popular, see Figure 2.1 and 2.3.

All of the studies are both sand stabilization and reinforcement were lab based. There was no evidence of any of the studies taken to a field test stage as there was little or no field data. The lab studies seemed to be focused on just determining the level of improvement due to the addition of a stabilizer and/or reinforcement.

Only one of the twenty-two a sand stabilizer focused on the application of studies (Kumar and Singh, 2008) on roads. In term of reinforcement, only two of the fifty-one studies focused on applications (Al-Refeai and Al-Suhaibani, 1998, Santoni et al., 2001) which use polypropylene fibre. It was observed that the class C fly ash has not been used to stabilize the sand.

There are no robust investigations for the polypropylene fibre and the fly ash stabilized sand for road construction. The investigations include the resilient behaviour and the permanent deformation which are the main parameters of pavement design. Therefore, the pavement design procedures and the behaviour of the subgrade layer and the reinforcement materials are considered carefully in this chapter.

None of the studies seems to test on durability in terms of the effect of reinforcement and stabilization and/or reinforcement on repeated loading, frost susceptibility and wetting and drying.

2.2 Pavement Design

The pavement is a structure consisting of layers of materials of specific properties chosen such that they can act as a composite to provide secure support to the vehicles (acceptable riding quality, adequate skid resistance, favourable light reflecting characteristics, and low noise pollution0 and enable the transfer of traffic load to the subgrade layers without failure and to protect the latter (subgrade) from subgrade from the deleterious effects of the environment.

There are two pavement design methods which are empirical pavement method and mechanistic-empirical design method. The empirical pavement design procedures depend on the previous projects or the experience for road construction. The pavement performance was also important to evaluate the deformation of the pavement structure.

In 1960, the AASHTO design guide was based on road trails tests and the empirical methods were developed by the fitting of the experimental results and/or test track experiments. The disadvantage of the empirical methods is that the methods are only accurate if they are used with the same materials and environmental conditions.

Nowadays, with the development of new techniques and materials for improving subgrade and other structural layers in the pavement, it has become necessary to modify road design procedure, which also takes account of failure mode and can investigate method procedure under simulated loading. Therefore, failure modes such as rutting, fatigue, and deflection need to be considered for pavement design. The early procedures were The Asphalt Institute method (Asphalt Institute, 1982, 1991) and the Shell method (Claussen et al., 1977; Shook et al., 1982). The mechanism of these procedures is a linear-elastic concept which used to obtain

the strains; as well as the empirical models were used to evaluate the allowed number of loads for flexible pavement. In linear-elastic theory, there are important factors for pavement design which did not assess such time, temperature, and anisotropy in materials properties. Therefore, new better models were needed to evaluate the mechanistic of pavement performance.

The mechanistic empirical design method is a hybrid concept. The procedure includes two parts which are; the mechanistic properties that assume the materials are homogenous and use the static as in linear elastic theory, while the empirical part fills in the gap between the mechanic and the pavement performance. Therefore, the mechanistic empirical design method is a better approached as bridge the gap between empirical and mechanistic design methods and correlated more suitable for pavement design.

Following section review the pavement designs methods: empirical and mechanistic-empirical design method.

2.2.1 Empirical Pavement Design method

The empirical design method depends on both experimental and field experience. The empirical method requires a number of observations such loads, materials properties and environment to obtain the outcome for the design by correlations models. However, the correlations do not have scientific principle. The benefit of empirical models is that it can be used to relate cause and effect of a complex phenomenon which cannot be explained early on a scientific basis.

In 1920, the first soil classifications materials were developed, and the first empirical pavement design procedure was also developed. The California Bearing Ratio (CBR) strength

test was developed by the Public Roads soil classification system (Huang, 2004). The CBR value was used to determine the layer thickness that can prevent subgrade shear failure. During the Second World War, the CBR test was developed by United State Corps of Engineers (USCE) and became the common procedure. It is still widely used in pavement design across the world.

In 1945 Public roads soil classification system was developed by the Highway Research Board (HRB). HRB classified the soil into seven groups from A-1 to A-7. The layers thickness and properties were estimated by public roads soil classification system.

After the California Bearing Ratio (CBR) strength test, many procedures were created based on the subgrade shear failure. Terzaghi's bearing capacity formula was utilized to obtain the pavement thickness by Barber (1946, after Huang (2004)). McLeod (1953, after Huang (2004)) also used the bearing capacity after using logarithmic spirals.

The first trail of measuring the pavement structure capacity was obtained by determining the surface vertical deflection (Huang, 2004). In 1947, the Kansas State Highway Commission developed the first procedure which is Boussinesq's equation and the limit of the subgrade deflection was 2.5mm. In 1953, the U.S. Navy used the theory of Burmister's two-layer elastic and set the deflection to 6.35mm (AASHTO, 1993). These limitations can be easily measured in the field but the pavement layers are failed due to excessive stress and strain instead of deflections.

The American Association of State Highway and Transportation Officials (AASHTO) design method has been modified based on the experience and the theory (AASHTO, 1993). This modification allows using the method for other materials and different conditions. The benefit

of the models is that they can be applied to interpret the factors that affect the pavement. The first AASHTO Guide was in 1972 then 1986 and the final guide is AASHTO 1993. The next section describes the procedure of AASHTO 1993.

2.2.1.1 Design Inputs

Design period

The good pavement design is that the design period cost of the road will be the minimum to a given terminal condition. This whole life cost is made up of two factors: construction cost, maintenance cost. For heavy traffic road, the design life is acceptable to be 20 years. The pavement thickness for 20 years and the traffic of 80 msa do not change the pavement thickness for 40 years (AASHTO, 1993).

Traffic loading

The main factor in both pavement design methods empirical or mechanistic is the traffic loading which measured in terms of vehicles classes and load distributions, classified by the axle type, and convert them into the equivalent single axle loads (ESALs). The equivalent single axle load was defined as the number of 18-kip single axles that causes the same pavement damage as the actual mix of axles loads (AASHTO, 1993).

$$LEF = \frac{W_{t18}}{W_{tx}} \qquad \text{Equation 2-1}$$

$$T_f = \sum (p_i * LEF_i) * A \qquad \text{Equation 2-2}$$

$$ESAL = AADT * T * T_f * G * D * L * 365 * Y \qquad \text{Equation 2-3}$$

Where

W_{tx} = Number of x-axle load applications applied over the design period,

W_{t18} = Number of equivalent 80 kN (18 kip) single axle loads over the design period,

T_f = Truck factor,

p_i = Percentage of repetitions for i^{th} load group,

LEF_i = LEF for the i^{th} load group,

A = Average number of axles per truck,

AADT = Annual average daily traffic,

T = Percentage of trucks,

G = Growth factor,

D = Trucks in design direction (%).

L = Trucks in design lane (%), and

Y = Design period.

Reliability

The reliability factor is the factor that defines based on the road classification. The factor was used to make sure that the traffic loading was predicted correctly up to the end of the design life. Therefore, the pavement design can be conducted regarding the predicted traffic loading. Reliability factors are specified in the range from 99.9% to 50%. These factors depend on the functional classification of the road and whether the road is urban or rural, for instance for

motorways this reliability factor ranges from 85% to 99.9%, while for local roads it could be within a range of 50% to 80%.

Material Properties for Structural Design

The empirical pavement design (AASHTO, 1993) considers the effect of the environment on the resilient modulus over the design life. The guide presents two procedures to obtain the resilient modulus. The first method determines the resilient modulus from the experimental test. Then the relative damage is calculated from Equation 2-4. The second method obtains the seasonal moduli which can be determined from correlations with soil moisture and temperature conditions or from non-destructive deflection testing. Then the relative damage is obtained from the chart which related to the resilient modulus for each a half month (Huang, 2004).

$$u_r = 1.18 * 10^8 * M_R^{-2.32}$$ Equation 2-4

Where

U_r = Relative damage factor, and

M_R = Resilient modulus.

Layer coefficients

The (AASHTO, 1993) guide focus to improve the subgrade and the unbound materials, consider the environmental condition and combine the drainage into the design. Therefore, it has developed an empirical formula that includes the layers coefficient and drainage coefficients as Equation 2-5.

$$SN = a_1 D_1 + a_2 D_2 m_2 + a_3 D_3 m_3$$ Equation 2-5

Where

SN = Structural number,

$a_{1, 2, 3}$ = Layer coefficient, and

$D_{1, 2, 3}$ = Layers thickness.

2.2.1.2 Performance criteria

Serviceability

The serviceability is defined as the quality of the pavement to serve the traffic (Huang, 2004). The initial serviceability index is a function of pavement type and construction quality. The terminal serviceability index is the lowest index that will be tolerated before rehabilitation, resurfacing, and reconstruction becomes necessary. The serviceability index is marked as a range from 0 to 5. Also, it is expressed by Equation 2-6.

$$\Delta PSI = P_0 - P_T \quad \text{Equation 2-6}$$

Where

P_o = Initial serviceability index, and

P_T = Terminal serviceability index.

Typical, the initial serviceability index is a range from 4.2 to 4.5 as reported in AASHO road test while the terminal serviceability index is 2.5 at the end of the road life for the major highway and 2 for the low roads.

2.2.2 Mechanistic-Empirical Pavement Design (M-E Pavement Design)

The mechanistic-empirical pavement design method considers the behaviour of the pavement materials and conduct iterative method to determine the thickness of the layers (Huang, 2004). The M-E pavement design procedure considers the strain, stress, and deflection that are due to the traffic loading and environmental conditions.

Kerkhoven & Dormon, (1953) proposed that the vertical compressive strain on the top of subgrade could be used as a failure criterion to reduce the permanent deformation. In 1960, Saal & Pell stated that the fatigue was controlled by horizontal tensile strain at the bottom of the asphalt layer. Shell and Asphalt Institute method proposed to use the strain as failure criteria in their M-E pavement procedures (Claussen et al., 1977, Shook et al., 1982; AI, 1992). Afterwards, the criteria of strain were used and further developed by The Departments of Transportation of the Washington State (WSDOT), North Carolina (NCDOT), and Minnesota (MNDOT) in their M-E pavement design methods. In 1990, the framework of Calibrated Mechanistic Structural Analysis Procedures for Pavements was reported by The National Cooperative Highway Research Program (NCHRP) in 1-26 project report.

In 2004, The NCHRP 1-37A project (NCHRP, 2004) incorporated the calibrated model that was developed by using traffic loading and environmental conditions. Also, it includes the Equivalent Single Axle Load (ESAL) of AASHTO pavement design method and vehicle class and load destruction. The performance of materials behaviour was considered under environmental conditions such as permeant deformation (rutting), fatigue cracking (both bottom-up and top-down), thermal cracking, and smoothness. The procedure and the requirements of mechanistic-empirical pavement design guide such design criteria, traffic

loading, materials properties, the empirical performance models, reliability and environmental conditions are described in the following section.

2.2.2.1 Design Inputs

Design Criteria

The design criteria consist of different types of distresses criteria. The distresses of flexible pavement are permanent deformation (rutting), fatigue cracking, thermal cracking, and roughness. The only functional distress predicted is roughness (Huang, 2004, NCHRP, 2004). The disadvantage is that the friction is not taken in to account in the M-E design method.

Two strains have been considered as the most critical strain for the design of asphalt pavement. One is the horizontal tensile strain at the bottom of the asphalt layer, which causes fatigue cracking. The other is the vertical compressive strain on the surface of subgrade which causes permeant deformation or rutting. These two strains are used as failure criteria in the asphalt institute method. The critical locations were demonstrated in Figure 2.5 and the definition for each point was described Table 2-6.

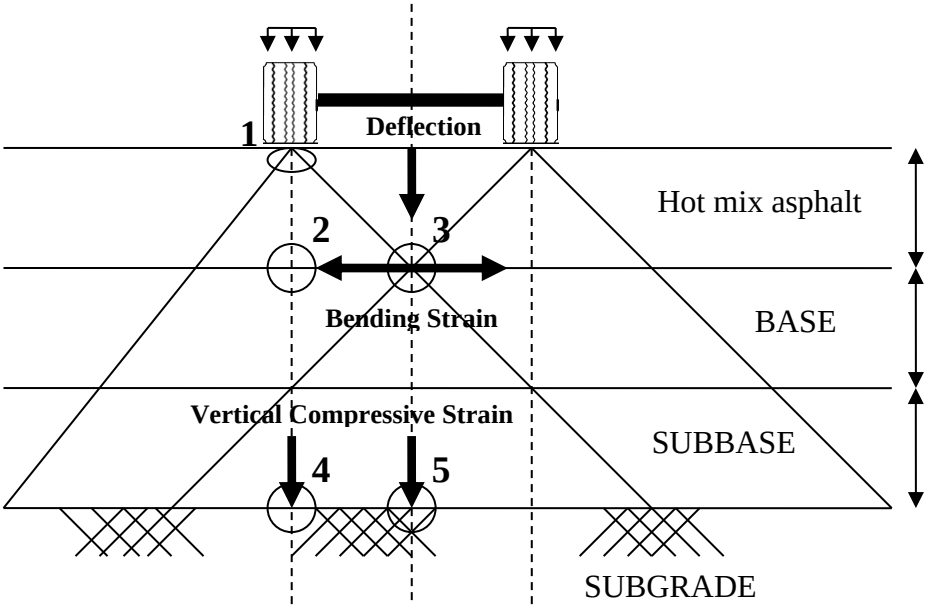

Figure 2.5 Illustrates the locations for critical points.

Table 2-6 Locations of critical points for flexible pavement (NCHRP, 2004)

Location	Critical response
Top of pavement layer (1)	Deflection (rutting)
Bottom of pavement layer (2)	Horizontal tensile strain (fatigue)
Top of base & subbase layer (3)	Permanent deformation (rutting)
Top of subgrade (4,5)	Permanent deformation (rutting)

Fatigue criterion: The allowable number of load repetition was determined by the tensile strain at the bottom of the asphalt layer for the fatigue cracking. In the Asphalt Institute Method, it was recommended to use Equation 2.7.

$$N_f = f_1(\varepsilon_t)^{-f_2}(M_r)^{-f_3}$$ Equation 2.7

Where

N_f = Allowable number of load repetition,

ε_t= Tensile strain at the bottom of the asphalt layer,

Mr = Resilient modules of asphalt layer, and

f_1, f_2 & f_3 = Coefficients of fatigue criterion (0.0796, -3.291 & -0.854, respectively).

Rutting criterion: The rutting was controlled by two vertical compressive strains which are on the top of both the asphalt layer and subgrade layer. The Asphalt Institute and Shell design methods recommended Equation 2.8 to determine the allowable number of load repetitions.

$$N_d = f_4(\varepsilon_c)^{-f_5} \quad \text{Equation 2.8}$$

Where

N_d = Allowable number of load repetition,

ε_c= Vertical strain on the surface of the subgrade, and

f_4 & f_5 = Coefficients of permanent deformation criterion (1 .365x10^{-9} & 4.477, respectively).

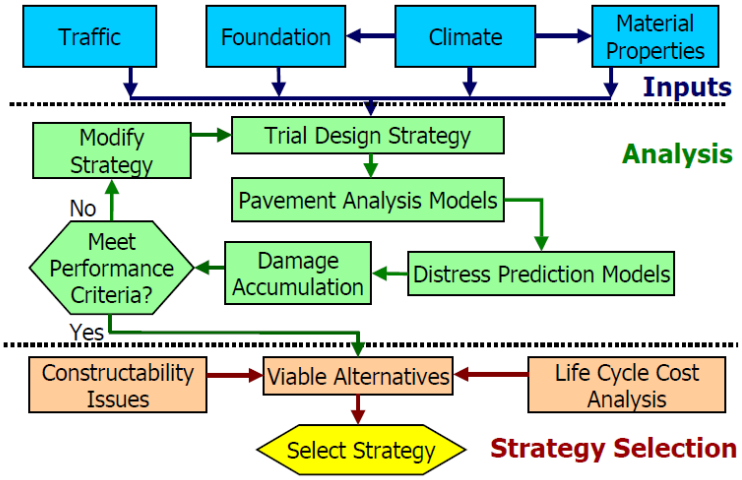

Figure 2.6 Flow diagram of design process for flexible pavements (After MEPDG, 2004).

Traffic loading

As mentioned in section 2.2.1, he equivalent standard axle loads (ESAL) of the empirical design methods have been used in the M-E pavement design guide to obtaining the traffic loading.

Environment effects

The (NCHRP, 2004) developed the Enhanced Integrated Climatic Model (EICM). The EICM model requires the hourly air temperature, hourly precipitation, Hourly wind speed, hourly percentage sunshine, and hourly relative humidity. The effect of environmental conditions and the effect of variation in water content are discussed in section 2.3.3. The following is the environmental factors that affect flexible pavements.

- Temperature variations for the asphalt concrete.
- Moisture variation for subgrade and unbound materials.
- Freezing and thawing for subgrade and unbound materials.

In this research, the moisture variation and freezing-thawing cycles are considered for reinforced and stabilized sand. Moreover, the research was extended to investigate the effect of these factors on both resilient modulus and permanent deformation.

Material Properties

This study is focusing on sandy soil that considers as granular or unbound soil, therefore only unbound materials and asphalt concrete are described. The design process requires three factors: the climate (temperature and precipitation), the pavement response (stress, strain state), and the distress models. The Mechanistic-Empirical Pavement Design requires two parameters as input: the dynamic modulus for asphalt concrete and the nonlinear stiffness model for unbound materials. The dynamic modulus is determined by simulating the temperature variation and loading rate in asphalt concrete. The recommended materials properties for the M-E pavement design are summarized in Table 2-7.

Section 2.3.1 provides the factors affecting the resilient modulus. These include the deviator stress, dry density, degree of saturation, and fines content. For the analytical pavement design, resilient modulus can be determined based on the design level of data (NCHRP, 2004). Level 1 is to determine the resilient modulus by the laboratory test, level 2 uses other parameters to evaluate the resilient modules while level 3 use the typical value of the resilient modulus as Table 2-7.

Table 2-7 Mechanistic Properties for Flexible Pavements

No.	Material	Property	Methods
1	Asphalt Concrete	Dynamic Modulus	Level 1: Determine by ASTM D3496. Level 2: Estimate from basic test results on AC. Level 3: Use typical values from a local database.
		Resilient Modulus	Level 1: Determine by SHRP P07 or ASTM D4123. Level 2: Estimate from basic test results on AC. Level 3: Use typical values from a local database.
		Poisson's Ratio	Level 1: Determine by SHRP P07 or ASTM D4123. Levels 2 & 3: Assume a typical value of 0.1, 0.35, and 0.5 At temperatures of 5, 25, and 40 °C.
2a	Base/Subbase (Untreated)	Resilient Modulus	Level 1: Determine by AASHTO T46. Level 2: Estimate from basic test results on the base. Level 3: Use a typical value from a local database.
		Poisson's Ratio	Levels 1-3: Assume a typical value of 0.35.
2b	Base/Subbase (Treated)	Resilient Modulus	Level 1: Determine by AASHTO T46 (ATB) or by ASTM D3496 (CTB, LCB). Level 2: Estimate from basic test results on treated base. Level 3: Select a typical value from a local database.
		Poisson's Ratio	Level 1: Determine by SHRP P07 or ASTM D4123. Levels 2 & 3: Assume typical values of 0.1, 0.35, and 0.5 at temperatures of 5, 25, and 40 °C
			Levels 1-3: Use a typical value of 0.15.
3	Subgrade	Resilient Modulus	Level 1: Determine by AASHTO T46. Level 2: Estimate from basic test results on subgrade soil. Level 3: Use a typical value for the soil type from a local database.
		Poisson's Ratio (μ)	Levels 1-3: Assume a typical value of 0.35.

2.2.2.2 Pavement Response Models

The Mechanistic-Empirical Design of New and Rehabilitated Pavement Structures guide (NCHRP, 2004) developed two methods to evaluate the stress, strain, and deflections such multi-layer linear elastic theory and finite element method. The pavement responses are evaluated under traffic loading and environmental conditions. The critical pavement responses variable include:

- Tensile horizontal strain at the bottom/top of the HMA layer (fatigue cracking).
- Compressive vertical stresses/strains within the HMA layer (HMA rutting).
- Compressive vertical stresses/strains within the base/subbase layers (rutting of unbound layers).
- Compressive vertical stresses/strains at the top of the subgrade (subgrade rutting).

Figure 2.5 describes the critical location within the pavement layer. Two flexible pavement analysis methods have been used in the design guide which is linear elastic and multilayer elastic theory. Multilayer elastic theory provides a better combination of analysis features, theoretical rigour, and computational speed for linear pavement analyses. Also, the nonlinearity of unbound materials was considered. The nonlinearity behaviour is considered by nonlinear finite element procedure for determining the pavement responses.

Multi-layer Linear Elastic Theory

Huang (2004) suggested that Boussinesq's solution (1885) can be applied to determine stress, strain, and deflection responses due to surface loading. The multi-layer concept was incorporative with two-layer and three-layer solutions in Burmister, (1945). Foster and Alvin,

(1954); Burmister, (1958); Jones, (1962); Huang, (1969), and (1973) improved the charts and tables of these solutions.

The theory of multi-layer analysis has its roots in the Burmister two-layer and three-layer solutions (Burmister, 1945); charts and tables summarizing these solutions were developed later (Foster and Alvin, 1954; Burmister, 1958; Jones, 1962; Huang, 1969, and 1973)

Finite Element Method (FEM)

The finite element method recommended method to determine the structural modelling of a multi-layer pavement where materials properties are various in both vertical and horizontal profile (NCHRP, 2004). Also, it is possible to consider various effects such as non-linear material behaviour, large strain effects, dynamic loading, and three-dimensional geometries. The finite element method (FEM) is suitable for structural evaluation and response prediction of pavements. It can be used to solve complex problems. However, FEM is consuming time.

The concept of FEM is that the FEM divides the part into rectangular finite elements (mesh) with a large number of nodes, and then the traffic loading and subgrade reaction are applied on the nodes. The M-E pavement design guide provided more features into the FEM as below.

1. Linearly elastic behaviour for asphalt concrete
2. Non-linearly elastic behaviour for unbound materials
3. Fully bonded, full slip, and intermediate interface conditions between layers

In this research, the KENLAYER software was used to obtain the pavement response for reinforced and stabilized subgrade layer. The KENLAYER Computer Program has accepted

software which can model pavement layers as linear or nonlinear elastic. The main core of KENLAYER software is used to set a solution for the elastic multi-layer system under a circularly loaded area. It can only be used to analyse flexible pavements with no joints. This program can use the superposition principle for multiple wheels. It can also use an iterative technique to solve non-linear problems (Ghadimi et al., 2014, Huang, 2004). It can be applied as single, dual, and dual-tandem wheel on each layer for the either linear or nonlinear elastic. Analytical design is described in detail in Chapter Six.

2.2.3 Discussion

The literature review showed that there are two main pavement design methods, empirical and mechanistic-empirical pavement design. The empirical pavement design (AASHTO, 1993) is based on correlation models. However, the models are only accurate when the correlation models used to relate to the materials for which they have been developed i.e. if correlation models have been used for specific silty sand, then using the same models used for clayey silty sand will give error results.

The Mechanistic-Empirical Pavement Design consists of two parts. The mechanistic aspect which assumes that materials layer are homogenous, and uses the linear elastic theory. While the empirical concept is used to explain the causes and the effects of the complex phenomenon (Huang, 2004).

It is acceptable that the design life is 20 years or more (AASHTO, 1993). Therefore, the current study was carried out the pavement design for 10, 20, and 30 years to evaluate the stabilizations and reinforcement materials for the subgrade layer. The empirical design method is used to obtain traffic loading as the equivalent single axle loads for each type of

vehicles. The materials properties are assessed by the resilient behaviour. Therefore, both empirical and mechanistic procedures recommended evaluating the resilient modulus under different environmental conditions.

The benefit of M-E pavement design method is that the ability to characterize the materials including subgrade and existing pavement structure. It accommodates changing load types as well as accommodation of new materials (NCHRP, 2004).

The pavement responses such the stress, stain, and deflection need to be obtained based on the traffic loading. Then the thicknesses of the layers can be determined based on the pavement responses. Therefore, the finite element model should be used in order to determine the effect of traffic loading and environmental condition during the design life (NCHRP, 2004). The layers thickness will construct based on the response of the material. While the empirical pavement design mothed, the thickness of the layers will determine based on experience or previous project.

In this research, the Mechanistic-Empirical Pavement method was used to carry out the pavement design as discussed in Chapter Seven. Three design periods (10, 20, 30 years) were proposed to investigate the pavement responses. Also, the traffic loading was recommended to be calculated based on (AASHTO, 1993), this was described in Chapter Seven.

The guide of pavement design recommended different experimental tests to simulate the effect of the environment on the road layers. Wet-dry and freeze-thaw durability tests are recommended in (AASHTO, 1993, NCHRP, 2004). Therefore, the resilient modulus and permeant deformation were investigated and reported after considering the environmental

conditions in Chapters Five and Six, respectively. Finally, pavement parameters were used to carry out the analytical pavement design in Chapter Seven.

2.3 Behaviour of Granular Subgrade Soil under Traffic Loading in a Pavement

Typical road construction comprises wearing course, base course, subbase, and subgrade. In instances where the subgrade soil is weak, a capping layer is placed between the subgrade and the subbase. Give a certain level of traffic, weaker subgrade will require thicker subbase. Thus, if subgrade material can be made stronger savings can be made in the quantity of suitable subbase used and possibly overlying base course material. To design the pavement structure, it is necessary to determine both permanent deformation and resilient modulus of the materials. Review of both permanent deformation and resilient modulus of granular materials and stabilized granular materials are described below.

2.3.1 Resilient Modulus

Resilient modulus is the main factor in pavement design. It allows determining the response of the layers in term of a determination under repeated loading. Resilient modulus is defined as the ratio of deviator stress to the recoverable strain as shown in Equation 2-9.

$$M_r = \frac{\sigma_d}{\varepsilon_r} \qquad \text{Equation 2-9}$$

Deviator stress, density, water content, grading fines content aggregate types and methods of compaction affect the resilient modulus (Lekarp et al., 2000a).

2.3.1.1 Deviator stress

The literature review shows that the cyclic deviator stress has a significant effect on the resilient modulus of granular materials (Salour et al., 2014, Brown, 1996, Lekarp and Dawson, 1998, Lekarp et al., 2000a). They found that the resilient modulus of granular materials has been significantly affected by confining pressure and sum of principal stresses. The results confirmed that the improvement of resilient modulus was 500% when the confining pressure increased from 20 to 200kPa as reported by (Monismith et al., 1975). Lekarp et al. (2000a) observed that a 50% improvement of the resilient modulus when increasing the principal stress from 70 to 140kPa. Morgan (1966) conducted a resilient modulus test and found that the resilient modulus was slightly decreased with increase the deviator stress at constant confining pressure. Therefore, it can be concluded that the effect of confining pressure is much more than the stress level.

Both constant confining pressure and variable confining pressure were applied to investigate the resilient modulus. Allen and Thompson (1974) conducted a comparison between the constant and the variable confining pressure. The higher resilient modulus was obtained by the constant confining pressure. Lekarp et al. (2000a) reported that the resilient modulus at the constant confining pressure was equal to the mean of resilient modulus at the variable confining pressure.

2.3.1.2 Dry density

Lee et al. (1995) investigated the effect of the density on the resilient modulus for dune sand and the results show that at the same density, the resilient modulus decreased at 13.8kPa but after increasing the deviator stress the resilient increased.

Lekarp et al. (2000a) stated that the increase in density is due to increase in the resilient modulus. The density results showed 50% difference in the resilient modulus between the loose and dense sand. Barksdale (1972) carried out the resilient modulus test and the results showed that the density showed a significant effect on the results but less effective at high deviator stress. The density of granular soil increases the strength and the stiffness.

The density of granular soil also has influences on Poisson's ratio. It was observed that the Poisson's ratio decreased with increase in the density (Allen and Thompson, 1974, Lekarp et al., 2000a).

2.3.1.3 Degree of saturation

The effect of moisture content or the degree of saturation on the resilient modulus was observed in both experimental and in situ work. Ahmed and Khalid (2008) observed that the resilient modulus was 214MPa at the optimum moisture content of 6.9% and the maximum dry density of 21.82kN/m^3. While the maximum modulus was 330MPa when the optimum moisture content is 5.7%. Lekarp et al. (2000a) reported that the resilient modulus in dry or partially dry cases was higher than the resilient modulus in the wet case. Therefore, it was recommended to carry out the resilient modulus at ±25% of optimum moisture content.

The effect of the water content of dune sand was evaluated by measuring the parameter k_1 and k_2 and the water content slightly affect both parameters (Lee et al., 1995). This because the test is the drained type and the sand is a free-draining material. Therefore, the resilient modulus remains the same when the effective stress was used to obtain the resilient modulus (Monismith et al., 1975).

2.3.1.4 Effect of Grading, fines content and aggregate types

There is an argument about the effect of the fine content on the resilient modulus. The reason of that as the fine content increases the resilient modulus decrease in partially crushed aggregate as reported by (Caicedo et al., 2011) but (Plaistow, 1994) stated that the grading has an indirect effect when the water content is controlled.

Two granular soils with different proportion of fines were tested by repeated loading test (RLT) to obtain more factors affecting the resilient strain. The results shown that the resilient strain was reduced by 30% when the fine content decrease from 7.5% to 4% as reported by (Ho et al., 2014b). Therefore, it was concluded that the fine content is more effective than the water content for both soils. Also, the fine content of soils requires more investigation. Similar results were reported by (Hornych and Abd, 2004).

The particle size destruction is one of the factors affecting resilient strain. The soils can resist both permanent and resilient strain when it consists of all particles as reported by (William B. Fuller and Sanford E. Thompson, 1907).

The resilient modulus decreases with an increase in the fines that is less than 0.074 mm. The increase of the water content is due to reduction of resilient modulus with high fines content. In the coarse soil, if the fine is small, then the bigger grains will distribute the load, thus the fine will fill the voids between the grains. In contrast, the increase of fine content will not allow the bigger grain to reach each other to distribute the load. Therefore, the resilient modulus is decreased by an increase in the fine content. It was confirmed that 10% of fine soil decreased the resilient modulus in the crushed rock by 15% compared with 4% of fine content (Kolisoja, 1998).

2.3.1.5 Methods of compaction

Two compaction procedures were conducted to obtain a higher density (Lee et al., 1995). These are the impact of the hammer and vibrating table. The highest resilient modulus was obtained using the vibrating compaction. Also, the permanent deformation was determined at 6.9kPa confining pressure and it was observed that the permanent deformation of impact compaction was higher than the vibrating one of about 2.5 times. Moreover, the resilient strain of the impact compaction was greater than the vibrating compaction. Therefore, it can be concluded that the density by the vibrating compaction is higher than the density by impact compaction. The reason for that is because the vibrating compaction is more uniform than the impact compaction.

2.3.2 Permanent Behaviour

One of the main aspects of the design philosophy for flexible road pavements is the limitation of the rut development in the pavement structure. Although measuring rut depth is normally considered to be a relatively simple task, the prediction of rut development is extremely complex. The problem is not only to characterize the pavement materials but also to assess the impact of the environmental conditions and calculate the appropriate stress distribution during the entire service life of the pavement. The first step in understanding the important role of granular materials in pavement rutting is to appreciate the nature of permanent deformation in such materials. Nevertheless, research in this area has revealed that plastic behaviour is affected by several factors as described below.

2.3.2.1 Effect of Stress Level

The threshold deviator stress values were stated for granular soils by (Brown, 1996). It was reported that 70% of the static shear stress can be applied in the repeated cyclic load test. It was also confirmed by (Chow et al., 2014) that 70% of the static shear stress obtained the higher permanent deformation. Equation 2-10 demonstrates the relationship between the applied shear stress and shear strength.

$$\text{Shear Stress Ratio} = \frac{\text{applied shear stress}}{\text{shear strength}} = \frac{\tau_f}{\tau_{max}} \qquad \text{Equation 2-10}$$

The deviator stress has a significant effect on the permanent strain as observed by (Kim and Siddiki, 2006). It was concluded that if the confining stress was kept constant and the change in the axial stress will affect the permanent deformation. It was stated that if the cyclic deviator stress is increasing at constant confining stress, the accumulation of permanent strain increases. Conversely, at constant stress level and reducing the confining stress the accumulation of permeant strain is reduced.

In Italy, (Cerni et al., 2012) were testing the construction and demolition wastes materials as aggregates for road construction. Repeated triaxial tests were carried out to determine the permanent deformation for these materials as the base or/and subbase layer. The samples were compacted at the maximum dry density and optimum water content. The repeated load test (RLT) was a constant confining pressure and carried out up to 10000 load cycles. The effect of different deviator stress level showed significant effecting on the results. The permanent deformation increases with increase in the axial stress while it reduces with an increase in the confining pressure.

Chauhan et al. (2008) also carried out repeated triaxial tests on unreinforced and reinforced sand. The fibre and fly ash were used to reinforce and stabilize the sand. The tests were carried out at a confining pressure of 25, 50 and 75kN/m^2 and six different deviator stresses. The permanent deformation for both unreinforced and reinforced samples decreases with increase in the deviator stress and the confining pressure. On the other hand, the resilient modulus increases with increases in the confining pressure and decrease the deviator stress and the number of cycles. Similar results were observed by (Kumar and Singh, 2008). It was confirmed by cyclic triaxial test that the permanent deformation of polypropylene fibre reinforced class F fly ash with 25% of sand soil was increased with an increase in the stress level.

2.3.2.2 Effect of moisture content/suction

Pinard et al. (2013) stated that the sand strength was improved by dry the soil to the equilibrium moisture content which is in the range of 0.6 to 0.7% of OMC. The soil suction can be observed over this range by soaked condition. The main point is that the moisture content of the pavement layers should not be above the OMC to retain the sand suction strength. It was also recommended that the typical compacted moisture content should be less than 80% of the saturation moisture content of the untreated sand.

Scott (1980) reported that the deformation resistance, cohesion, and stiffness increase with a decrease in the moisture content. The reason for that the soil suction improves the cohesion. The partially saturated is demonstrated in Equation 2-11.

$$s = u_a - u_w \qquad \text{Equation 2-11}$$

Where

s = Matrix suction,

u_a = Pore air pressure, and

u_w = Pore water pressure.

In the case of fully saturated soil, the pore air pressure is zero. As a result of Equation 2-12, the pore water pressure will be decreased with the increase of the soil suction (negative value). by using Equation 2-13, the effective stress will be increase as (CRONE, 1952) assumed.

$$u = s + \propto p \qquad \text{Equation 2-12}$$

$$p' = p - u \qquad \text{Equation 2-13}$$

Where,

s = Soil suction as a negative quantity,

u = Pore water pressure,

p = Total mean normal stress, and

p' = Effective stress.

In this meaning, the soil suction has significant influences on its effective stress. Also, the confining or hydrostatic pressures are governed by effective stress; therefore, the increase in confining pressure is due to improve materials strength.

Similar results were reported by (Caicedo et al., 2011). The influence of water content on the resilient modulus for non-standard granular materials was investigated. It was stated that

when the water content decreases the resilient modulus increased due to the increased suction. It was also stated that the water content has a significant effect on the soil that has more fines. The same conclusion was reported by (Cary and Zapata, 2011). The effect of water content on the resilient behaviour of non-standard unbound granular materials was investigated by (Coronado et al., 2016). The results showed that the water content has a more significant effect than the fines soil for secant modulus. The reason is that when the water content decreases the capillary forces increased, and then the secant modulus is significantly increased.

The effect of water content on the permanent deformation was investigated also by (Pumphrey and Lentz, 1986). It was observed that the permanent strain of compacted samples at optimum water content was greater than the permanent strain below the optimum water content after 10,000 cycles. It is reasonable, because of less water volume during compaction to produce a denser soil.

Lekarp et al. (2000a) reported that resilient modulus decreases with an increase in water content. It was observed that the increase of saturation degree from 70 to 97% is due to a reduction of 50% in the resilient modulus. it was observed that the resilient modulus did not change much if the analysis depends on the effective stress as reported by (Ho et al., 2014a). In addition, the Poisson's ratio decreases with an increase in the saturation degree. It was observed that the effective stress is not sufficient to interpret the change of Poisson's ratio.

2.3.2.3 Effect of number of load cycles

Kumar and Singh (2008) stated that the permanent deformation was increased with an increase in the number of load cycles. It was also reported that the permanent deformation can be obtained by the Equation 2-14.

$\varepsilon_p = a\ N^b$ Equation 2-14

Where,

N= Number of load cycles, and

a, b = Constants for types of soils.

Multistage repeated load triaxial test was carried out by (Arnold et al., 2002) to evaluate the effect of the number of cycles and increasing the deviator stress on two Good and Poor Northern Ireland unbound granular materials, Granodiorite and Sandy Gravel. It was observed that the permanent deformation was decreased with increase in the number of cycles until it reaches purely elastic. Because of the aggregates are getting stable after certain cycles.

2.3.2.4 Modelling of Permanent Deformation

A series of repeated loading triaxial tests were conducted on different materials to obtain permanent deformation with respect to the cycles number by (Barksdale, 1972). The results were expressed by logarithm cycle's number, different deviator stress level and confining pressure as expressed in Equation 2-15.

$\varepsilon_{1_p} = a + b \log(N)$ Equation 2-15

ε_{1p} = Permanent deformation,

N = Number of cycles, and

a and b = constant for stress level and confining pressure

The previous model was also investigated by (Sweere, 1990) after applying 10^6 cycles. The researcher stated that the log-normal approach is not fitting the experimental results.

$$\varepsilon_{1_p} = a\, N^b \qquad \text{Equation 2-16}$$

Wolff et al. (1994) developed a model based on the data from full-scale heavy vehicle simulator (HVS) at 10^6 of load cycles as expressed in Equation 2-17.

$$\varepsilon_{1_p} = (c * N + a) * (1 - e^{-bN}) \qquad \text{Equation 2-17}$$

The new approach was investigated by (Paute et al., 1996) in order to consider the stress level with the load cycles as shown in Equation 2-18. The experimental work shows that the model was fitted and in agreement with the experimental results.

$$\varepsilon_{1_p} = A * (1 - (\frac{N}{100})^{-B}) \qquad \text{Equation 2-18}$$

ε_{1p} = Permanent deformation after the first 100 cycles,

$A = \frac{m_{mob}}{b*(m-m_{mob})}$ = Limit of total permanent strain,

$m_{mob} = \frac{q_{max}}{p_{max}+p^*}$

q_{max} = Maximum deviator stress,

p_{max} = Maximum mean normal stress,

b = Regression parameter,

m = Slope of the static failure line, and

p^* = Stress parameter.

The factor of A is the limit of the total permanent deformation. Therefore, the A value is expressed as above (Burland et al., 1981).

Further effort for the Equation 2-19 model was carried out by (Pappin, 1979) to investigate the effect of the combination of the number of cycles and cyclic deviator stress level on the development of permanent deformation.

$$\varepsilon_{1_p} = a * \left(\frac{q}{p}\right)^b_{max} \left(\frac{L}{P_o N_{ref}}\right) \qquad \text{Equation 2-19}$$

Where

$\varepsilon_{1,\,p}$ = Accumulated permanent after N_{ref},

N_{ref} = Any given number of load cycles greater than 100,

L = Length of stress path,

p_o = A reference stress,

$(q/p)_{max}$ = Maximum shear stress ratio, and

a and b = Regression parameters.

The correlation between the permanent and resilient deformation of granular soil was investigated by Veverka (1979), (Lekarp and Dawson, 1998). The model was illustrated in Equation 2-20. The only disadvantage of this model is that it was not confirmed by other researchers.

$$\varepsilon_{1_p} = a * \varepsilon_r * N^b \quad \text{Equation 2-20}$$

Where

ε_r = Resilient strain.

Also, Khedr (1985) investigated the effect of a number of load cycles on the permanent deformation for crushed lime. It was stated that the permanent strain decreases logarithmically with increasing the load cycles; the model is expressed as Equation 2-21.

$$\varepsilon_p = A * N * N^{-m} \quad \text{Equation 2-21}$$

m = Material parameter.

Several permanent deformation models were assessed by (Ahmed and Erlingsson, 2013). The beginning was with Tseng and Lytton (1981) model in Equation 2-22.

$$\delta_a(N) = \beta_1(\frac{\epsilon_0}{\varepsilon_r})e^{-\left(\frac{\sigma}{N}\right)^{\beta}}\varepsilon_v h \quad \text{Equation 2-22}$$

Where

$\delta_a(N)$ = Permanent deformation (in),

β_1 = The laboratory to field correlation factor,

ε_0, β and ρ = The material parameters,

ε_v = Vertical resilient strain (in/in),

h = Thickness of layer,

logβ= - 0.61119 - 0.017638Wc,

logρ= 0.622685 0.541524Wc, and

Wc= Water content = $(M_R/2555)^{1/0.64}$.

Also, Gidel et al. (2001) developed a model to obtain the permanent deformation under the maximum stress and the maximum mean stress using the multi-stage triaxial test. In addition, the number of cycles and the stress level was taken into the account as well as the display in Equation 2-23.

$$\varepsilon_p(N) = \beta_1(1 - (\frac{N}{N_0})^{-B}) \left(\frac{L_{max}}{P_a}\right)^n (m + \frac{s}{p_{max}} - \frac{q_{max}}{p_{max}})^{-1} \quad \text{Equation 2-23}$$

Where

N_0 = The reference number of load, and

L_{max}, n, B, m, s and ε^0 = Materials parameters.

Then, Korkiala-Tanttu (2005) developed a model in which relationships between the stress point and the deviator stress ratio. The model is described in Equation 2-24. According to this model, the development of permanent deformation is directly related to the distance from the

stress point to the Mohr-Coulomb failure line expressed in q−p space and it also relates the effect of stress on the permanent deformation through a hyperbolic function.

$$\varepsilon_p(N) = \beta_1 C N^b \frac{R}{A-R} \qquad \text{Equation 2-24}$$

Where

β_1 = The laboratory to field correlation factor,

C and b = Materials parameters,

A = Independent factor of the materials (A=1.05), and

$R = \frac{q_{max}}{q_f}$ = The deviator stress ratio.

The permanent deformation in the subgrade layer was obtained by Equation 2-25. Erlingsson (2012) developed (Tseng and Lytton, 1981) model. The contribution of the model was to estimate the permanent deformation in the top part of the subgrade which was divided into 10 sublayers and each layer is 20 cm. In (Erlingsson, 2012) model, it added integrating $ae^{-kz_{end}}$ to obtain the deformation in the lower part of the subgrade.

$$\delta_{sg} = (\frac{\varepsilon_{v1}}{k})(1 - e^{-kz_{end}})\varepsilon_0 e^{-(\sigma/N)^\beta} \qquad \text{Equation 2-25}$$

Where

δ_{sg} = Permanent deformation in the lower part of subgrade,

ε_0 = Materials constant,

ε_{v1} and ε_{v2} = The vertical strain at the surface of subgrade, and

Z = The required depth of the subgrade.

Cerni et al. (2012) considered post-compaction in his model. The model includes two parts, the first part demonstrates the relation with the cycles load number, and the second part is obtaining the strain that was generated by the post-compaction. The results of the model shown that the permanent deformation increased with an increase the numbers of loading cycles but decrease with the post compaction.

$$\varepsilon_p(N) = A + B * N - C * e^{-DN} \quad \text{Equation 2-26}$$

Where

A, B, C and D = Regression parameters.

The model in Equation 2-27 was proposed by (Chow et al., 2014). Laboratory experimental results of repeated load tests on four aggregates (two granitic particles and basalt and limestone) were used to propose a model. The model includes two factors stress level and shear stress.

$$\varepsilon_P(N) = AN^B\sigma_d^C\left(\frac{\tau_f}{\tau_{max}}\right)^D \quad \text{Equation 2-27}$$

$\tau_{max} = c + \sigma_f tan\emptyset$ = Shear strength, and

τ_f = Applied shear stress.

2.3.3 Durability of Pavement Layers

As previously mentioned, there are several factors which affect the resilient modulus. To evaluate the resilient modulus, the following factors are required to consider the stress level, density, water content and freezing-thawing cycles. The first three factors were explained in section 2.3.1. While the freezing-thawing cycles are described in this section. The current tests procedures for different materials were also summarized in Table 2-8.

The pavement is subjected to water variation and traffic loading, subjected to the freezing and thawing as well. During the winter, the resilient modulus of unbound materials shows the highest value and smallest in spring. The ice bonding between particles in base, subbase and subgrade layers increased due to an increase in the resilient modulus. In contrast, the thawing in the spring season is due to the saturated case. Therefore, the resilient modulus decreased as explained in section 2.3.1.

The effect of freezing-thawing cycles on the resilient modulus of class C fly ash stabilized limestone aggregate was investigated by (Khoury et al., 2010). The freezing-thawing cycles were considered from -25 Co for 24hr and 21.7 Co for 24hr with a relative humidity of 90%. The samples also were subjected to 28days of curing and 30cycles of F-T shows that the resilient modulus reduces when compared with 90 days of cured samples. The temperature affected the reaction of the pozzolanic fly ash. Also, during the thawing phase, the voids between the particles were filled with the water.

Simonsen and Isacsson (1999) carried out resilient modulus tests after freezing-thawing cycles. The cycles were conducted on both coarse and fine-grained subgrade soils. The sample was kept at -10o C then up to room temperature. It was observed that the resilient

modulus decreases to about 60% of clay soils and 25% of coarse gravelly sand. Also, the observations include increasing in volume after freezing-thawing cycles and losing the structure of the sample. Similar results were reported by (Gupta, 2014). The resilient modulus of soil decreased after freezing, and the water content increased due to thawing.

The comparison of resilient modulus between sand and clay soil in wetting and drying were investigated by (Khoury and Zaman, 2004). The sand was compacted at -4% of the optimum water content then wetted to about +4% of OMC, the resilient modulus was reduced by 60%. The results show that the resilient modulus improved to 200% when the samples were compacted at the optimum water content. While the resilient modulus increase by 80% when the samples were compacted at -4% of the optimum water content. The same behaviour of resilient modulus was reported by (Kim and Kim, 2007). AASHTO T307 test was carried out on sand-silty-clay and silty-clay. The samples were compacted at ±2% of the OMC. The results indicated that the resilient modulus increased with a reduction in the water content.

Multistage repeated triaxial tests were conducted according to the CEN on three materials by (Uthus et al., 2006) to determine the resilient and the permanent deformation. The test was conducted at different water content and a constant confining pressure of 150kPa and different deviator stress level. The results shown that the resilient modulus of the three materials was significantly affected by water content at the same deviator stress level. Also, the permanent deformation increased after the increase in water content as mentioned in section 2.3.2. During the thawing, the water content increased due to the permanent deformation increases. On the other hand, the resilient modulus increased when the water content decreases.

It can be concluded that the resilient modulus test is more suitable to measure after freezing-thawing cycles; the resilient modulus test is appropriate to simulate the field condition better than the unconfined compressive strength test as shown in Table 2-9.

Table 2-8 Summary of Laboratory Procedures for freezing-thawing durability test

Reference	Materials	Procedure		
ASTM D560	Soil cement	Freezing at constant temperature not warmer than (−23C°) for 24 h; then thawing at (21C°) for 23 h; brush the specimen with a wire scratch brush; after being brushed, specimens shall be subjected to another FT cycle; apply up to only 12 cycles	Soil-cement loss, moisture changes; and volume changes	Kalankamary and Donald（1963) reported that evaluating the durability based on the weight loss is overly severe and does not simulate the field conditions.
ASTM C666	Concrete	One cycle consists of lowering the temperature of the specimens from 5 C°F to -18C° and raising it from -18 to 5C° in not less than 2 nor more than 5 h; apply 300 cycles	Resonant frequency of the samples is measured to a relation of this frequency to elastic modulus is used to determine FT durability	Not applicable
ASTM C671	Concrete	Test cycle consists of cooling the specimens in silicone oil or water saturated kerosene from 2 C° to 10C° at a rate of -15C°/h followed by immediate return of specimens to the water bath (2C°), where they shall remain until the next cycles; one test cycle lasts for 2 weeks	Specimen length changes per unit length and the cooling temperatures during the cooling cycle	Not applicable
ASTM C593	Fly ash and other pozzolan	Specimens are tested for FT cycles by means of the vacuum saturation strength testing procedure; five and 10 cycles are used	Unconfined compressive strength	Not applicable
Iowa FT test	Soil cement	Wetted specimens (24) h subjected to gradient temperature; freezing the specimen from the top (7C°), water provided from the bottom at 2C°; 10 cycles	Unconfined compressive strength	To simulate temperature gradient as occurs in the field

Table 2-9 Summary of Relevant Studies

Reference	Materials	Procedure	Parameter	Results	Comments
Berg (1998)	CFA aggregate for road bases	(1) ASTM D593 (2) Sealed cured specimens for 5 days in a plastic bag, soaked specimens for 2 days; and then subject them to FT cycles. FT consists of placing specimens in a freezer at 0°F for 3 days, then in a plastic bag at room temperature for 4 days; specimens were subjected to 16 cycles (3) Curing specimens for 7 days, freeze specimens for 3 days (same temperature), then immersing specimens in water for 4 days; repeated until 50% loss of weight	UCS Weight loss without brushing the specimen Weight loss	Not applicable	Not applicable
Zaman et al. (1999)	CKD stabilized aggregates	Placing cured specimens in a freezer not warmer than −15°C for 24 h and then placing it in a cabinet having a temperature of 71°F with Rh greater than 95% for 24 h	M_R	(1) FT cycles have remarkable adverse effects on the resilient modulus of CKD-stabilized specimens; (2) MR decrease 65%, 67.5%, and 54% due to 4, 8, and 12 cycles, respectively; and (3) layer coefficient dropped significantly due to FT cycles	M_R simulates better the engineering property in the field compared to UCS

Table 2-9 Summary of Relevant Studies
Continued….

Reference	Materials	Procedure	Parameter	Results	Comments
Nunan and Humphrey (1990)	Cement stabilized aggregate	7-day cured specimens were placed in a freezer at −15°F for 24 h; then in a humidity room at 70°F and a relative humidity of 90% for 23 h; (same as ASTM D560)	Percent loss	5% cement stabilized specimens had a soil-cement loss less than 14%	Not applicable
Miller et al. (1999)	Shales and sand stabilized with CKD/lime	7-day cured specimens were placed in a freezer at −9.4°F for 24 h; then in a humidity room at 70°F and a relative humidity of 90% for 24 h; (same as ASTM D560);1,3, 7, and 12 cycles	UCS	All specimens survived 12 cycles of FT actions	Use of UCS as an indicator of durability due to FT action may not be very appealing because field-loading situations are rarely unconfined; Thompson and Smith (1990) concluded that the UCS is not a good indicator of the actual strength of an in-service granular base subjected to moving vehicles
Syed et al. (2000); Barbu and Scullion (2006)	Unbound and bound aggregate bases	Tube suction test: see Syed et al. (2000); Barbu and Scullion (2006)	Dielectric Constant	Maximum permissible dielectric constant is 16 for unbound aggregate bases and 10 for stabilized aggregate bases	Not applicable

Table 2-9 Summary of Relevant Studies
Continued….

Reference	Materials	Procedure	Parameter	Results	Comments
Khoury and Zaman (2007a)	Aggregate bases stabilized with CFA; cement kiln dust and fluidized bed ash	28-day cured specimens, freezing specimens at −25°C in a FT cabinet for 24 h, and then thawing at 21.7°C for another 24 h with a relative humidity of approximately 98%. Membranes around the specimens were removed during the freezing and thawing to expose specimens to moisture changes.	M_R	MR values of stabilized specimens decreased with increasing FT cycles up to 30. Decrease in MR values varies with type of stabilizing agents. The CKD-stabilized Meridian and Richard Spur aggregates exhibited a higher reduction in MR values than the corresponding values of CFAand FBA-stabilized specimens. The CFA-stabilized Sawyer specimens performed better than their CKD- and FBA-stabilized counterparts.	MR simulates better the engineering property in the field compared to UCS
Guthrie et al. (2008)	Aggregate base stabilized with CFA	ASTM D560; ASTM C593; tube suction	UCS	(1) CFA specimens exhibited an increase in UCS values; (2) ASTM C593 is more severe than ASTM D560; cement-treated specimens had lower dielectric values than the others; (3) Strength and durability depend upon material type, stabilizer type, and stabilizer concentration.	Use of UCS as an indicator of durability due to FT action may not be very appealing because field-loading situations are rarely unconfined; Thompson and Smith (1990) concluded that the UCS is not a good indicator of the actual strength of an in-service granular base subjected to moving vehicles

2.3.4 Discussion

Among the many factors affecting the flexible pavement, resilient modulus, permanent deformation, and environmental conditions are described in (NCHRP, 2004). The effect of deviator stress, confining pressure, density, water content, grading fines content aggregate types, methods of compaction and environmental conditions on resilient modulus and permanent deformation were discussed in this section.

The literature review showed that the deviator cyclic stress depends on the confining pressure. Increase the confining pressure due to increase the resilient modulus and decrease the permanent deformation. Also, the density has a significant effect on both resilient modulus and permeant deformation. The maximum dry density of sandy soil was obtained by the vibration compaction method. The density of granular soil increases strength and stiffness. The number of load cycles is causing an increase in the resilient modulus and permeant deformation of granular soils. This can due to the post-compaction of the soil.

The durability of the pavement layer was also reviewed to demonstrate the effect of environmental conditions on the pavement layers. There are two durability tests, wetting-drying and freezing-thawing durability tests. Previous researcher (Khoury and Brooks, 2010) showed that the resilient modulus decreases during the spring season but increase during the winter season. The ice bonding between particles in base, subbase and subgrade layers increased due to an increase in the resilient modulus. While the thawing in spring season was due to saturated case. Therefore, the resilient modulus decreased.

In Table 2-8, different durability tests were described for the construction materials. Only ASTM D560 and ASTM C593 were established for stabilized soils. However, these

procedures are 10 or 12 cycles that simulate 10 or 12years. While (NCHRP, 2004, AASHTO, 1993) recommended 20yearsor more as design life. Finally, the experimental investigation should take these parameters into the account.

2.4 Reinforced and Stabilized of Sand

2.4.1 Synthetic Fibre

2.4.1.1 Polypropylene (PP) Fibres

The polypropylene fibre is a common fibre used in reinforced sand as illustrated in Figure 2.3. The effect of incorporating fibre in properties of sand is discussed in this chapter. In addition to that, it also includes a discussion of parameters required for the design of pavement structures. This section of the literature review shows the available experimental work on fibre reinforced sand.

Shear Strength

AI-Refeai (1991) investigated the behaviour of two different sand using a series of triaxial tests. The study investigated the effect of the fibre length and content, particles size and shape on both strength and stiffness. Fine dune sand with subrounded particles and medium sand with subangular particles were used together with three fibre types as shown in Table 2-10.

Table 2-10 Types of fibre used by (AI-Refeai, 1991).

Fibre	Length, mm
Fibrillated	25and 50
Pulp	12
Glass Fibre	10, 25, 50, 75 and 100

It was concluded that reinforced sands showed significant improvement in the load capacity. The short fibres required a higher confining pressure to prevent the bond failure whatever the size and shape of sand particles. Moreover, the particles interlock was also improved by incorporating the fibre with subrounded particles rather than subangular particles. The fibre content was determined by the triaxial test results which were 0.5% of the dry weight of soil. It was observed that the internal friction angle was significantly affected by the shape of the particles. The shear strength of fibre reinforced sand experiencing bond failure was characterized by an apparent friction angle that was greater than that of unreinforced specimens

Consoli et al. (2007a) investigated the behaviour of fibre reinforced sand using a series of ring shear tests at large shear strain with different fibre length, fibre content. The used polypropylene fibre lengths were 6, 12 and 24mm length and 0.023mm in diameter. The samples were prepared at a relative density of 50% and 0.71 void ratios. It was found that there was a significant improvement in shear strength as shown in Figure 2.7. The strength increased with longer fibre without any reduction in the strength with large displacement. This was because the fibres elongated before some of the fibre was broken. This was noted for the 24mm fibre length. Moreover, the shear displacement was bigger with the short fibre due to the fact that fibre was elongated before broken at the failure strain. Also, higher density increases the ultimate shear strength.

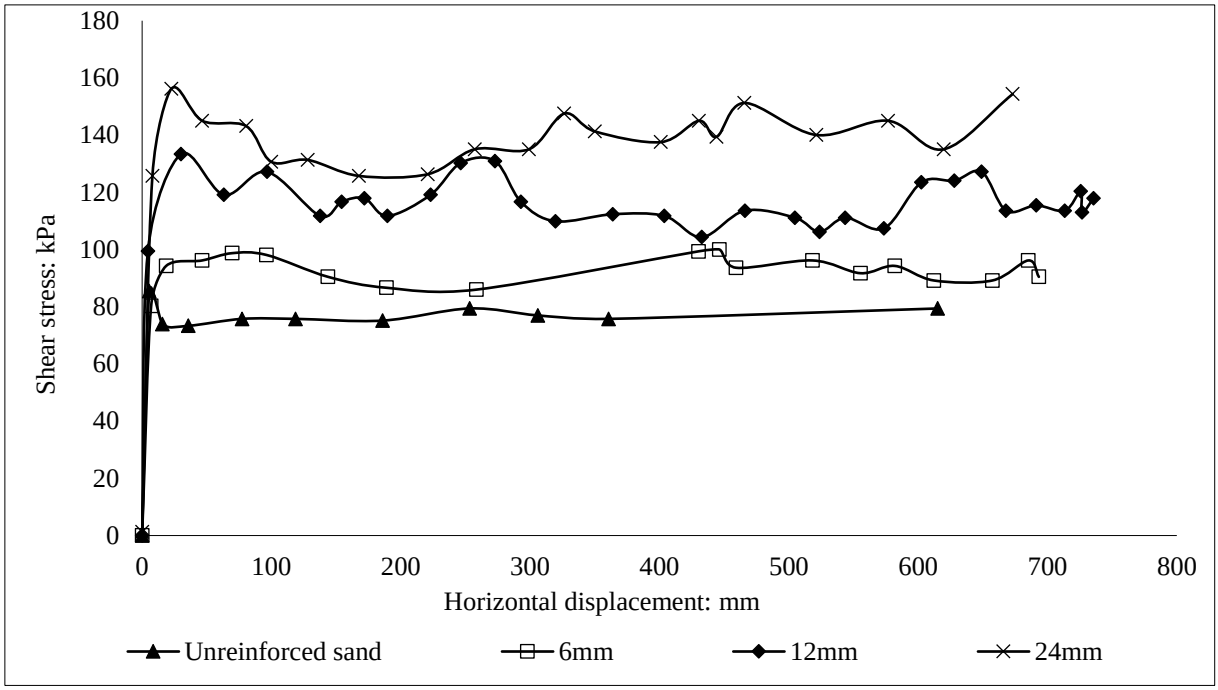

Figure 2.7 Comparison of shear stress between unreinforced and reinforced sand with different fibre lengths for relative density of 50% and normal stress of 200kPa (after (Consoli et al., 2007a))

Diambra et al. (2010) conducted the conventional drained triaxial compression and extension tests for reinforced sand with 35mm polypropylene fibre length. The test was conducted using 0.3, 0.6 and 0.9% fibre content investigate the mechanical behaviour of fibre reinforced sand. The fibre content was obtained based on the void ratio. It was suggested that the fibre should be considered as part of the solid sand particles. Therefore, the fibre content was 0.9% of the dry weight of soil and this was because the maximum void ratio of the sand was 0.99%.

A similar trend was observed by (AI-Refeai, 1991, Al-Refeai and Al-Suhaibani, 1998, Consoli et al., 2007a) whereas (Diambra et al., 2010) shows the increase of the internal friction angle and shear strength. The fibre diameter and the voids ration affected the shear strength as shown in Figure 2.8. Table 2-11 described the properties of sand and the fibre. It

was observed that the fibre diameter should be less than the particles size to improve the interaction between the particles.

Table 2-11 Sand and fibre properties used by (AI-Refeai, 1991, Al-Refeai and Al-Suhaibani, 1998, Consoli et al., 2007a, Diambra et al., 2010)

Reference	D50	Maximum void ratio	Fibre diameter, mm	Fibre length, mm
(AI-Refeai, 1991)	0.18	0.78	0.4, 0.1	25
(Al-Refeai and Al-Suhaibani, 1998)	0.3	--	0.4, 0.43	50,25
(Consoli et al., 2007a)	0.16	0.85	0.023	6, 12, 24
(Diambra et al., 2010)	0.32	0.84	0.1	35

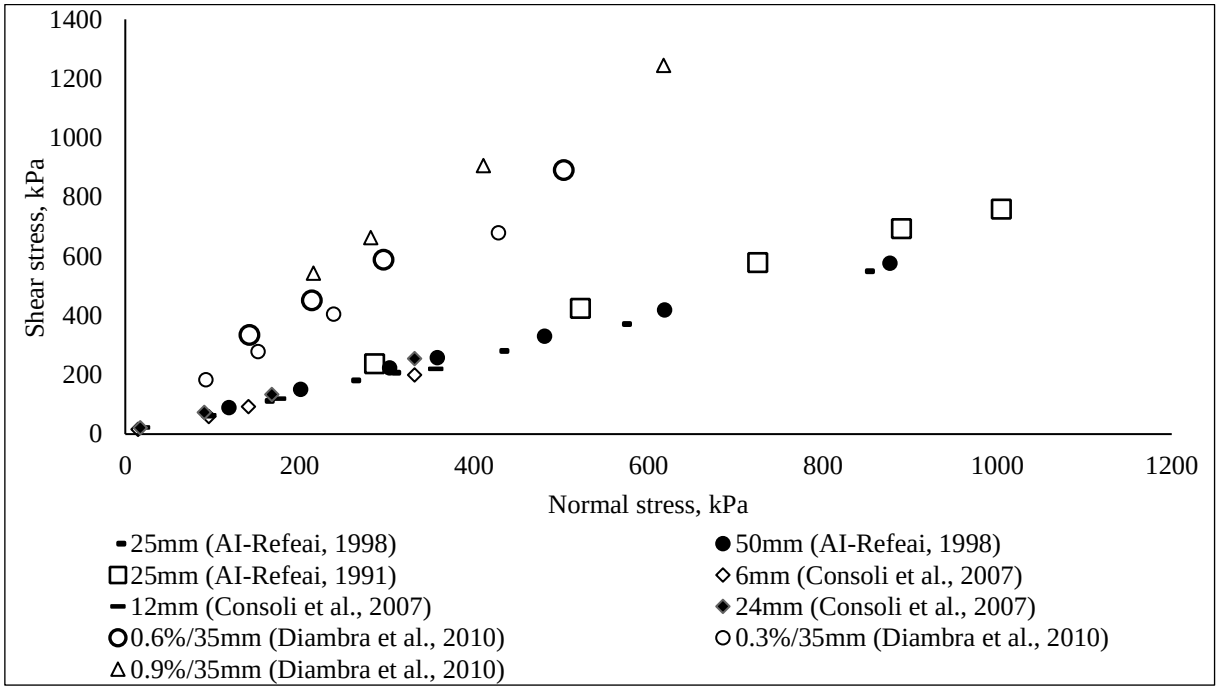

Figure 2.8 The comparison of triaxial test results for fibre reinforced sand (after (AI-Refeai, 1991, Al-Refeai and Al-Suhaibani, 1998, Consoli et al., 2007a))

Unconfined Compressive Strength

This part discusses few studies which were conducted to determine the unconfined compressive strength for reinforced sand with polypropylene fibre. Girija (2013) conducted unconfined compressive tests on unreinforced and reinforced specimens using fibre length of 15mm and content varying from 0 to 0.7% of the dry weight of soil. The results showed that the optimum fibre content was 0.6% of the dry weight of soil and, the corresponding failure strain of fibre reinforced sand was higher than that for un-reinforced soil. Also, it was observed that the fibre reinforced sand improved the strength by 2.5% of the unreinforced sand.

Santoni et al. (2001) carried out an unconfined compressive test for six different sand types, four fibre types, five fibre lengths, and different fibre content. From the research, the available data was only for silty sand reinforced with fibrillated and monofilament fibre at 0.6 and 1% fibre contents respectively and 51mm long fibre.

Santoni and Webster (2001) also conducted the unconfined compressive strength test on poorly graded sand reinforced with 50mm long fibre. The purpose of the research was to determine the optimum fibre content and the benefits of the fibre in airfield and road construction. The samples were compacted at optimum water content and 1% fibre content.

In the conclusion of the findings of the above researchers (Santoni et al., 2001, Girija, 2013, Santoni and Webster, 2001), the results were replotted in Figure 2.9. The optimum fibre content was 0.6% of the dry weight of soil for different fibre lengths. The incorporation of fibre improved the unconfined compressive strength. Also, the inclusion of up to 8% of silt

does not affect the performance of the specimens while fibre also increased both the cohesion and the internal friction angle of the specimens.

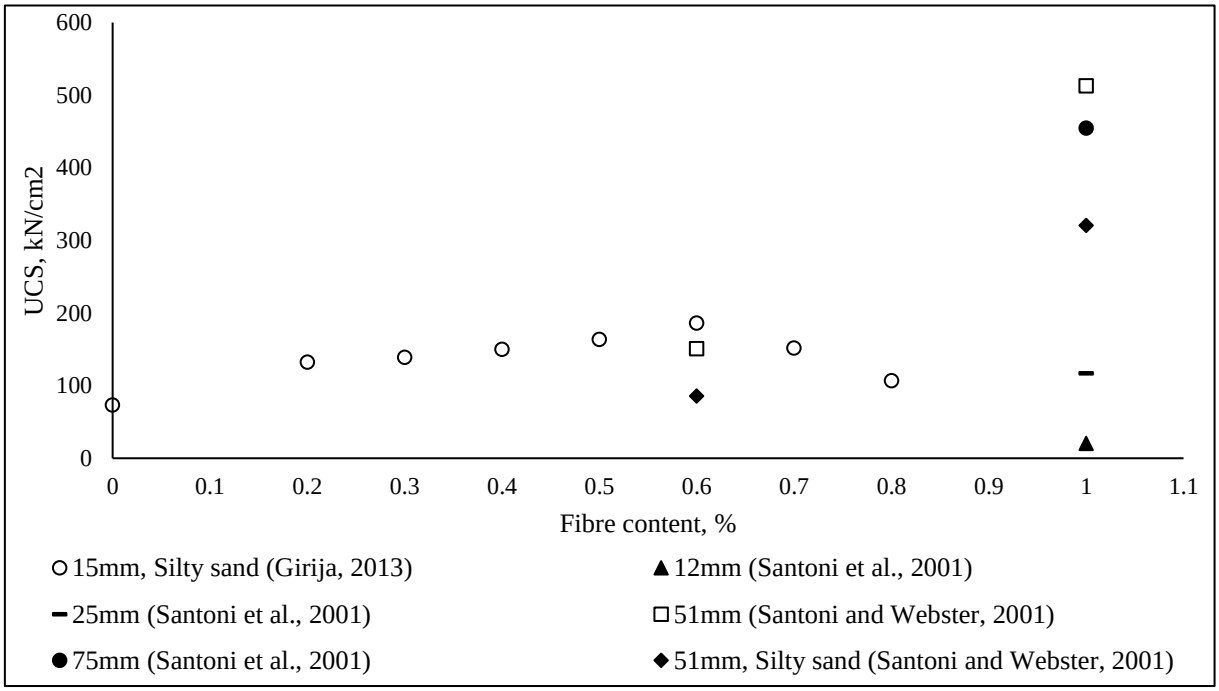

Figure 2.9 The comparison of unconfined compressive strength test results for fibre reinforced sand (after (Girija, 2013, Santoni et al., 2001, Santoni and Webster, 2001))

California Bearing Ratio (CBR)

The California bearing ratio results were plotted in Figure 2.10 for the available data. Few researches about the CBR test were conducted on reinforced sand with synthetic fibre. The fibre and sand properties which were used in (Al-Refeai and Al-Suhaibani, 1998) investigation that described earlier section. The test was carried out for different fibre contents. It was observed that the fibre content of 0.6 to 0.8% of the dry weight of soil behaved like strain hardening materials. The fibre contents of 0.2 to 0.4% of the dry weight of soil showed a slight increase in stress.

The improvement of load penetration was marked by reinforced sand with fibre. Tiwari and Sharma (2013) conducted the CBR test on fibre reinforced/unreinforced sand under soaked and unsoaked condition. The sand was classified as fine sand and the fibre lengths 30mm. A significant improvement of the CBR was obtained due to reinforced sand with fibre at the fibre content of 0.6 to 1% of the dry weight of soil. Moreover, the fibre showed a stiffer response against the penetration. This results increased the potential of using the fibre for subgrade, subbase, and base layer under heavy loads.

Generally, the CBR value at 2.5 mm penetration was higher than at 5 mm penetration. The results of both researches showed that the CBR at 5 mm penetration was higher than that at 2.5 mm penetration. The results indicated that the fibre helped to increase the resistance to penetration. The improvement of strength of reinforced sand with fibre could be explained by the increase in the tensile strength with reinforcement of the sand with the fibre. On the other hand, the unreinforced specimen was characterized by strain-softening behaviour while strain hardening was recorded for the reinforced sand.

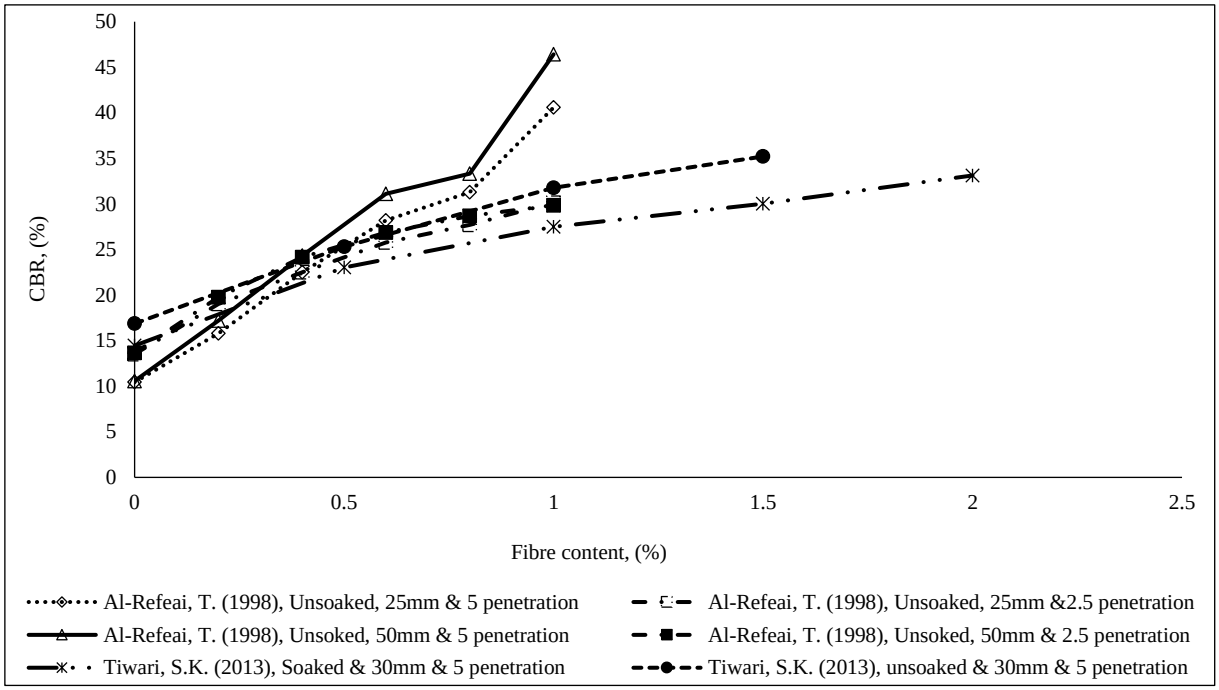

Figure 2.10 The compression of the CBR results fibre reinforced sand (after (Al-Refeai and Al-Suhaibani, 1998, Tiwari and Sharma, 2013))

Resilient Modulus

(Al-Refeai and Al-Suhaibani, 1998) was the only available researcher who investigated the resilient modulus of fibre reinforced sand. Al-Refeai and Al-Suhaibani (1998) investigated the effect of reinforced dune sands reinforced with polypropylene on resilient modulus. Two fibre lengths were used which are; 25mm and 50mm long and the effect of fibre reinforced sand was determined by the resilient modulus parameters to understand the resilient modulus results, the researcher used the Equation 2-28.

$$M_R = K_1 (\sigma_d)^{K2} (\sigma_3)^{K3}$$ Equation 2-28

Where

K_1, K_2 and K_3 are the model parameters (regression constants) which depend on soil type and the physical state of the soil.

The parameters values shown that the fibre reinforced sand decreased effect of the deviator stress and confining stresses on the resilient modulus. Also, the permanent deformation of reinforced sand with fibre decreased as shown in Figure 2.11.

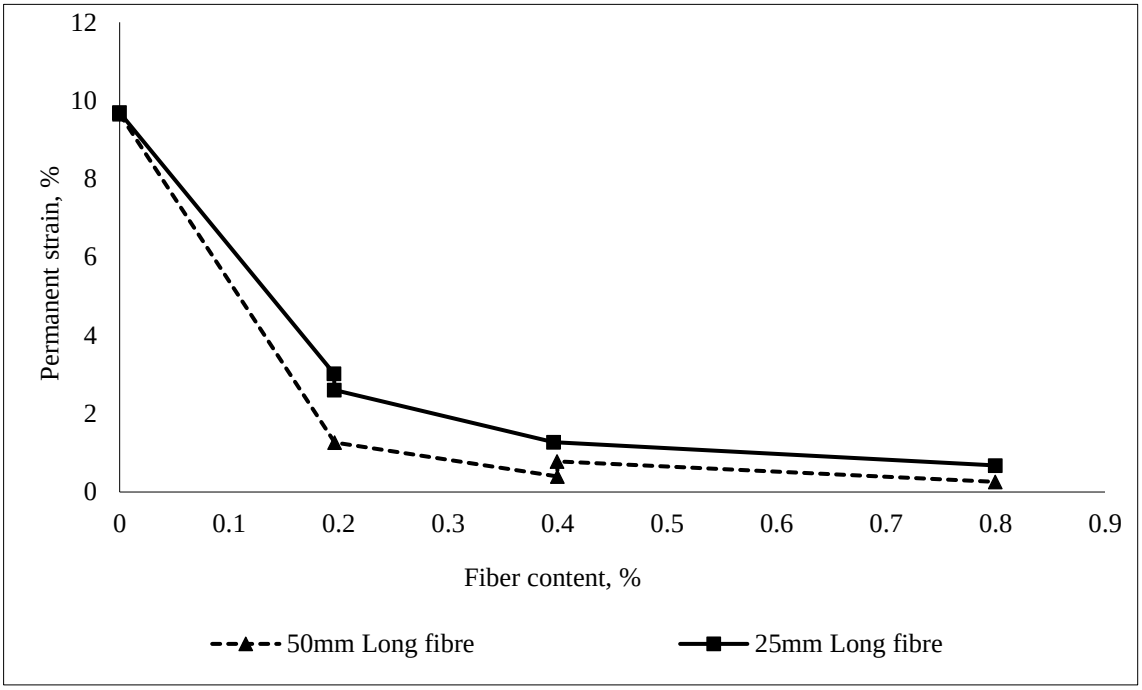

Figure 2.11 Influence of fibre content on permanent strain.

Mechanism of Fibre Reinforced Sand

Interfacial properties of fibre reinforced soil were examined by (Tang et al., 2010) using shear direct test and pull out test. The stiffness and vertical effective stress had a significant effect on the pull-out behaviour. Figure 2.12 illustrates the mechanism of interlocking.

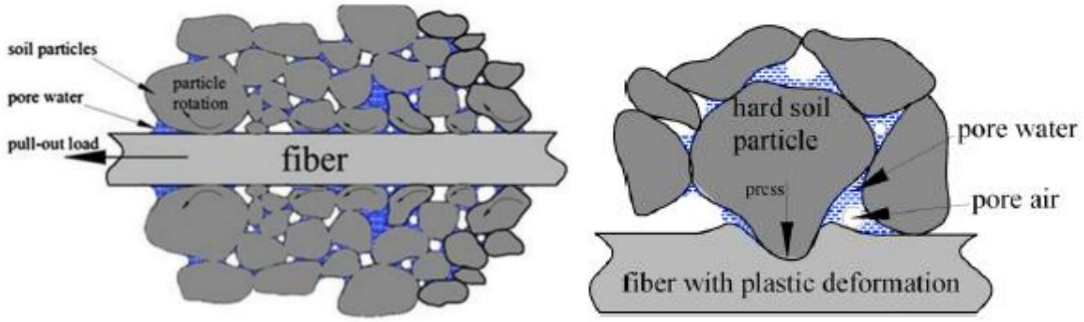

Figure 2.12 The schematic of fibre and soil interaction (after (Tingle et al., 2002)).

The mechanism of fibre reinforced sand was explained by (Yang Yunhua and Shengguo, 2008). The fibre distribution in soil was explained as bending and interleaving mechanism as shown in Figure 2.13. During the loading, the fibre is in tension, therefore in the soil, both friction and pressure will be produced by the curved fibre. On the other hand, when the fibre reinforced soil is loaded, the interleaved fibre in the soil develop tensile stresses and retrace movement in all directions of the interleaving mechanism as shown in Figure 2.13.

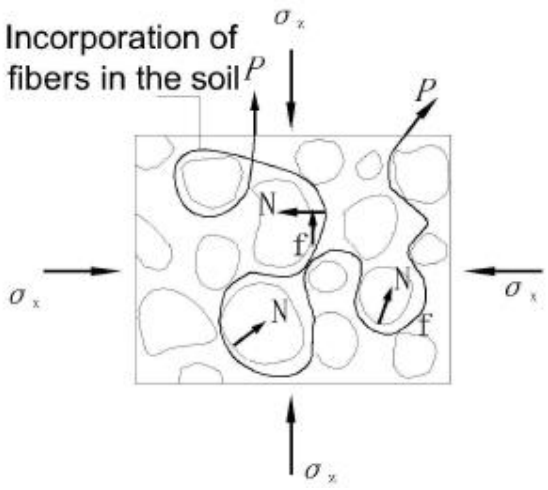

Figure 2.13 The mechanism of fibre reinforced sand (after (Yang Yunhua and Shengguo, 2008)).

The mechanism of fibre reinforced sand was also interpreted by (Tiwari and Sharma, 2013) as shown in Figure 2.14. When the load is applied, particle C is pushed between particles A and

B. The fibre than will prevent the particle movement unless it fails, or the particle entry between the other particles A and B. The resistance to movement (provided by the fibre) results in an increase in strength.

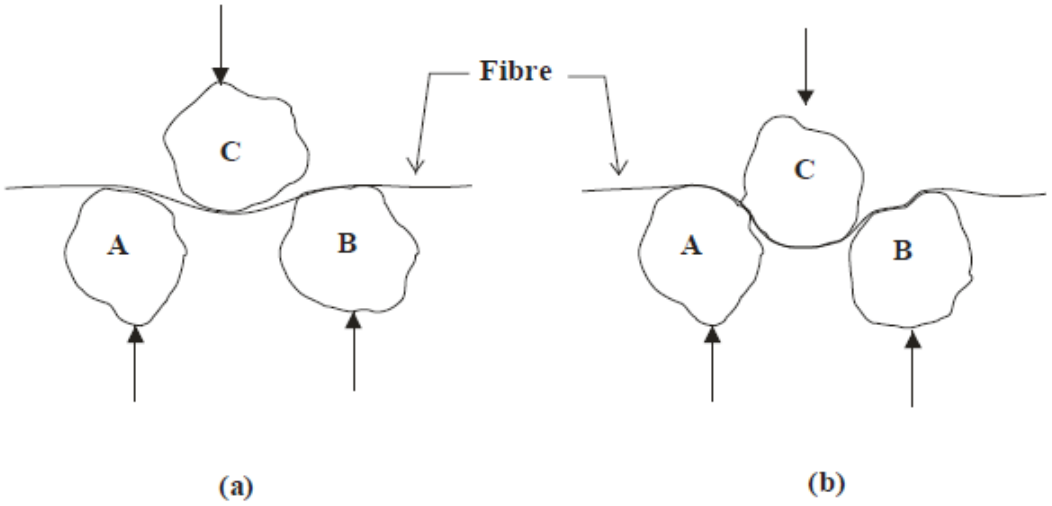

Figure 2.14 diagram of fibres position with soil particles; (a) before loading, (b) after loading (after (Tiwari and Sharma, 2013)).

Also, the compaction procedures are still under investigation for fibre reinforced sand. Table 2-12 summarizes the different compactions which have been applied. The properties for both sand and fibres used throughout the previous investigations are summarized in Table 2-5.

Table 2-12 Summary of maximum dry density and method of compaction

Reference	MDD, (kN/m^3)	Compaction test	No. of layers	Specification of Mould	
				Mould dimension, (mm)	Type of mould used
Al-Refeai, T. (1998)	18.9	AASHTO T99	3	152*177	
Anagnostopoulos, C.A. (2013)	16.6, 14.4	Modified	Nil	Nil	Nil
Chauhan, M.S. (2008)	19	Modified	Nil	Nil	Nil
Consoli, N.C. (2005)	17.5	Static	3	100*200	Split Mould
Consoli, N.C. (2003)	17.4	Static	3	50*100	Split Mould
Consoli, N.C. (2009)	16.7	Vibrating	Nil	Nil	Nil
Consoli, N.C. (2009)	16.7	Static	3	100*200	Split Mould
Consoli, N.C. (2007)	16.7	Static	3	50*100	Split Mould
Consoli, N.C. (2004)	16.7	Static	3	50*100	Split Mould
Consoli, N.C. (2012)	16.7	Vibrating	Nil	Nil	Nil
Consoli, N.C. (2009)	16.7	Static	Nil	50*100	Split Mould
Consoli, N.C. (2003)	16.7	Vibrating	Nil	Nil	Nil
dos Santos, A.P.S. (2010)	17.5	NB	3	50*100	Nil
Hamidi, A. (2013)	18.5	NB	8	100*200	Spilt Mould
Michalowski, R.L. (2003)	19.2, 17.8	Vibrating	5	Nil	Nil
Santoni, R.L. (2001)	18.86	Vibrating	Nil	Nil	Nil

2.4.2 Conventional Materials

Large quantities of materials are required for pavement construction. In the same time, the amount of waste and recycles materials have been increased every day. Athanasopoulou and Kollaros (2015) stated that conventional materials have a high potential for use in road construction. The materials can be used in other applications such as stabilized base, granular base, asphalt concrete, embankment and Portland cement concrete.

In addition, different waste including coal fly ash, coal bottom ash/boiler slag, steel slag, baghouse fines, blast furnace slag, kiln dust, foundry sand, mineral processing wastes, nonferrous slags, flue gas desulfurization, scrap tires, scrubber material, quarry by-products, reclaimed concrete material, reclaimed asphalt pavement, sewage sludge ash, municipal solid waste incinerator ash, sulfate wastes, waste glass, etc. can be used in road construction.

The soil stabilization can modify the physical and chemical soil properties and the soil stabilization can be defined as the improvement of physical properties. Therefore, the shear strength would be improved and prevent the shrink/swell, and therefore the load bearing will be able to support the pavement layers and the foundation. The stabilization is sufficient for clays to granular soils to achieve the engineering properties. The improvements of stabilization consist of improvement of the compaction, reduction of the permeability, decreasing the pavement thickness and reducing the plasticity.

2.4.2.1 Fly ash

The fly ash is produced by burning of pulverized coal in coal-fired electric power and steam generating plants. Two sizes of ash are produced: coarse – typical size range – and fine - typical size range. Fly ash has many applications and is used in construction. Therefore, the ASTM published the Fly Ash and Natural Pozzolans Standard ASTM C 618 classifying the cementitious materials including Fly Ash. Classifications of fly ash materials were shown in Table 2-13 below.

Table 2-13 The classification of fly ash materials

Materials	Classifications
Class N	Diatomaceous earths, opaline cherts and shales, tuffs and volcanic ashes or pumicites, calcined or uncalcined, and Calcined clays and shales.
Class F	pozzolanic properties
Class C	Fly ash with pozzolanic and cementitious properties

Bhardwaj and Mandal (2008), Chauhan et al. (2008) stated that the density and the water content of stabilized sand with fly ash were significantly affected. The fly ash increased the density but reduced the water content due to filling the void between the particles. On the other hand, the density decreased when incorporated the fibre with fly ash to stabilize the sand while the water content increases.

Shear Strength

Due to the difference in materials properties, in Table 2-4 represents the materials and sand properties. Therefore, the findings of various researchers were discussed below while the results were discussed at the end.

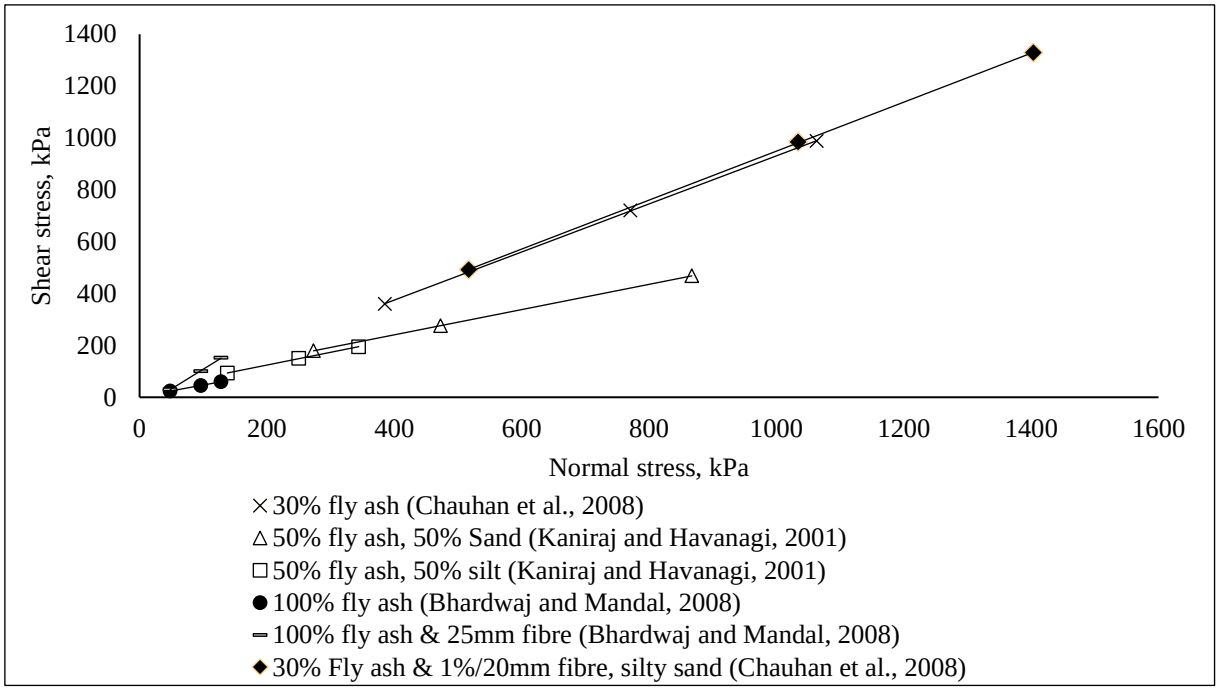

Figure 2.15 The comparison of triaxial test results for fly ash with/without fibre stabilized sand (after (Chauhan et al., 2008, Bhardwaj and Mandal, 2008, Kaniraj and Havanagi, 2001))

Bhardwaj and Mandal (2008) carried out the standard proctor compaction test on 15 % sand, 79 % silt, 6 % clay of sample, 25m fibre length and 1% fibre content. The results show that due to the mixing of fibre in the soil, the maximum dry density decreases, and optimum moisture content increases.

Chauhan et al. (2008) conducted the static triaxial test to obtain the shear strength of both stabilized sand with fly ash or fly ash with fibre. The specimens were compacted at the optimum water content and fibre content of 0.4% by dry weight of soil. The results show that, the deviator stresses of 720 kN/m^2 and 984 kN/m^2 were obtained at 25 kN/m^2 confining pressure for fly ash and fibre with fly ash reinforced sand, respectively. The results show that, the fly ash improved the shear stress at small confining pressure comparing with fibre.

Chauhan et al. (2008), Bhardwaj and Mandal (2008) findings were plotted in Figure 2.15. They showed that the soil type, the fibre length, and diameter affected the shear strength.

Table 2-4 described the properties of the fibre used in previous studies. The fibre affected the interlock between the sand particles. Thus, the fibre diameter should be close to the particles size as shown in the previous researches.

The effect of fly ash with fibre on the density was investigated by (Chore et al., 2011). Figure 2.16 shows the results of 6 and 12mm long fibres with different fly ash content of 25, 50, 65 and 75% of the dry weight of soil. The results show that the increase in the fibre content increases the water content. The density did not change much while the water content increased with the incorporation of the fibre as shown in Figure 2.16 and 2.18, respectively. The water content increased beyond 0.4% fibre content.

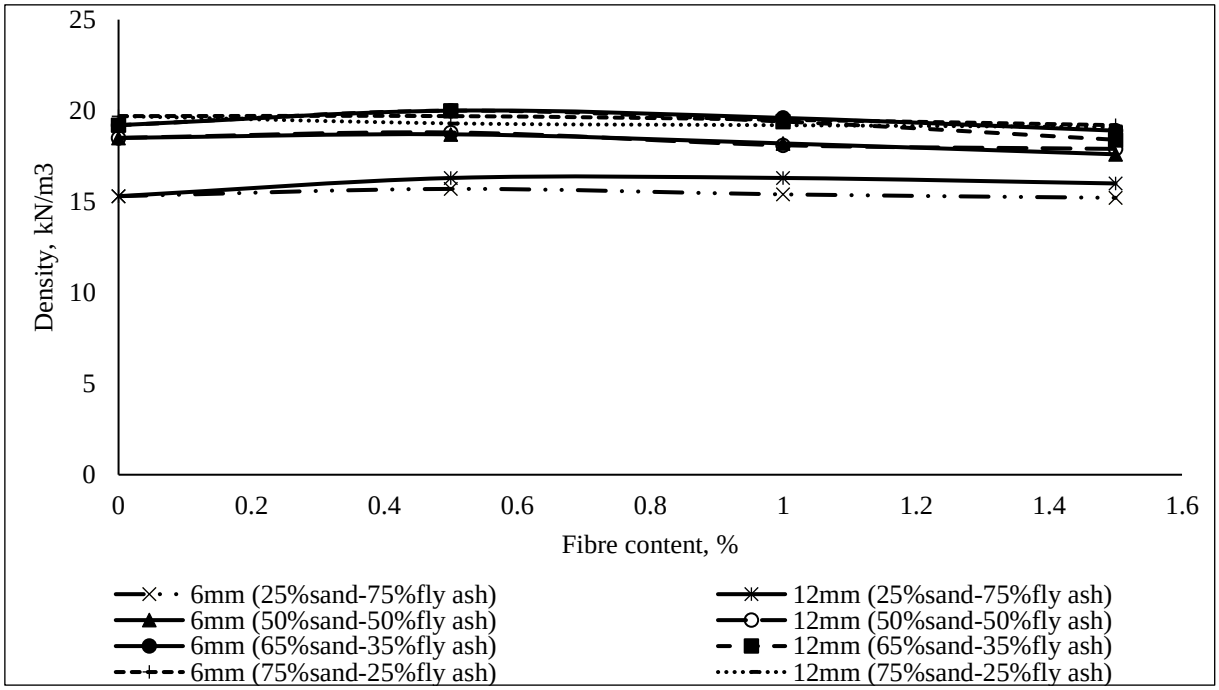

Figure 2.16 Compaction test results (after (Chore et al., 2011)).

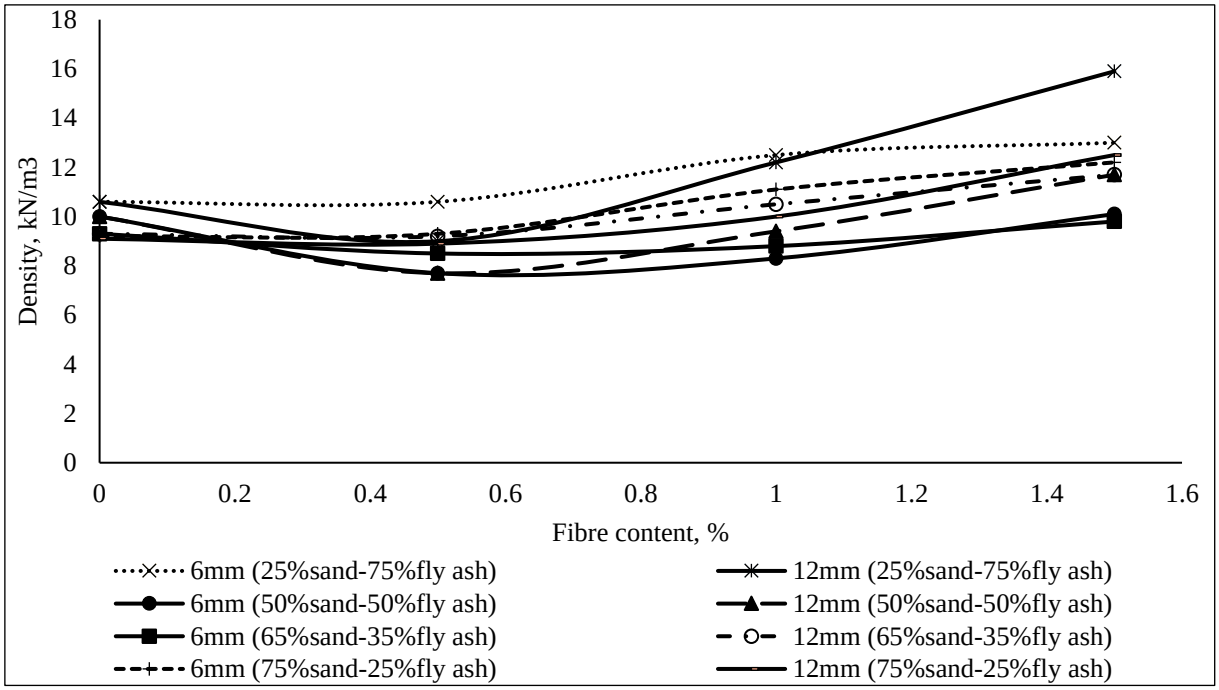

Figure 2.17 Density to fibre content relationship (after (Chore et al., 2011)).

Unconfined Compressive Strength

The unconfined compressive strength was obtained by (Bhardwaj and Mandal, 2008). It was observed that the shear strength was increased when the fibre reinforces the soil. Moreover, the fibre decreased displacement. Also, the failure of unreinforced sand usually is brittle while it becomes ductile when reinforcing it with fibre.

Chauhan et al. (2008) reported that the proportion of 30% of fly ash, 70% silty sand and 1% fibre content were optimum for both. This result was also confirmed by the unconfined compressive strength test. This proportion was near to that recommended in NCHRP 1976. If the fly ash increases the optimum moisture content increases but the maximum dry density decrease. The effect of fly ash on sand compaction was demonstrated also by (Zabielska-Adamska, 2008). The density increased with finer fly ash than the coarse one, this was

because the porosity of fly ash sample reduced due to the increase in the density while the moisture content decreases.

The effect of fibre with fly ash reinforced sand on the stress-strain relationship were investigated by (Jadhao and Nagarnaik, 2008). The fibre content of 1% of the dry weight of soil was used with 12mm long fibre. It was observed that the strength of sand stabilized with fly ash was improved as shown in Figure 2.18.

To conclude the results of (Bhardwaj and Mandal, 2008, Chauhan et al., 2008, Jadhao and P.B.Nagarnaik, 2008), the optimum fly ash content was between 30 to 40% of the dry weight of soil. The fibre length of 20mm was the best while the fibre content was 0.5% of the dry weight of soil. Also, the particles size plays the principal role to determine the fibre dimension. It is important to mention that the previous studies were conducted using only class F fly ash.

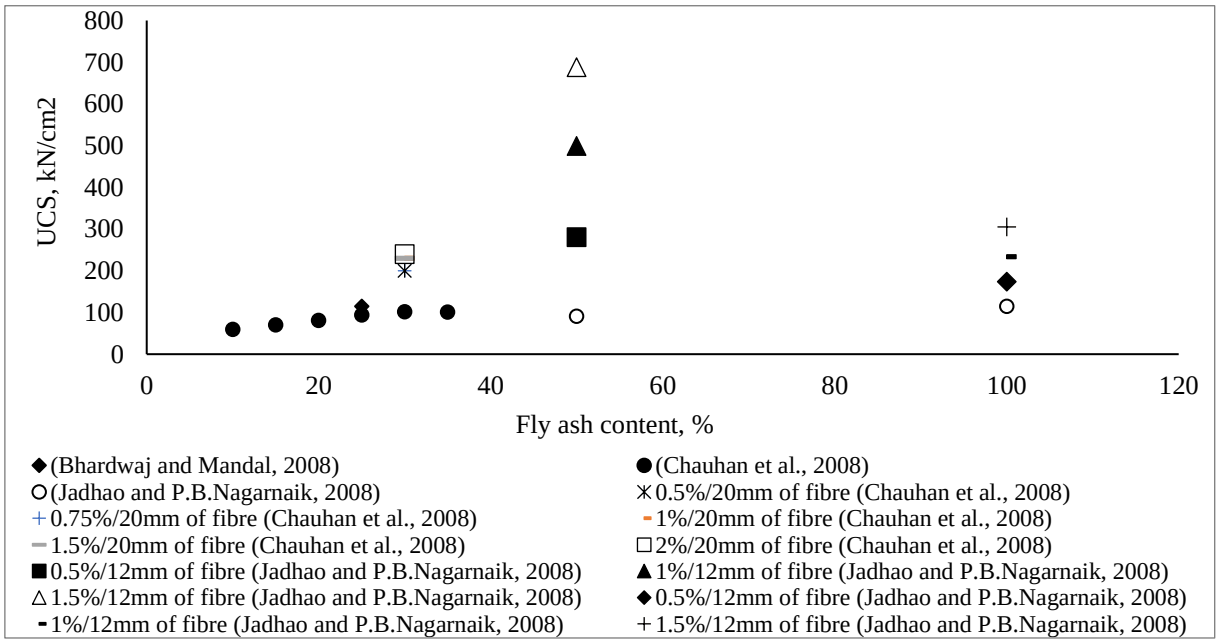

Figure 2.18 Unconfined compressive strength to fly ash content relationship (after (Bhardwaj and Mandal, 2008, Chauhan et al., 2008, Jadhao and Nagarnaik, 2008))

California Bearing Ratio (CBR)

The California Bearing Ratio (CBR) tests were carried out by (Al-Refeai and Al-Suhaibani, 1998, Jadhao and P.B.Nagarnaik, 2008, Tiwari and Sharma, 2013) on fibre reinforced sand and fly ash stabilized sand and fibre with fly ash reinforced sand, and shown in Figure 2.19 to compare the behaviour of all mixtures.

Chore et al. (2011) conducted a series of CBR tests for sandy soil and the test conditions include fibre contents of 0 to 1.5%, the fibre length of 6mm and 20mm and 25%, 50%, 65% and 75% fly ash content. The CBR value decreased when the fly ash content exceeds 25% of the dry weight soil while fibre with fly ash reinforced sand shows significant improvement. The optimum fibre content was 1% of the dry weight of soil.

The fine percent shows a significant effect on the CBR value as reported by (Jadhao and Nagarnaik, 2008). The silt was replaced by the Class F fly ash to evaluate the CBR value. The optimum fibre content was obtained at 1% of the dry weight of soil. There was no improvement in CBR value after 1% fibre content. Figure 2.19 demonstrates the CBR value for fibre and fly ash with fibre stabilized sand.

The available publications about fly ash stabilized sand are summarized in Table 2-4.

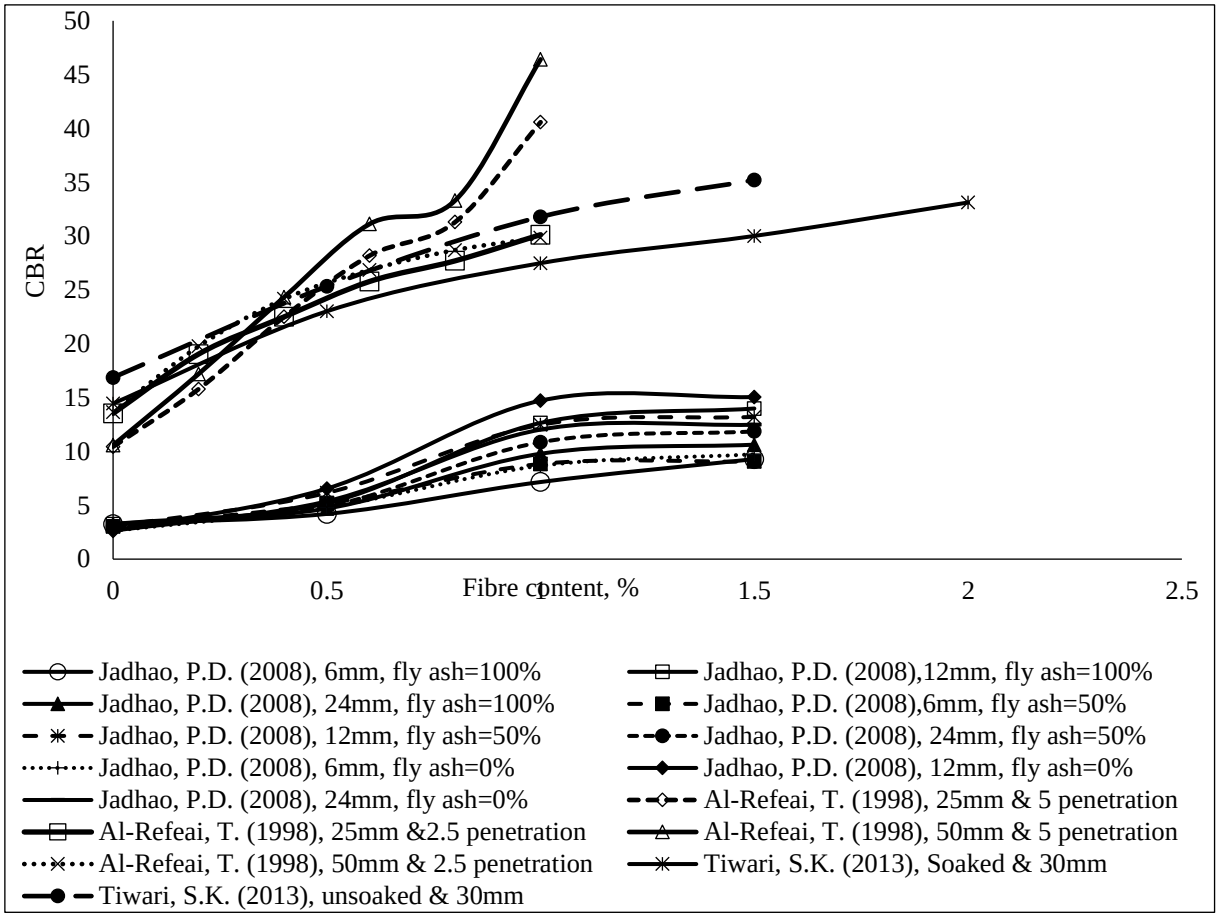

Figure 2.19 The comparison of CBR improvement between fibre and fly ash (after (Jadhao and P.B.Nagarnaik, 2008, Tiwari and Sharma, 2013, Al-Refeai and Al-Suhaibani, 1998))

2.4.2.2 Slag

The thermal plasma treatment of wastes is a common procedure which changes the mechanism of the particle (Keeley et al., 2017). Typically, it is made by heating or melting to disconnect the particles. The advantages of thermal plasma are that higher temperature, high density, non-ionising radiation, big treated amount and Low gas flow rate. The plasma is generated by different procedures which are: DC non-transferred arc plasma torches, DC transferred arc plasma torches and RF inductively coupled discharges. Table 2-14 summarizes recycles materials based on plasma generation devices. The next section includes several

waste materials. Table 2-14 summarizes wastes materials that are treated using the plasma generation devices.

Firstly, residues from waste to energy facilities are produced in incinerator bottom ash (IBA), fly ash, and/or air pollution control residues. The incinerator bottom ash consists of unburned materials and non-combustible materials. They are volatilized during burning and intensify; the residue's heavy metals are lead, cadmium, and mercury. Also, incinerator bottom ash is not considered as hazardous material while the fly ash and air pollution control residues are registered as hazardous materials according to the European Waste Catalogue. The air pollution control residues consist of the high volume of soluble/volatile salts, lead, cadmium, and mercury. Because of that, the treatment will be difficult as reported in the European Waste Catalogue.

Secondly, asbestos-containing residues are produced from the commercial factory in France. An asbestos residue is treated at high temperature in order to transfer it to solid or non-leachable. The main problem is that it leads to fatal pulmonary disease even if a low amount of asbestos fibre is in the lungs as reported by (Gomez et al., 2009). Also, in the UK, the asbestos residues are treated to solid materials at 1600^{o}C by transferred arc plasma furnace's Tetronics Limited. The treatment succeeds to transfer the asbestos to a solid solution.

Also, the healthcare wastes are getting by different resources such as hospitals, medical and dental surgeries, maternity units, nursing homes, and medical research facilities. Therefore, it could be divided into two groups which are; general wastes and hazardous wastes that need special requirement for disposal. In the Technical University of Lodz in Poland where the treatment of the fly ash in a DC thermal plasma reactor showed that the treatment was succeeding at 1550-1600^{o} C for 30 min, it was noted that the form after heating called

crystalline phase. This phase has high mechanical resistance. The bottom fly ash was also collected from the same plasma furnace and was mixed with coal fly ash. The fly ash was homogeneous and vitreous.

Moreover, wastes of steelmaking, huge quantities of sludge-containing, and dust are generated from the steel factories. These wastes are recorded as hazardous materials. It is valuable waste materials if they were recycled. The waste materials normally consist of stable oxides (calcia, silica, and alumina), volatile metals (zinc, lead, and cadmium), and oxides of iron, chromium, nickel, manganese and phosphorus. Several treatment procedures are available for vitrification into a glassy slag. It was stated that the plasma can treat all these materials.

Also, aluminium dross is registered as hazardous materials. The reason for that is become the waste materials consist of leachable chlorides and fluorides. Also, it releases gas such as methane and ammonia. The proportion of aluminium dross is about 1-5% as stated by (Gomez et al., 2009).

Finally, the common type of the other wastes treated is fibre reinforced polymeric matrix composite (FRPC) materials. It is used for aircraft, chemical tanks, and cars. At 1250^{o} C the process is due to the vitrification process. The vitrified slag is treated by further heating of glass and ceramic. The filtration of the iron and aluminium as shown that the produced material is glassy network as stated by (Gomez et al., 2009).

Table 2-14 Wastes materials based on plasma generation devices.

Reference	Plasma generation source	waste
K. Katou, T. Asou, Y. Kurauchi, R. Sameshima, Melting municipal solid waste incineration residue by plasmamelting furnace with a graphite electrode, Thin Solid Films 386 (2001) 183–188.	DC transferred arc (Takuma Co. Ltd.)	Bottom ash from municipal incinerator
H.I. Kim, D.W. Park, Characteristics of fly ash/sludge slags vitrified by thermal plasma, J. Ind. Eng. Chem. 10 (2004) 234–238.	DC non-transferred arc (experimental equipment)	Fly ash and sludge from waste water treatment
T. Inaba, M. Nagano, M. Endo, Investigation of plasma treatment for hazardous wastes such as fly ash and asbestos, Electrical Eng. Jpn. 126 (1999) 73–82.	DC non-transferred arc (experimental equipment)	Fly ash from sanitation centre, asbestos
K. Cedzynska, Z. Kolacinski, M. Izydorczyk, W. Sroczynski, Plasma vitrification ofwaste incinerator ashes, in: International Ash Utilization Symposium, Centre for Applied Energy Research, University of Kentuky, 1999.	DC transferred arc (Technical University of Lodz, Poland)	Bottom ash from hospital incinerator, fly ash from a power plant
J.P. Chu, Y.T. Chen, T. Mahalingam, C.C. Tzeng, T.W. Cheng, Plasma vitrification and re-use ofnon-combustible fiber reinforced plastic, gill net andwaste glass, J. Hazard. Mater. B148 (2006) 628–632.	DC non-transferred arc (Institute Energy Research, Taiwan)	Fibre reinforced plastic composites (FRPC), gill net, waste glass
J. Szepvolgyi, I. Mohai, J. Gubicza, I. Saray, RFThermalPlasmaSynthesis ofFerrite Nanopowders From Metallurgical Wastes, in Euro Ceramics Viii, Pts 1–3, Trans Tech Publications Ltd., Zurich-Uetikon, 2004, pp. 2359–2362.	RF plasma reactor (Tekna Plasma Systems)	Dried sludge from hot galvanising process and a converter flue dust from steelmaking
T.E. Best, C.A. Pickles, In-flight plasma reduction of electric arc furnace dust in carbon monoxide, Can. Metall. Q. 40 (2001) 61–78.	AC plasma arc furnace	Zinc oxide from electric arc furnace
K. Ramachandran, N. Kikukawa, Plasma in-flight treatment of electroplating sludge, Vacuum 59 (2000) 244–251.	DC transferred and non-transferred arc	Electroplating sludge
H. Nishikawa, M. Ibe, M. Tanaka, M. Ushio, T. Takemoto, K. Tanaka, N. Tanahashi, T. Ito, A treatment of carbonaceous wastes using thermal plasma with steam, Vacuum 73 (2004) 589–593.	DC plasma torch+RF plasma torch (experimental equipment)	Charcoal with NaCl (carbonaceous wastes)
A.L.V. Cubas, E. Carasek, N.A. Debacher, I.G. De Souza, Development of a DC-plasma torch constructed with graphite electrodes and an integrated nebulization system for decomposition of CCl4, J. Braz. Chem. Soc. 16 (2005) 531–534.	DC plasma torch with nebulisation system	Chlorine-containing wastes

As mentioned above, the vitrified slag can be produced by several procedures. It is been used in a landfill the EU. It is accepted by the reasons of low cost and low leachable and several applications can use the slag. In the road construction, the granulated slag is used for concrete aggregate and roadbed. Moreover, it can be used for interlocking blocks, tiles, and bricks. Gomez et al. (2009) stated that in Japan, they made water-permeable blocks by adding cement or gravel to the slag and the strength was acceptable. The main advantage of using slag is that the cost of raw materials compared with the original materials which are required to be imported to the site. Notwithstanding, there is a disadvantage of using slag, the production of glass-ceramics needs electricity as energy and this is not economical.

Pozzolanic such as granulated blast furnace slag was used to replace the cement (Altun and Yilmaz, 2002, Ghataora et al., 2004, Das et al., 2007, Arribas et al., 2014). The main benefit of using pozzolanic in cement paste is that improve the early strength gain (Kourti et al., 2013).

Arribas et al. (2014) tested the durability of the slag from the Electric Arc Furnace (EAF). Freezing thawing cycles consist of 4 hrs at 20^{o} C, 2 hrs heating then 4 hrs at 15^{o} C and 2 hrs cooling. The failure was obtained by the dynamic modulus and breakage of samples. The alkali reaction was used to react with the slag. The strength of slag concrete was better than the limestone concrete under the durability conditions. The reason for that is due to less loss of adhesion in the slag concrete compared with the limestone. Also, this could be caused by keeping the slag concrete in humidity and high temperature; the samples improve itself with time.

Brand and Roesler (2015) test the durability for two kinds of slag these are; Basic Oxygen Furnace (BOF) slag and Electric Arc Furnace (EAF) slag to determine the effect of freezing-

thawing cycles on strength. Also, an autoclave expansion test was conducted. It was concluded that it uses low free CaO better than the high one in the application of expansion slag in concrete. Both slags demonstrated high compressive strength, but the slag resource has affected on the strength. The slags showed 95% confidence. It can be concluded that the untreated slag can be used as unbound aggregate materials as recommended in ASTM D4792. After treating to reduce the CaO and MgO, the strength and the durability will be acceptable for certain applications. Similar recommendations were reported by (Das et al., 2007).

The potential of using steel slag for road construction was studied by (Aziz et al., 2014). It was stated that the steel slag cannot be separated under the required road testing. The slag produced higher density during the compaction test. The effect or temperature or heating were also investigated and it was found that the slag holds the heat for a longer period of time than the traditional aggregate. Therefore, there is good potential for use in hot areas like India, Italy, Malaysia, and Saudi Arabia as mentioned. The improvement of friction is caused by the self-cementation, and then the compressive strength increased. The main benefit is that the pavement thickness is less than the normal because the slag improves itself as stated by (Arribas et al., 2014). Also, research was carried out to study the potential for the use of slag in cement, base layer, and asphalt concrete. The investigation showed that the slag can be used as a granular base due to it's the mechanical properties. For the purpose of the geotechnical applications, the researcher recommended more investigation about the slag especially since the slag has the desired properties such as friction and self-cementation.

Emery (1982) reviewed used the slag using in pavement construction. It was discussed that the ferrous slags were appropriate for concrete slag and asphalt concrete. They appeared high skin resistance in asphalt concrete. One of the ferrous slags is the Air-Cooled Blast Furnace

Slag which is used as the granular base, ballast, trench fill, and backfill. This shows high CBR values and friction angle of 45^{o}. Moreover, it was sufficient to stabilize the soft soil and very durable and non-susceptible. In contrast, air-cooled blast furnace slag was not suitable with cement as reported by (Ouf, 2001). When the slag was crushed, it will be more appropriate as aggregate, and it was confirmed that the slag increases the friction angle and needs more water content due to the porosity increased.

2.4.3 Discussion

The literature review has shown that the reinforcement sand with fibre or/and mixed with fly ash improved the mechanical properties of sand (Chauhan et al., 2008). Inclusion polypropylene fibre improved the shear strength when compared with unreinforced sand. The internal friction angle also showed an increase with the fibre. Also, the effect of water content was an important factor for road construction, however, the previous studies were only conducted at the optimum water content (Anagnostopoulos et al., 2013, Consoli et al., 2005, Diambra et al., 2010). The detailed literature review showed that there are no studies on the effect of stabilization and reinforcement of sand on its durability and only studied the effect of strength sand resilient modulus (Al-Refeai and Al-Suhaibani, 1998, Bhardwaj and Mandal, 2008, Jadhao and Nagarnaik, 2008).

The fly ash improved the shear strength and the density as well as reducing the required water for the compaction (Kumar and Singh, 2008). The utilization of fly ash as cement replacement material in concrete or as an additive in cement introduced many benefits from economical, technical, and environmental points of view. However, also the literature review showed no studies were conducted on cyclic load testing as fly ash and reinforced sand with fly ash for use in pavement design.

Generally, the max dry density decreased with an increase in fly ash content, while OMC increased while the fibre improves the shear strength and interlock between the particles (Athanasopoulou and Kollaros, 2015). Therefore, this is promoting to use both materials for stabilization the sand.

Reinforced sand with fibre shows a decreasing effect of both the deviator and confining stresses on the resilient modulus. Also, the permanent deformation of reinforced sand with fibre decreased.

2.5 Summary

It is expensive to import good quality of imported materials as they may be remote from the construction site. Thus, desert sands have to be stabilized in the same manner to give the required performance for road construction. Stabilisation of sands can take many forms – importing different materials and mixing them with other sand to achieve physical stability or using chemical stabilisation agents such as cement or other binders.

The use of hydraulic binder utilizes expensive cement and requires water and likely to be a scarce commodity in the desert for hydration and thus, the costs can be high. In addition to this, hydraulically bound materials tend to be rigid and ground movements can cause cracking if the strength of the concrete or stabilized sand is not adequate.

The literature review chapter represents different pavement design procedure and their requirements. The pavement design procedures were considered in details in order to assess the sand reinforcement as subgrade layer for road construction. As the focus of this research is on subgrade soils, the properties of reinforcement and stabilization sand should meet the requirement of pavement design. The systematic review was conducted to identify the

reinforcement and stabilization materials as shown in this chapter. Also, the laboratory tests that are needed to be conducted for road construction such as static, cyclic tests and the durability test of subgrade layer soil. The available durability experimental tests are considered to assess the behaviour of resilient modulus and permanent deformation of reinforced sand for the long term. Either ASTM D560 or ASTM C593, the tests procedures measure the unconfined compressive strength, soil-cement loss, moisture content and volume changes. The pavement design parameters such as resilient modulus and permanent deformation need to be evaluated after the durability.

The vitrified slag was not investigated yet, but the chemical investigation showed high potential to use in construction application. Therefore, the pilot test was prepared to assess the slag stabilized sand. The pilot tests were prepared depending on the research time and the required parameters for pavement design.

To address this, a robust experimental plan is described in Chapter Three. The resilient modulus and permanent deformation are the main parameters in the pavement, therefore, they are described in Chapter Four and Five respectively. Also, in Chapter Seven, developed correlation models for fly ash and fibre are needed to obtain the resilient modulus by using other simpler test such unconfined compressive strength test which was provided in Chapter Five. Then, the results of resilient modulus and permanent deformation are used to obtain the pavement response and used in analytical pavement design in Chapter Seven.

CHAPTER 3 LABORATORY TESTING & MATERIALS

3.1 Introduction

Findings of the literature review described in Chapter Two were used to inform the work plan for this study as a flow chart in Figure 3.1. This included the development of a laboratory testing programme to classify sand, determine its engineering properties, and study the effect of adding fibres, fly ash, and slag. It also included the determination of parameters to enable pavement design to be undertaken.

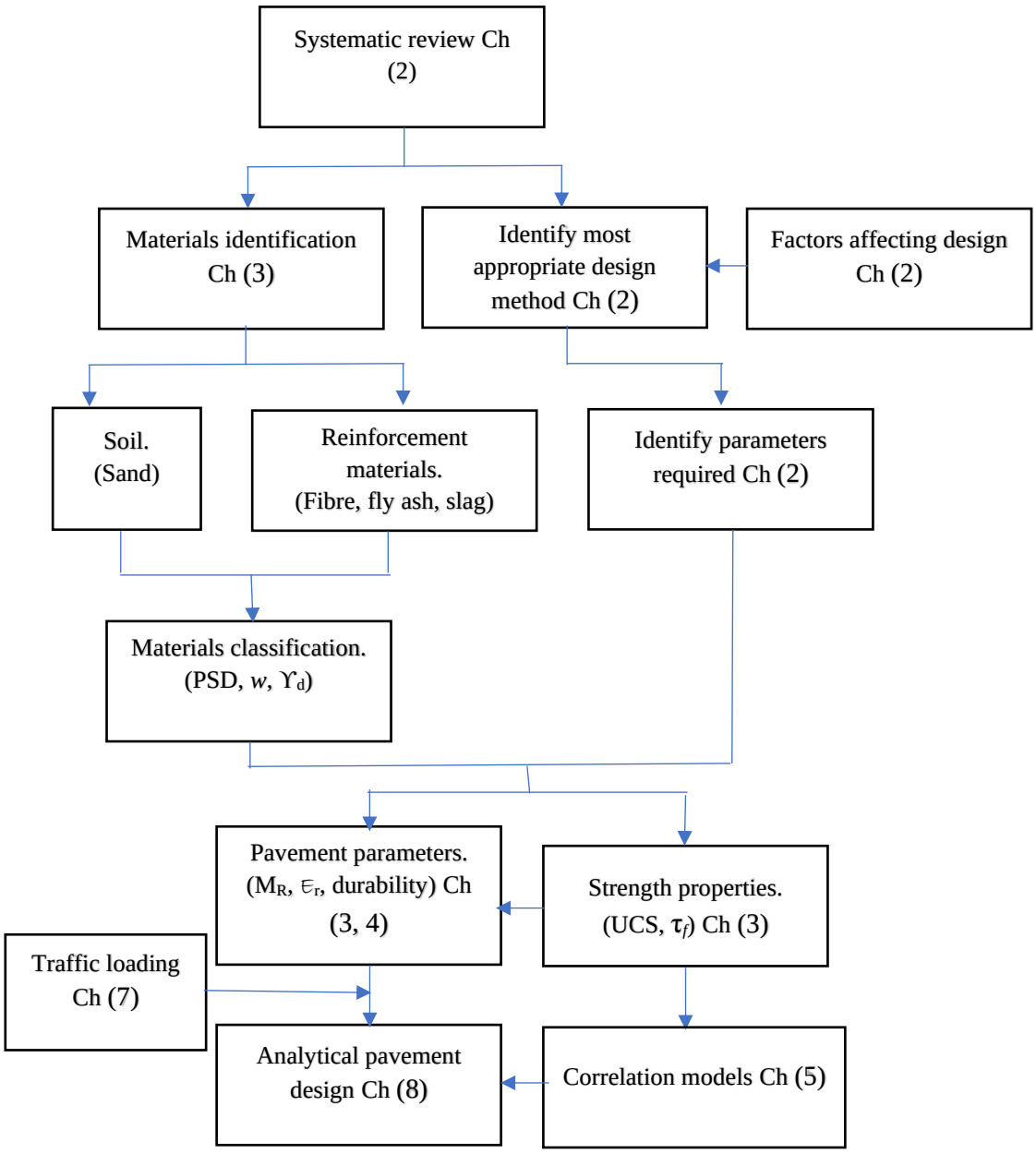

Figure 3.1 Flow chart for the research work.

3.2 Properties of Materials

3.2.1 Sand

Traditional crushed rock is extensively used in road construction and maintenance. However, much of Libya landmass is covered by sand (part of Sahara Desert), and crushed rock supply is often very remote from where it is needed for road construction. Therefore, to conserve the

limited crushed rock resources, it is important to consider the use of sand for road pavement construction.

Thus, as stated in the research aim and objectives, it was proposed to investigate the possibilities of using typical desert sand obtained from Libya for road pavement construction. However, since sand from Libya could not be imported into the UK, the typical particle size distribution of Libyan Desert sand was obtained by private communication due to a scarce in the published data and plotted in Figure 3.2. Sand, closely resembling the Libyan Desert sand was sourced from an Aggregate Industries, called Levenseat quarry in Scotland as shown in Figure 3.4. This sand is also known as LV100 and it is single size particles. Its particle size distribution is also plotted in Figure 3.2. About 2 tons of Levenseat sand was used for this study. It's characteristic and properties are summarized in Table 3-1. The resilient modulus test was conducted in accordance with AASHTO T307-99. The sand used in this study was classified as soil Type 2 because more than 70% was finer than 2mm sieve (No.10) whilst less than 20% passed through the 75μm sieve (No.200).

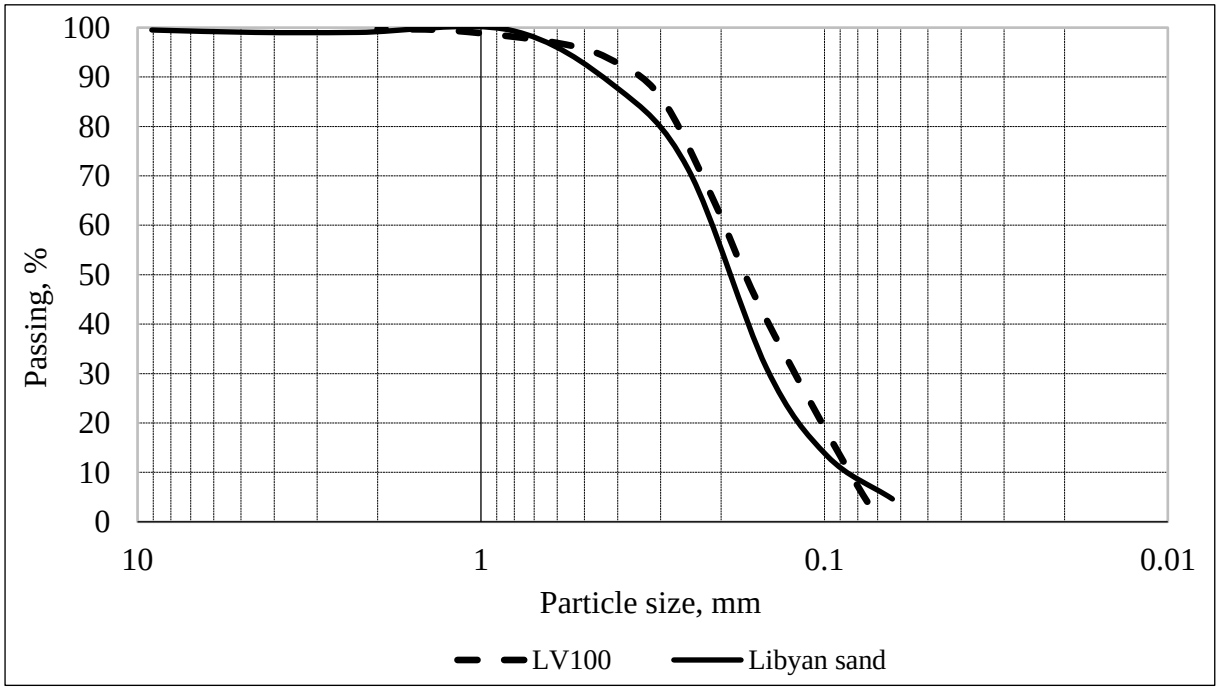

Figure 3.2 Gradation curve of sand.

Table 3-1 Physical and mechanical properties of the LV100 (Levenseat quarry).

Physical property	Relevant standard	(LV100) sand
D_{10} (mm)	BS 1377-2:1990	0.085
D_{30} (mm)		0.13
D_{50} (mm)		0.18
D_{60} (mm)		0.2
Coefficient of uniformity (Cu)		2.35
Coefficient of curvature (Cc)		0.99
Minimum dry density $\Upsilon_{dry\ min}$ (kN/m^3)	BS 1377-4:1990	14.8
Maximum dry density $\Upsilon_{dry\ max}$ kN/m^3		16.75
Optimum Moisture Content, OMC (%)		6.1
Maximum void ratio, e_{max}		0.8
Minimum void ratio, e_{min}		0.6
Maximum porosity of the sand		0.4
Minimum porosity of the sand		0.375
Porosity of the sand		0.4
Relative density (RD), %		65
Soil classification: ❖ Unified Soil classification. ❖ AASHTO classification.		 SP A-3
Sphericity:		Medium
Specific gravity	BS 1377-2:1990	2.67

3.2.2 Reinforcement and Stabilizers Materials

3.2.2.1 Fibres

Polypropylene is a 100% synthetic fibre. Polypropylene fibres are composed of crystalline and non-crystalline regions (Hejazi et al., 2012). The spherulites developed from a nucleus can range in size from fractions of a micrometre to centimetres in diameter. Polypropylene fibre is the type used in this study. It is commonly used in concrete to reduce cracking of the concrete surface. However, many researchers have used these fibres for reinforcing sand (Al-Refeai and Al-Suhaibani, 1998, Anagnostopoulos et al., 2013, Consoli et al., 2005, Diambra et al., 2011, Gray, 1983, Ibraim et al., 2012) as demonstrated in Figure 2.3.

AI-Refeai (1991) carried out a series of triaxial test on reinforced fine sand with sub-rounded particles and medium sand with sub-angular particles by glass fibre and polypropylene fibre. The fibre reinforcement decreases the effect of both deviator stress and confining pressure on resilient modulus. In addition, the permanent deformation of sand samples decreased. Also, the short fibres require higher confining pressure to prevent the bond failure irrespective of type of sand. Finally, the maximum stiffness and strength were obtained with polypropylene fibre compared to glass fibre. The particles interlock was also improved by adding the fibre, especially with sub-rounded fine sand. Ud-din et al. (2011), Eldesouky et al. (2015) and Anagnostopoulos et al. (2013) concluded that the fibre increases the dilatancy for both fine and coarse sand. Santoni and Webster (2001) recommended that future investigations need to be addressed by using fibrillated fibres and recycled materials in road construction application. In (Freed, 1988) patent shows that the incorporation of 0.5%, by weight of dry soil, can increase shear strength of sand by up to 50%.

Previous studies shown that optimum length of fibre may be between 12 and 50mm (Santoni et al., 2001, Consoli et al., 2005, Tiwari and Sharma, 2013, Chore et al., 2011). To improve the workability and increase the density, the fibre content is a value between 0.2 to 0.75% of dry weight of soil as reported in (Chore et al., 2011).

In this research, fibre concentrations ranging from 0.1% to 0.75% (by wt of dry soil) were used, with fibre lengths of 12, 19 and 50mm and diameter of 0.15mm were investigated. PP fibres were supplied by Propex Concrete System Ltd. Properties and characterizations of fibre used were shown in Table 3-2. PP fibres are graded fibrillated fibre as shows in Figure 3.3. The fibre is alkali proof and therefore, it can be mixed with alkali solution. It also reduces the freeze-thaw damage (Propex concrete system Ltd, 2013).

The fibre content in this study was determined through a series of pilot tests included series of compaction test and static triaxial test. The compaction test was conducted for different fibres lengths and contents to obtain the highest density and the optimum water content. Then, the triaxial test was conducted to obtain the shear stress. The resilient modulus test was also conducted on the samples that have higher shear strength.

In the AASHTO (1993) guide stated that the wet and dry state of the water content of subgrade soil should be investigated. Also, the strength of subgrade layer was affected by increase the water content. Therefore, it became necessary to conduct the experimental investigation at different water contents such as 80, 100, and 120% of optimum moisture content. Results of these tests are described in Chapter Four Section 3.6.

Table 3-2 Characteristics of fibres (Propex concrete system Ltd, 2013)

Characteristics	Value
Fibre type	Fibrillated
Length, (mm)	12, 19 & 50
Colour	White
Specific gravity	0.91
Diameter, (mm)	0.15
Aspect ratio	80, 124 & 333
Young's modulus, (GPa)	3.5
Linear denity, (deniers)	1000
Ignition Point	593^{o} C
Melting point	162 ^{o} C
Absorption	Nil
Acid & salt resistance	High
Alkali resistance	Alkali Proof
Electrical conductivity	Low

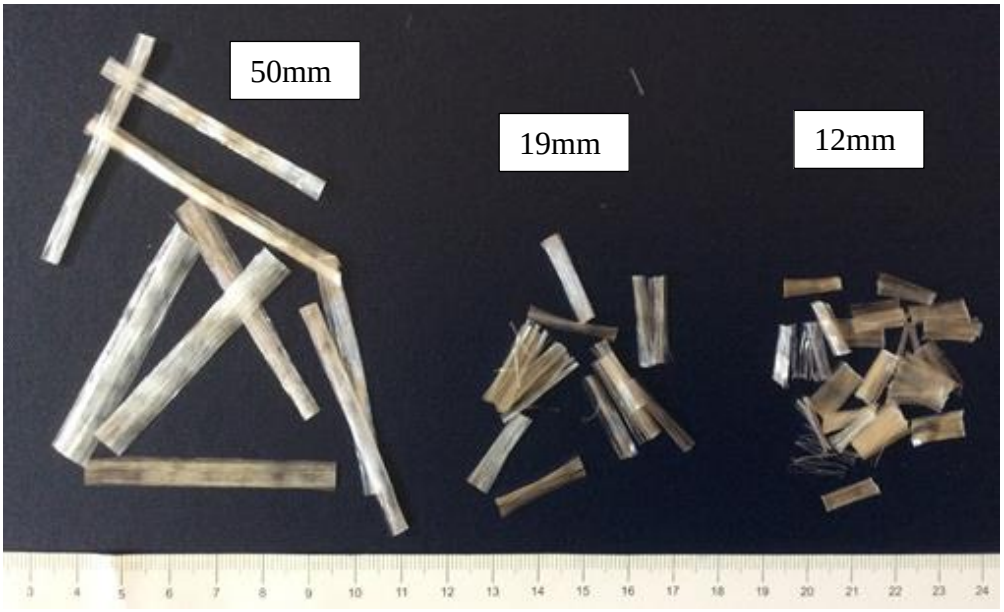

Figure 3.3 Polypropylene fibre (Propex concrete system Ltd, 2013).

3.2.2.2 Fly ash

Fly ash is typically fine as shown in Figure 3.4. Fly ash consists of silt-sized particles which are generally spherical, typically ranging in size between 10 and 100 microns. Fly ash consists primarily of oxides of silicon, aluminium iron, and calcium. Magnesium, potassium, sodium, titanium, and sulfur are also present to a lesser degree as represented in Table 3-3. When used as a mineral admixture in concrete, fly ash is classified as either Class C, Class F or Class N based on its chemical composition.

The previous studies (Chauhan et al., 2008, Chore et al., 2011, Takhelmayum et al., 2013, Jadhao and Nagarnaik, 2008, Kumar and Patil, 2006, FHWA-IF-03-019, 2003) showed that the fly ash was an effective agent for chemical and/or mechanical stabilization of soils. It improved soil density, water content, plasticity, and strength of soils. Typical applications are soil stabilization, soil drying, and control of shrink-swell. Fly ash can be used as a borrowed material to construct fills and embankments. When fly ash was compacted in lifts, a structural fill was constructed that can support highway buildings or other structures. Fly ash has been

used in the construction of structural fills/embankments that range from small fills for road shoulders to large fills for interstate highway embankments. Fly ash stabilized base courses were proportioned mixtures of fly ash, aggregate, and an activator (cement or lime) that, when properly placed and compacted, produce a strong and durable pavement base course.

Table 3-3 Typical percentage of composition for class C fly ash (BS EN ISO 14688-2:2004+A1:2013).

Chemical component	SiO_2	Al_2O_3	CaO	MgO	Fe_2O_3	SO_3
Oxide (wt %)	39.9	16.7	24.3	4.6	5.8	3.3

Properties of Fly Ash

Fineness: The particle size of the fly ash was important for pozzolanic activity and the workability of the concrete. The required grain size should be more than 66% passing from sieve No 0.044 mm (FHWA-IF-03-019, 2003).

Chemical composition: The main components of fly ash are silica, alumina, iron oxide, and calcium, with different amounts of carbon, as measured by the loss on ignition (LOI). Lignite and sub-bituminous coal fly ash were characterized by higher percentages of calcium and magnesium oxide and reduced percentages of silica and iron oxide, as well as lower carbon content, compared with bituminous coal fly ash (Thomas, 2007, ASTM, 2000). The ASTM specification of fly ash is summarized in Table 3-4. American Society for Testing Materials classified the fly ash into two classes which are based on the percentage of (SiO_2 + Al_2O_3 + Fe_2O_3) and the lime if it is more than 70% the fly ash is class F while if it is more than 50% the fly ash is class C (ASTM, 2000).

Table 3-4 ASTM Specification for class C Fly Ash.

Class	Description in ASTM C618	Chemical requirements (min %)
F	Fly ash normally produced from burning anthracite or bituminous coal that meets the applicable requirements for this class as given herein. This class of fly ash has pozzolanic properties.	$SiO_2 + Al_2O_3 + Fe_2O_3 \geq 70\%$
C	Fly ash normally produced from lignite or sub-bituminous coal that meets the applicable requirements for this class as given herein. This class of fly ash, in addition to having pozzolanic and cementitious properties.	$SiO_2 + Al_2O_3 + Fe_2O_3 \geq 50\%$

Carbon content: It is important that the percentage of unburned carbon in the fly ash should be determined by Loss of Ignition (LOI). The unburned carbon requires more water content due to the increase in the voids ratio in the mixture.

The investigation includes fly ash stabilized sand both with/without fibre. The compaction test was carried out for a range of fly ash content ranging from 5 to 50% at 5% interval by weight of dry soil to determine the maximum dry density and optimum water content. For the reason of using class C fly ash, the samples were cured for 7, 14, 28, and 56 days.

Thereafter, the mixture of samples was prepared by the optimum fibre content and the optimum fly ash content. The mixture was tested with and without curing at the optimum water content for the unconsolidated undrained triaxial test, unconfined compressive strength test, resilient modulus test, and determination of permanent deformation. The results are presented and discussed in detail in Chapters Four, Five and Six, respectively.

3.2.2.3 Vitrified slag

An alternative, non-Portland cement, preferably based on waste materials was sought during the study. Tetronics International in Swindon, UK uses a plasma-enhanced process to recover high-value materials from waste feedback. It produces slag generated by vitrification of air pollution control residue. In order to change the slag to that produced by plasma processes, the slag was produced by adding Titanium dioxide (TiO_2), Calcium oxide (CaO), Silicon dioxide (SiO_2) and Aluminium oxide (Al_2O_3) powder, then the slag with the powders was heated at 1600^o C in a muffle furnace to re-melt the mixture before forming the vitreous materials by the air. The slag was then ground down to sub - 150μm particles size using a planetary disc mill.

Keeley et al. (2017) carried out a chemical investigation to determine the chemical components of the slag as shown in Table 3-5. The analysis was obtained by X-ray fluorescence (XRF). In addition, the vitreous nature of the slag prior to alkali activation was confirmed by special preparation as Bruker D2 Phaser powder diffractometer and a wavelength dispersive Bruker S8 Tiger XRF. In addition, X-ray diffraction (XRD) was also conducted and represented in Table 3-5.

Table 3-5 X-Ray fluorescence analysis of the slag components (Keeley et al., 2017).

Chemical component	SiO_2	Al_2O_3	CaO	TiO_2	Na_2O	MgO	Fe_2O_3	P_2O_5
Oxide (wt %)	43.7	9.8	41.7	1.2	0.2	1.5	1.2	0.5

The analysis of the slag shows that there was no crystalline phase while there was at least 95% glassy solid. Thus, the slag was significantly affected by alkali-activation. Therefore, the strength of activated slag was dependent on the percentage of slag dissolution in an alkaline solution. The percentage of slag dissolution increased with a reduction in the polymerisation

of slag (Keeley et al., 2017). Hence, it was suggested that the activated slag could be used as cementitious materials. Therefore, there was good potential to use the slag material to stabilize the sand.

Figure 3.4 Fly ash, ground slag, and sand used.

Figure 3.5 Raw slag.

The experimental work of this study was designed to investigate the possibility of using slag to stabilize the sand. Figure 3.5 shows the raw slag as delivered from the factory. The raw slag was grounded down from about 35x15mm dimension to less than 150μm by using a planetary disc mill. The resulting powder used for stabilization is shown in Figure 3.4.

In the investigation, 6Mol of sodium hydroxide (NaOH) was used to activate the slag as suggested by (Keeley et al., 2017). Therefore, to prepare the solution, 240g of sodium hydroxide was dissolved in 1 litre of water. The chemical reaction increases the strength of the slag due to reduction in the polymerisation of slag binder. Also, it was noted that the particle size is one of the main factors which influence on pozzolanic activity.

Numbers of modified proctor compaction tests were carried out for ranging of slag contents from 10 to 50% at 10% interval (by weight of dry soil) to determine the maximum dry density and optimum water content in accordance with BS1377-4:1990. Based on the compaction test results, the specimen was prepared for unconfined compressive strength test, resilient modulus test, permanent deformation determinations, and durability test.

It was worth mentioning that the available triaxial apparatus's load cell capacity was not enough to test the slag stabilized sand. A similar issue occurred with an unconfined compressive strength test. For this, the compression test machine for crushing concrete specimens was used to obtain the unconfined compressive strength for both slag with /without fibre reinforced sand. The investigation was carried out on optimum water content due to limited available time for the research since slag was identified as a stabilizer for sand towards the end of the study.

3.2.3 Compaction Test (Moisture – Density Relationship)

Consoli et al. (2005) stated that the highest density of sandy soil has been obtained by the vibrating compaction test. In the current study, the vibration compaction test was conducted on the samples of fibre reinforced sand. The result showed that the vibration method separates the sand and fibres. Therefore, the modified proctor compaction test was used for the compaction. The modified proctor compaction test then was used through the study to have the constancy of results.

The cyclic load triaxial test for unbound mixtures of BS EN 13286-7:2004 require that the heavy compaction test should be conducted to obtain the maximum dry density and optimum water content for pavement design. A series of compaction tests were conducted to determine the maximum dry density and the optimum water content for unreinforced and reinforced

sand, fly ash, and slag mixture in accordance with BS1377-4:1990. The test involves dropping 4.5 kg of rammer weight through a drop height of 450mm and 27 times per layer, in five layers in a compaction mould with a volume of a litre.

The results of dry density/moisture content determination were shown in Figure 3.6. Unconsolidated undrained triaxial (UU) and unconfined compressive strength tests (UCST), together with the resilient modulus (M_R), and permanent deformation determinations (PD) were undertaken on the specimen at 95% of maximum dry density and 80, 100, and 120% optimum water content as shown in Table 3-6.

The compaction tests were conducted on the sand with 12, 19, and 50mm fibre lengths at different fibre contents as shown in Figure 3.7, 3.8, and 3.9, respectively. The maximum dry density was obtained at 0.5% fibre concentration. The density achieved was only greater than the maximum of density achieved with 12mm long fibre at the same fibre content 0.5%. However, 19mm fibre length was used throughout the research because the maximum dry density was obtained by it. It was noted that the workability of samples was better than others.

Different fly ash and slag content were used to obtain the maximum dry density and the optimum water content as shown in Figure 3.10 and 3.11, respectively. It was found that the optimum fibre content occurred of 0.5% of the dry weight of soil, the fly ash at 35% of the dry weight of soil and the slag at 40% of the dry weight of soil. Also, it is important to note that, the inclusion of the fibre increases the compaction energy required to bring the specimen to the required density. Because of the fibre, the sand needs more effort to place it in the position. And the fibres curves resist the compaction load, this also requires to increase the energy.

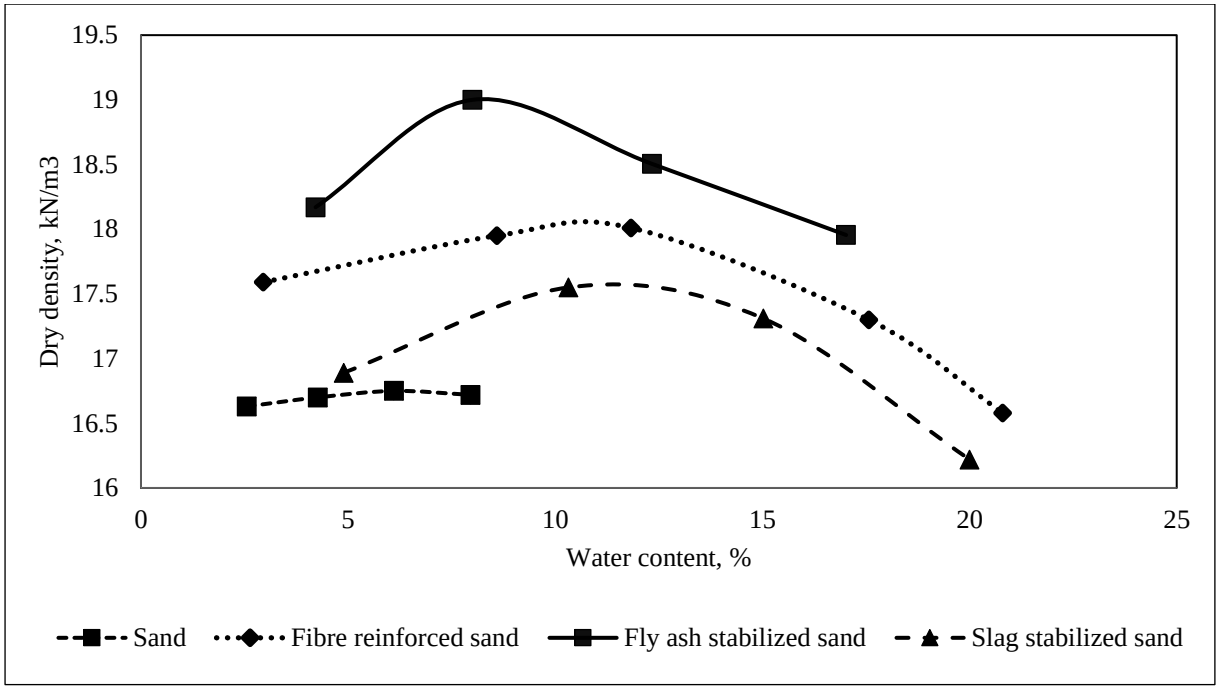

Figure 3.6 Moisture to density relation for reinforced and stabilized sand.

Table 3-6 Maximum dry density and optimum moisture contents for reinforced and unreinforced sand.

Soils	MDD, kN/m^3	OMC, %	Relevant standard
Unreinforced sand	16.75	6.1	BS1377-4:1990
Fibre reinforced sand	18	12	
Fly ash stabilized sand	19	8	
Slag stabilized sand	17.5	10.3	
Fibre with fly ash reinforced sand	19	8	
Fibre with slag stabilized sand	17.5	10.3	

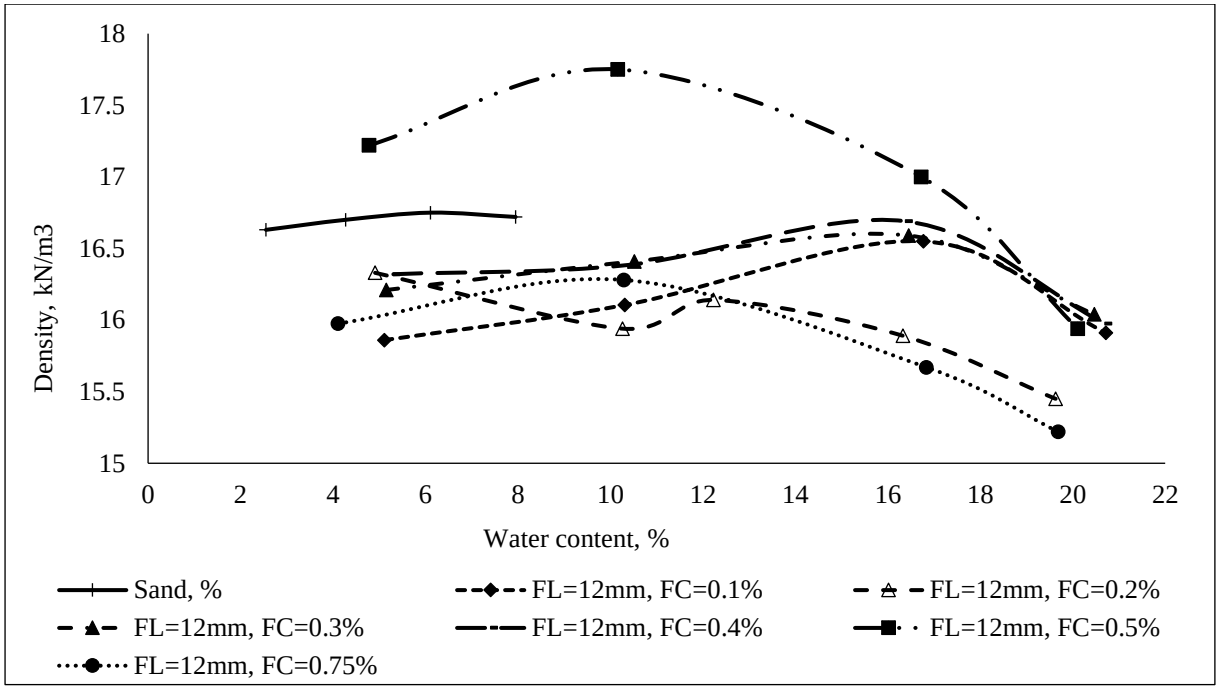

Figure 3.7 Moisture to density relation for fibre (12mm) reinforced sand with different fibre contents.

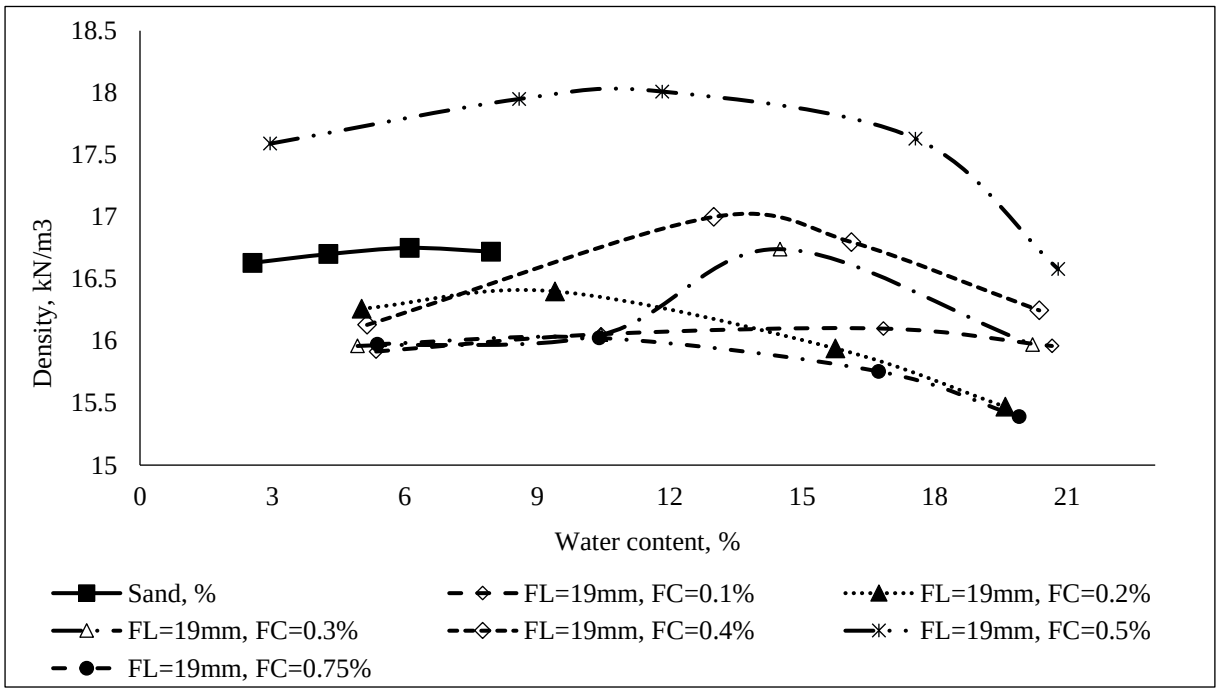

Figure 3.8 Moisture to density relation for fibre (19mm) reinforced sand with different fibre contents.

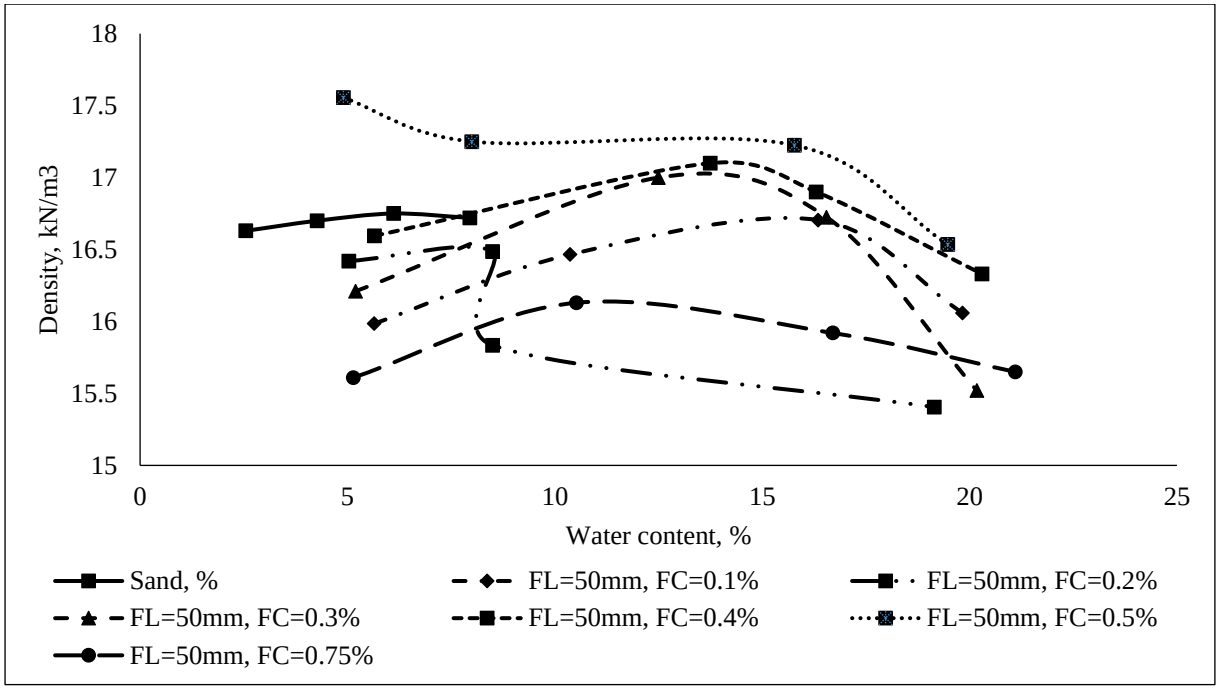

Figure 3.9 Moisture to density relation for fibre (50mm) reinforced sand with different fibre contents.

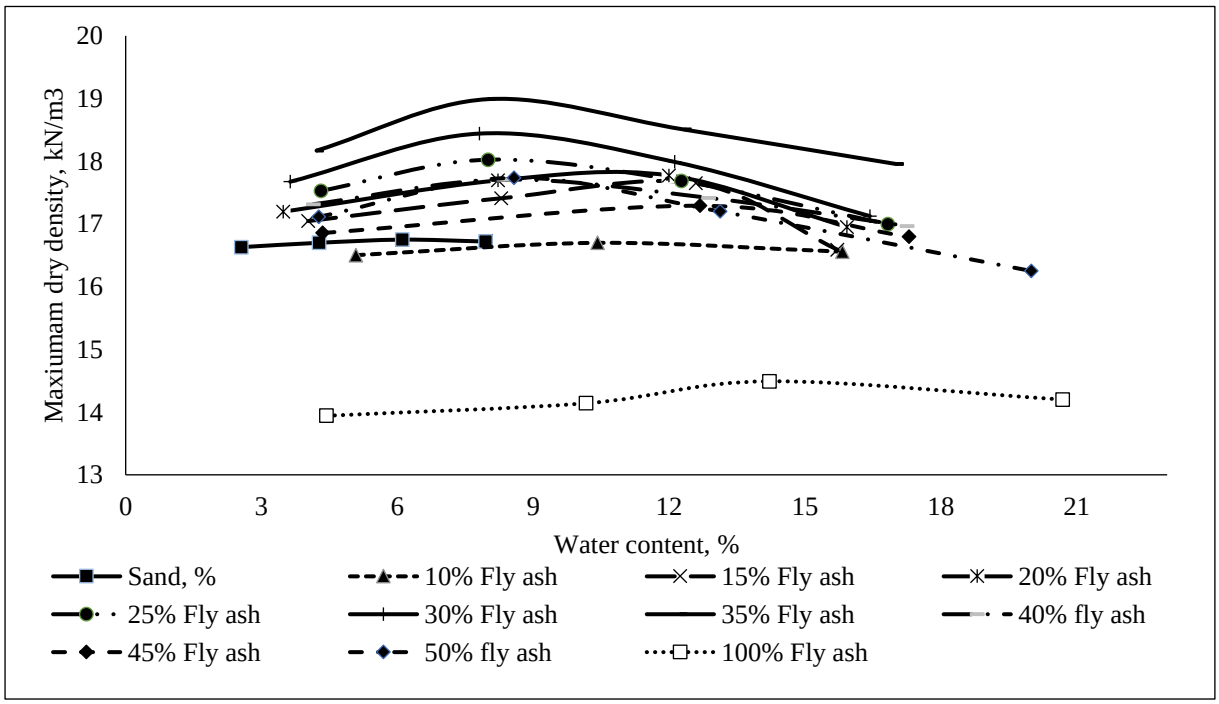

Figure 3.10 Moisture to density relation for fly ash stabilized sand with different fly ash contents.

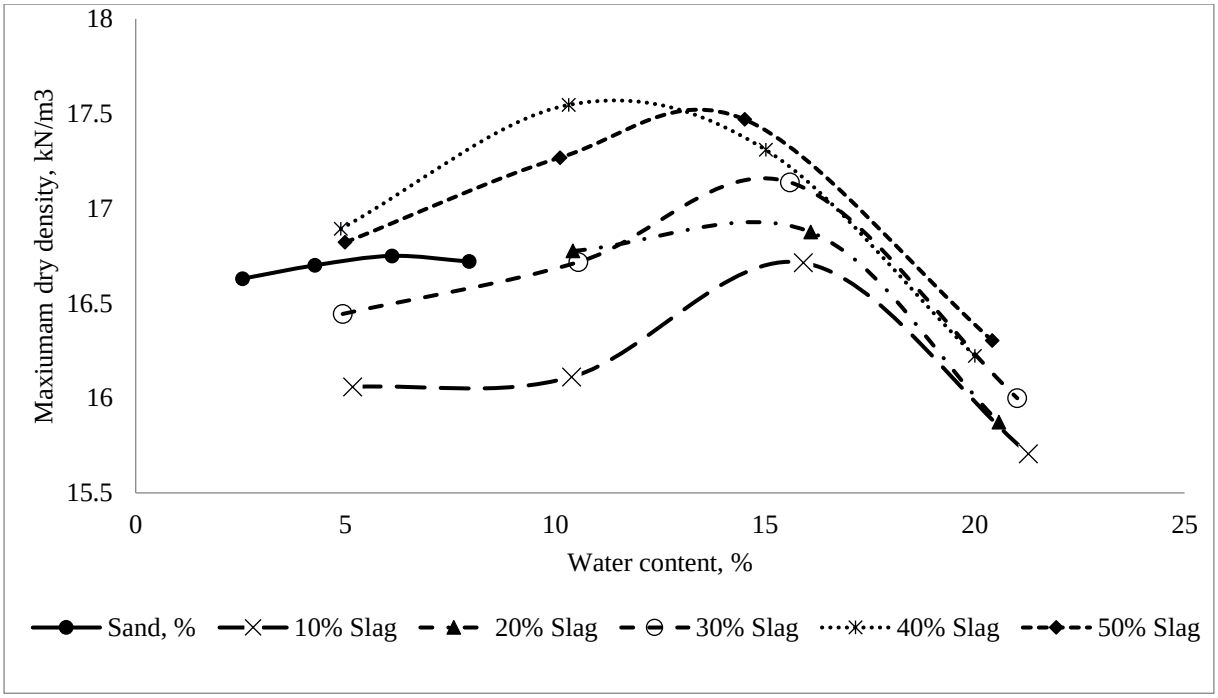

Figure 3.11 Moisture to density relation for slag stabilized sand with different slag contents.

3.2.4 Unconsolidated Undrained Triaxial Test (UU)

A series of monotonic triaxial tests were performed on unreinforced and reinforced sand to determine the static deviator stress of soil at failure for the different mixtures (Brown, 1996, Huang, 1993). Then, use the values to determine a cyclic stress ratio (CSR) that use in the cycle triaxial test. The cyclic stress ratio was obtained by Equation 3-1 that is the cyclic deviator stress and the static deviator stress of soil at failure, the ratio was used to set the in repeated load deformation testing (Salour and Erlingsson, 2015, Brown, 1996, Chow et al., 2014).

$$CSR = q_{cyclic} / q_{failure} \qquad \text{Equation 3-1}$$

Where:

CSR = the cyclic stress ratio,

q_{cyclic} = the cyclic deviator stress, and

$q_{failure}$ = the static deviator stress of reinforced soil at failure.

Werkmeister et al. (2001) applied the shear stress ratio of 50% of the materials stress at failure for sandy gravel. Brown (1996) recommended that the range of applied stress level for the sand is 20 to 60% while (Elliott et al., 1998) applied 20 to 70% for clay soil.

In this research, the test was conducted in accordance with BS1377-7:1990. Test specimens were 100mm in diameter and 200mm in height. The confining pressures (σ_3) were 10, 25, & 40kPa and the strain rate was 3 mm/min. The confining pressures were chosen based on the confining pressure in the subgrade layer which is similar to the confining pressure in the resilient modulus test. Figure 3.12 shows the triaxial apparatus used throughout the research. The shear strength was investigated at 80, 100, and 120% of OMC in order to consider the effect of moisture variation in the wet and dry state (AASHTO, 1993).

To determine the maximum applied cyclic stress numbers of repeated triaxial tests were conducted. The elasticity of samples was controlling the maximum applied cyclic stress. The load actuator was stuck when the applied cyclic stress was above 0.66 of the static deviator stress. The resilient modulus apparatus was designed for testing untreated subgrade soils and untreated base/subbase materials.

It is important to mention that the slag with/without fibre was not possible to test with the triaxial apparatus because the load cell of triaxial apparatus had a capacity of only 10kN while the samples stabilized with slag were stronger than the load cell capacity. The results of the unconsolidated undrained triaxial test were described in detail in Chapter Four.

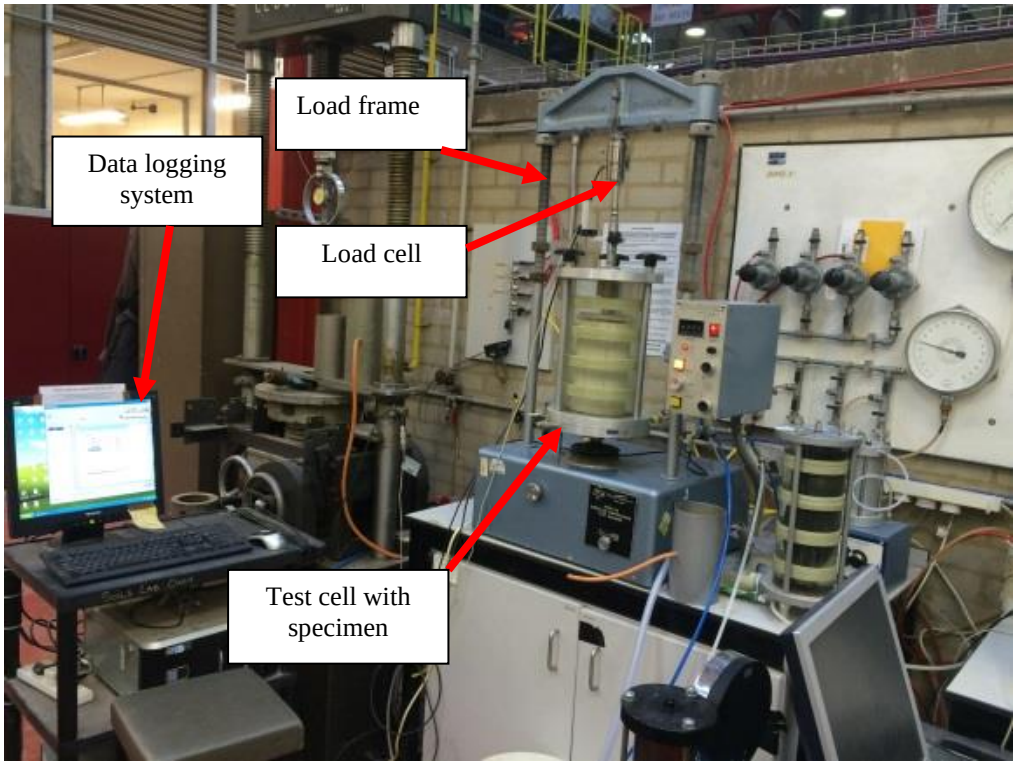

Figure 3.12 Unconsolidated Undrained Triaxial Apparatus

3.2.5 Unconfined Compressive Strength Test (UCS)

The UCS determination was undertaken on different mixtures at different water contents. The guide for the mechanistic-empirical design for pavement (NCHRP, 2004) recommends the correlations models for lean concrete, cement-treated aggregate, open-graded cement stabilized, soil cement, lime-cement-fly ash, and lime stabilized soil. Correlations models for fibre, class C fly ash, and slag were not included in the guide. Hence, the results of UCS tests were used to develop correlations with other properties to obtain the resilient modulus value for design purpose.

Unconfined compressive strength tests were conducted in accordance with BS 1377-7:1990. Samples dimensions were 100mm in diameter and 200mm in height. The samples were prepared based on the compaction test results in Table 3-6. The tests were performed on samples prepared at 95% maximum dry density and at 80, 100, and 120% of optimum water

content. The strain rate of 1.5% was used as recommended by (Head, 1994). The samples of fly ash and slag were cured for 7, 14, 24, and 56 days before testing. The test set up for UCS determination using a 10kN load cell is shown in Figure 3.13, while the slag samples were tested using a 50kN load cell, the test set up is shown in Figure 3.14.

Figure 3.13 (10) kN load cell with unconfined compressive test apparatus.

Figure 3.14 (50) kN load cell with unconfined compressive test apparatus.

3.2.6 Specimen Preparation

The samples were static compacted as given in AASHTO T307, ANNEX C for the proposed experimental tests while the mould dimension used is 100mm in diameter by 200mm high. The mould consists of six spacers to compact the soil in five layers. The samples were prepared for both fibre and fly ash with three different water contents (80, 100, and 120%) of optimum water content (OMC) and 95% of the maximum dry density while slag, slag with fibre, fly ash with fibre were only tested at 100% of OMC and 95% of the maximum dry density. The specimens were tested after 0 & 7 days of curing for all experimental tests. For further investigation, the unconfined compressive strength test samples were cured for 0, 7, 14, 28, & 56 days of curing, respectively.

To achieve uniform compaction throughout the thickness, the mixtures were divided into five parts. This was based on the volume and the weight of the mixture. The compaction procedure was described as following; the static load was applied for 2 minutes with the same compaction energy in accordance with AASHTO T307-99. The mixture was divided into five layers. The first layer of the mixture was placed in the middle of the mould with the longest spacers and followed by the second, third, fourth and fifth layer with the place the spacer respectively. After the compaction, the extractor was used to take the sample out.

The specimens were prepared by mixing dry soil, water, and/or fly ash, slag and polypropylene fibres. In the fibre reinforced samples, the water was added to the sand before adding the fibres into the mixture. The designated fibres were weighed according to the desired dosage rate and mixed in small increments. Only the slag mixture used sodium hydroxide (NaOH) with the water in order to react to the slag.

3.3 Design of Testing Programme

This section includes two main tests which are the repeated load triaxial tests and durability test. The testing program was designed to evaluate the reinforced sand in road application. The repeated load tests were conducted in accordance with British Standard EN 13286-7 while the Freeze-Thaw durability test was carried out in accordance with ASTM D 560.

3.3.1 Repeated Load Triaxial Tests (RLTT)

Resilient modulus and permanent deformation tests were carried out in this research with the purpose of investigation the resilient modulus and the permanent deformation characteristics of stabilized and reinforced sand in the subgrade layer. The test was conducted in accordance with AASHTO T307 using apparatus shown in Figure 3.15 supplied by Cooper Technology Ltd.

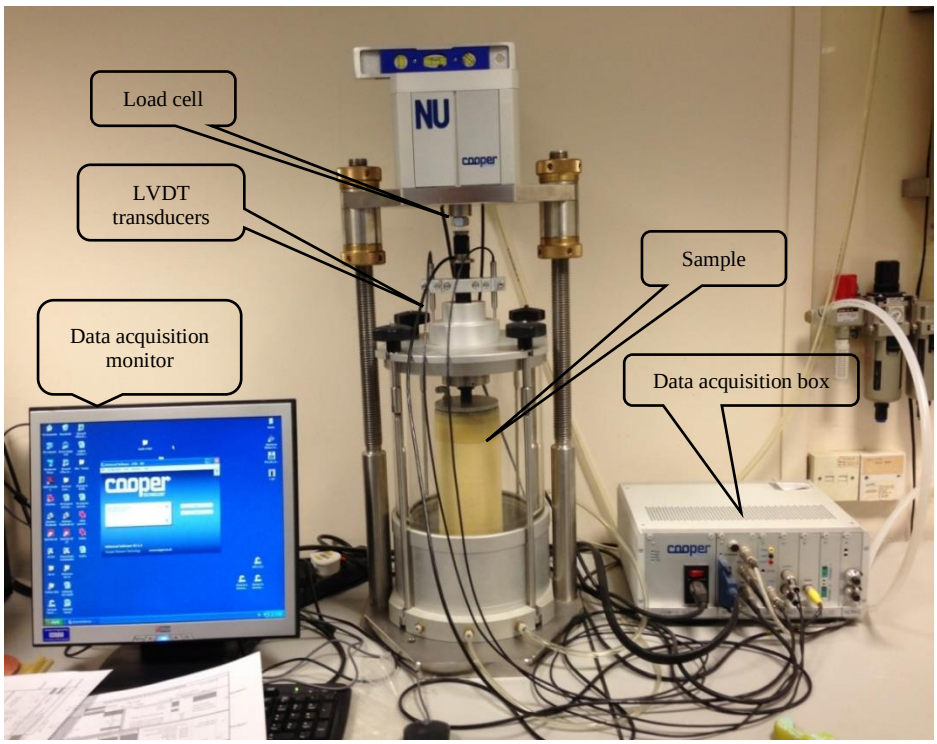

Figure 3.15 Repeated Load Triaxial Apparatus

3.3.1.1 Resilient Modulus Tests M_R

The resilient modulus test apparatus had a pneumatic loading system. The procedure requires loading duration of 0.1 second and cyclic duration of 0.9 seconds. Dynamic cyclic stress and a static confining stress were applied during the test. The resilient modulus procedure is applied 2000 cycles and the first 500 cycles are called a conditioning stage while the remaining of 1500 cycles were divided into 15 sequences, each one with confining pressure of 13.8, 27.6 & 41.4kPa, respectively. And each confining pressure was fixed for stress levels of 12.4, 24.8, 37.3 49.7 & 62kPa. The resilient modulus test was carried out to evaluate resilient modulus in different conditions as described below:

- According to AASHTO T307, for fibre reinforced sand, fly ash stabilized sand, slag stabilized sand, fibre with fly ash reinforced sand and fibre with slag reinforced sand.
- According to AASHTO T307 after 7 days of curing for fly ash stabilized sand, slag stabilized sand, fibre with fly ash reinforced sand, and fibre with slag reinforced sand.
- According to AASHTO T307 after 10, 20, & 30 Freeze-Thaw cycles.
- According to Multi-Stage permanent deformation test for fibre reinforced sand, fly ash stabilized sand (with/without curing), slag stabilized sand (with/without curing), fibre with fly ash reinforced sand (with/without curing) and fibre with slag reinforced sand (with/without curing).
- According to Multi-Stage permanent deformation test after 10, 20 & 30 of Freeze-Thaw cycles for fibre reinforced sand, fly ash stabilized sand, slag stabilized sand, fibre with fly ash reinforced sand and fibre with slag reinforced sand.

The resilient modulus tests were conducted at different water content 80, 100, and 120% of OMC and different stabilizers and reinforced material. Only fibre with fly ash or slag

reinforced sand specimens were tested at 100% of OMC. The results were presented and discussed in Chapter Five.

3.3.1.2 Permanent deformation test

The aim of permanent deformation test was conducted to investigate the effect of stress level on the permanent strain at different water content. The British Standard EN 13286-7 provides two procedures which are a single-stage repeated load triaxial test SS RLT and Multi-stage repeated load triaxial test MS RLT for determining the permanent strain as shown in Figure 3.16. The test consumes the time when different stress conditions are needed.

A single-stage repeated load triaxial test SS RLT is defined as one load pulse of constant magnitude. The disadvantage of this method is that it consumes time, and requires a new sample for each new stress level. Also, the procedure does not allow obtaining the effect of stress history.

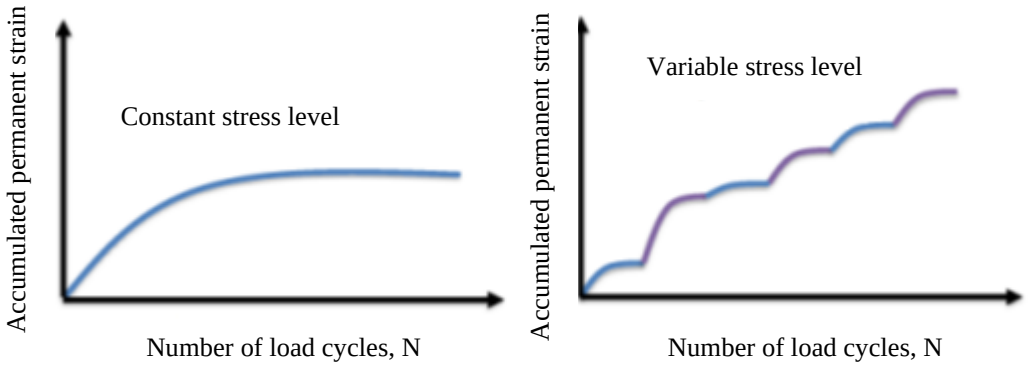

Figure 3.16 Single & Multi-Stage Repeated Load (Rahman, 2015).

While the Multi-Stage Repeated Load Triaxial test MS RLT allows to; Study the stress history, minimize both the effort and time of studying different stress levels, it is more reliable to simulate the field condition and investigate the material behaviour as stated by (Salour and Erlingssonc, 2015, Rahman, 2015, Saevarsdottir and Erlingsson, 2013).

Therefore, the comparison between the SS RLT and MS RLT was illustrated in Figure 3.17. In the case of a Multi-stage repeated load test, after applying the first stress level for several cycles $\mathbf{N_1}$ on the sample the accumulated strain $\mathbf{\varepsilon'_{p1}}$ would be along the line **OA**. Stress path **2** produced the accumulated strain $\mathbf{\varepsilon'_{p2}}$ after $\mathbf{N_2}$ cycles at the second stress level as **AC** line shown in Figure 3.17. While the Single-stage repeated load test could be simulated by the stress path 2, the accumulated strain would be developed from $\mathbf{\varepsilon'_{p2}}$ to $\mathbf{\varepsilon'_{p2'}}$ for N2 cycles within the second stress level for stress path 2. The difference between SS RLT and MS RLT is shown in point E & A, the line of OEBFD & OAC and the distance between A & B.

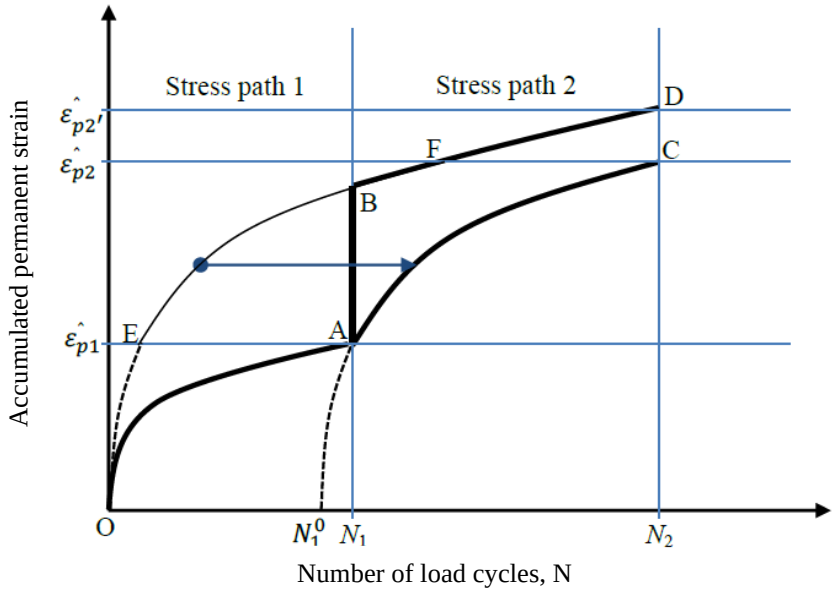

Figure 3.17 The comparison between single-stage and multi-stage repeated load tests after (Rahman, 2015).

To study the behaviours of pavement materials and to determine the maximum deviator stress level before the failure, the MS-RLT was conducted in accordance to BS EN 13286-7 at confining pressure of 27.6kPa for the specimens while a series of stress levels were applied. The confining pressure was obtained as recommended by BS EN 13286-7. The minimum confining pressure was 20kPa as recommended by BS EN 13286-7. The minimum confining pressure of AASHTO T307 was 13.6kPa. Therefore, the current confining pressure was

chosen as the second confining pressure in resilient modulus test procedure which is 27.6kPa. The stress levels were obtained based on the results of the unconsolidated undrained triaxial test. 50,000 cycles were applied for cured and non-cured samples with 5 sequences of 10,000 cycles each. The test procedure involved taking reading during the first 20 cycles as recommended by BS EN 13286-7. Then, the last three cycles are recorded throughout the test.

Also, it was important to mention that, the samples stabilized with slag or slag with fibre could not be tested at the stress level higher than 150kPa. This was because of the capacity of the load cell that is10kN. Therefore, in the beginning, numbers of slag and slag with fibre samples were tested to determine the cyclic deviator stress level that could be applied.

The permanent deformation test was conducted as follows:

- According to Multi-Stage permanent deformation test for fibre reinforced sand, fly ash stabilized sand (with/without curing), slag stabilized sand (with/without curing), fibre with fly ash reinforced sand (with/without curing) and fibre with slag reinforced sand (with/without curing).
- According to Multi-Stage permanent deformation test after 10, 20 & 30 of Freeze-Thaw cycles for fibre reinforced sand, fly ash stabilized sand, slag stabilized sand, fibre with fly ash reinforced sand and fibre with slag reinforced sand.

3.3.2 Freezing and Thawing Durability (F-T) test

The durability of pavement materials could be simulated by wetting-drying and freeze-thaw durability tests as recommended in (NCHRP, 2004). This should be adjusted based on the environment/climate where the road is constructed. In a desert scare, freeze-thaw is likely to

prevalent the condition that will affect durability. Therefore, all the proving mixtures were subjected to freeze-thaw tests. The wetting-drying test could not be applied on sandy soil. Because of the reinforced sand did not stand in the bucket. Also, there is no available F-T cycle's durability test for class C fly ash, fibre, and slag. Available procedures of freezing-thawing durability tests are listed in Table 3-7. They were conducted to measure the volume change, moisture change, loss in weight and unconfined compressive strength. In this research, the ASTM D560 test procedure was modified in terms of numbers of cycles and parameter measured to simulate the life design of pavement design.

The resilient modulus and permanent deformation are the main factors of the pavement design as stated in the (AASHTO, 1993) and MEPDG (2004). Therefore, the resilient modulus and permanent deformation were measured instead of volume change, loss in weight and unconfined compressive strength. Moreover, the resilient modulus test was considered to be more appropriate to conduct on the samples than the unconfined compressive strength test after the durability test (Gupta, 2014).

Figure 3.18 shows the test apparatus which includes chest freeze, moist box, humidity, and temperature controller. Also, the standard test (ASTM D 560) includes 12 freeze-thaw cycles, while the modified freeze-thaw test was carried out up to 10, 20 & 30 cycles in order to evaluate the resilient modulus and permanent deformation to represent 10, 20 and 30 years. The specimens were tested in accordance with AASHTO T307 used for the preparation of the resilient modulus and permanent deformation test. Specimens were stored in the freezing cabinet for 24 hours at -23^{o}C. Thereafter, specimens were thawed in the moist box at 21^{o}C and relative humidity of 100% for 23 hrs as discussed in (ASTM D 560).

Table 3-7 Summary of the laboratory Freezing-Thawing durability procedures

Reference	Materials	Procedure	Parameter used
ASTM D560	Soil cement	Freezing at temperature of −23°C for 24 h; then thawing at 21°C for 23 h; brush the specimen with a wire scratch brush; after brushing, specimens shall be subjected to another FT cycle; apply up to only 12 cycles	Volume changes, soil-cement loss and moisture changes
ASTM C666	Concrete	The cycle procedure is cooling the sample from 40°F to 0°F. Then, warm up it from 0 to 40°F. The cycle time is 2 to 5 hours. It is applied for 300 cycles	Use the elastic modulus to measure the durability by resonant frequency of the samples.
ASTM C671	Concrete	The cycle procedure is cooling the sample in water saturated kerosene or silicone oil from 2°C to -10°C for 5 hours, then, warm it again at 2°C for 2 weeks.	Strain during the cooling cycle
ASTM C593	Fly ash and other pozzolan	The specimen is subjected by the vacuum saturation strength testing procedure for 5 to 10 cycles.	Unconfined compressive strength

Figure 3.18 The Freezing-Thawing system.

3.4 Discussion

This chapter presented the experimental work and the reinforcement materials used in this study. The aim of the study was to reinforce the subgrade layer for road construction. Therefore, the resilient modulus and permanent deformation were important factors to be investigated for the reinforcement sand. Then these parameters were used in analytical pavement design.

Using synthetic fibre was to improve the strength, resilient modulus, and density. Based on the compaction test and unconfined compressive strength test, the fibre length of 19mm improves the density and workability when compare it with 12 and 50 mm fibre length. It also gains the highest shear strength. By contrast, 12mm fibre length improved the workability but resulted in a decrease the density while 50mm fibre resulted in decreases both the workability and the density. The results of the compaction tests were discussed in Section 3.2.3 and the unconfined compressive strength test later in Chapter Four, Section 4.3.

The systematic review shows that the fly ash improves the strength, workability, and the durability of road layers in Chapter Two, Section 2.3.3. Fly ash is used as Portland cement replacement and used in concrete to improve the strength, increase the resistance to sulphate and alkali-silica reactivity, and reduce the shrinkage and the bleeding.

The principal components of both fly ash and slag are silica, alumina, iron oxide, and calcium, with varying amounts of carbon. The pozzolanic materials are characterized by higher concentrations of calcium and magnesium oxide and reduced percentages of silica and iron oxide, as well as lower carbon content, compared with non-pozzolanic materials.

According to British Standard (EN ISO 14688-2:2004+A1:2013), the ash minimum containing 50% of SiO2, Al2O3 and Fe2O3 are defined as cementitious materials. This was used to compare the chemical constituents of vitrified slag with class C fly ash as shown in Figure 3.19. Also, the percentage of calcium hydroxide that reacts these components at ordinary temperatures and in the presence of moisture to form compounds possessing cementitious properties. This chemical reaction between the siliceous and/or siliceous-alumina components in the pozzolan, calcium hydroxide, and water is called the pozzolanic reaction. The high-calcium value of slag improved significantly the cementitious properties

(self-hardening when reacted with water). Figure 3.19 shows the comparison between Class C fly ash and activated slag with the amount of calcium and the silica, alumina, and iron content in the ash.

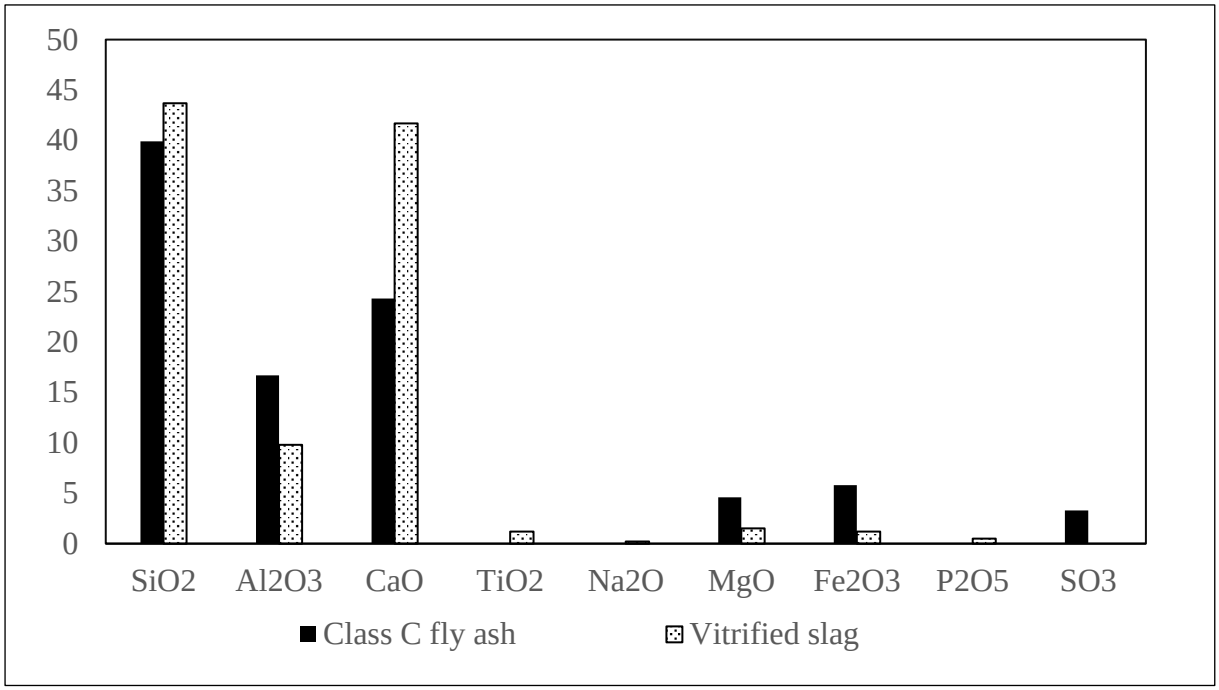

Figure 3.19 Percentage of chemical components for class C fly ash and vitrified slag.

CHAPTER 4 MONOTONIC LOADING RESULTS AND DISCUSSION

4.1 Introduction

As reported in Chapter Three, both monotonic and dynamic load tests were conducted on reinforced and stabilized sand. Results of monotonic loading are presented and discussed in this chapter. The monotonic tests are the unconfined compressive strength (UCS) and unconsolidated undrained triaxial (UU) tests. Both tests were conducted under the conditions of a range of moisture contents, confining pressures and different stabilizers and reinforced materials.

The results of UU tests were used to determine the cyclic deviator stress that will be applied in the permanent deformation tests, whilst the UCS tests were used to assess the degree of improvement in strength due to fibre reinforcement and addition of both fly ash and slag. Also, the results of unconfined compressive strength test were used to develop corrections models. The aim of the correlation models was to determine the resilient modulus value by using a simple test instead of the expensive equipment test.

4.2 Unconsolidated Undrained Triaxial Test (UU)

In order to set the deviator stress and confining stress for both resilient modulus and permanent deformation tests, it was necessary to determine the shear stress of the materials at failure. The resilient modulus test standard, AASHTO T307, recommends three confining pressure and five stress level (cycling deviator stress) as explained in Chapter Three. For determining permanent deformation, Brown (1996) applied the deviator stress ratio from 20 to 60% of the static shear stress strength for granular soil. While (Elliott et al., 1998) applied

the deviator stress ratio from 20 to 70% of the static shear stress strength for clay soil. Also, (Brown, 1996) stated that the plastic strains and pore pressure below the threshold stress are negligible.

The monotonic triaxial test was carried out to obtain the cycling deviator stress for the reinforced and stabilized sand. It is important to note that the slag and slag with fibre were not possible to test using the available standard triaxial test apparatus, due to limitation of the available load cell which has a capacity of (10kN). Thus, this reflects that a small confining pressure does not have an effect on the slag or slag with fibre.

Numbers of slag specimen were tested at different deviator stress values using the permanent deformation test in order to determine the threshold stress level. The AASHTO T307 apparatus is a standard apparatus for untreated soils, and due to the fact that slag samples are stiff material, the load cell was stuck after the stress of 150kPa. The maximum stress level of fly ash with fibre also was obtained to be 148kPa. Therefore, cyclic deviator stress of 150kPa was applied on slag and slag with fibre.

4.2.1 Sand

The shear strength parameters of unreinforced sand were obtained for specimens compacted to 95% of maximum dry density and ± 20% of optimum moisture contents. Typical shear stress and normal stress relationship for unreinforced sand were shown in Figure 4.1. It was observed that the internal friction angles and the cohesion were 21.4, 19.2 to 23 degrees and 12, 16, and 5kPa with the change in the water content from 80% to 120% of OMC, respectively. The results showed that the highest cohesion was obtained at the optimum water content, but the lowest value was observed at 120% OMC. Figure 4.1 shows that the difference of the shear strength was negligible between the stress at 80% and OMC. Figure 4.2 illustrates the relationship between

the shear stress at failure and confining pressure. Also, the increase in water content affected the stress as demonstrated in Figure 4.3, 4.4, and 4.5, respectively. It can be seen when plotting the shear stress against the confining pressure.

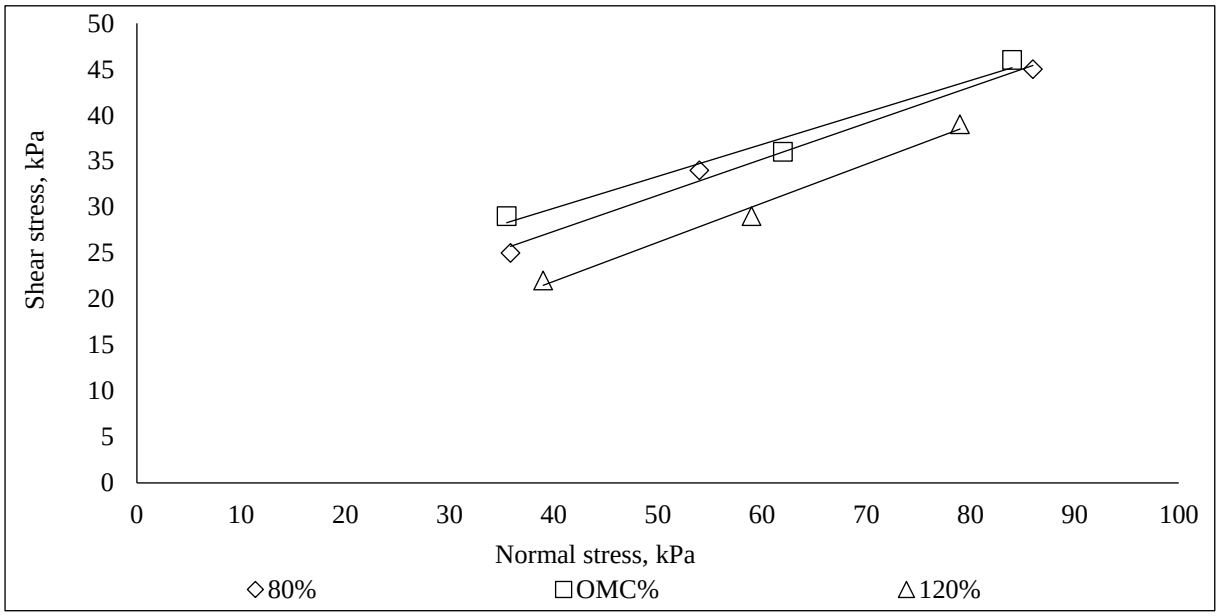

Figure 4.1Shear stress to normal stress relation of unreinforced sand at 80, OMC & 120% and confining pressure of 10, 25, & 40kPa.

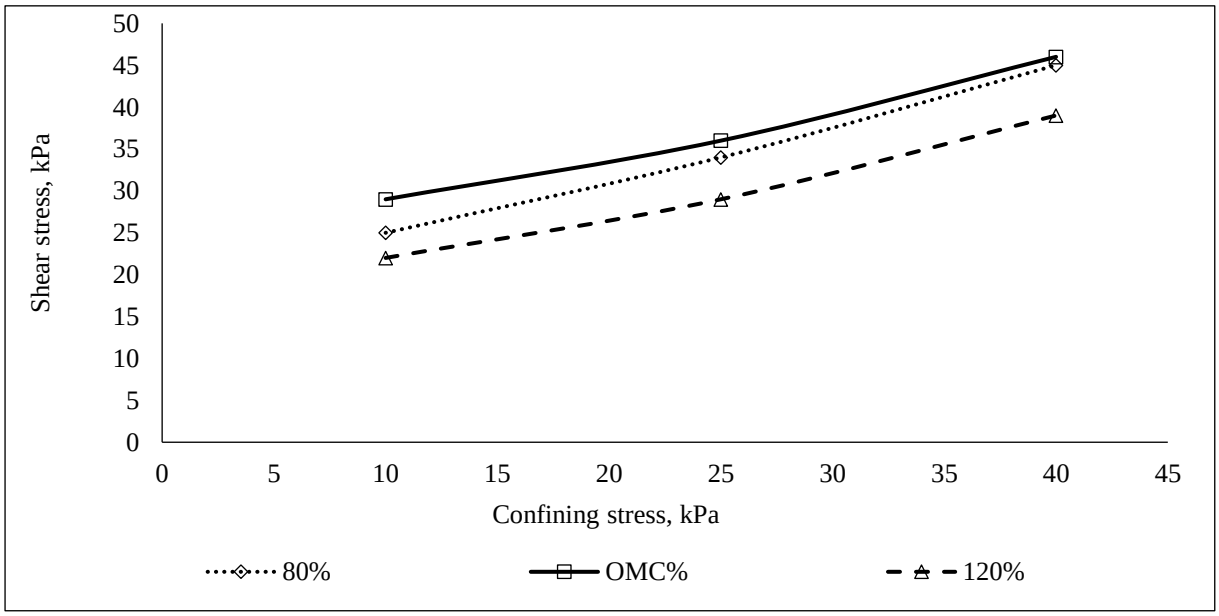

Figure 4.2 Confining stress to stress relation of unreinforced sand at 80, OMC & 120%.

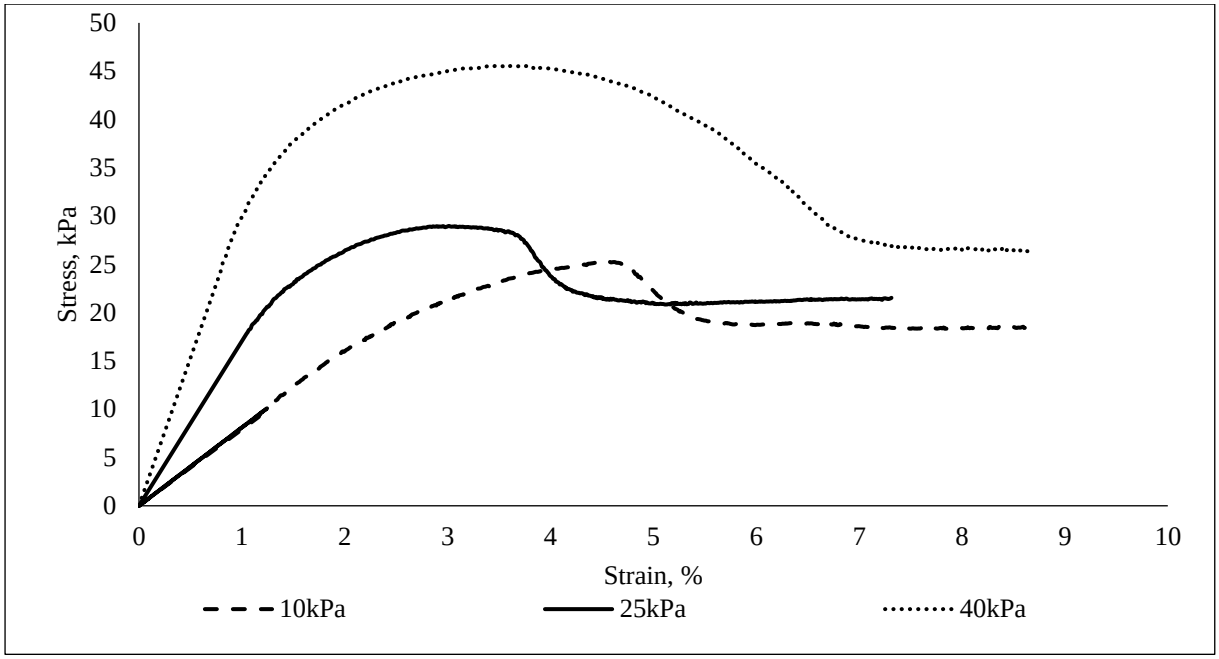

Figure 4.3 Stress-strain relationship for unreinforced sand at confining pressure of 10, 25, and 40kPa at 80% of OMC.

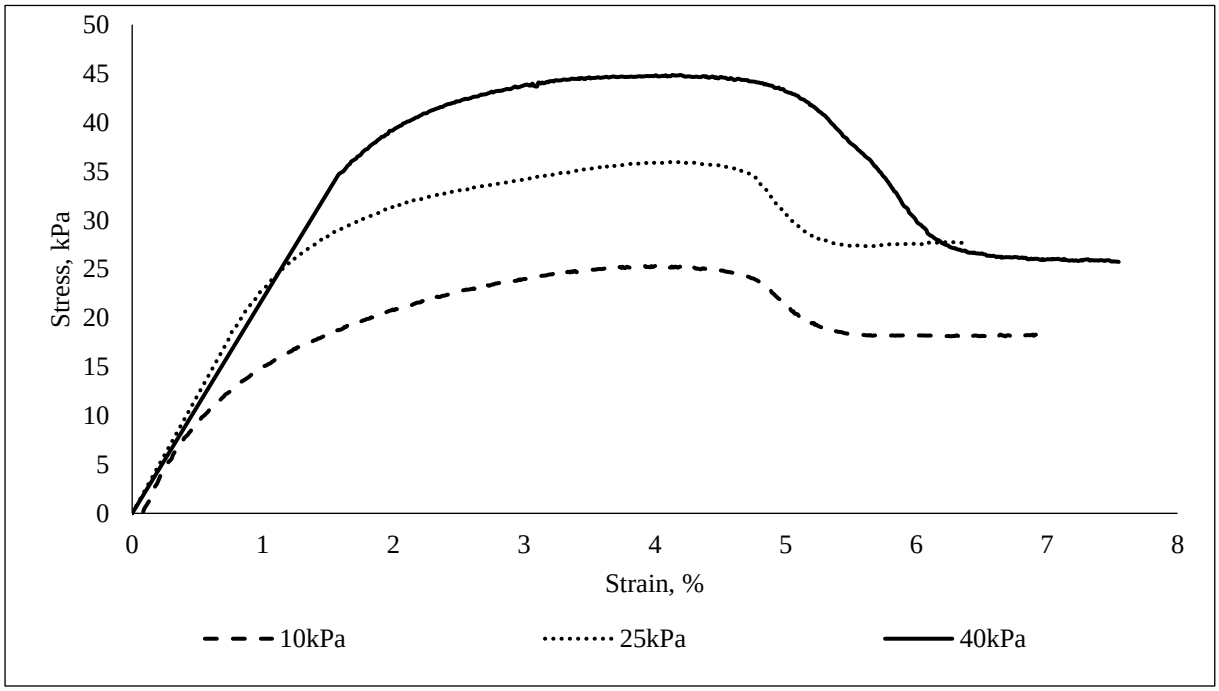

Figure 4.4 Stress-strain relationship for unreinforced sand at confining pressure of 10, 25, and 40kPa at OMC.

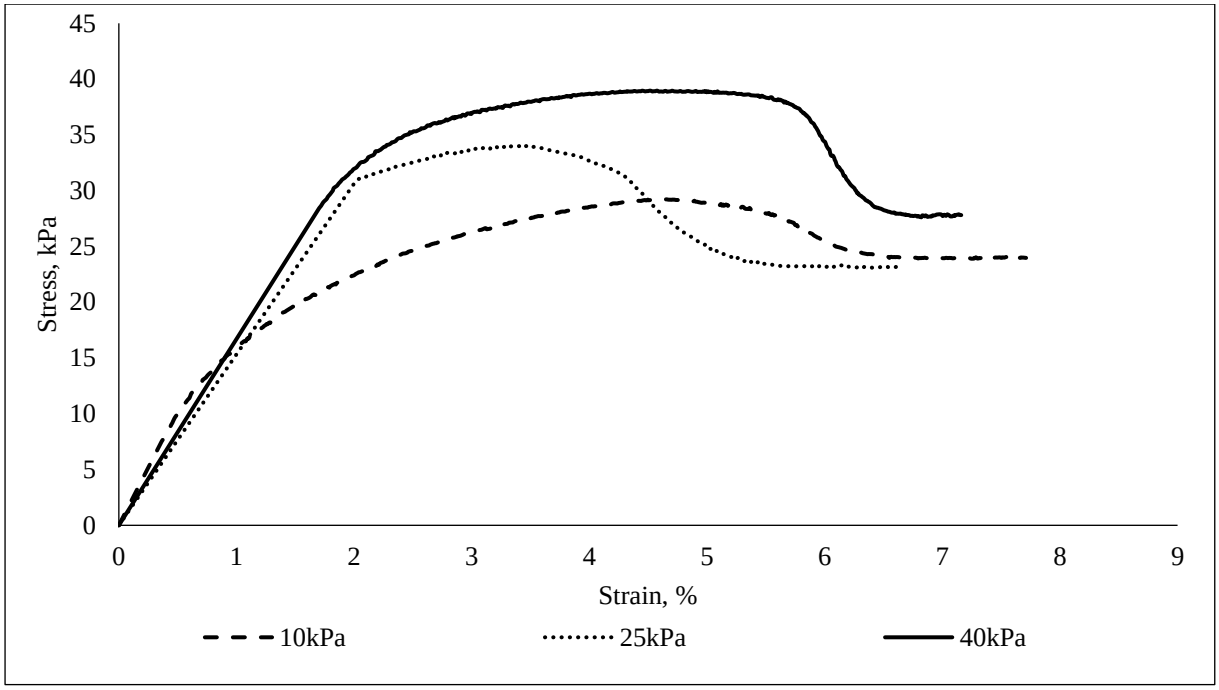

Figure 4.5 Stress-strain relationship for unreinforced sand at confining pressure of 10, 25, and 40kPa at 120% OMC.

4.2.2 Fibre Reinforced Sand

The shear strength parameters also were obtained for sand reinforced with 12, 19, & 50mm long fibrillated polypropylene fibre. All the samples were compacted at 95% of MDD and three water contents of 80% and ±20% of OMC. The optimum fibres content was obtained from the compaction test as explained in Chapter Three section 3.2.3. It was found that the fibres content are 0.5% of the dry weight of soil for 12, 19, and 50mm long fibres. Typical normal stress versus shear stress at failure for 12, 19, and 50mm long fibre at 80%, OMC and 120% water content were plotted in Figure 4.6, 4.7, and 4.8, respectively. It was observed that the fibre length of 19mm at different water contents showed the highest shear stress and the internal friction angle. The shear stress at the failure to confining pressure relationship was shown in Figure 4.9, 4.10, and 4.11, respectively. Figure 4.10 demonstrates that the highest strength was obtained by 19mm long fibre at OMC. It can be explained by the

interlock between the particles and fibre of 19mm. The performance of 19mm long fibre was better than other fibre lengths during the mixing. Three mixers were broken during mixing fibre 50mm long fibre with sand.

Shorter fibre 12mm was not sufficient to prevent pull-out failure. Inclusion of fibres modifies the stress condition in the specimens as loading results in the generation of tensile stress in the fibre resulting enlargement of zone of failure as shown in Figure 4.6, 4.7 and 4.8, respectively. The short fibre also requires higher confining pressure. These results were confirmed by (Al-Refeai and Al-Suhaibani, 1998).

It was expected that the maximum dry density of optimum fibre length can provide the optimum strength of the fibre. The highest density was obtained by 19mm long fibre while the least density was obtained by 12mm long fibre as shown in Chapter Three section 3.2.3.

Figure 4.12, 4.13 and 4.14 show the shear stress-strain relationship of sand reinforced with 12mm long fibre. The shear stress changed much with an increase in the strain. The 19mm long fibre showed a reduction in shear stress with an increase in strain. But the ultimate shear strength was higher than the peak shear strength of 12mm and 50mm long fibres as shown in Figure 4.15, 4.16, and 4.17, respectively. The 50mm long fibre showed similar behaviour as 19mm long fibre. Also, the tangling and the reduction in the fibre effecting become a problem with the fibre longer than 19 mm. This was also confirmed by (Consoli et al., 2009a). Thus, the 19mm fibre length was used throughout the research.

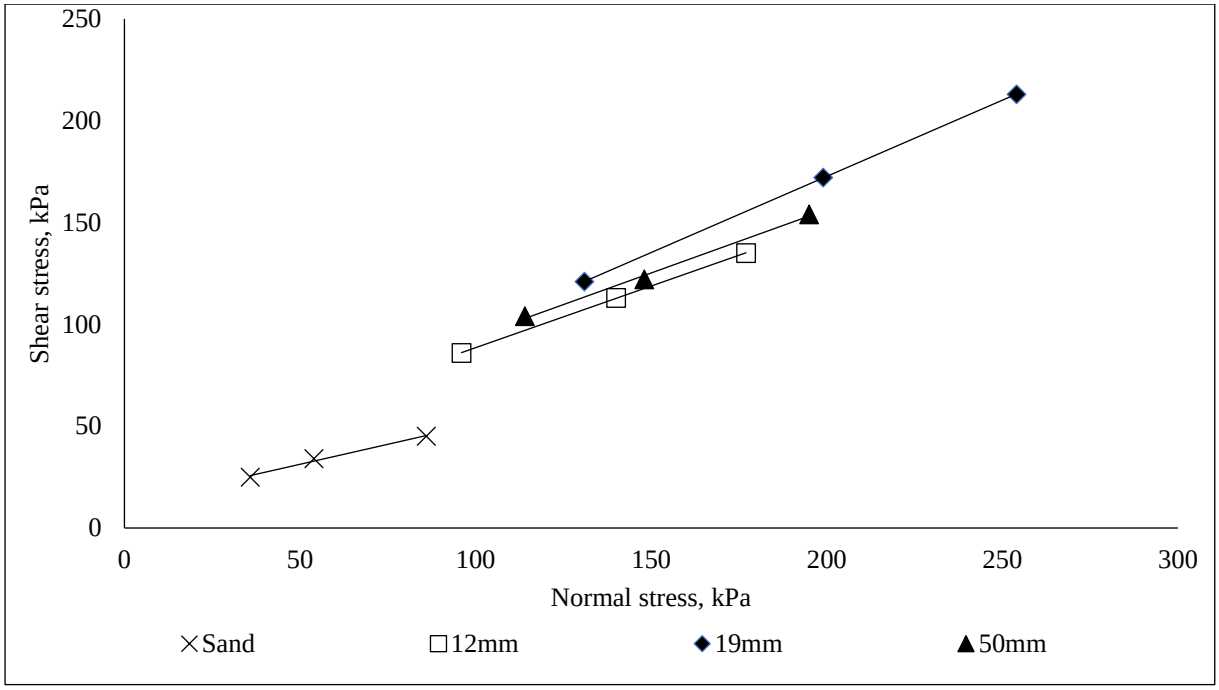

Figure 4.6 Shear stress to normal stress relation of reinforced and unreinforced sand at 80% of OMC.

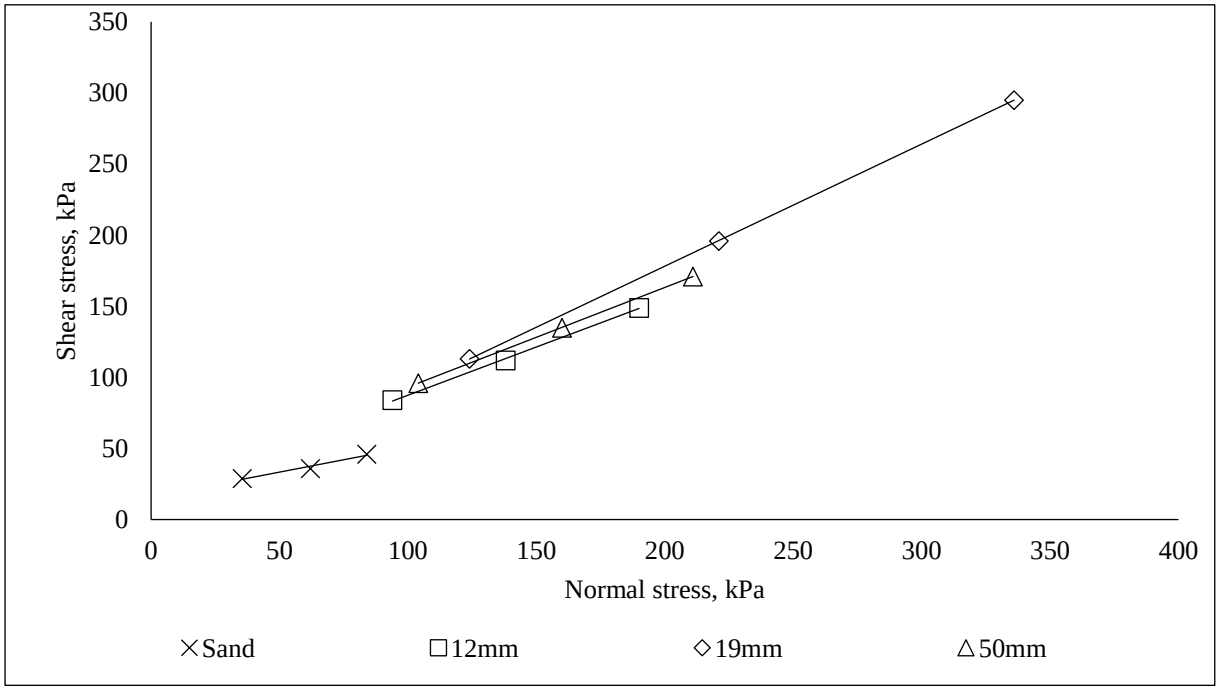

Figure 4.7 Shear stress to normal stress relation of fibre reinforced sand at OMC.

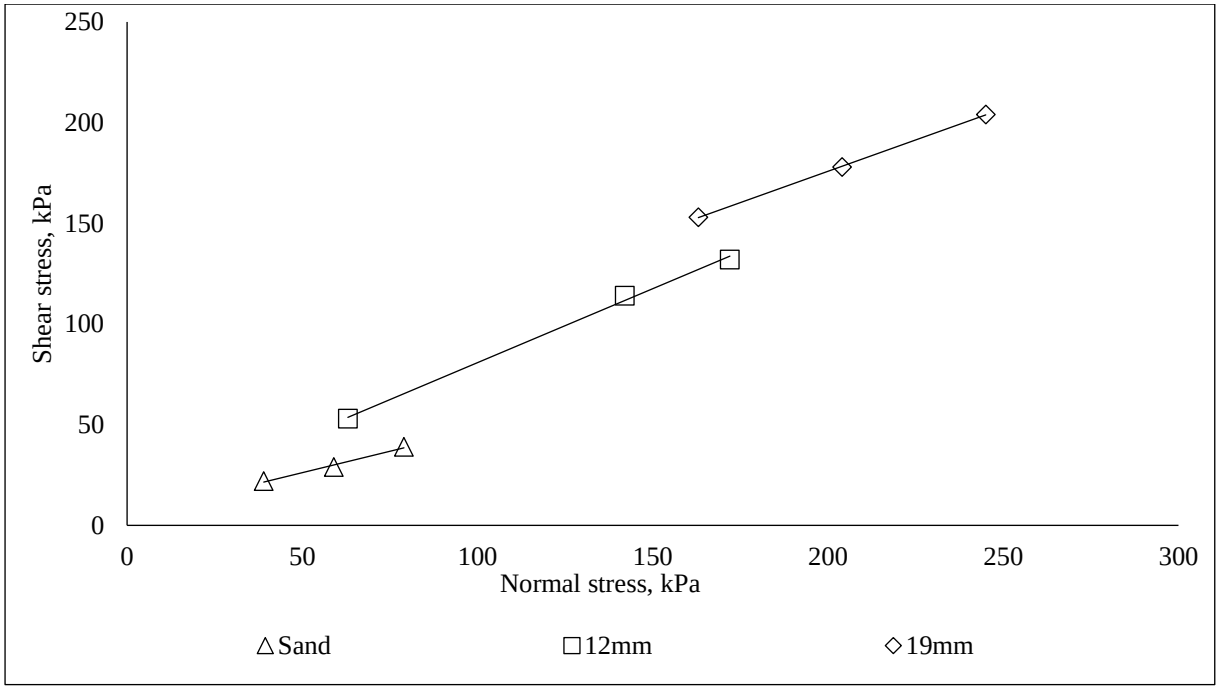

Figure 4.8 Shear stress to normal stress relation of fibre reinforced sand at 120% of OMC.

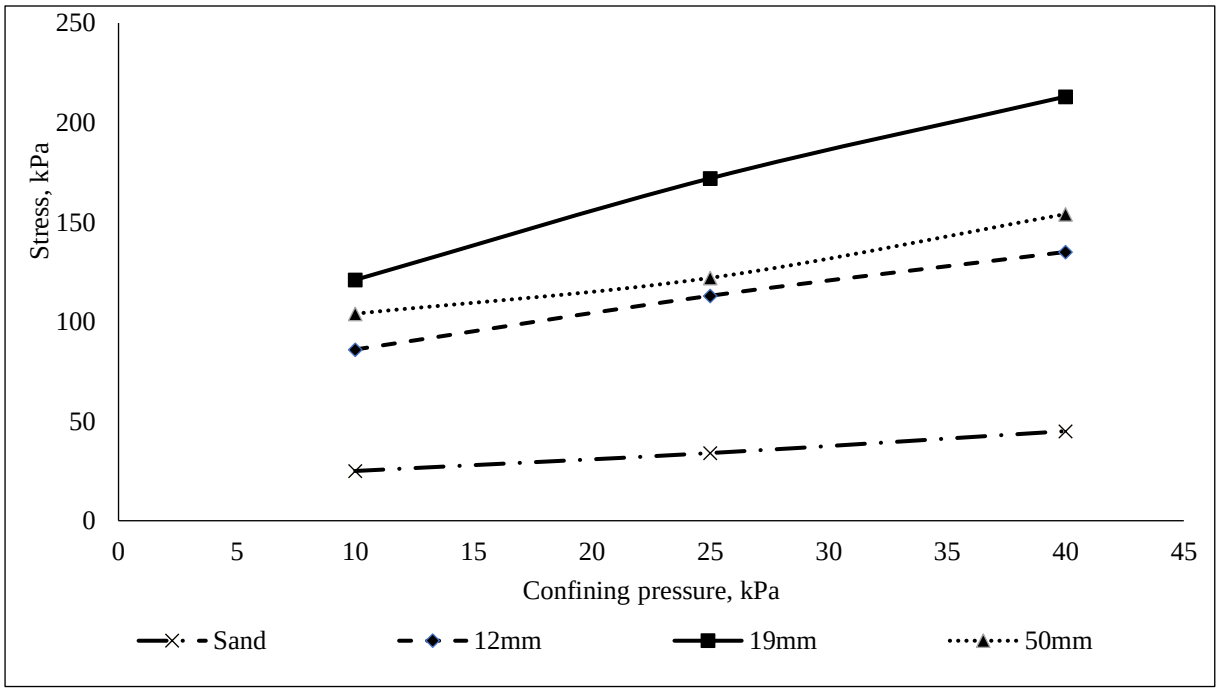

Figure 4.9 Confining stress to stress relation of reinforced & unreinforced sand at 80% of OMC.

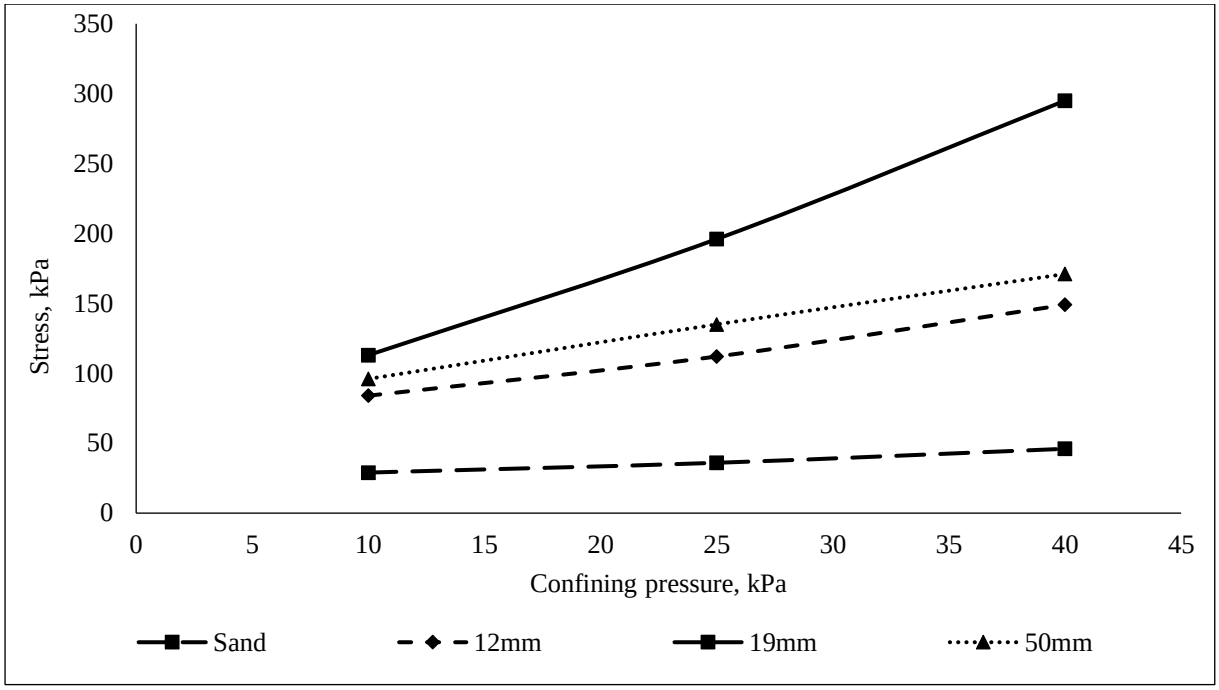

Figure 4.10 Confining stress to stress relation of reinforced & unreinforced sand at OMC.

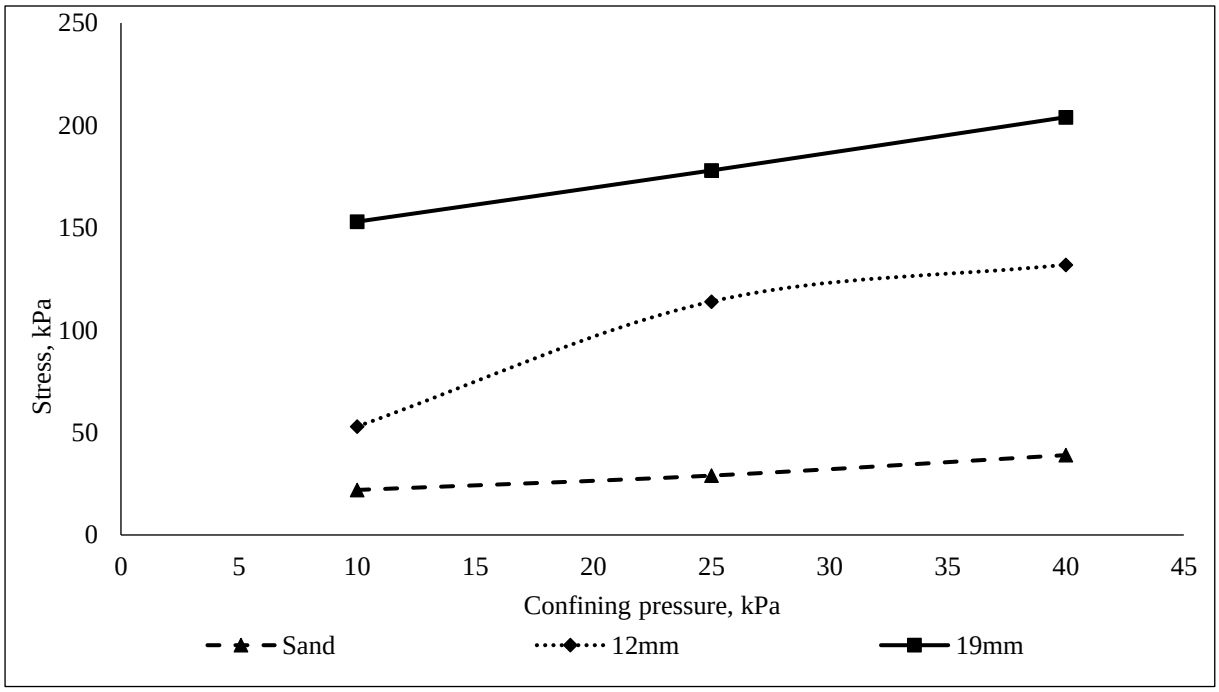

Figure 4.11 Confining stress to stress relation of reinforced & unreinforced sand at 120% of OMC.

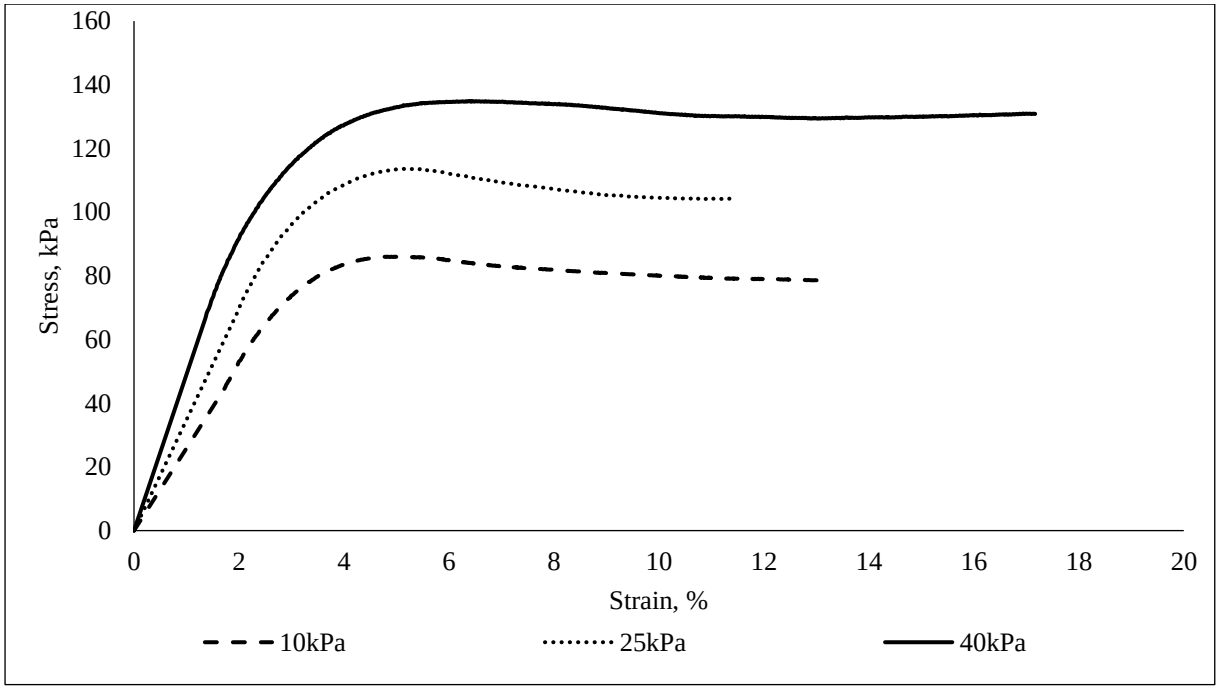

Figure 4.12 Stress-strain relationship for fibre (12mm) reinforced sand at different confining pressure and 80% OMC.

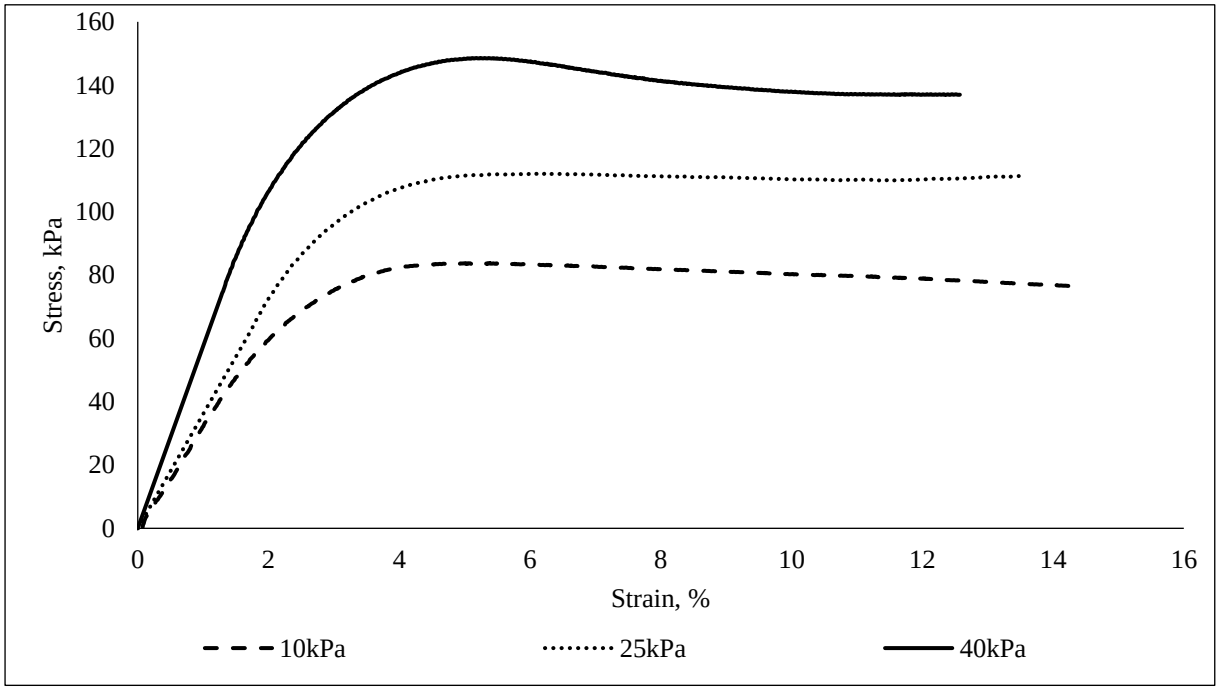

Figure 4.13 Stress-strain relationship for fibre (12mm) reinforced sand at different confining pressure and OMC.

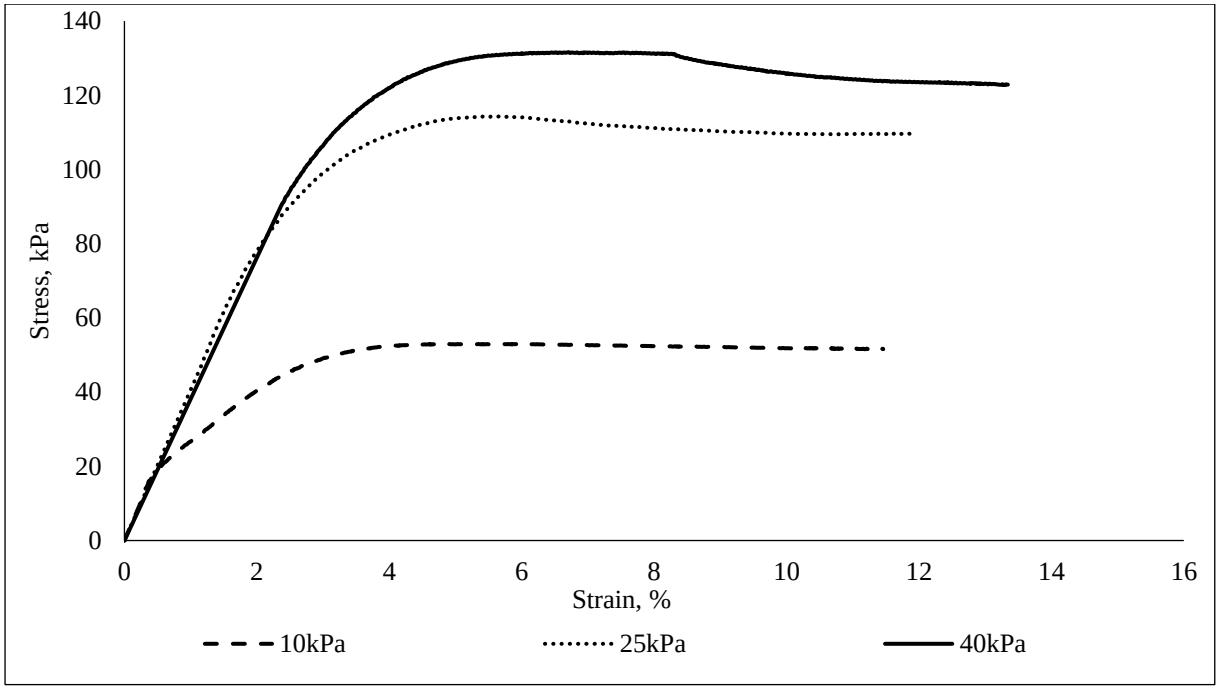

Figure 4.14 Stress-strain relationship for fibre (12mm) reinforced sand at different confining pressure and 120% OMC.

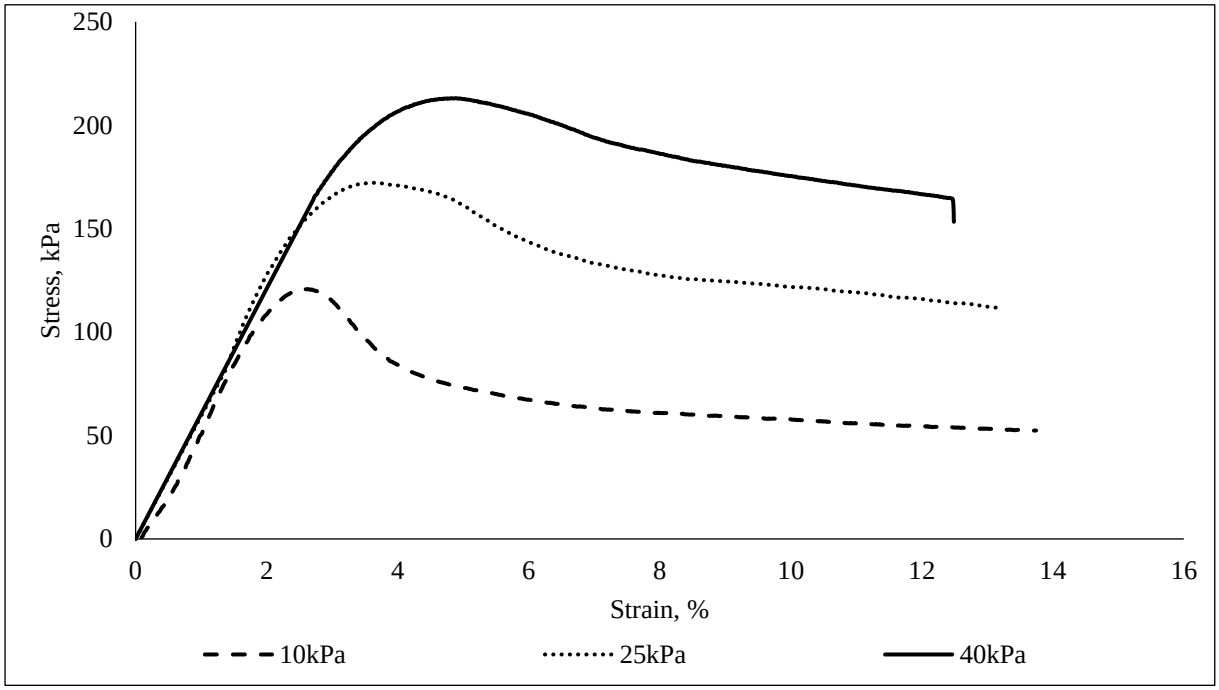

Figure 4.15 Stress-strain relationship for fibre (19mm) reinforced sand at different confining pressure and 80% OMC.

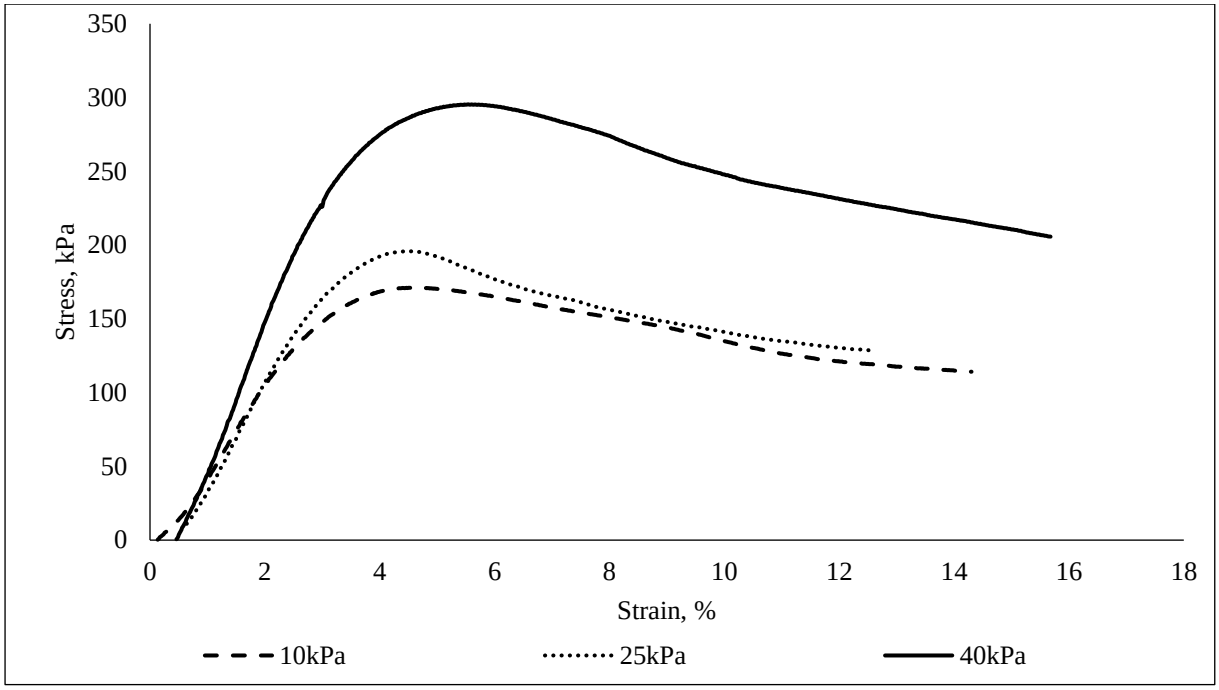

Figure 4.16Stress-strain relationship for fibre (19mm) reinforced sand at different confining pressure and OMC.

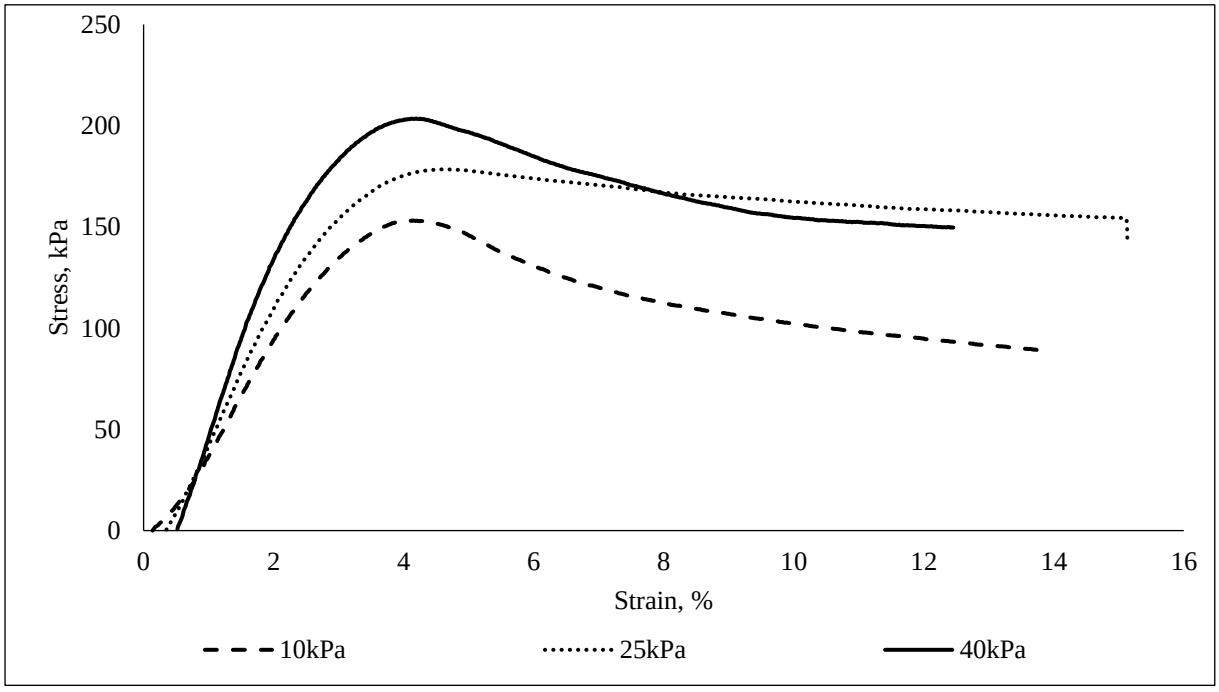

Figure 4.17 Stress-strain relationship for fibre (19mm) reinforced sand at different confining pressure and 120% of OMC.

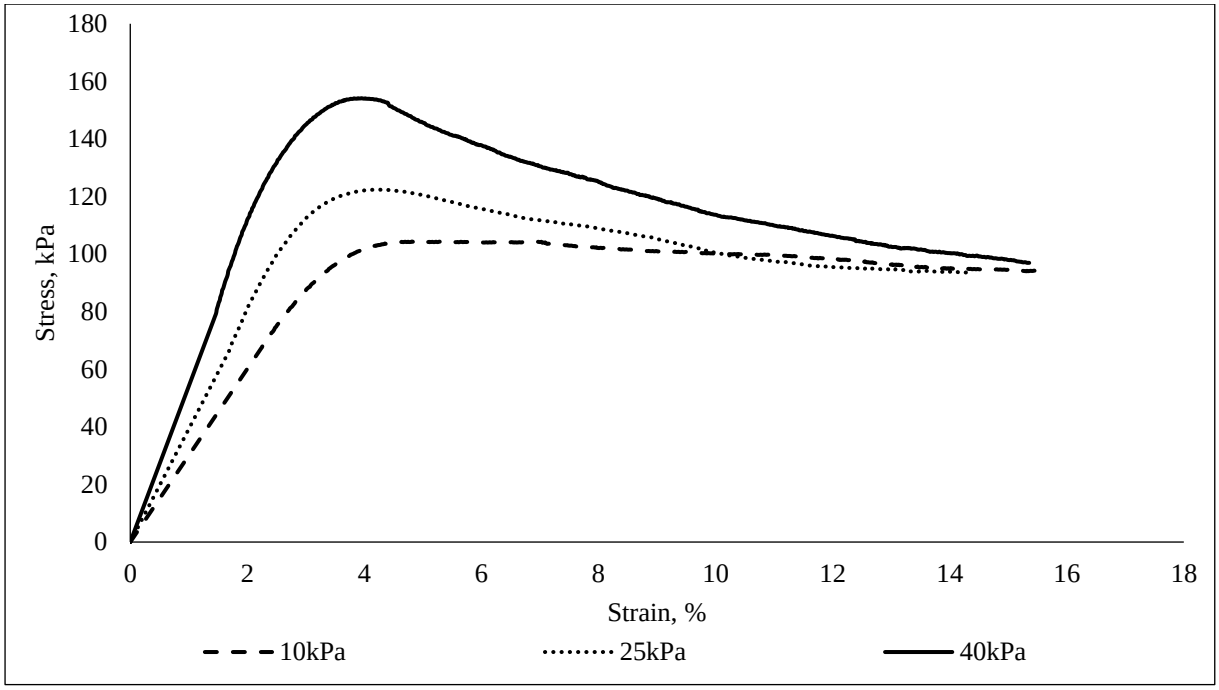

Figure 4.18 Stress to strain relation for fibre (50mm) reinforced sand at different confining pressure and 80% OMC.

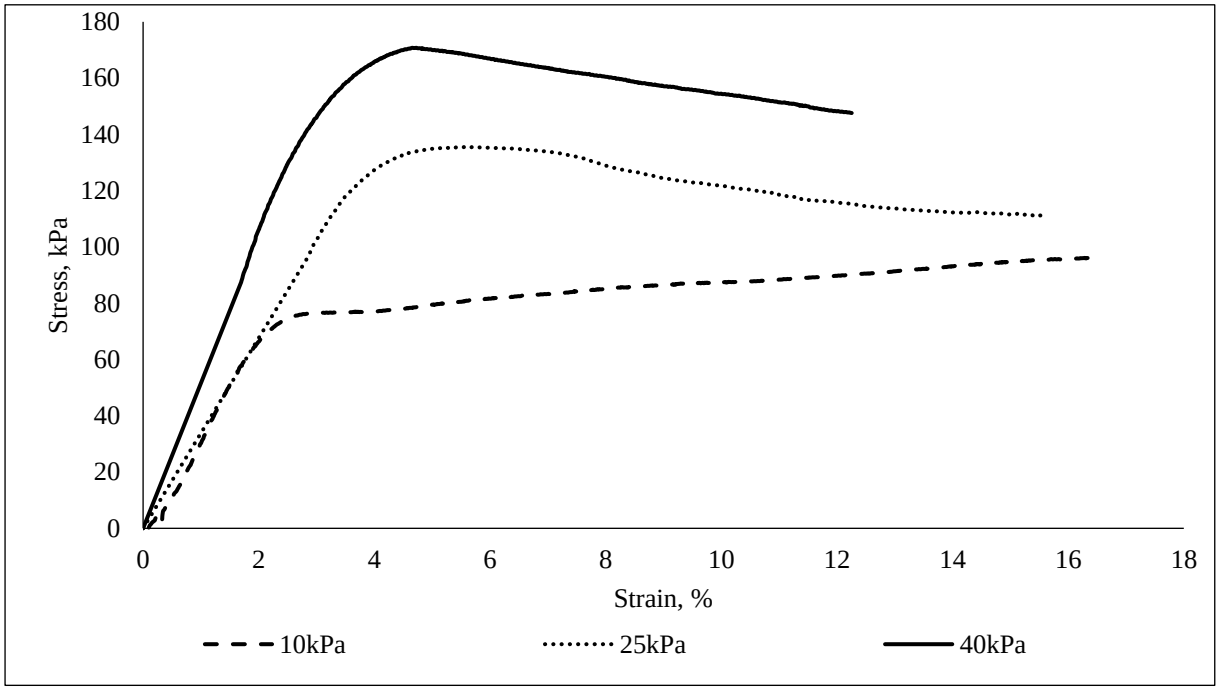

Figure 4.19 Stress to strain relation for fibre (50mm) reinforced sand at different confining pressure and OMC.

4.2.3 Fly Ash with/without Fibre Stabilized Sand

Unconsolidated undrained triaxial tests were carried out on both cured and raw fly ash samples. The samples were compacted at a different water content of 80%, ±20% of OMC and 95% of MDD. The sand stabilized with class C fly ash was also cured for 7 days in order to improve the strength. Typical shear stress at failure and normal stress relationship of raw and cured fly ash stabilized sand are plotting in Figure 4.20. Thereafter, the shear stress at failure and normal stress relationship of stabilized and unstabilized sand with fly ash are presented in Figure 4.21. It was observed that the cohesion and the internal friction angle increased with the addition of fly ash when compared with unreinforced sand.

The shear stress and confining pressure relationship illustrates the effect of water content on fly ash mixture as shown in Figure 4.22. The fly ash reduces the volume of voids, this lead to increase the density. Therefore, the required water content was reduced as shown in the compaction test results in Chapter Three section 3.2.3.

It was observed that the cementitious properties of class C fly ash led to improve the cohesion between the particles. The effect of fly ash on the internal friction angle was less than that of fibre at different water contents. For example, at OMC the internal friction angle for sand, fibre reinforced sand and fly ash reinforced sand was 19, 25, and 41 degrees, respectively. Figure 4.23, 4.24, and 4.25 showed the shear stress to strain relationship. As expected, the highest shear stress was obtained at the OMC.

Few researchers who investigated the effect of the mixture of the fibre with fly ash in the soil as (Kumar and Singh, 2008, Chauhan et al., 2008, Chore et al., 2011, Jadhao and Nagarnaik, 2008). They concluded that there was a significant improvement on the strength as well as the internal friction angle of fibre with fly ash reinforced sand. Therefore, after testing fibre

reinforced sand and fly ash stabilized sand separately; it was suggested to add 19mm fibre to the fly ash in order to improve the shear strength parameters. Due to limited time for the experimental work, the samples were compacted at 95% of MDD and OMC only. The curing period improved the shear strength of fly ash with fibre as shown in Figure 4.26. The shear stress to strain relationship was plotted in Figure 4.28 and the results show that the internal friction angle was increased when compared with fibre or fly ash alone. In addition, the mixture of fibre with fly ash showed significant improvement in peak shear strength. The reason for that the fibre with fly ash improved the interlock between the particles and the bonding increases the cohesion between the particles. Moreover, the specimen reinforced with fibre and fly ash show high strength with an increase in the strain as shown in Figure 4.28.

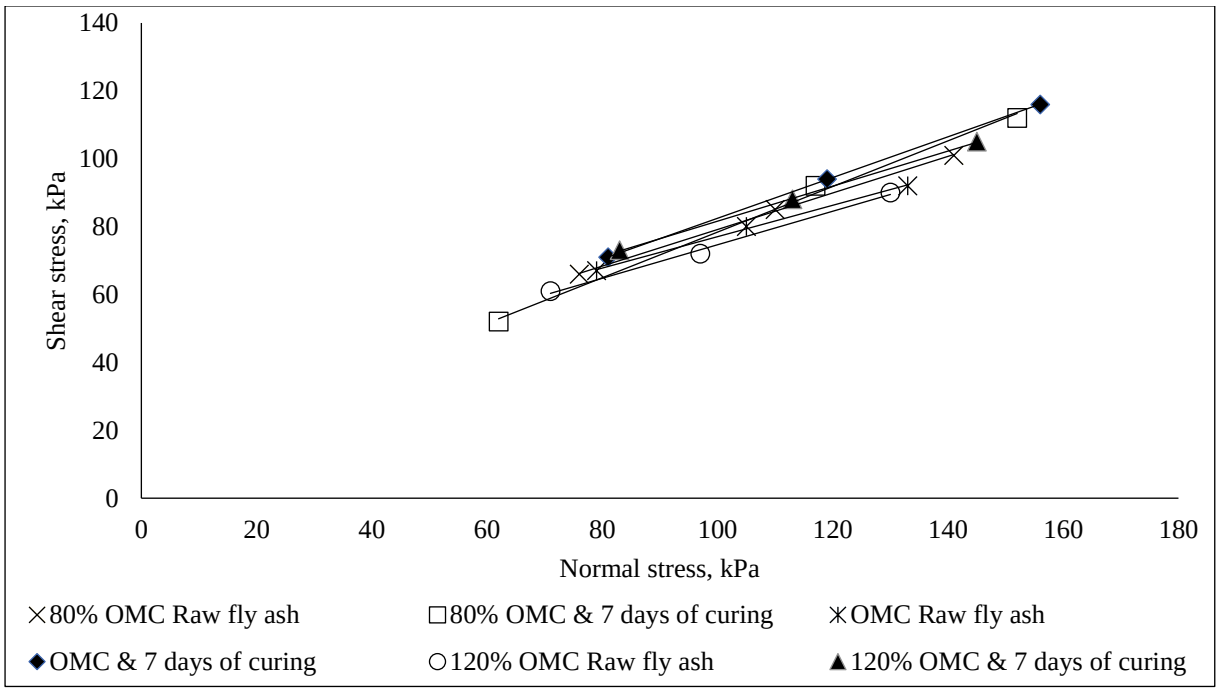

Figure 4.20 Normal stress to shear stress relation for raw and curing fly ash stabilized sand at different water content and 7 days of curing.

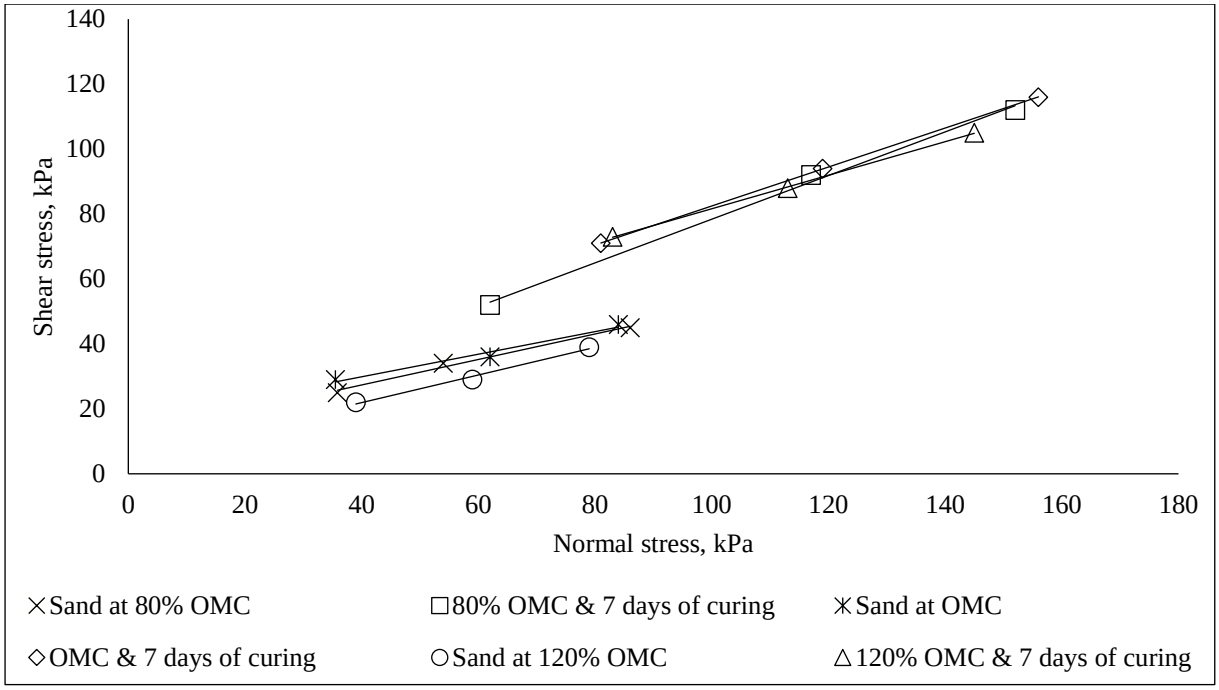

Figure 4.21 Normal stress to shear stress relation for stabilized and unstabilized sand with fly ash at different water content and 7 days of curing.

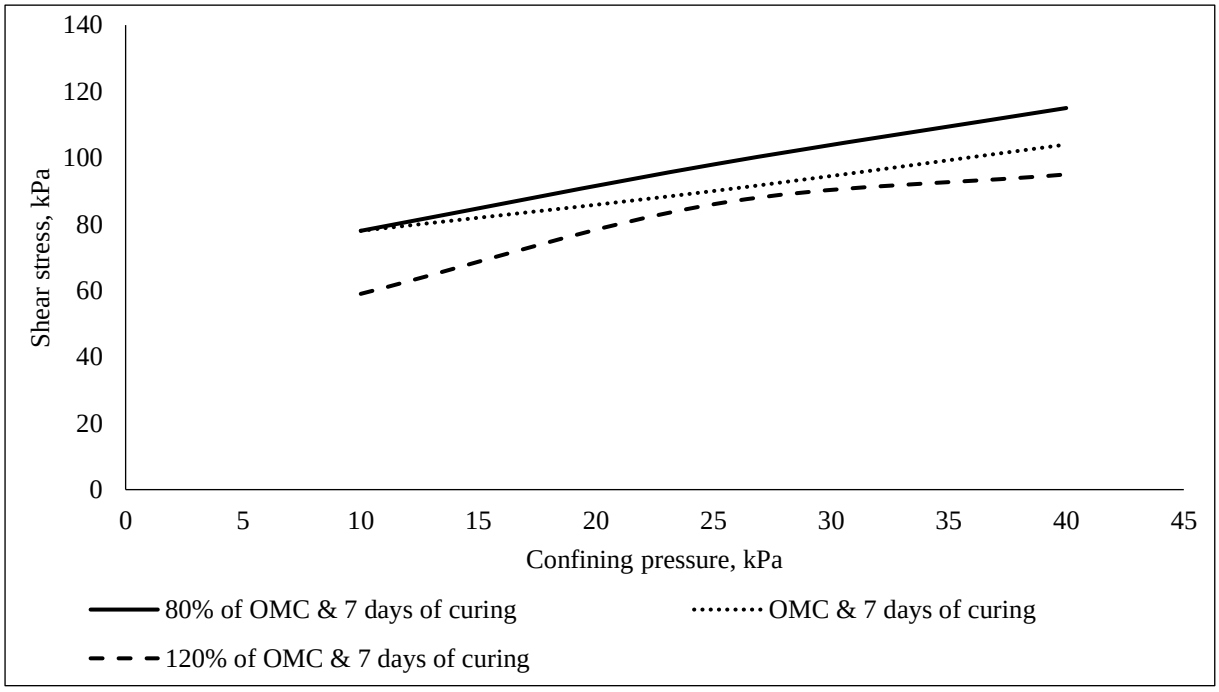

Figure 4.22 Confining stress to shear stress relation for fly ash stabilized sand at different water content and 7 days of curing

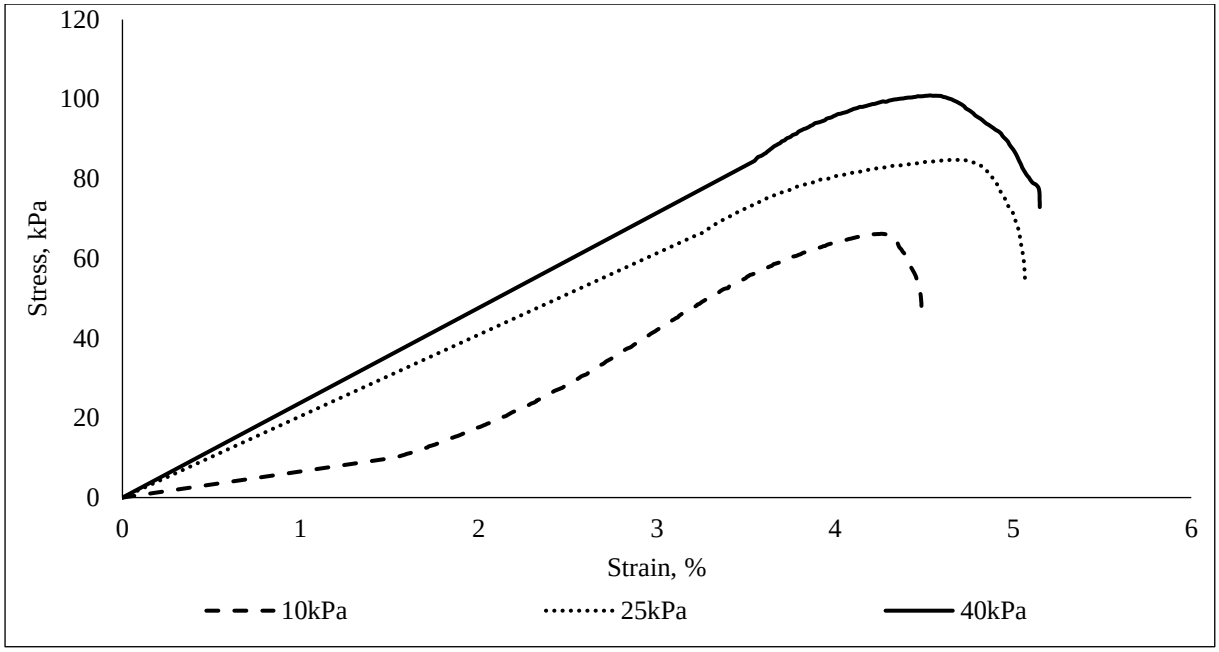

Figure 4.23 Stress to strain relation for fly ash stabilized sand at 80% of OMC and curing for 7 days.

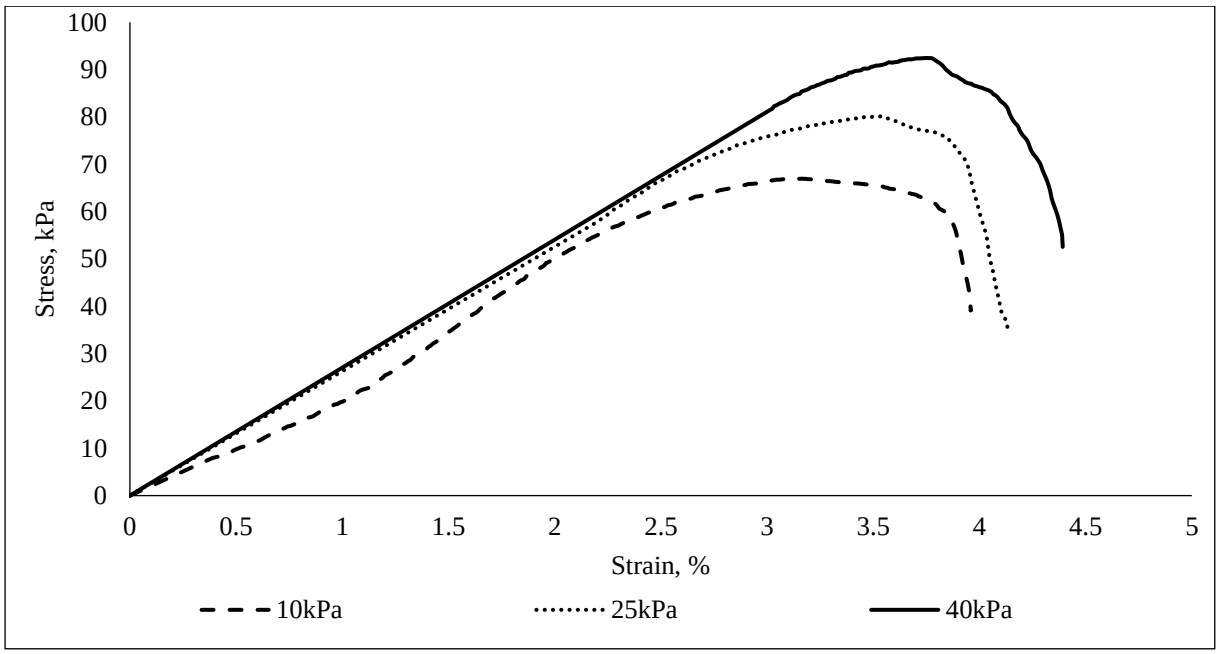

Figure 4.24 Stress to strain relation for fly ash stabilized sand at of OMC and curing for 7 days.

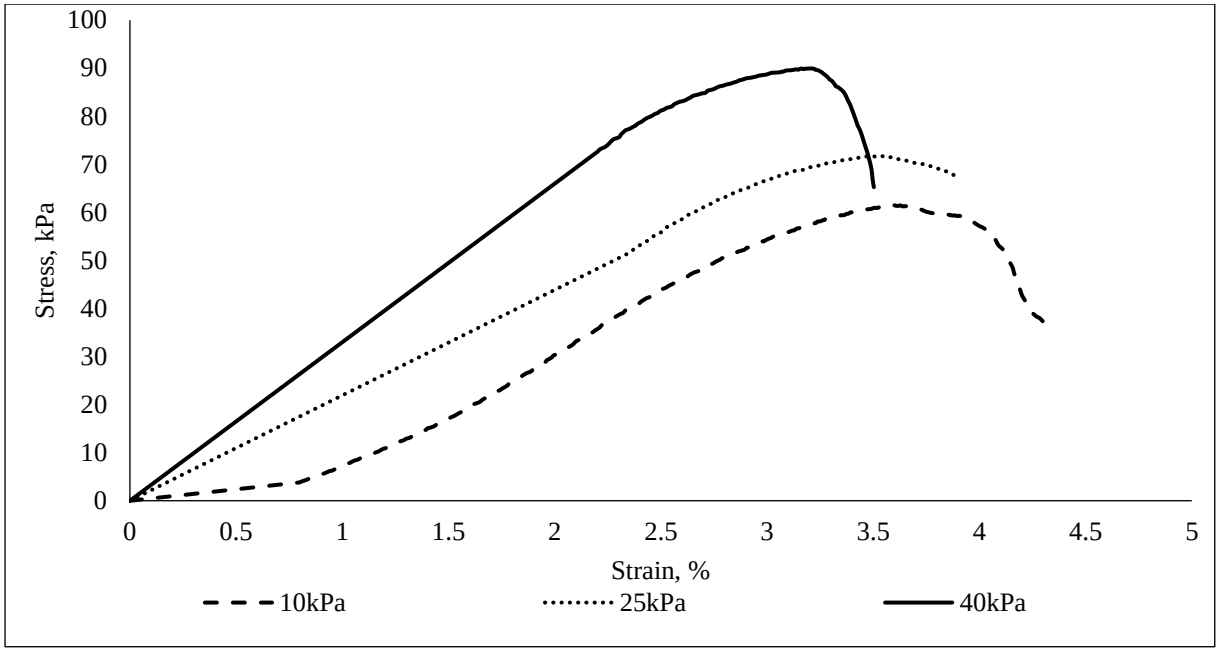

Figure 4.25 Stress to strain relation for fly ash stabilized sand at of 120% of OMC and curing for 7 days.

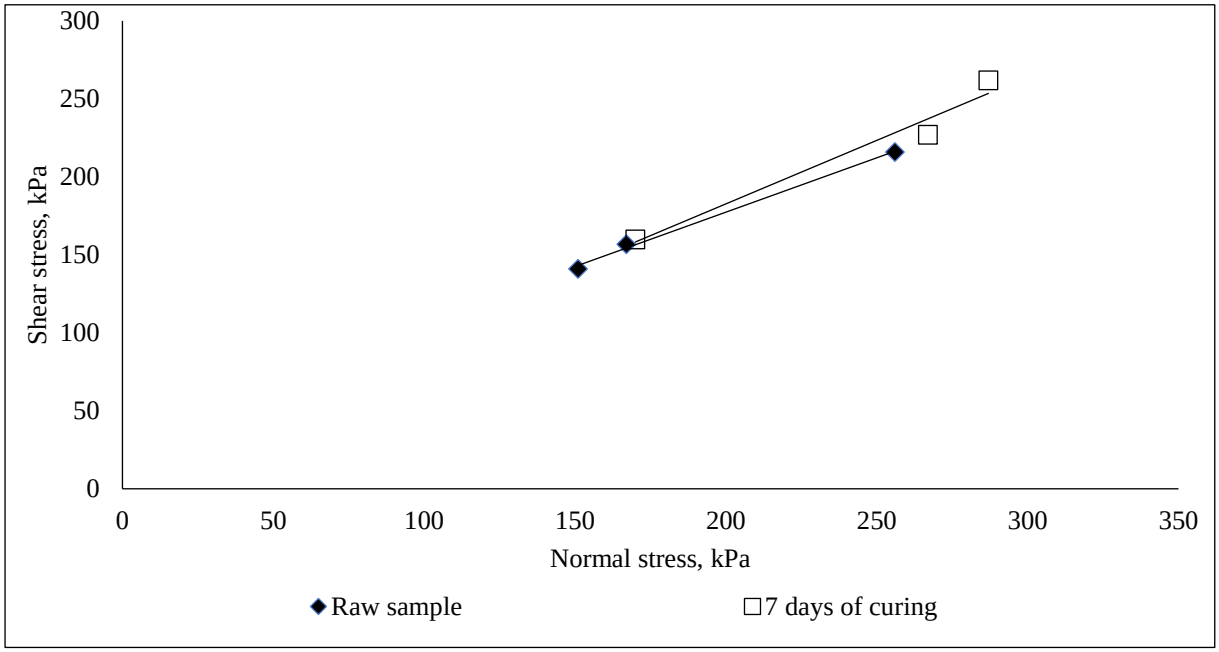

Figure 4.26 Normal stress to shear stress relationship for fly ash and fibre reinforced sand at OMC and 0 & 7 day of curing.

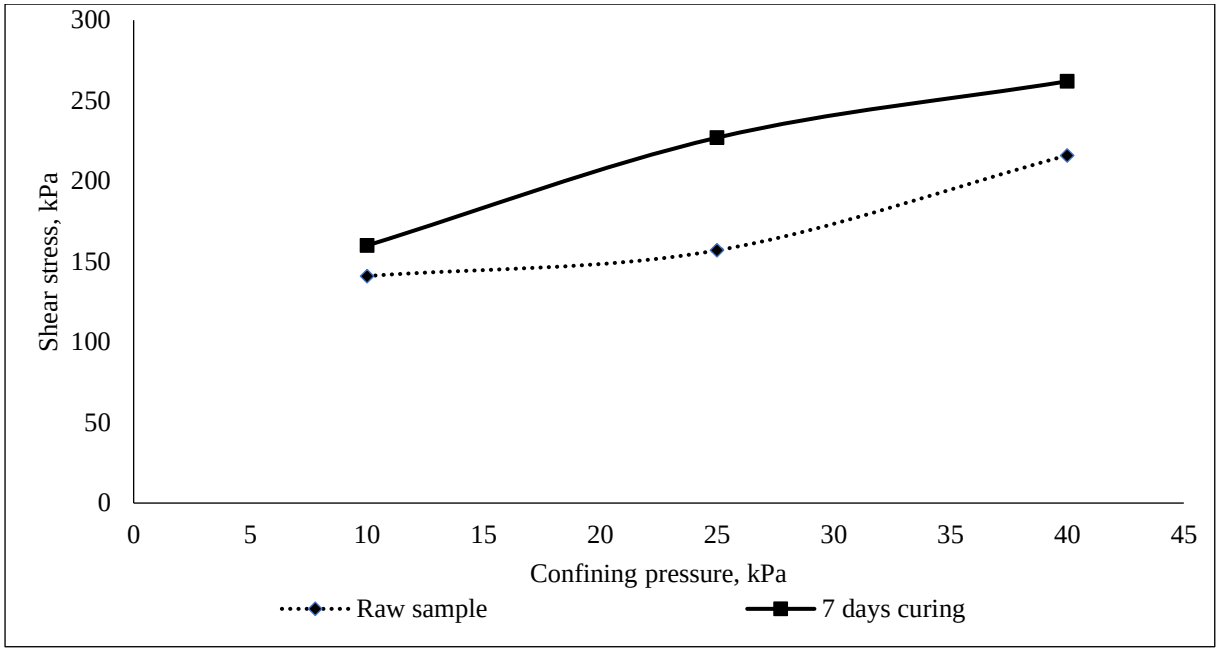

Figure 4.27 Confining stress to shear stress relationship for fly ash and fibre reinforced sand at OMC and 0 & 7 day of curing.

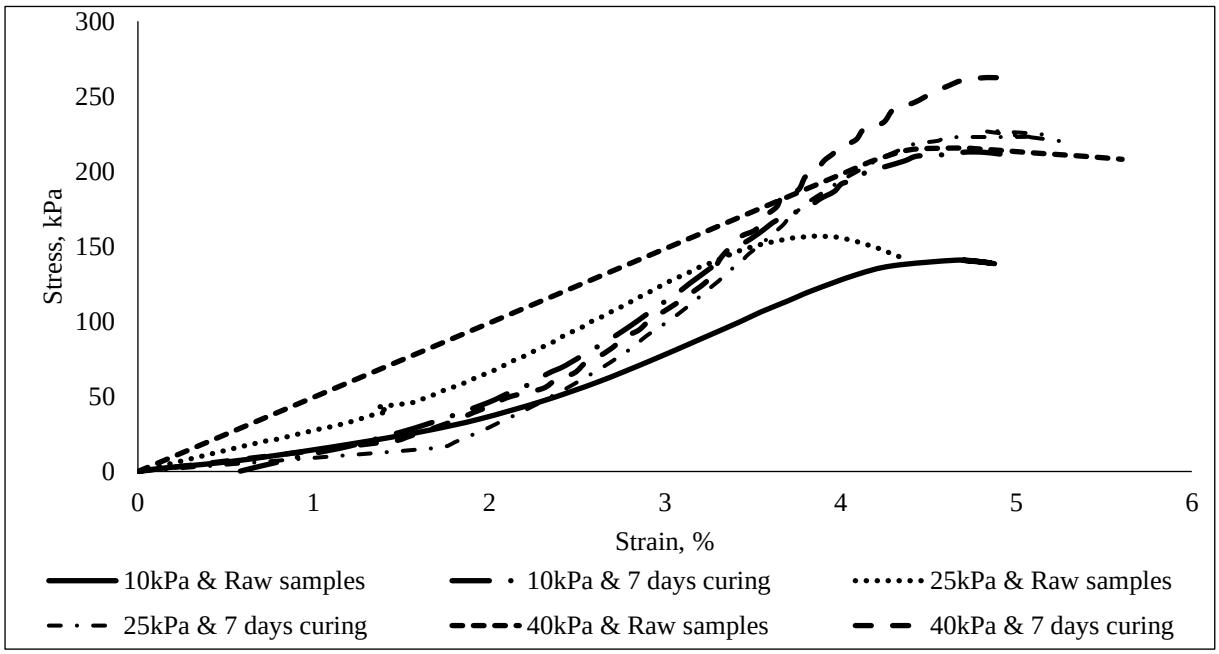

Figure 4.28 Stress to strain relationship for raw and cured fly ash with fibre reinforced at OMC and 7 days of curing.

4.3 Unconfined Compressive Strength Test

The purpose of the unconfined compressive strength test is: to develop a correlation model to obtain the resilient modulus, to compare the strength of different stabilizers and reinforcement materials at different water contents. Samples dimensions were 100mm in diameter and 200mm in height. They were prepared at 95% of maximum dry density and different water contents of 80%, 100%, and 120% of optimum water content. The strain rate was adjusted at 1.5% (Head, 1994). The samples of fly ash and slag were cured for 0, 7, 14, 24, and 56 days and tested. The samples were tested using a 10kN load cell with unconfined compressive test apparatus while the slag samples were tested in a 50kN load cell.

4.3.1 Sand

Unconfined compressive strength test was conducted on unreinforced soil at different water content. Figure 4.29 demonstrates the stress to strain relationship of sand. The results indicate that the water content does not have much effect on the strength at 80% and OMC.

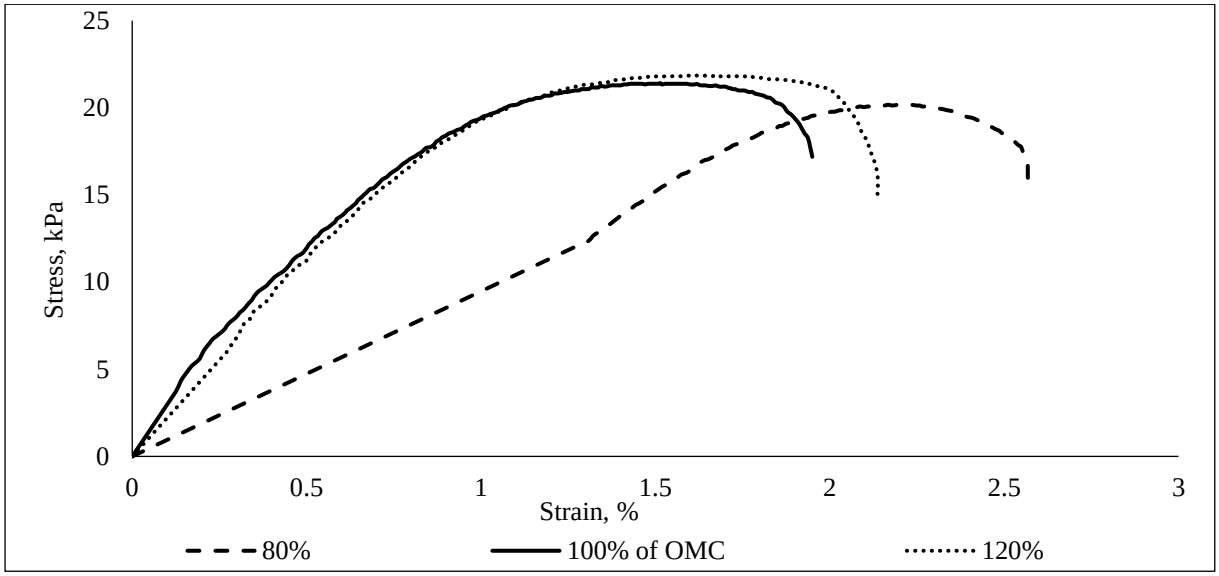

Figure 4.29 Stress to strain relationship of unreinforced sand with three different moisture contents.

4.3.2 Fibre Reinforced Sand

Unconfined compressive strength test was conducted on 19mm fibre length only. As a result of the unconsolidated undrained triaxial test, 19mm long fibre has the highest shear strength, therefore, it was nominated to use throughout the research. Figure 4.30 represents the stress-strain relationship of fibre reinforced sand at different water contents. The results show that the compacted samples at OMC demonstrate higher stress. This improvement can be explained by the interlock and rearrangement the particles.

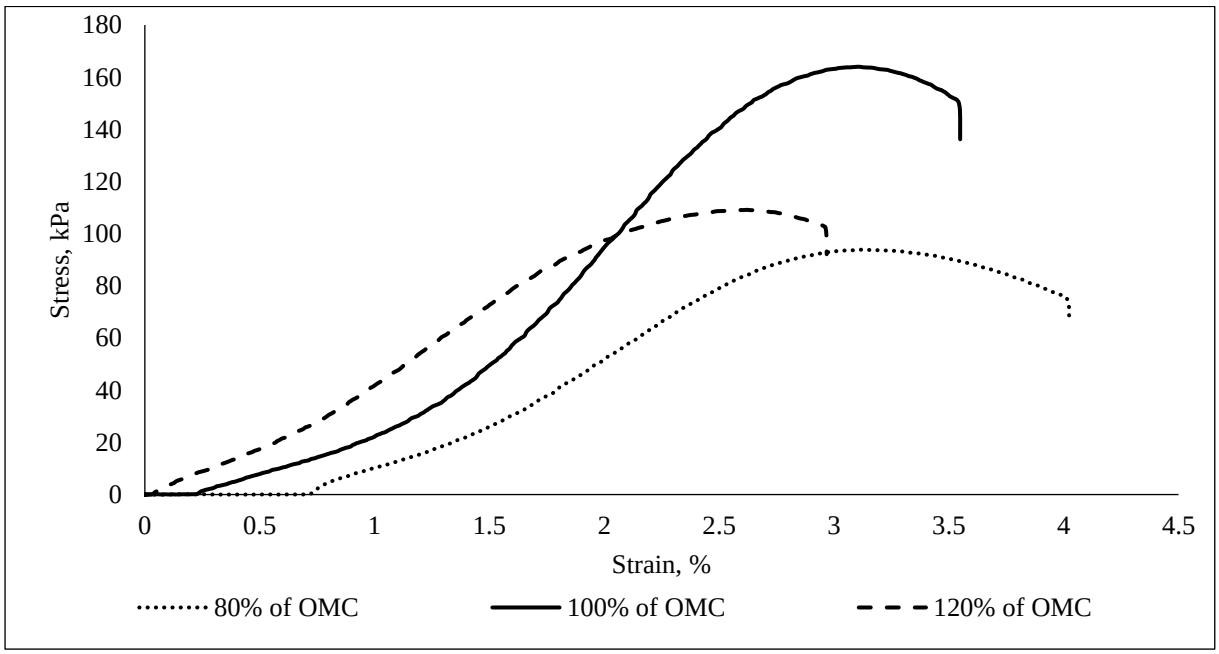

Figure 4.30 Stress to strain relationship of fibre reinforced sand with three different moisture contents.

Figure 4.31 provides a mechanism for fibre and soil interaction. The distribution of fibre in the soil can be explained as bending and interleaving mechanism. After mixing the fibre with sand, a lot of curved transitions of fibre were gained that is in the bending case. During the loading, the fibre was in tension, therefore in the soil, the curved fibre produced both friction and pressure, and this was the sense of using fibre to reinforce the soil. On the other hand, when the fibres were loaded, and because of the interwoven of the fibre in the soil, the

displacement took place and was prevented by Figure 4.31. This explains the interleaving mechanism.

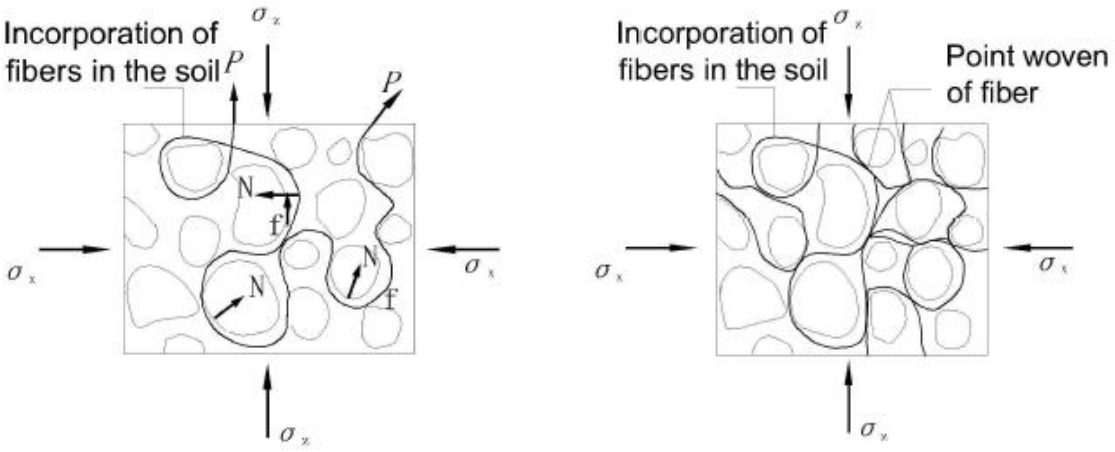

Bending mechanism **Interleaving mechanism**

Figure 4.31 The mechanism of fibre reinforced sand.

4.3.3 Fly Ash with/without Fibre Stabilized Sand

The pozzolanic reaction of the Class C fly ash played the principal role in improving the strength as shown in Figure 4.32. It demonstrated strain to stress relationship after 0 and 7 days of curing at OMC. Figure 4.33 shows the stress to strain relationship after different curing periods and OMC. The fly ash increases the density by filling the voids. Also, the bonding between the particles was improved. This indicated that there was a significant improvement in strength.

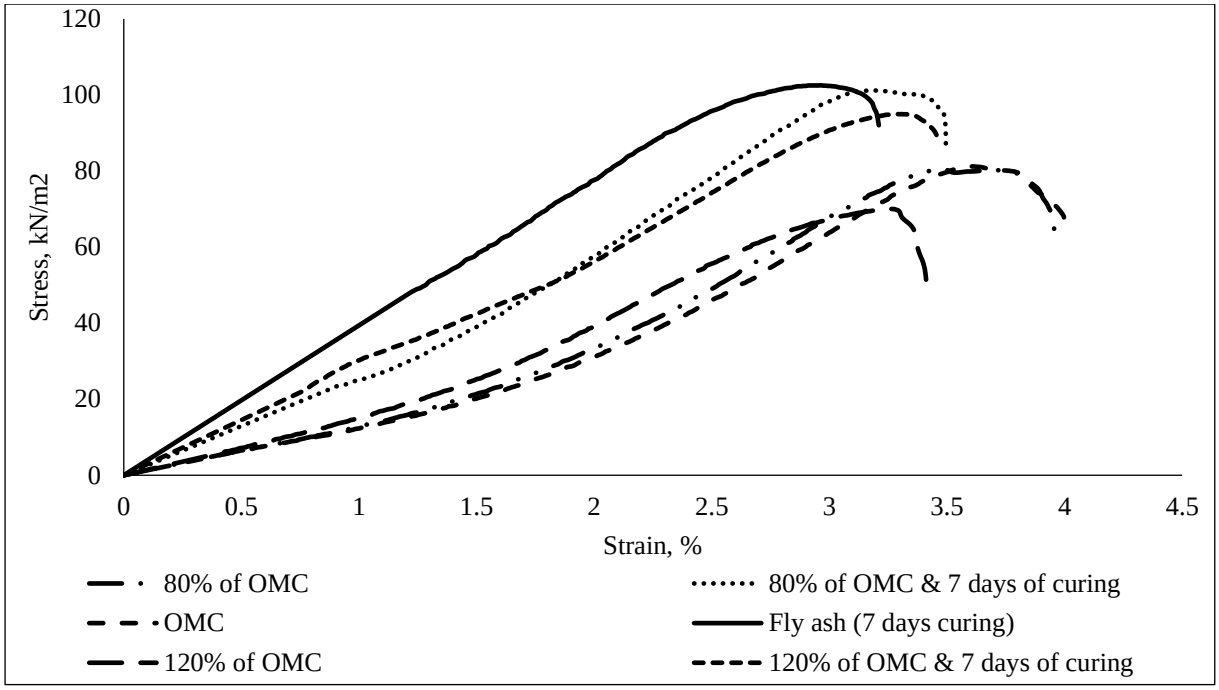

Figure 4.32 Stress to strain relationship of fly ash stabilized sand with different moisture contents and 0 & 7 days of curing.

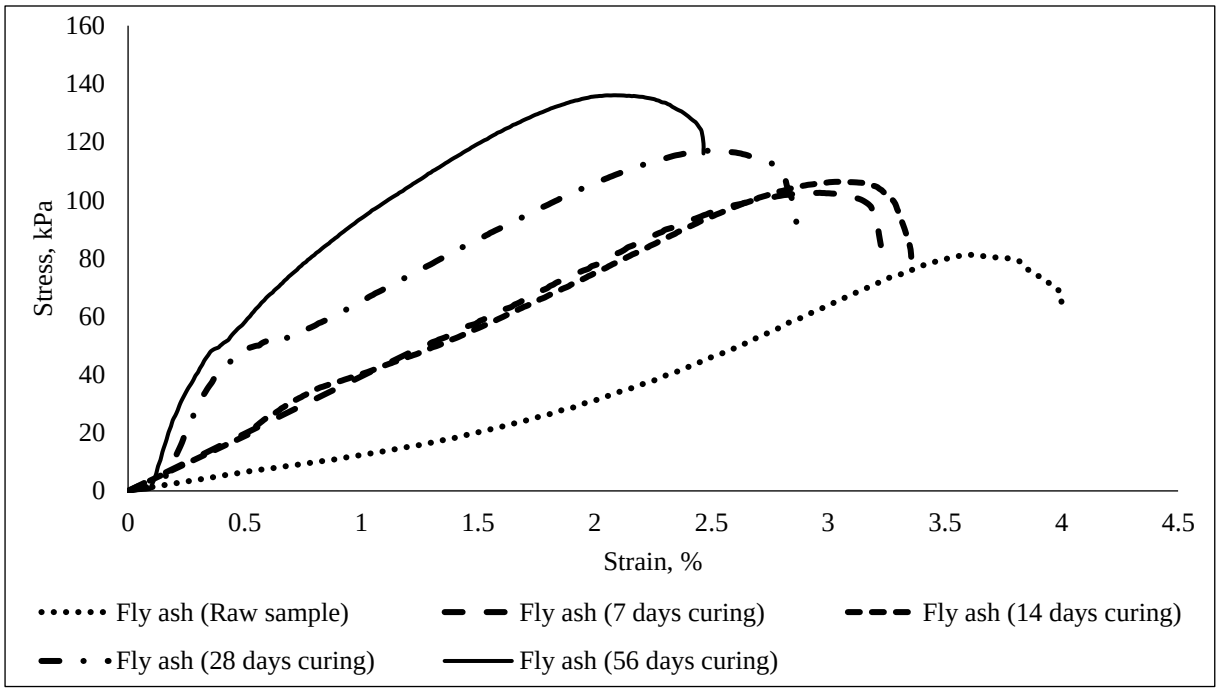

Figure 4.33 Stress to strain relationship of fly ash stabilized sand at OMC and different curing periods.

The unconfined compressive strength of fly ash with/without fibre were tested. The incorporation of the fibre of 0.5% of the dry weight of soil with the fly ash increased the

unconfined compressive strength. However, the fibre increases the strength but it was not linear. The fibre incorporated into granular soil improves its strength by interacting with the soil particles mechanically through surface friction and also by interlocking as shown in Figure 4.34.

The bonding and interlocking between the particles and fibre caused the transfer of the tensile strain developed in the mass to the reinforcement and thereafter, the tensile strength of the reinforcement was mobilized and helps in improving the load capacity of the reinforced mass. Figure 4.34 demonstrates stress to strain relationship of fly ash and fly ash with fibre for raw and cured samples. The graph shows the improvement in the use of fibre to improve shear strength. This indicates that the inclusion of fibre gives ductility to the specimens. It was further noticed that the reduction in the post-peak strain of a reinforced sample is comparatively lower than the unreinforced sample.

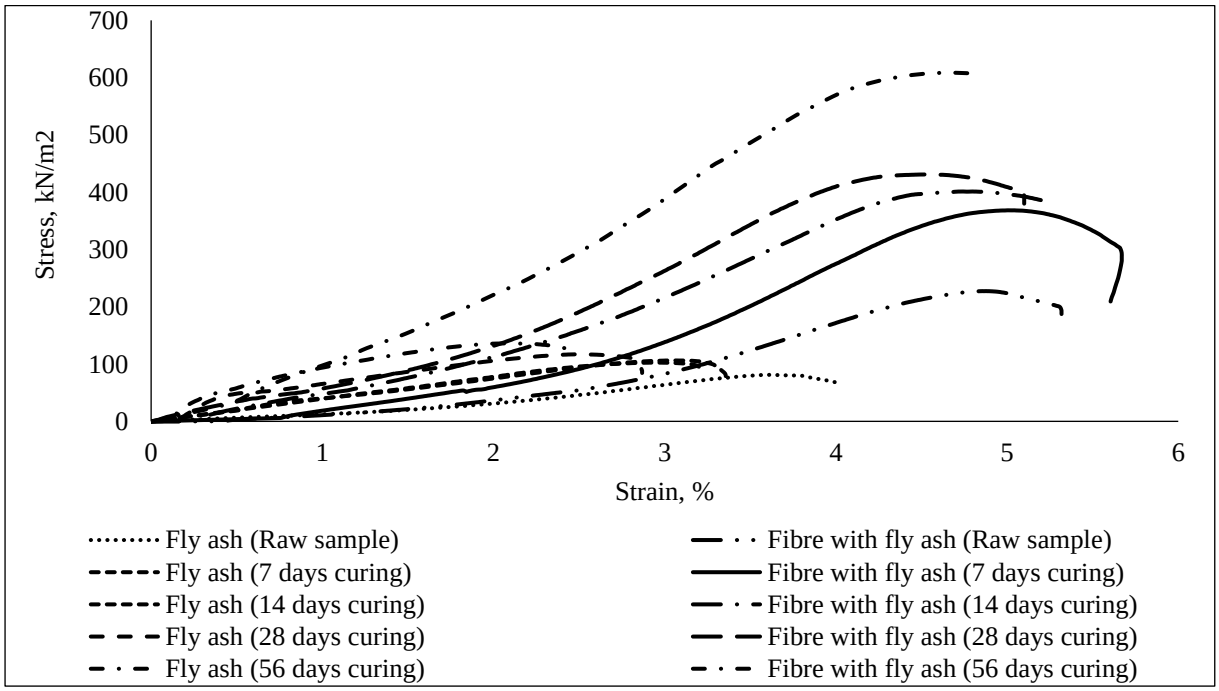

Figure 4.34 Comparison of stress to strain relationship of fly ash and fly ash with fibre stabilized sand at OMC and different curing periods.

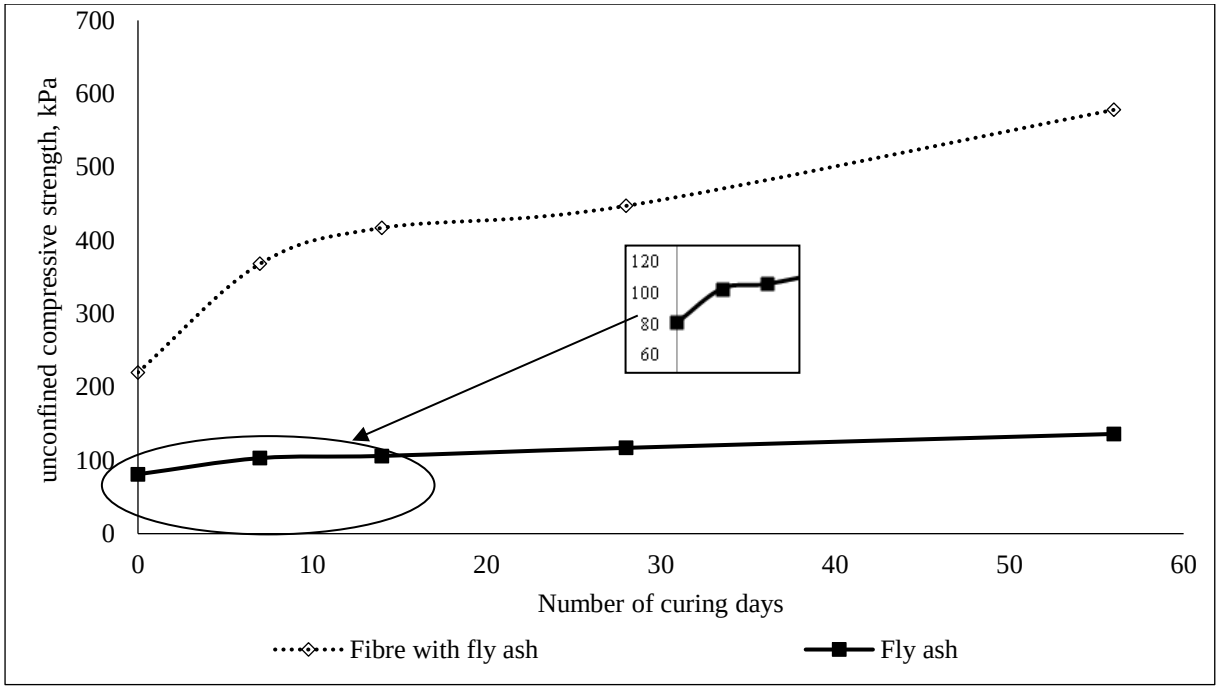

Figure 4.35 UCS to different curing period's relation of fly ash and fly ash with fibre reinforced sand at OMC.

4.3.4 Slag with/without Stabilized Sand

Vitrified slag was tested by unconfined compressive strength test. Keeley et al. (2017) stated that the strength of activated slag develops on the percentage of slag dissolution in an alkaline solution. The chemical reaction decreases the polymerisation of slag. It was confirmed that the chemical composition of the slag can be increasing the strength after reacting the slag.

Although numbers of inactivated samples were tested, the results did not show much improvement as shown in Figure 4.37. Thereafter, the slag was activated by the alkaline solution (Sodium hydroxide). The slag was mixed with 40% of the dry weight of soil. The samples dimension is 100 in diameter and 200mm in length and compacted at 95% of MDD and OMC. The samples were cured for 7, 14, 28, and 56 days, respectively. The results are illustrated in Figure 4.38. The test was carried out on both slag and slag with fibre. It can be said that the slag improvement is linear while the slag with fibre shows the high strength at the beginning then gradually increasing. Figure 4.36 shows the behaviour of failure for slag

stabilized sand with/without fibre. As mentioned in Chapter Three, it was not possible to test the samples of slag or slag with fibre by triaxial test apparatus.

(a) **(b)**

Figure 4.36 Unconfined compressive strength test: (a) Slag stabilized sand, (b) Fibre with slag stabilized sand.

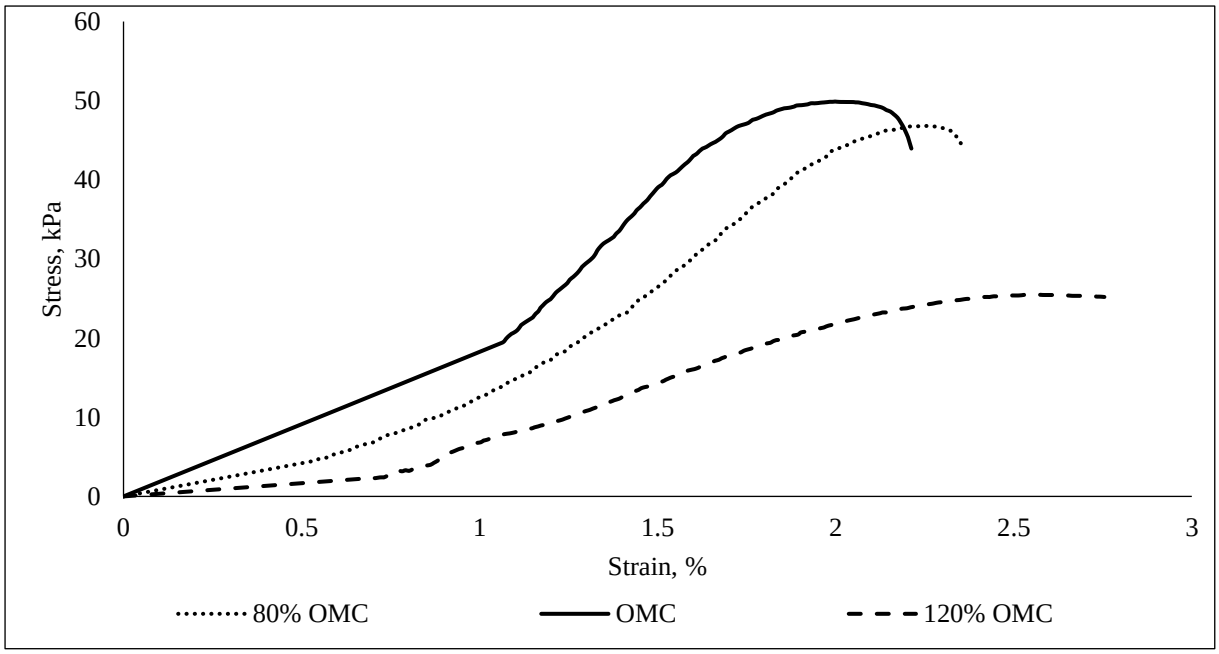

Figure 4.37 Stress to strain relation for raw slag stabilized sand.

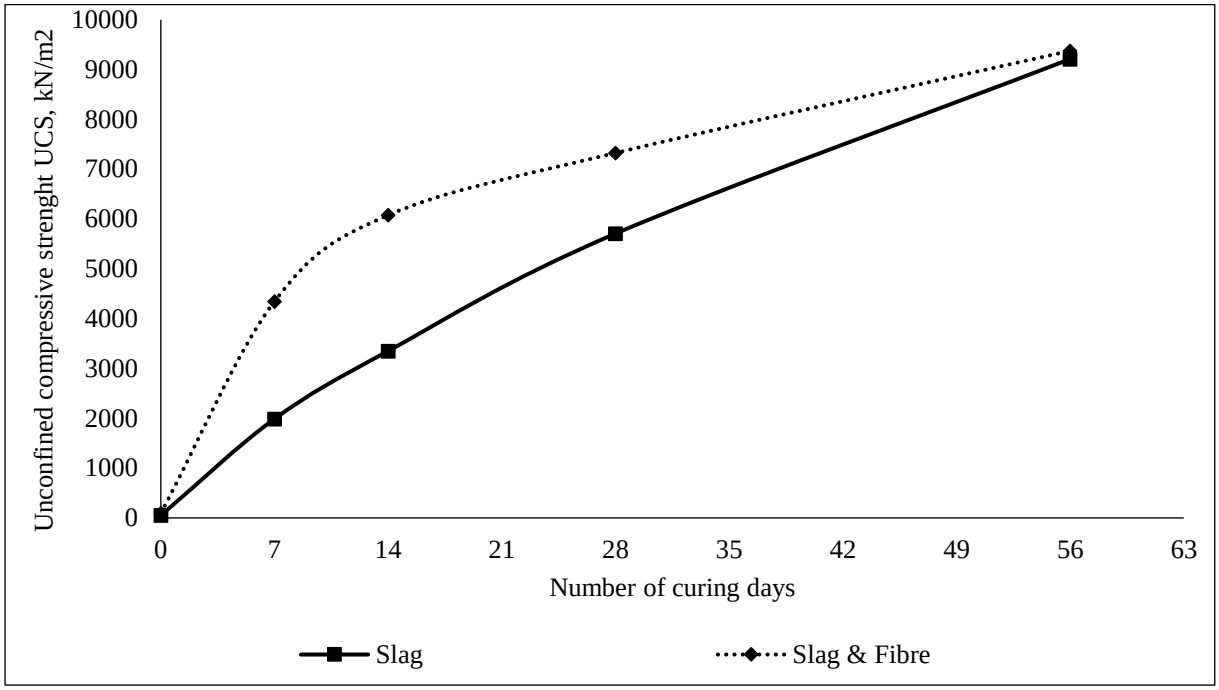

Figure 4.38 UCS to different curing period's relation of slag and slag with fibre stabilized sand at OMC.

4.4 Discussion

4.4.1 Unconsolidated Undrained Triaxial Test Results

4.4.1.1 Fibre reinforced sand

Results of the unconsolidated undrained triaxial test together with results of other researchers (AI-Refeai, 1991, Al-Refeai and Al-Suhaibani, 1998, Consoli et al., 2003, Consoli et al., 2007a, Diambra et al., 2010) were demonstrated in Figure 4.39 in terms of the ratio of shear strength to confining pressure. 19 mm fibre length showed significant improvement in shear strength against the confining pressure. The previous studies and the current study indicated that the optimum fibre content is between 0.5% and 1% of the dry weight of soil. Also, the fibre diameter affects the strength of the samples. Also, it was observed that the density was decreased with reinforced sand by Polypropylene (PP) fibres; this finding was confirmed in the literature review.

It can be concluded that the fibre decreases the density but increase the interlocking between the particles. This could be explained by the difference between the voids ratio in the current research and (Diambra et al., 2010) investigation. The voids ratio (Diambra et al., 2010) was higher than that in the current research. This was due to the difference in fibre length and the fibre should be considered as a part of the solid. On the other hand, increasing the fibre length at the constant fibre content could create a sponge effect as stated in (Santoni et al., 2001).

In addition, the inclusion of fibre in sand decreases the density. It increased due to the voids between the particles. This problem reduced with increase the fine or with fine soil (Diambra et al., 2010). Thus, the fibre diameter and particles size should be taken into account.

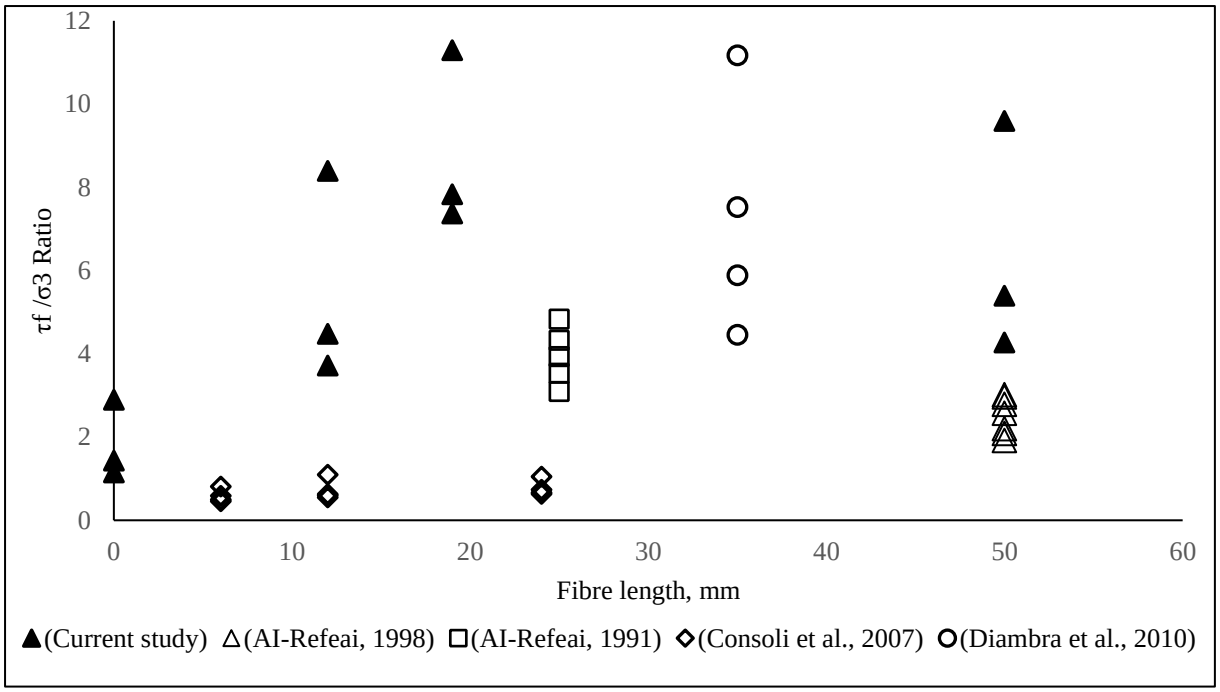

Figure 4.39 Normalised shear stress against PP fibre length and sand soil.

Figure 4.40 illustrates the principle of stress against the confining pressure for the current research and the available published data. The confining pressure to principal stress relationship shows a similar trend for the different fibre dimensions into the sand while the

19mm long fibre shows an ideal increase in shear strength with increase in the confining pressure. On the other hand, it is concluded that the fibre diameter is also important as well as the fibre length (AI-Refeai, 1991, Al-Refeai and Al-Suhaibani, 1998, Diambra et al., 2010, Consoli et al., 2009a). The particles size should be equal or near to fibre diameter then the fibre length is determined.

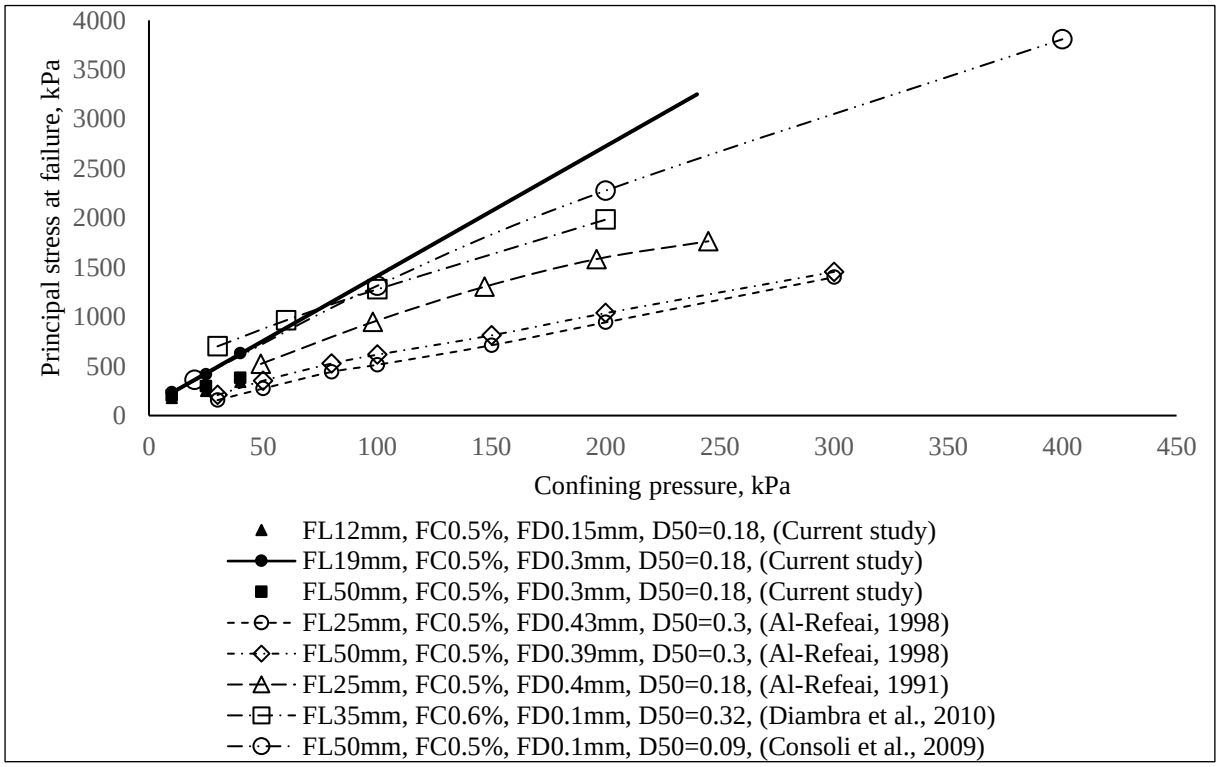

Figure 4.40 Principal stress to confining stress relationship for different fibre dimensions reinforced sand (FL=fibre length. FC=Fibre content & FD=Fibre diameter).

4.4.1.2 Fly ash stabilized sand

Figure 4.41 represents the results of the current study and the results of previous research for fly ash and fly ash with fibre reinforced sand. Chauhan et al. (2008) used fibre of 20mm long fibre and 0.048 fibre diameter and 1% fibre content with 30% of fly ash. This was because the soil was silty sand and its average particles size is 0.11mm and 1.1% of the maximum voids ratio. Also, higher confining pressure was applied. The results could be justified by the

high voids ratio of the silty sand as shown in Figure 4.42. The researcher used the fly ash to fill the voids while the fibre increases the interlocking between the particles. This result also supports the conclusion of the importance of fibre diameter by using 0.048mm fibre diameter.

In the current study, the trend line for fly ash with fibre shows that the fine proportion should be increased to a certain amount to fill the voids between the particles and between the fibre and particles. In the current study, class C fly ash was used to stabilized sand and the benefit of using class C could be seen by comparing the results with (Kaniraj and Gayathri, 2003) results. The 30% of class C fly ash instead of 50% of class F fly ash was used. Both results show the same shear strength but with different proportion and properties of the fly ash.

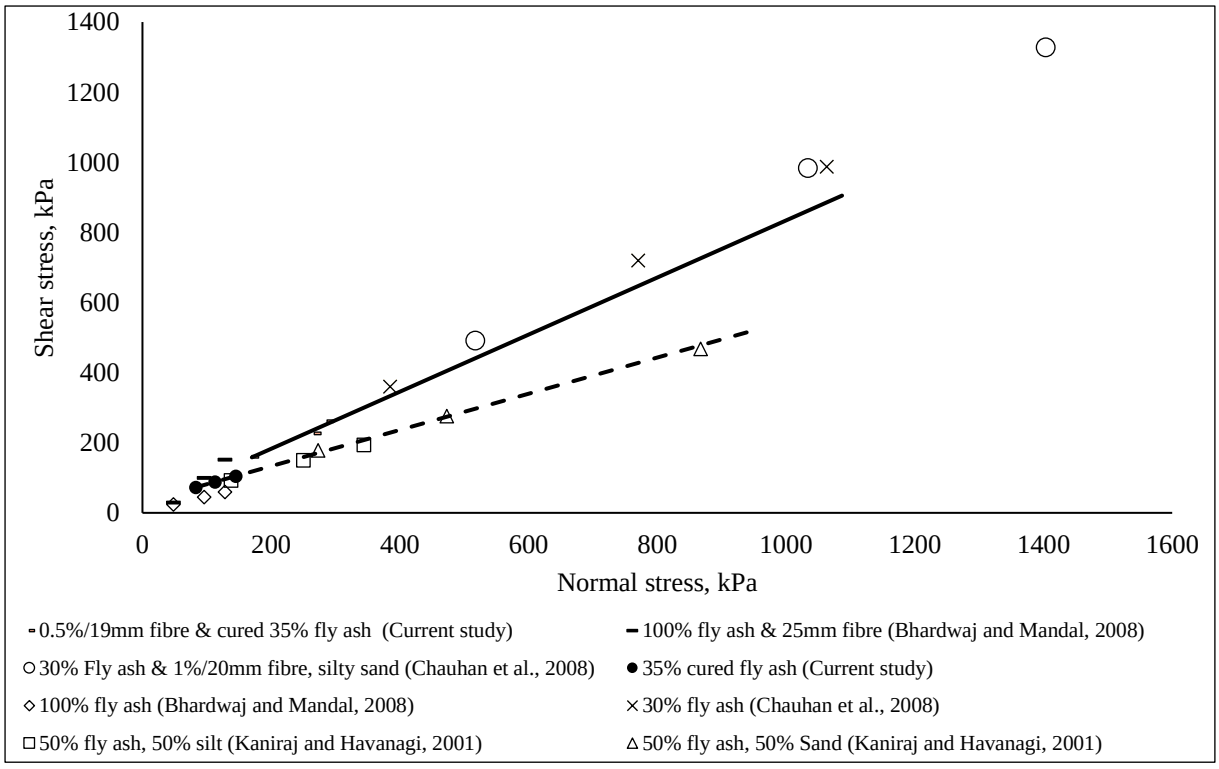

Figure 4.41 Shear stress to normal stress relationship for the current study and the previous studies of fly ash and fly ash with fibre reinforced sand.

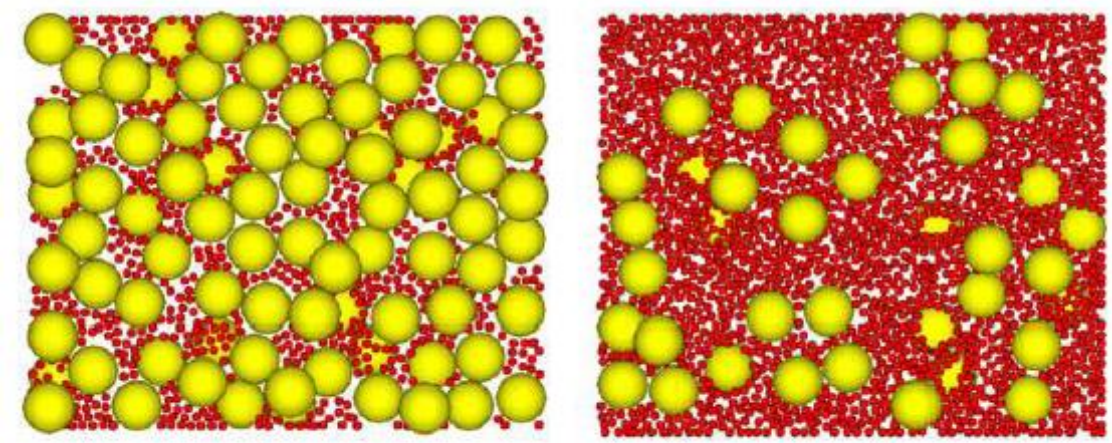

(a) (b)

Figure 4.42 Two types of packing structure (a) low fines content, (b) high fines content.

4.4.2 Unconfined Compressive Strength Test results

4.4.2.1 Fibre reinforced sand

In section 4.2.2, the analysis of UU test results revealed that the optimum fibre length and content were 19mm and 0.5% dry weight of soil, respectively. In this research, the unconfined compressive strength test was conducted only for 19mm long fibre. The current research and the previous researches (Santoni et al., 2001, Girija, 2013) indicated that the optimum fibre content for the fibre reinforced sand materials is between 0.5 to 1.0% of the dry weight of soil as shown in Figure 4.43. It was observed that the inclusion of synthetic fibres significantly improved the unconfined compressive strength of all sand types. However, the silt content affected the strength as stated by (Santoni et al., 2001), due to the internal friction angle and cohesion of reinforced sand were increased.

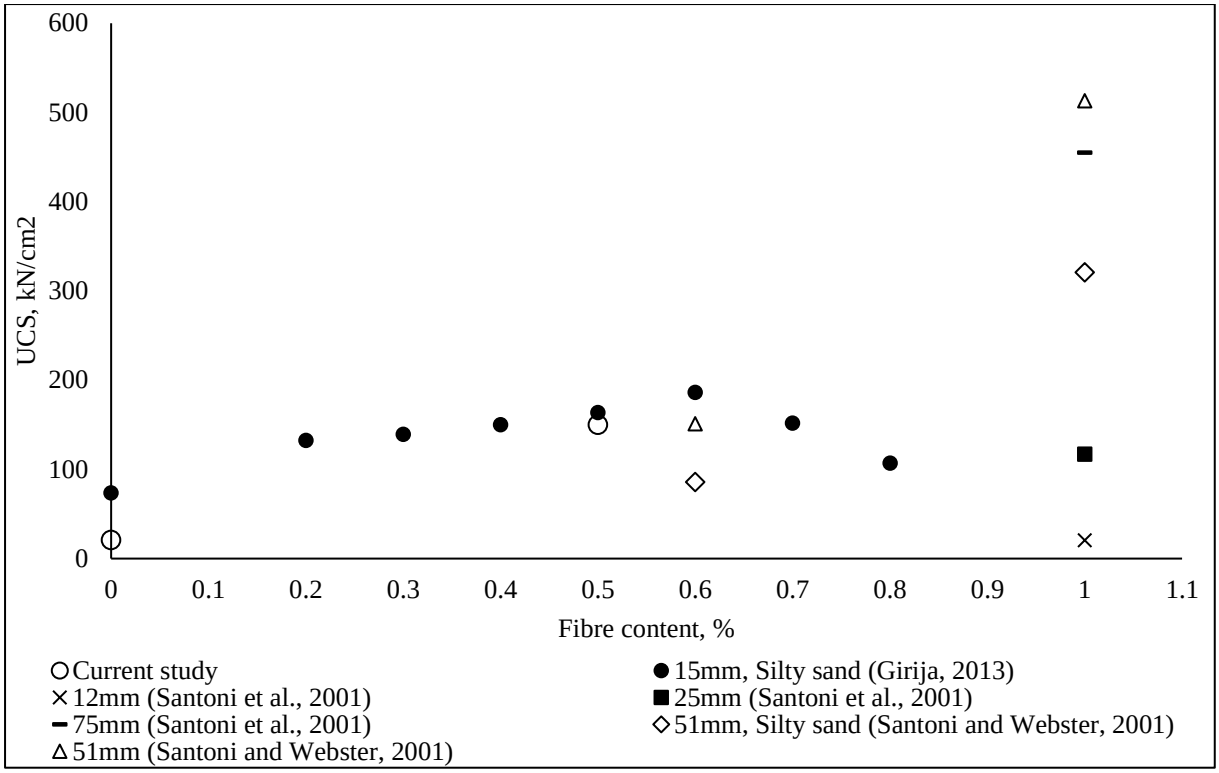

Figure 4.43 Comparison between current study and previous researches for fibre reinforced sand.

4.4.2.2 Fly ash with/without fibre stabilized sand

Figure 4.44 illustrates the available literature (Chauhan et al., 2008, Jadhao and Nagarnaik, 2008) and the research results. Using class C fly ash instead of class F fly ash decrease the required amount of fly ash by about 10% as shown in (Jadhao and Nagarnaik, 2008). Also, it was observed that the optimum fly ash content is between 30% to 40 % of the dry weight of soil. Also, after 0.5% of fibre content does not show any significant improvement in the strength as shown in (Chauhan et al., 2008, Jadhao and Nagarnaik, 2008).

To conclude that sand stabilized with fly ash and fly ash with fibre show improvement in unconfined compressive strength. The cohesion between the particles was increased especially with class C fly ash. The density was significantly affected by the addition of fly

ash into the sand. Moreover, the fibre reinforcement showed significant improvement with fly ash in the sand.

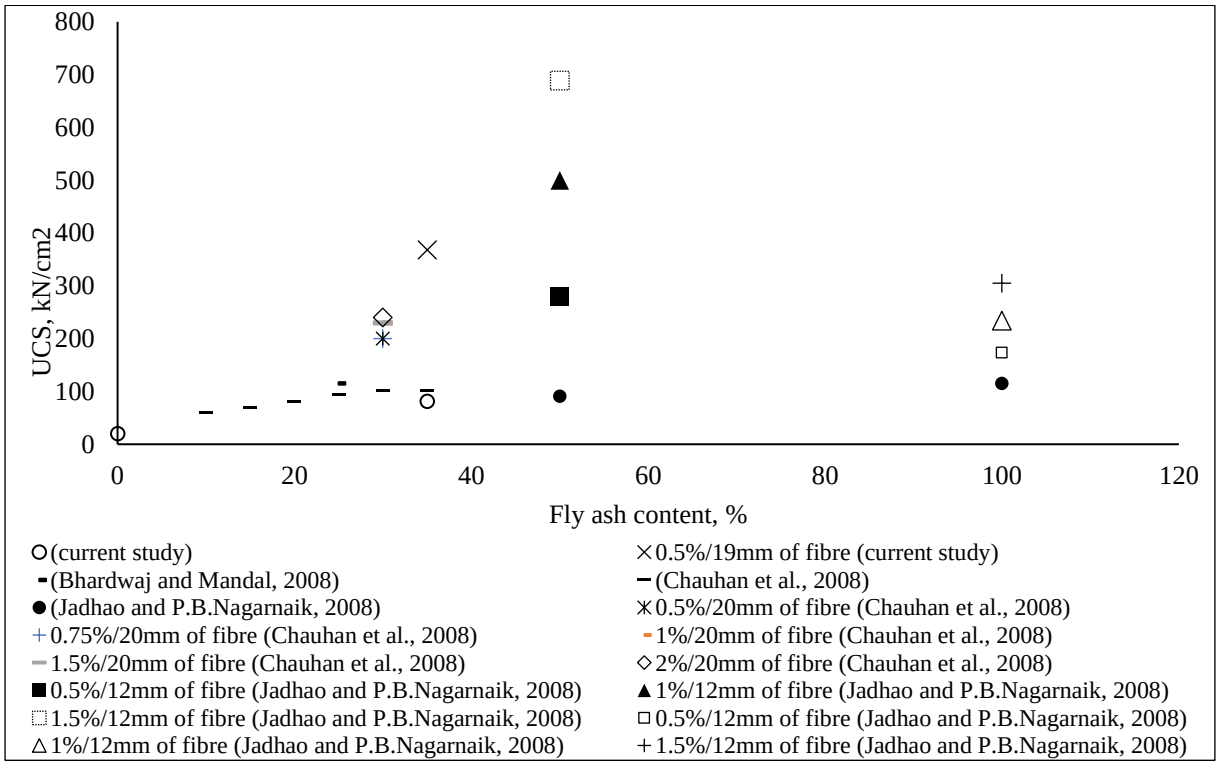

Figure 4.44 UCS to fly ash relationship for fly ash and fly ash with fibre reinforced sand for current study and previous researches.

4.4.2.3 Slag with/without fibre stabilized sand

The development of alkali-activated binders seems to present a greener alternative to ordinary Portland cement. In this research, pilot test program was carried out to evaluate the potential of stabilized sand by vitrified slag. There is no research about the vitrified slag.

In this research, the slag content was 40% of dry weight of soil. The sand stabilized with slag shows significant strength which may be more than the required for road application. Therefore, in the future research, the amount of slag should be considered concerning the required strength. It is worth to mention that the particles size of grounded slag affect the dissolution process.

4.5 Conclusion

This chapter presents the static triaxial test results and discussion. Since the research focused on the resilient modulus and permanent deformation of subgrade soil, it was necessary to carry out both static triaxial test and unconfined compressive strength test to determine the threshold cycling deviator stress for the materials. The results of the unconfined compressive strength test were used to developed correlation models to obtain the resilient modulus by simple test. Table 4-1 summarized the stress ratio for reinforced and stabilized sand. These results are used in Chapter Six for permanent deformation test. The slag and slag with fibre shown significant strength. Therefore, the slag is strongly recommended to stabilize the sand road construction.

Table 4-1 The applied cyclic deviator stress ratios.

Materials	Cyclic deviator stress ratios, %				
Fibre Reinforced Sand	7	19	32	45	57
Fly Ash Stabilized Sand	13	27	40	53	66
PFA & Fibre Reinforced Sand	6	17	28	38	66
Slag Stabilized Sand	6	17	28	38	66
Slag & Fibre Reinforced Sand	6	17	28	38	66

CHAPTER 5 RESILIENT MODULUS

5.1 Introduction

Resilient modulus is one of the main parameters required for analytical pavement design. Therefore, it is important to understand the behaviour of the soil under different conditions. Huang (2004) stated that the granular soil has different response to increase in the stress level than fine soil. The resilient modulus of granular soil increases with increase in the stress level, but it decreases with increase in the stress level in the fine soil. Many researchers stated that, the granular soils show nonlinear response under traffic loading. To consider and understand the nonlinear behaviour, the resilient response of the granular soil is defined by the resilient modulus. The resilient modulus test was conducted in accordance to AASHTO T307. The samples were performed at 95% of maximum dry density as the in-site condition. In this chapter, the results of resilient modulus determinations of stabilized and reinforced sand are discussed at different conditions such:

- A range of water content,
- Resilient modulus after permanent deformation test,
- Resilient modulus from AASHTO T307 and permanent deformation test and;
- Resilient modulus from AASHTO T307 and permanent deformation test after cycles of freezing and wetting.

It is important to mention that, it was not possible to test the unreinforced sand because the specimens would collapse since sand has no cohesion strength. Also, it might be the shear stress high or the confining pressure low. For this reason, it was not possible to test unreinforced sand.

5.2 Factors Affecting Resilient Modulus

Lee et al. (1995), Lekarp et al. (2000a) and Rahman et al. (2017) studied the behaviour of granular materials, using laboratory and in situ testing techniques. For design purposes, it is important to investigate the resilient behaviour with the change in influencing factors. From the studies found in the literature, it appears that the resilient behaviour of unbound granular materials may be affected, with varying degrees of importance, by several factors such as stress, dry density, particles size distribution, soil type, moisture content, stress history, number of load cycles and load duration, frequency and load sequence.

5.2.1 Effect of Stress on Resilient Modulus

Resilient modulus response is based on the soil type. In fine-grained soils, the resilient modulus decreases with increase in the cyclic deviator stress, but in the granular, coarser soils, resilient modulus increases with increase the cyclic deviator stress (Lekarp et al., 2000a, Huang, 2004). In addition, the previous researchers (Lekarp et al., 2000a, Salour et al., 2014) stated that the resilient modulus of untreated granular materials is affecting by the confining pressure and the sum of principal stresses. The resilient modulus increases with an increase in confining pressure and the sum of principal stresses.

In this research, the experimental results of the resilient modulus test demonstrated a different trend for reinforced sand with fibre and fly ash. The resilient modulus values were affected by deviator stress. On the other hand, water content has a negligible effect on reinforced sand with fibre or fly ash as well as confining pressure as shown in Figure 5.1 and 5.2, respectively.

Figure 5.3 shows the resilient modulus of reinforced sand with fibre and fly ash. The specimens were compacted at OMC and 95% of MDD as mentioned in Chapter Three section 3.2.4. The confining pressures of 13.8 and 27.6kPa have a similar trend of resilient modulus response. While the deviator stress shows less effect on the resilient modulus at confining pressure of 41.4kPa. The inclusion fibre to stabilized sand with fly ash increase the resilient modulus at lower stress level as shown in Figure 5.3. Figure 5.4 shows the resilient modulus of stabilized sand with vitrified slag. The results indicate that there was little change in resilient modulus at lower confining pressure. This could be explained by the strength of activated slag stabilized sand. As reported from the unconsolidation undrained triaxial test, the small confining pressure does not have any effect on the slag stabilized sand. This result reflects the strength of the slag. Also, the samples of slag stabilized sand show a slight difference with the increase in the deviator stress at the last 500 cycles and confining pressure of 13.8kPa as illustrated in Figure 5.4. This was due to the post-compaction of the samples which played the principal role. Figure 5.5 shows the results of fibre with slag stabilized sand. The resilient modulus values were affected by the confining pressure and it was increased with increase in the confining pressure as well as the deviator stress. On the other hand, the resilient modulus was reduced with the addition of fibre with slag into the sand. This observation was due to the impact of fibre while can see a reduction in density due to an increase in the void ratio.

Multi-stage (MS) triaxial test results show the superiority of using fibre, class C fly ash and vitrified slag into the sand. The MS test used a constant confining pressure test which was fixed at 27.6kPa. The resilient modulus increased with increase in the cycle loads number. This may be interpreted as: the increase in load cycles causes an increase in the density, thereafter loading change in the behaviour. Also, the resilient modulus is increased due to the

bonding that is generated by the cementitious materials. Moreover, the slag shows great improvement in resilient modulus after the activation and the curing. Figure 5.8, 5.9, and 5.10 demonstrate the resilient modulus after 50,000 load cycles.

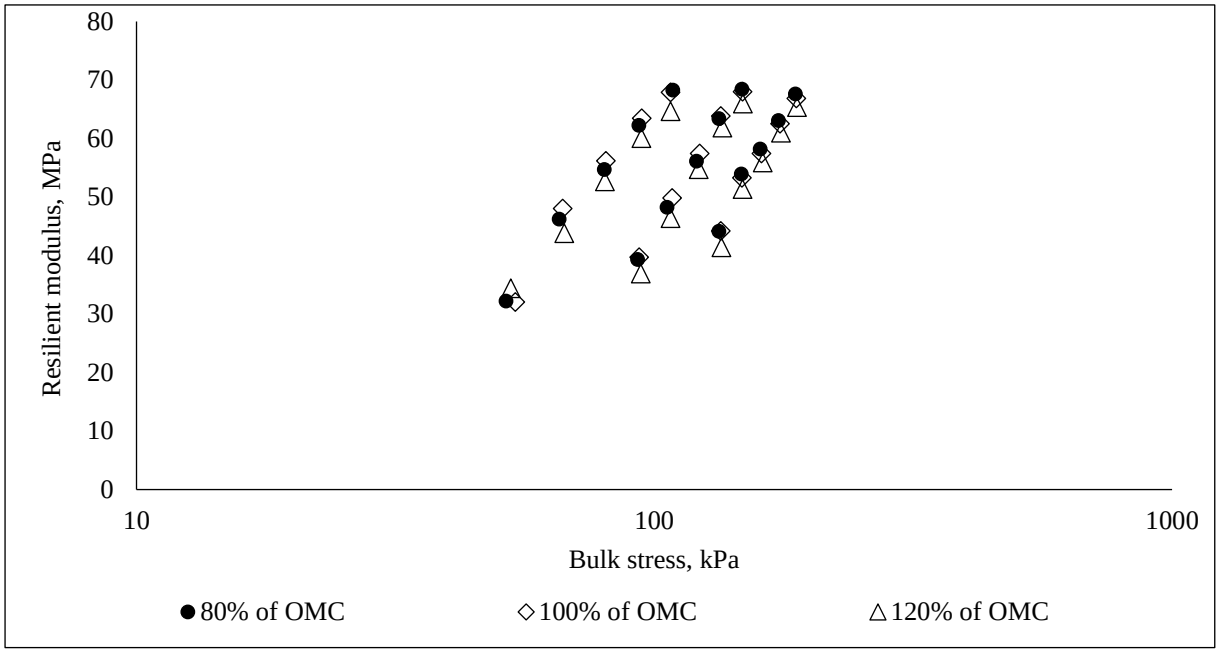

Figure 5.1 The resilient modulus of fibre reinforced sand at 80%, OMC and 120% of OMC.

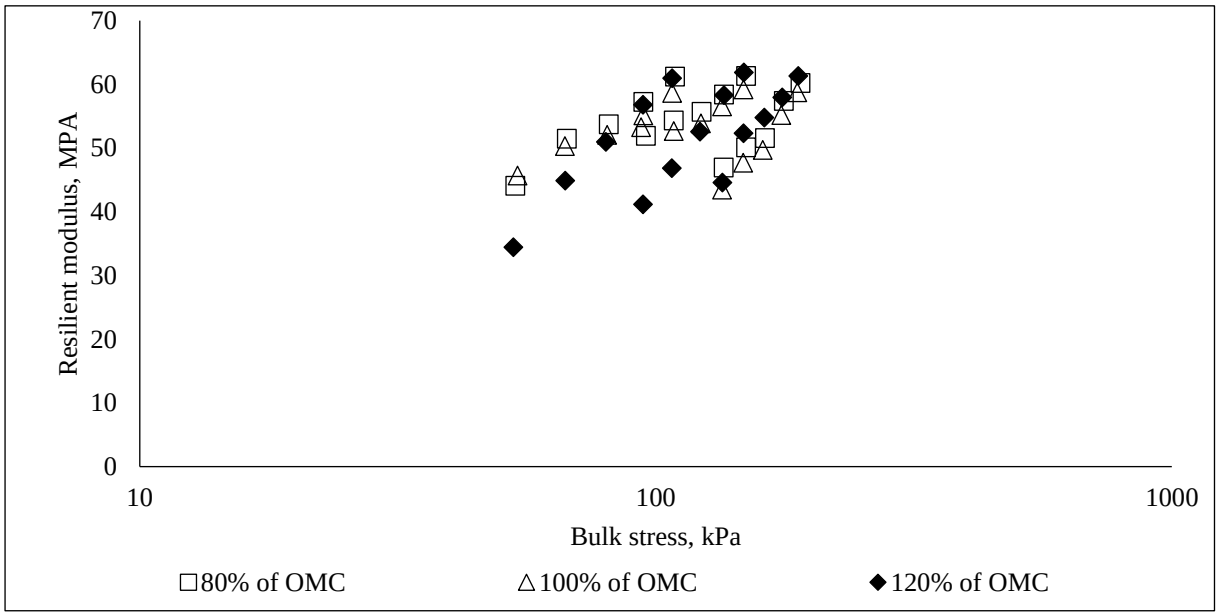

Figure 5.2 The resilient modulus of fly ash stabilized sand at 80%, OMC and 120% of OMC and 7 days of curing.

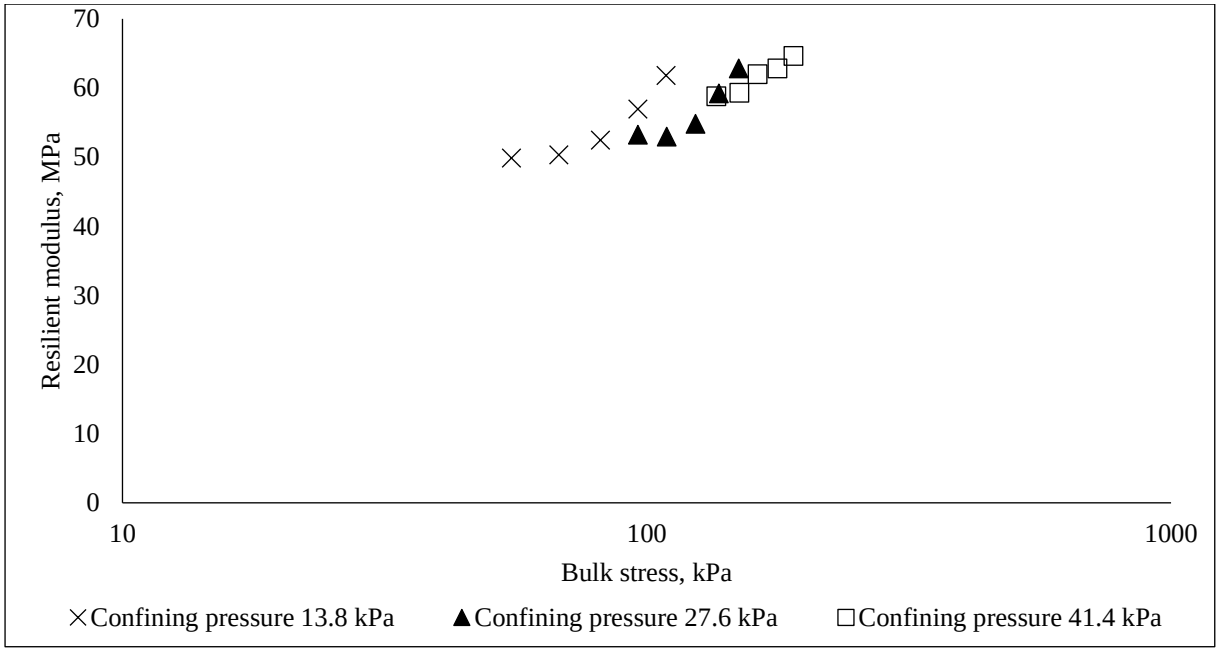

Figure 5.3 The resilient modulus of fibre & fly ash reinforced sand at OMC and 7 days of curing.

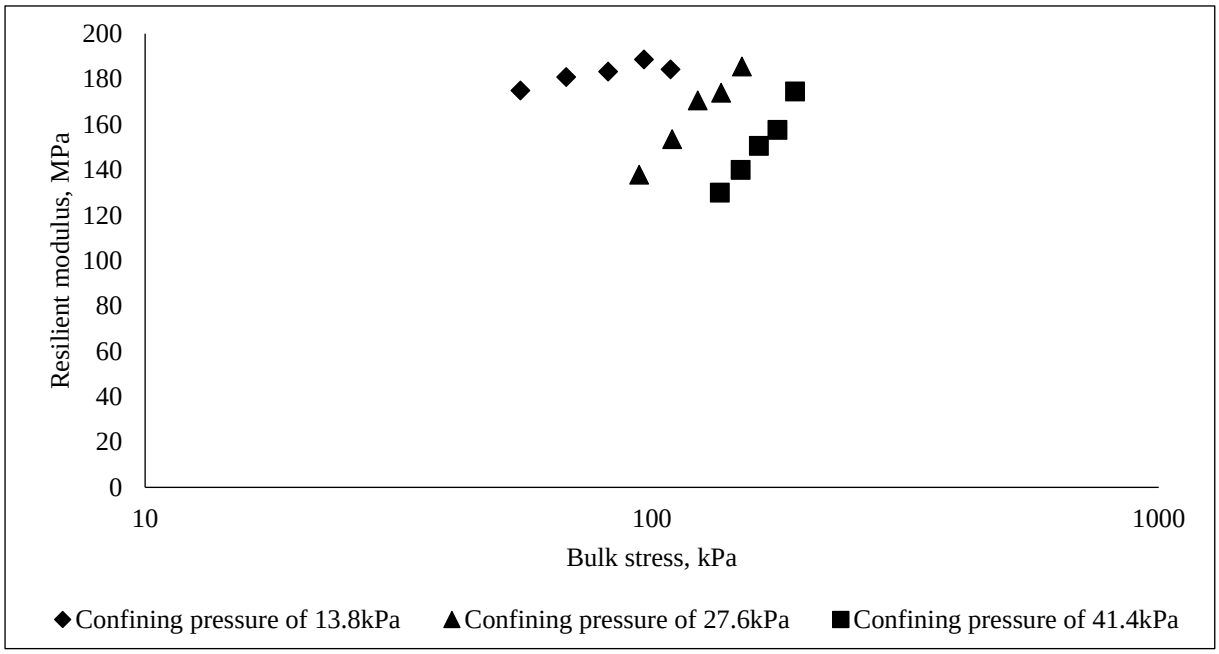

Figure 5.4 The resilient modulus of slag stabilized sand at OMC and 7 days of curing.

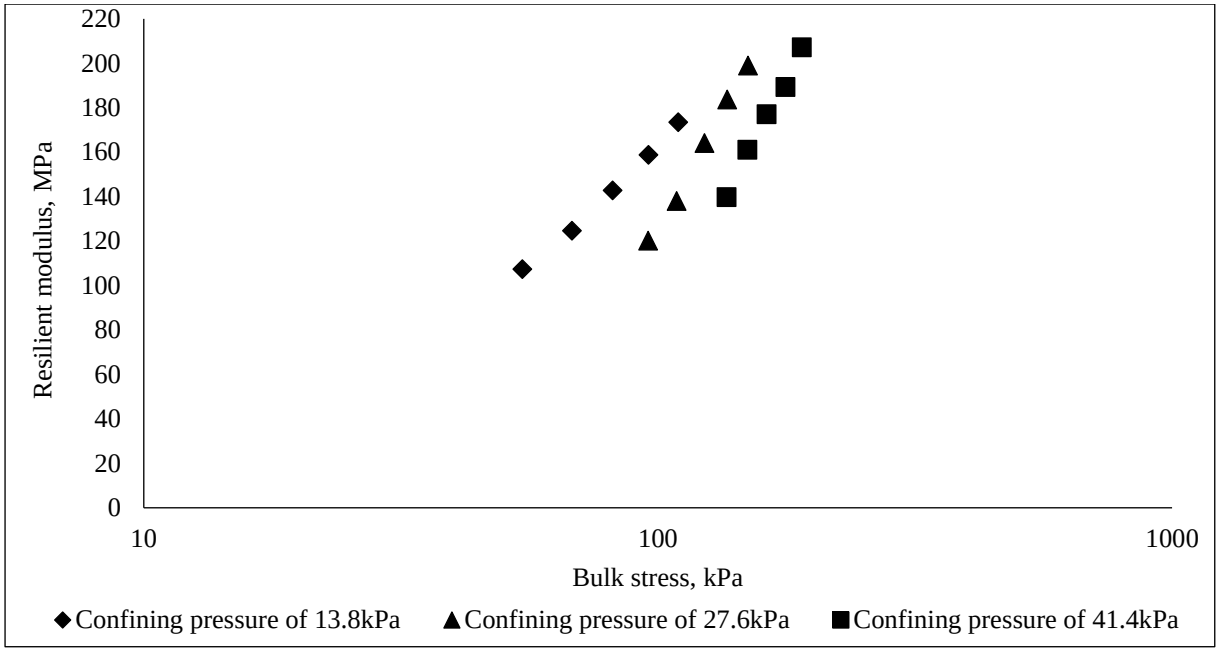

Figure 5.5 The resilient modulus of fibre with slag reinforced sand at OMC and 7 days of curing.

5.2.2 Effect of Moisture Content

In the road pavement, it is desired to compact the subgrade layer at optimum water content. In the field, the compaction is usually conducted at about 95% of the maximum dry density and the nearest optimum water content for the subgrade to able to support the highways (AASHTO, 1993). The repeated triaxial test was performed at the optimum moisture content and ± 20% of the OMC to simulate the field in wet and dry state. The effect of moisture content was explained by the increase in the pore pressure caused reduction in the effective stress and decrease both resilient modulus and strength (Brown, 1996, Scott, 1980). The effect of the degree of saturation on the resilient modulus was argued by (Mitry, 1964; Seed et al. 1967; Hicks, 1970 and Pappin, 1979). It was stated that, the resilient modulus decreases if the stress is obtained by total stress, but the resilient modulus slightly changes when the stress is obtained by effective stress.

The results of this research for both fibre and fly ash stabilized sand shows that, the resilient modulus was not affected by the increase in the water content as shown in Figure 5.1 and 5.2, respectively. Brown (1996) explained that the resilient modulus will not be affected with an increase in the water content if the soil suction was kept below the critical value. Figure 5.6 shows the water content range for the unreinforced and reinforced sand. The results show that the fly ash reduces the required water while the fibre requires more water. Table 5-1 summarized the materials and water content for the mixtures.

Table 5-1 Materials and water contents.

Materials	Materials contents, gm				Water content, % of OMC		
	Sand	Fibre	Fly ash	slag	80%	100%	120%
Sand	2501	--	--	--	122	153	183
Sand+Fibre	2675	13	--	--	254	318	382
Sand+Fly Ash	1834	--	988	--	181	226	271
Sand+Slag	1576	--	--	1051	217	271	325
Sand+Fibre+Fly Ash	1820	14	988	--	181	226	271
Sand+Fibre+Slag	1563	13	--	1051	217	271	325

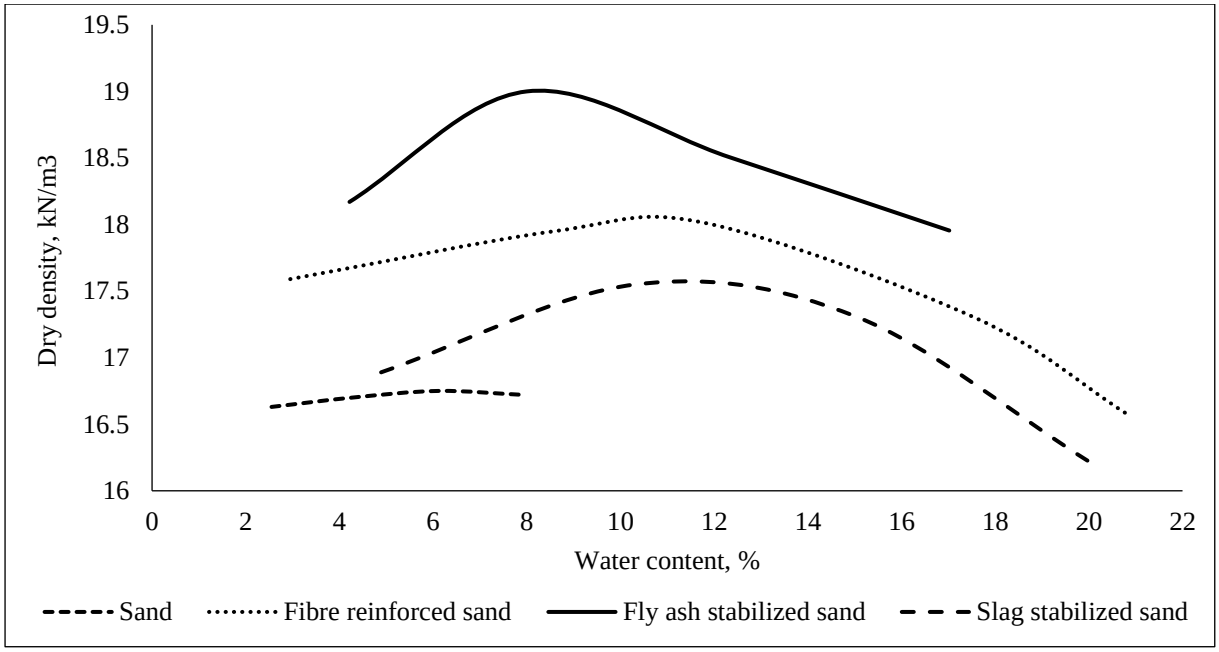

Figure 5.6 The compaction test results of the stabilizers and reinforced material

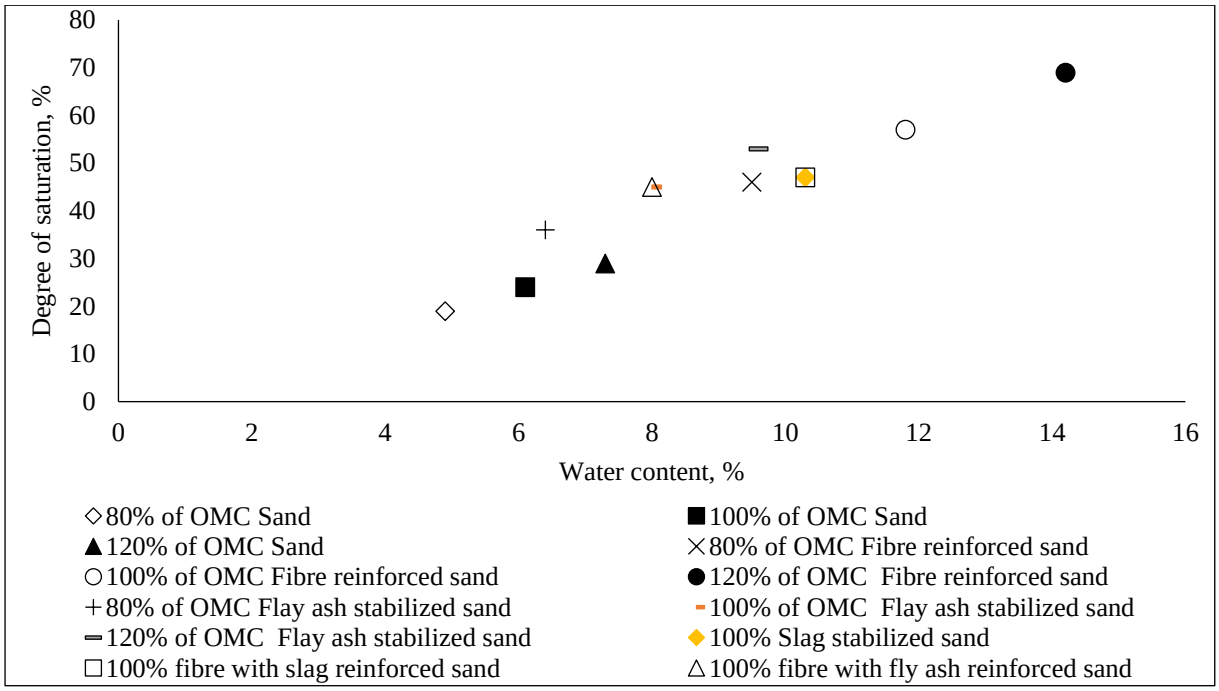

Figure 5.7 Degree of saturation against the water content.

5.2.3 Effect of Stress History and Number of Load Cycles

The literature review showed that the effect of stress history appears as a result of progressive densification and particle rearrangement under a number of load cycles. Hicks (1970) stated

that the stress history has slight effect after 100 cycles. In addition, the resilient modulus increased with an increase in the number of load cycles (Lekarp et al., 2000a). In this research, the effect of stress history for reinforced sand showed a similar result to Hicks (1970) results. These results show that fibre was more effective when some moisture was present than when the specimen was dry of optimum. The samples remained effective at 120% of optimum water content which is near the saturation point as shown in Figure 5.8 shown. The results in this research confirmed the work by (Puppala et al., 2009).

The results of the resilient modulus of fly ash stabilized sand showed that the resilient modulus was not affected by the increase in the number of loads cycles. These results were different with (Chauhan et al., 2008, Kumar and Singh, 2008) results. Their results indicated that the resilient modulus decreased with an increase in the number of load cycles. This can be interpreted by; both used class F fly ash with silty sand. In this research, class C fly ash was used in order to improve the friction and bonding between the particles and the increase of fine soil proportion developed the density. Figure 5.9 illustrates the effect of water content on resilient modulus of fly ash stabilized sand. The results demonstrated that the compacted sample at optimum water content produced the highest resilient modulus. As reported, the 50,000 load cycles were applied in this research compared to 10,000cycles applied by (Chauhan et al., 2008, Kumar and Singh, 2008). It was clear that the resilient modulus stabilized after 10,000 load cycles. Moreover, the fly ash stabilized sand with fibre improved the resilient modulus up to about 200% of stabilized sand with fly ash only as shown in Figure 5.10. This improvement gains after 30,000 cycles, the resilient modulus stable. The resilient modulus of slag with or without fibre shows significant improvement with an increase in the number of load cycles as illustrated in Figure 5.10. On the other hand, the fly ash with fibre was stabilized at 20,000 cycles load, and then the resilient modulus decreased

and kept stable till the end of the test. This may be due to densification of the sample caused by the increase in the number of the load cycles.

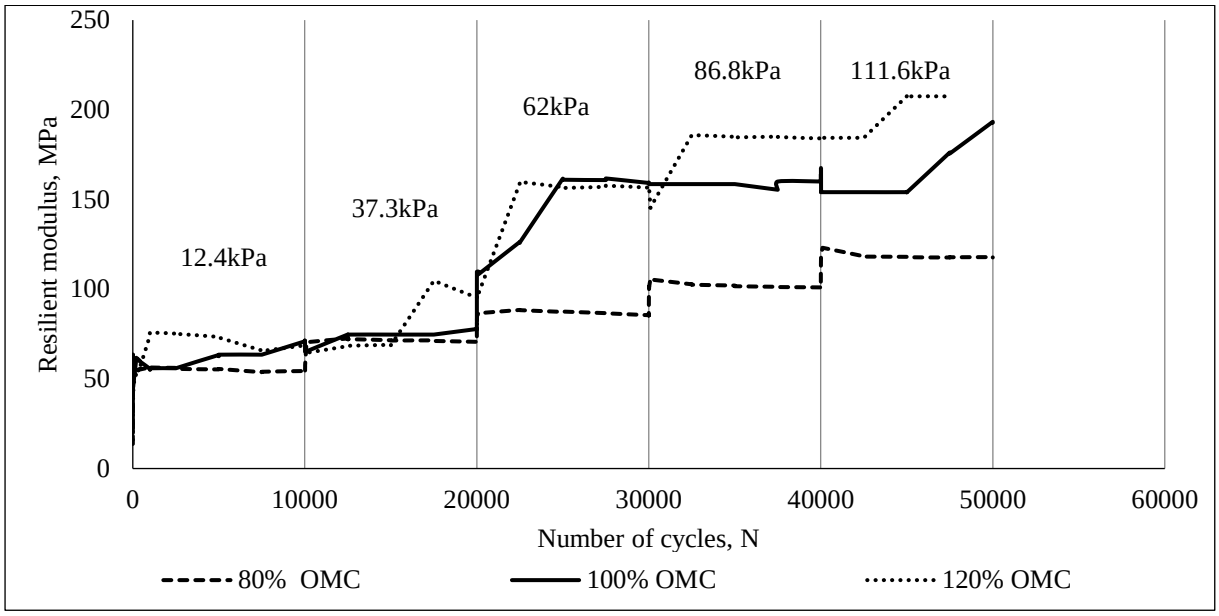

Figure 5.8 Resilient modulus of fibre reinforced sand at 27.6kPa confining prssure, different stress level and water contents.

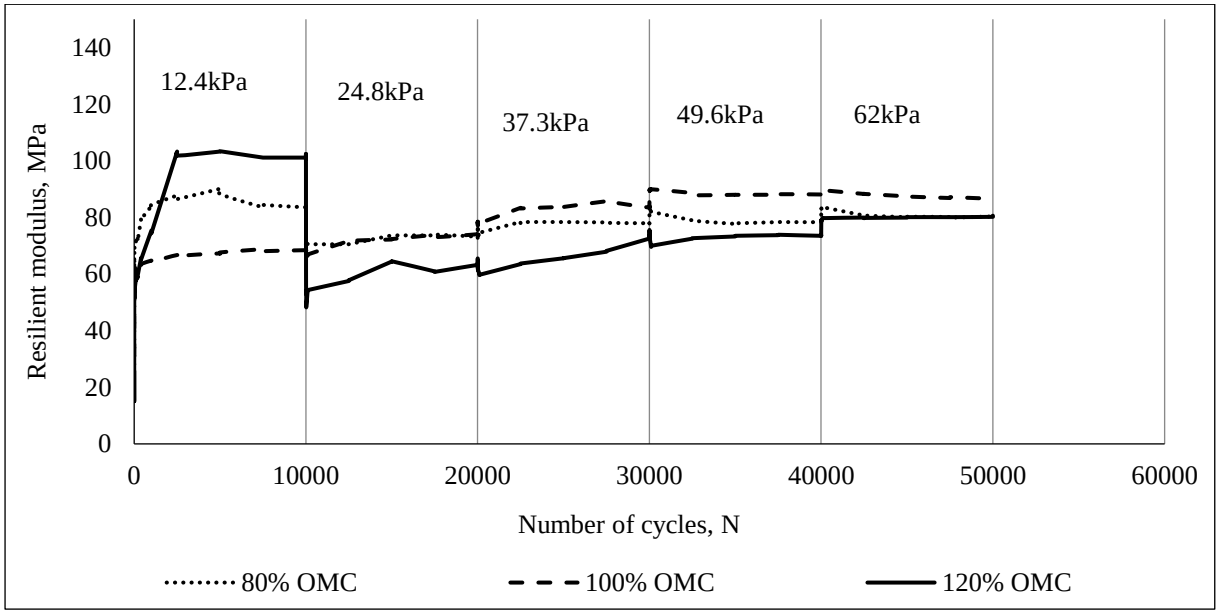

Figure 5.9 Resilient modulus of fly ash stabilized sand at 27.6kPa confining prssure, different stress level and different water content.

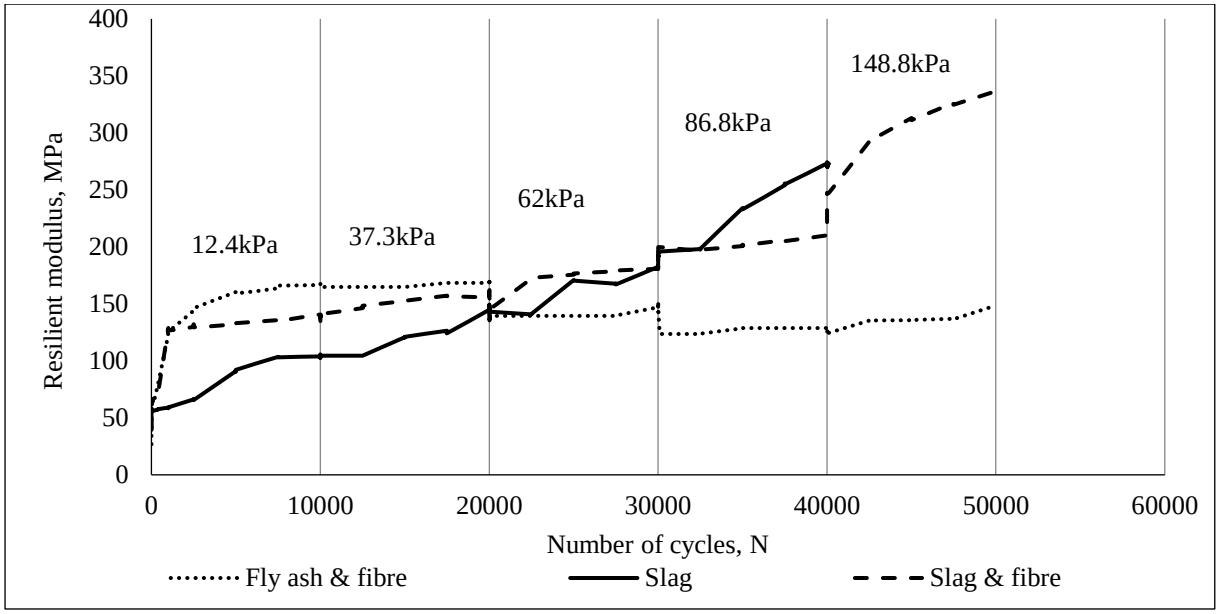

Figure 5.10 Comparsion between fly ash with fibre, slag, slag with fibre reinforced sand at 27.6kPa confinng pressure, different stress level at OMC.

5.2.4 Effect of Stabilizers and Reinforced Materials

To compare the effect of reinforced sand by different stabilizers and reinforcement material, the sand was stabilized using class C fly ash and vitrified slag with and without fibrillated polypropylene fibre. The slag and fly ash content were obtained based on the maximum dry density. Thus, 40% of slag was used throughout the research and 35% of fly ash. The findings showed that, the slag improved the strength and resilient modulus of sand. The slag content needs more investigation in terms of the required strength.

However, due to the necessity of carrying out a huge number of tests of the static triaxial test resilient modulus, permanent deformation and durability test as well as the complexity and time constraints, only 40% of slag content and 35% of fly ash with fibre at the optimum water content was investigated in this research. Figure 5.11 represent the results of the resilient modulus for all the mixtures.

The fibre length and content were obtained by the compaction test. The fibre content was 0.5% of the dry weight of soil. As mention in section 3.2.3, the raw slag was grounded from about 35mm*15mm dimension to pass through 150μm sieve by using a planetary disc mill. The grounded slag was mixed with a 6Mol of sodium hydroxide (Na OH) to activate the slag. The curing time was taken in account and therefore, the samples were tested before and after the curing. The samples were curing for 7days to determine the resilient modulus and permanent deformation. Many factors such as stabilizers content, curing time and soil type were considered to improve the strength of sand soil. In this research, it was found that the size of the slag particle was also important.

Figure 5.11 compares all the five mixtures. The mixtures were compacted at OMC and 95% of the maximum dry density. The fibre improves the resilient modulus in both mixtures of fly ash with fibre and slag with fibre. The resilient modulus of slag stabilized sand increased continuously while the fly ash stabilized sand remains stable without visible change. On the other hand, the fibre with slag reinforced sand shows increasing in resilient modulus every 20,000 load cycles. Fibre reinforced sand remains stable after 20,000 load cycles. The behaviour of fly ash reinforced sand with fibre was slightly different, the resilient modulus decreased gradually until become stable after 30,000 cycles to obtain about 130MPa.

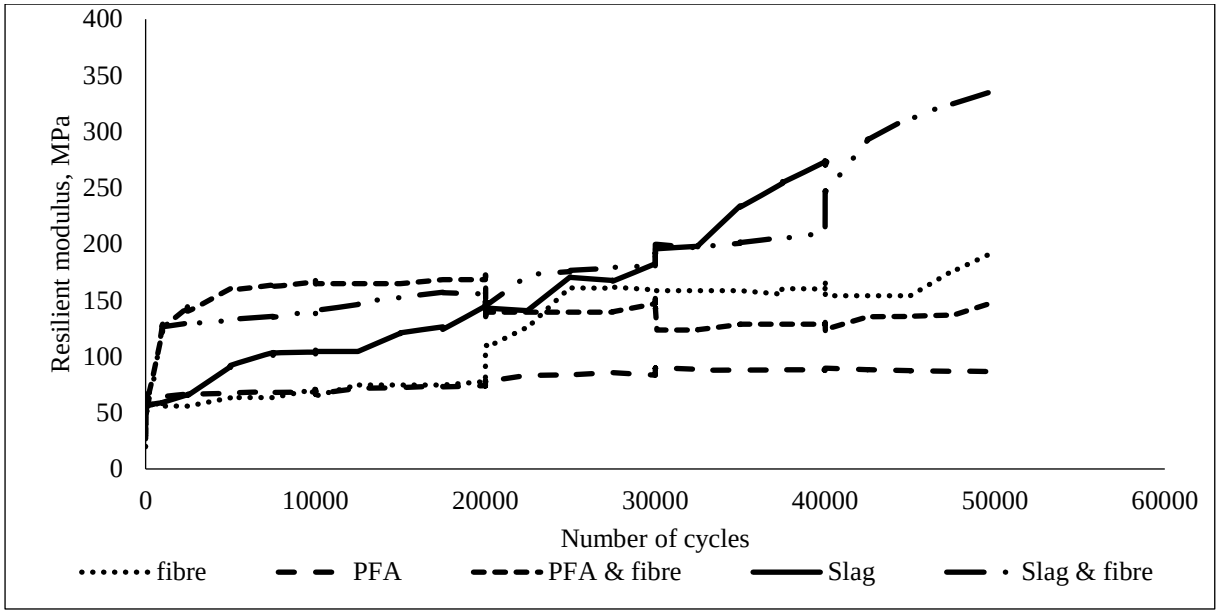

Figure 5.11 The effect the stabilizers and reinforce materials on the resilient modulus at OMC

5.2.5 Discussion

The resilient modulus of sand subjected to cyclic loading is affected by many factors including stress, density, particle size distribution, moisture content, soil type, stress history, the number of load repetitions, and the loading sequence. The effects of these factors on resilient modulus is discussed in this Chapter. The influence of the stress on resilient behaviour is considered to be the most significant factors (reference) and is included in constitutive models for resilient modulus prediction and determination. Granular soils have different responses to the increase in stress levels than fine-grained soils, as their resilient modulus increases with an increase in the stress level or stress Harding; while for fine-grained soils, the resilient modulus decreases with an increase in the stress level or stress softening.

In this research, the field in the wet and dry state were simulated by 95% of the maximum dry density and the nearest optimum water content. The results of the experimental investigations shown that the water content has a negligible effect on reinforced sand with fibre or fly ash as well as confining pressure. This change of behaviour is different from the general concept of

the effect of water content on the behaviour of granular soil. The reinforcement technique changes the behaviour of soil. Moreover, the result was in agreement with Brown (1996) result, the resilient modulus will not be affected with an increase in the water content if the soil suction was kept below the critical value.

The cementitious properties of the vitrified slag into sand provided high resilient modulus at lower confining pressure. This result was in parallel with the results of the unconsolidated undrained triaxial test result. The small confining pressure did not have any effect on the slag stabilized sand. This result reflects the strength of the slag. The resilient modulus of fibre with slag stabilized sand was slightly decreased; inclusion fibre was due to decrease the density and increase the void ratio.

The long-term investigation was obtained by Multi-Stage triaxial test. The number of load cycles increased the density under the term of the post-compaction. Increase the density of granular soil was due to the increases in strength and stiffness. Then the resilient modulus increases with an increase in the number of cycles. When some moisture was present, it helps to increase the density, the loading cycles is due to rearranging the particles.

In case of fly ash stabilized sand, the resilient modulus of fly ash stabilized sand was not affected by the increase in the number of loads cycles. The fly ash with fibre was stable at 20,000 cycles load, and then the resilient modulus decreased and kept stable till the end of the test. This may be due to densification of the sample caused by the increase in the number of the load cycles and the increase of the proportion of the fine soil. Also, the bonding that was created by class C fly ash.

5.3 Resilient Modulus after Freezing-Thawing Cycles

Brandl (2008) stated that the freezing behaviour of soils and other granular material was influenced by numerous factors: grain size distribution, fine grains, organic components, soil chemistry, water content, degree of saturation, density, permeability, temperature conditions, overburden and composite behaviour of the structure (multi-layered road system, etc.). As mentioned, the resilient modulus was more appropriate to measure after Freezing and Thawing cycles for durability study; the resilient modulus test was suitable to simulate the field condition better than the unconfined compressive strength test as stated in Chapter Two, section 2.3.3. The test was performed in accordance with ASTM D560, at 24 hrs under -18 C^o and then 24hrs in 21C^o with a relative humidity of 100%. The test was described in Chapter Three. Also, it should be noted that the membranes were removed during the F-T cycles to expose samples to moisture changes.

The water content has a significant effect on the resilient modulus of pavement layer as demonstrated in section 5.2.2. Therefore, the resilient modulus was determined at 10, 20, and 30 cycles of F-T in order to simulate 10, 20, and 30years. Figure 5.12 to 5.14 represented results of the resilient modulus of fibre reinforced sand for the three periods. A negligible reduction in resilient modulus was observed after 10 and 20 of F-T cycles at different water contents. By contrast, significant improvement of resilient modulus after 30 cycles was obtained at 80% OMC, 120% OMC, and then 100% OMC.

There was no available research to investigate the resilient modulus of fibre reinforced sand after F-T cycles. Therefore, the resilient modulus behaviour of AASHTO T307 was validated by the multi-stage triaxial test results. Both results were in agreement as demonstrated in Figure 5.12 to 5.14 and Figure 5.15 to 5.17, respectively. Therefore, it could be said that the

F-T cycles did not have an influence on the fibre reinforced sand. Ghazavi and Roustaie (2010) applied 10 cycles of F-T on polypropylene fibre reinforced clay and concluded that the change in the strength of the samples was not significant after 10 cycles since the equilibrium condition became predominant on the samples.

Figure 5.18 to 5.20 demonstrate the resilient modulus results of fly ash stabilized sand at 80%, OMC and 120% OMC. The results of the resilient modulus test show that the F-T cycle's sand increase in the resilient modulus of fly ash stabilized. These results were confirmed by (Khoury et al., 2010). At three water content, the Freezing and thawing cycles improved the resilient modulus. Also, M-S triaxial tests were conducted and the results agreed with the AASHTO T307 test as illustrated in Figure 5.21 to 5.23.

The strength of fly ash specimens could be improved by the cementitious properties of class C fly ash for the long-term construction by the freeze-thaw cycles. The result indicated that 24 hrs of thawing was sufficient to improve the pozzolanic reaction.

The combination of fibre with fly ash show significant improvement in resilient modulus. The result of the combination was almost like the summation of the improvement for each one separately. The fibre improves the interlock between the particles and the fly ash increase the cohesion. Figure 5.24 demonstrates the AASHTO T307 results. Also, Multi-Stage triaxial tests were conducted to confirm the behaviour of fibre with fly ash reinforced sand as shown in Figure 5.25.

Figure 5.26 shows the resilient modulus results of slag reinforced sand. The results show that the improvement in the resilient modulus of slag stabilized sand was better than what was obtained in fibre with fly ash reinforced sand. The slag stabilized sand has been improved by increasing the F-T cycles. It was worth to mention that the vitrified slag has not been

investigated before. The slag stabilized sand after freezing and thawing cycles shows similar trending to before the freezing and thawing.

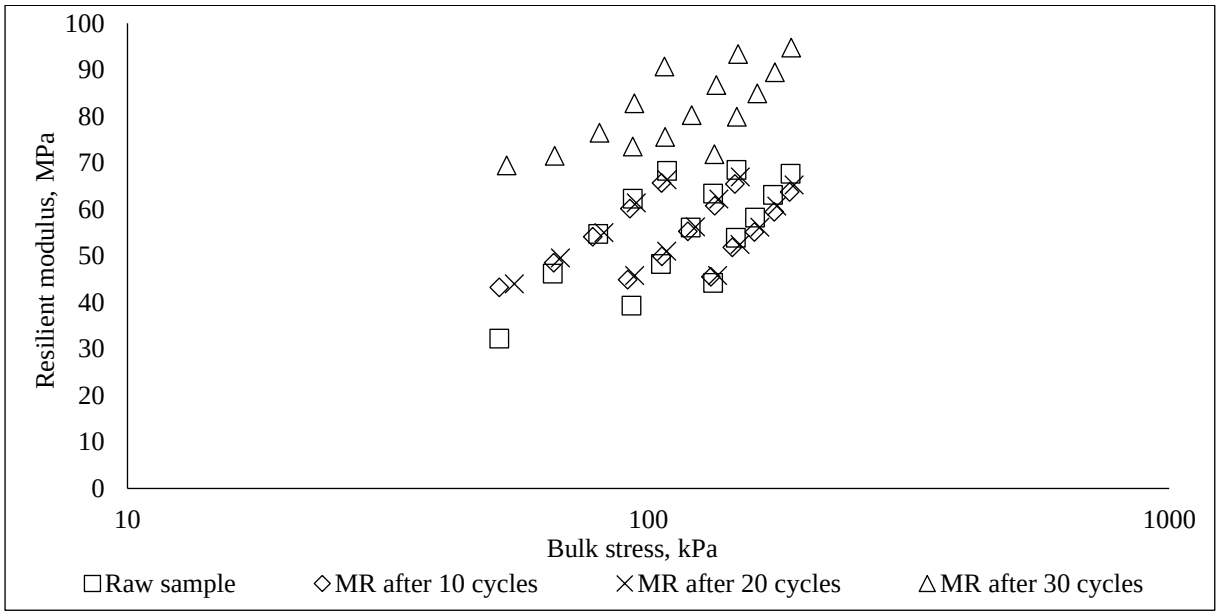

Figure 5.12 The comparison between the resilient modulus of fibre reinforced sand before and after the F-T cycles & 80% OMC.

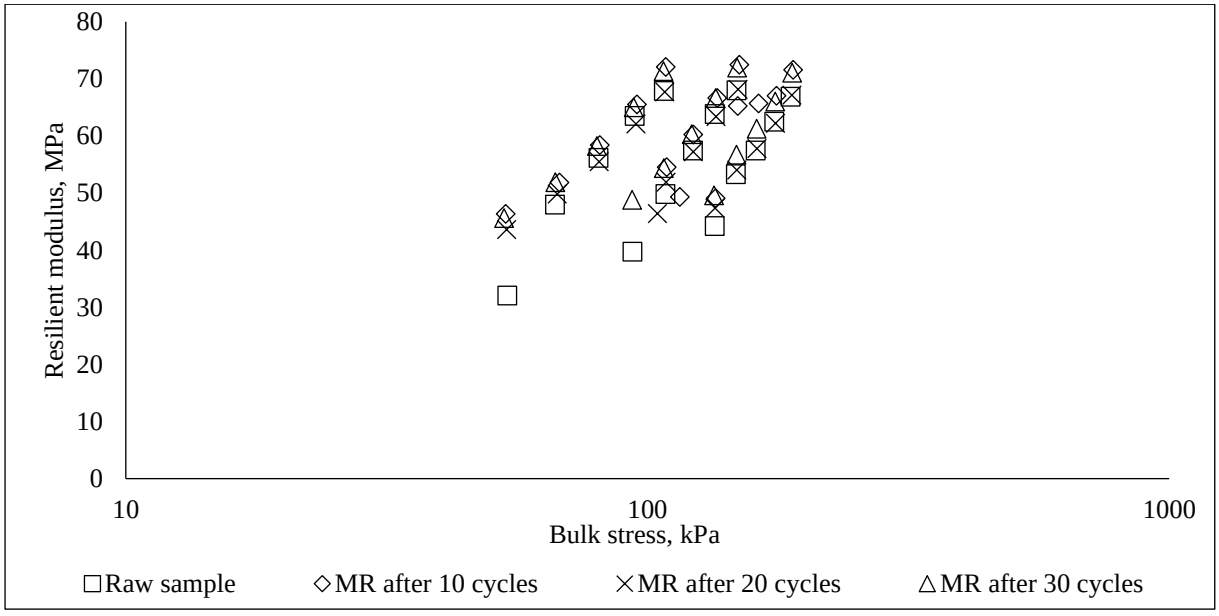

Figure 5.13 The comparison between the resilient modulus of fibre reinforced sand before and after the F-T cycles27.6kPa & OMC.

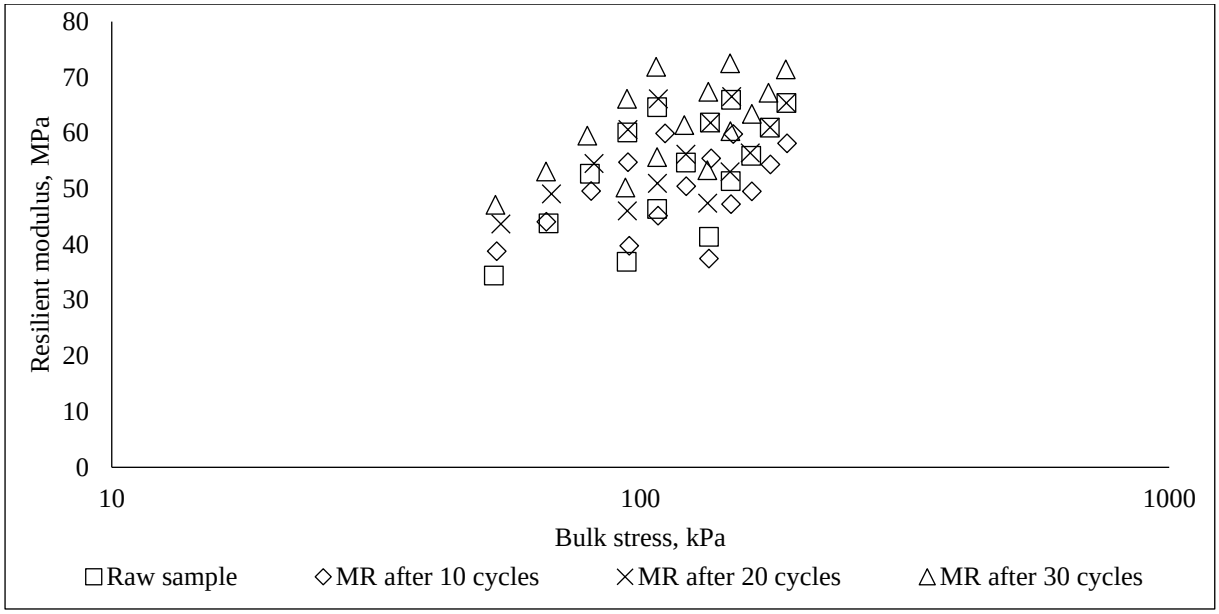

Figure 5.14 The comparison between the resilient modulus of fibre reinforced sand before and after the F-T cycles kPa & 120% OMC.

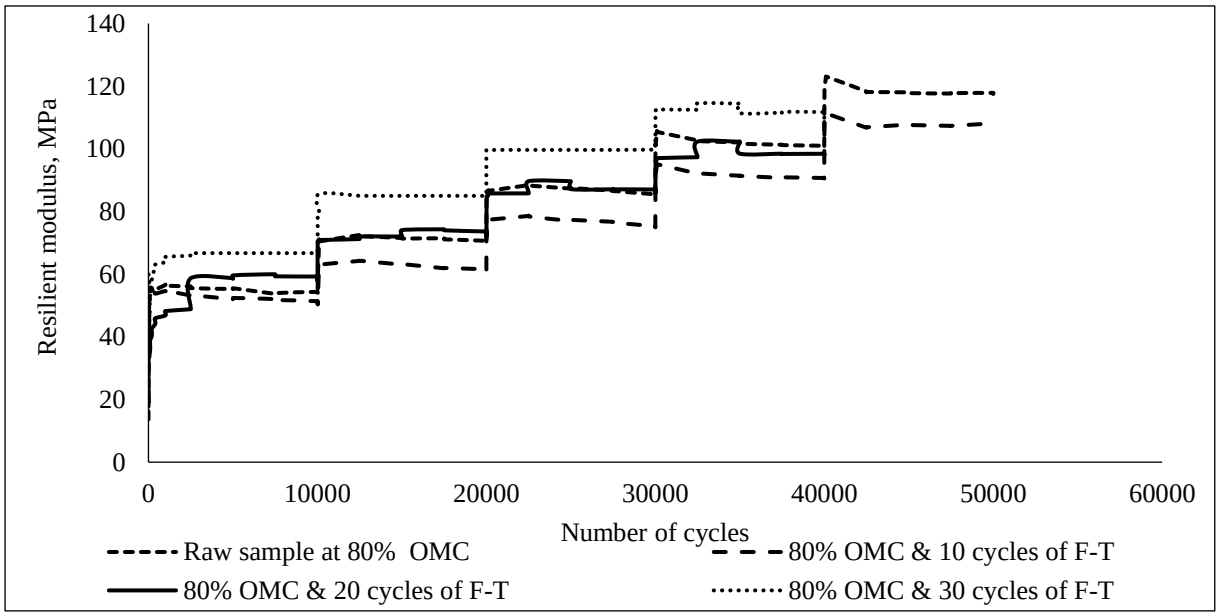

Figure 5.15 The comparison between the resilient modulus of fibre reinforced sand before and after the F-T cycles at 27.6kPa & 80% OMC.

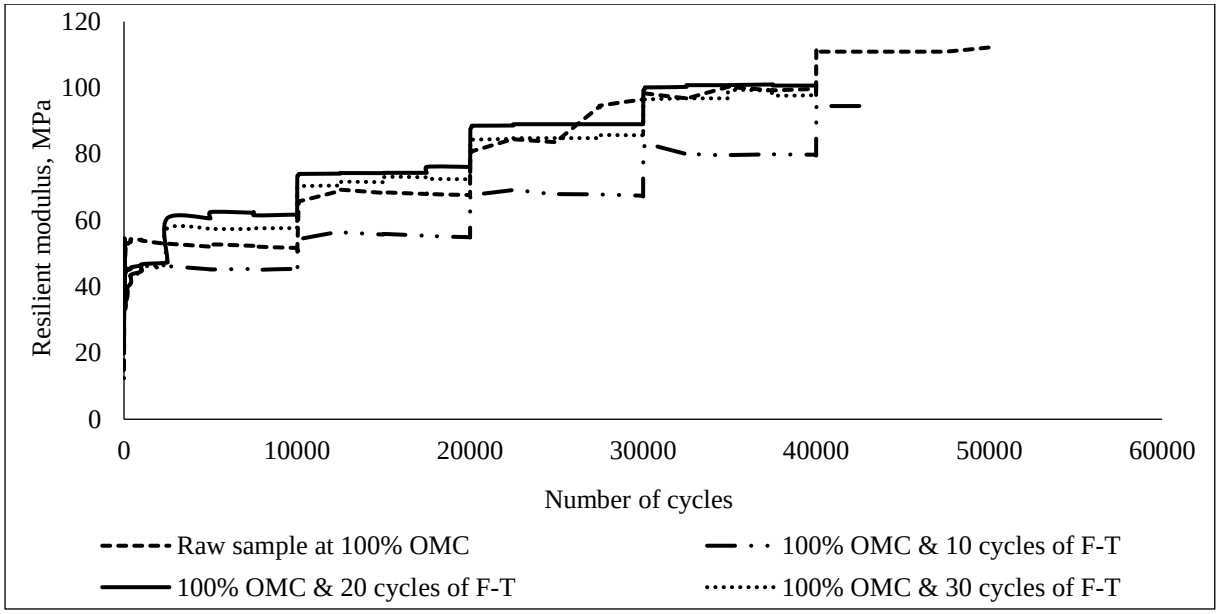

Figure 5.16 The comparison between the resilient modulus of fibre reinforced sand before and after the freezing-thawing cycles at 27.6kPa & 100% OMC.

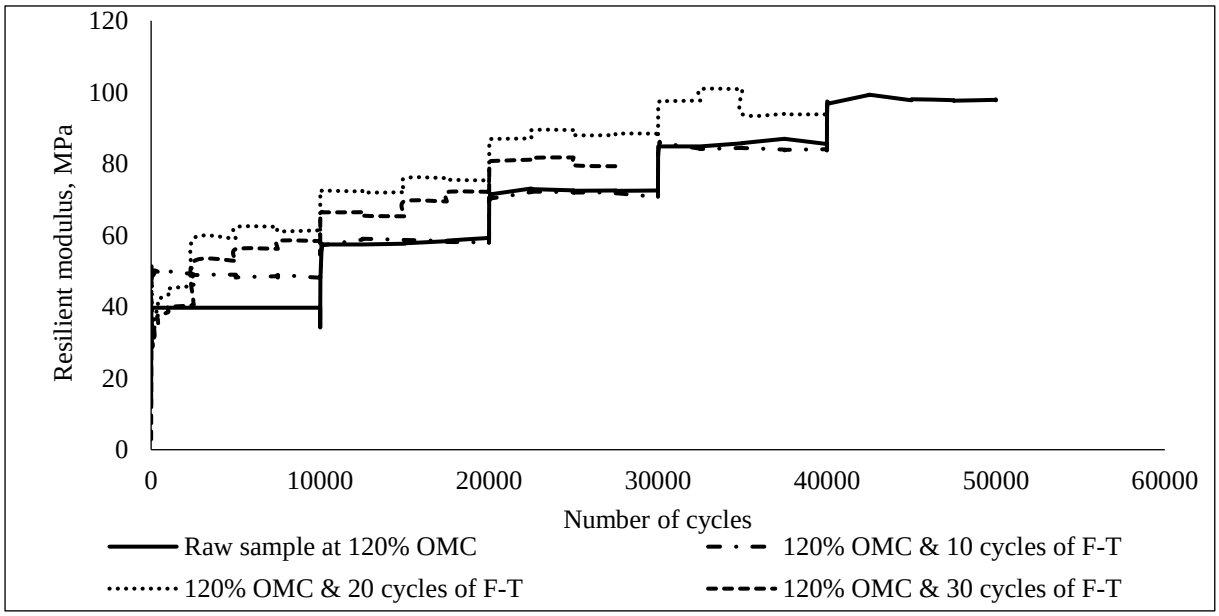

Figure 5.17 The comparison between the resilient modulus of fibre reinforced sand before and after the freezing-thawing cycles at 27.6kPa & 120% OMC.

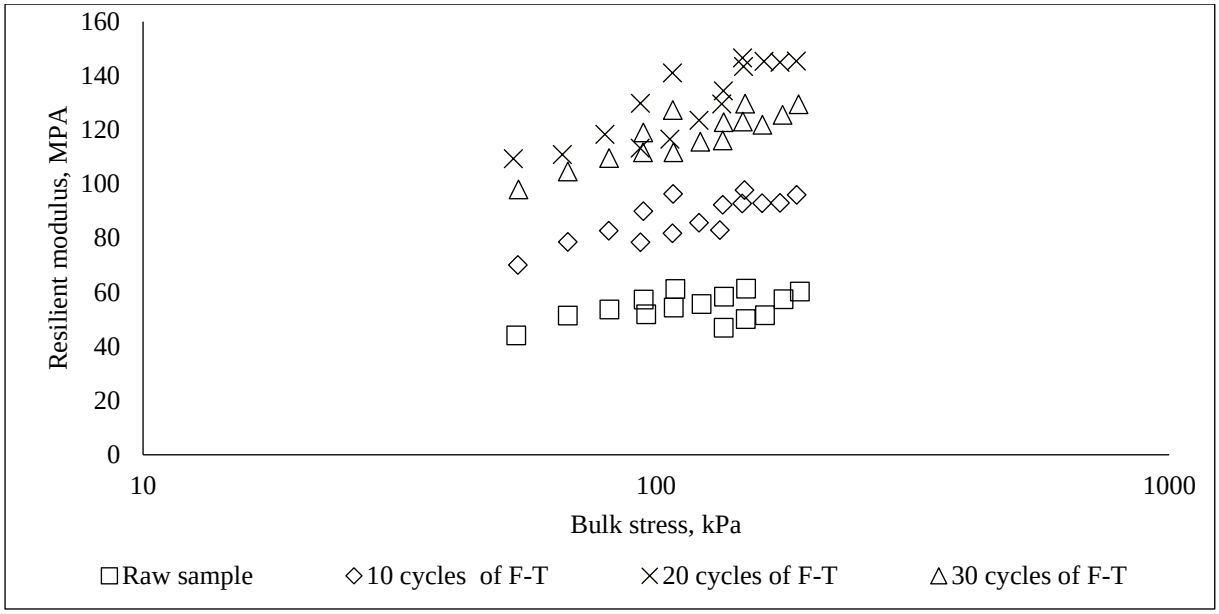

Figure 5.18 The comparison between the resilient modulus of fly ash stabilized sand before and after the freezing-thawing cycles & 80% OMC.

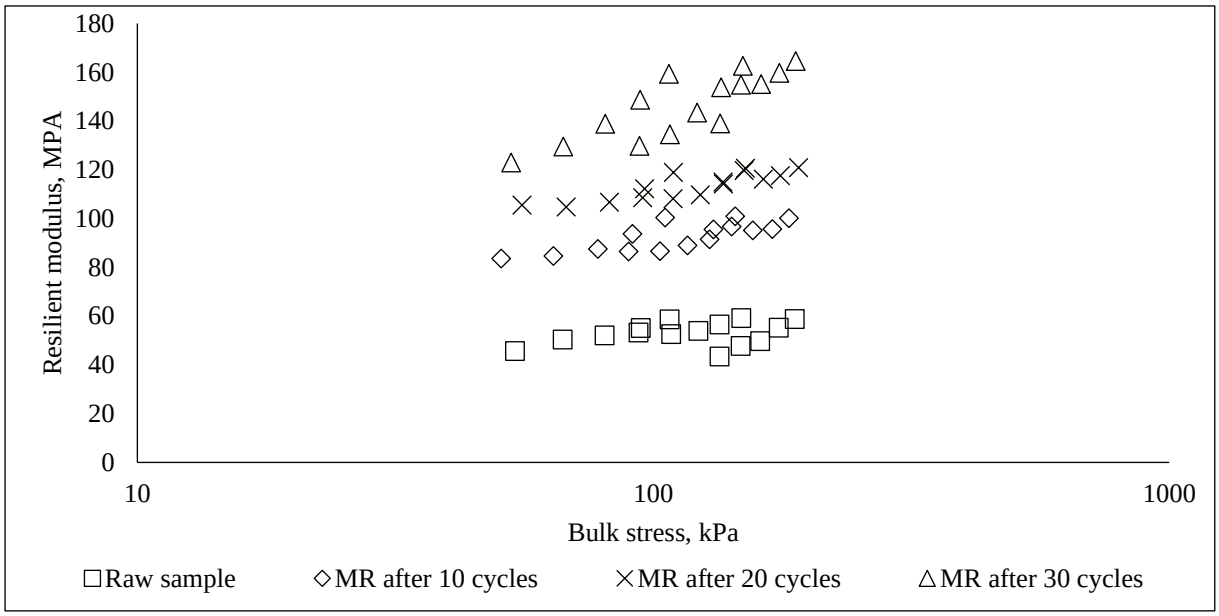

Figure 5.19 The comparison between the resilient modulus of fly ash stabilized sand before and after the Freezing-Thawing cycles & 100% OMC.

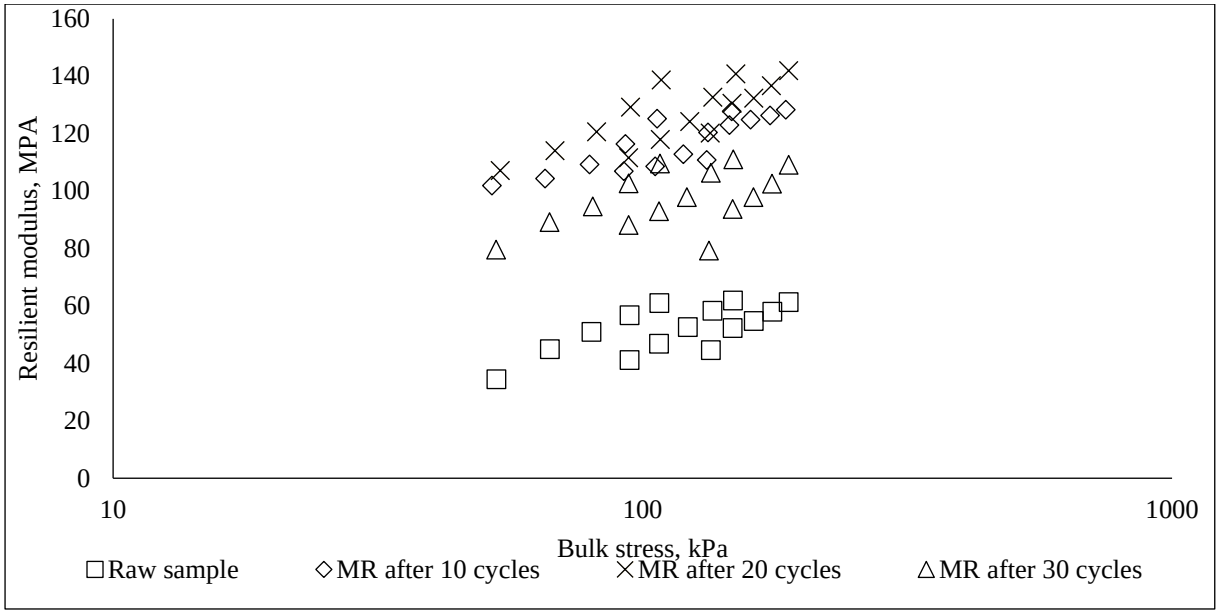

Figure 5.20 The comparison between the resilient modulus of fly ash stabilized sand before and after the Freezing-Thawing cycles & 120% OMC.

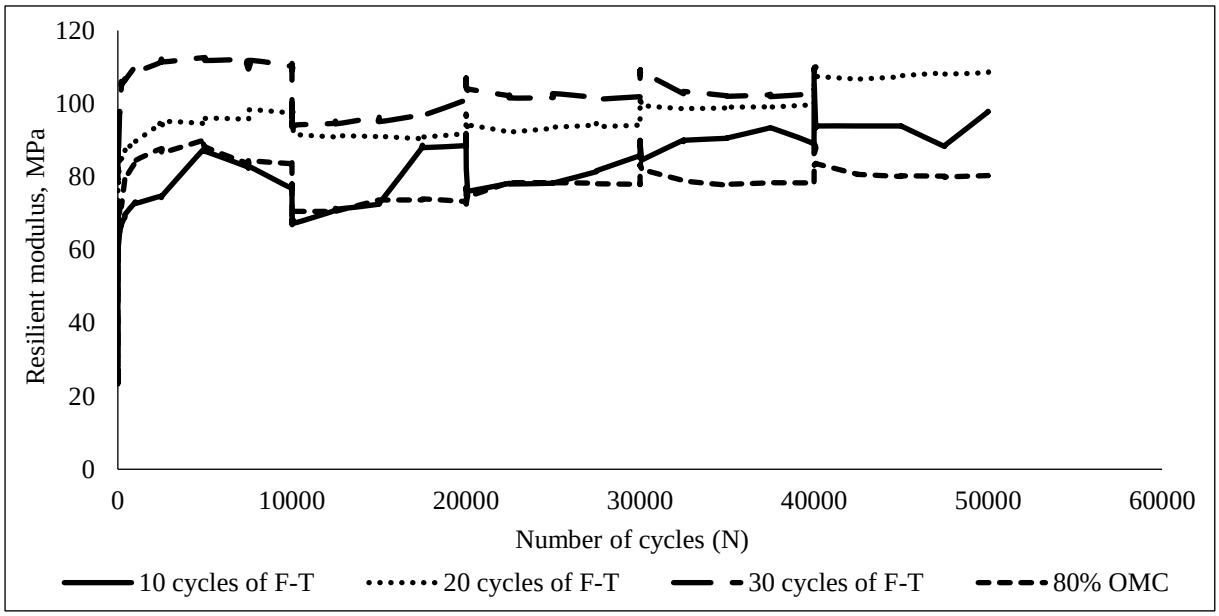

Figure 5.21 The resilient modulus of fly ash stabilized sand after 50000 cycles load, 80% OMC& Freezing-Thawing cycles.

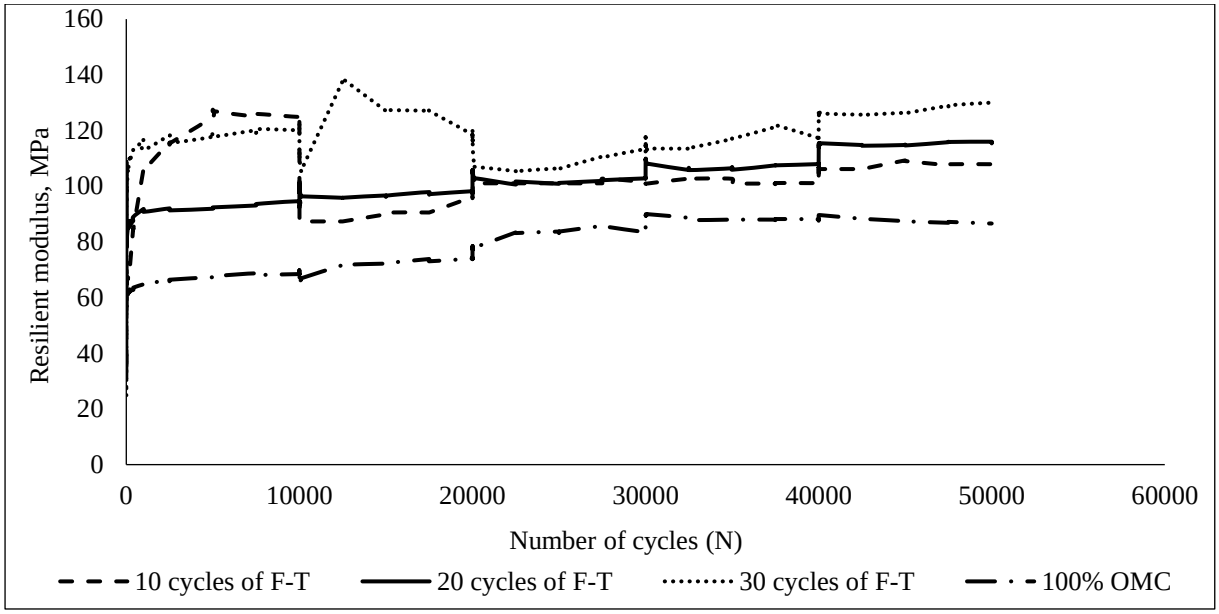

Figure 5.22 The resilient modulus of fly ash stabilized sand after 50000 cycles load, 27.6kPa, 100% OMC& Freezing-Thawing cycles.

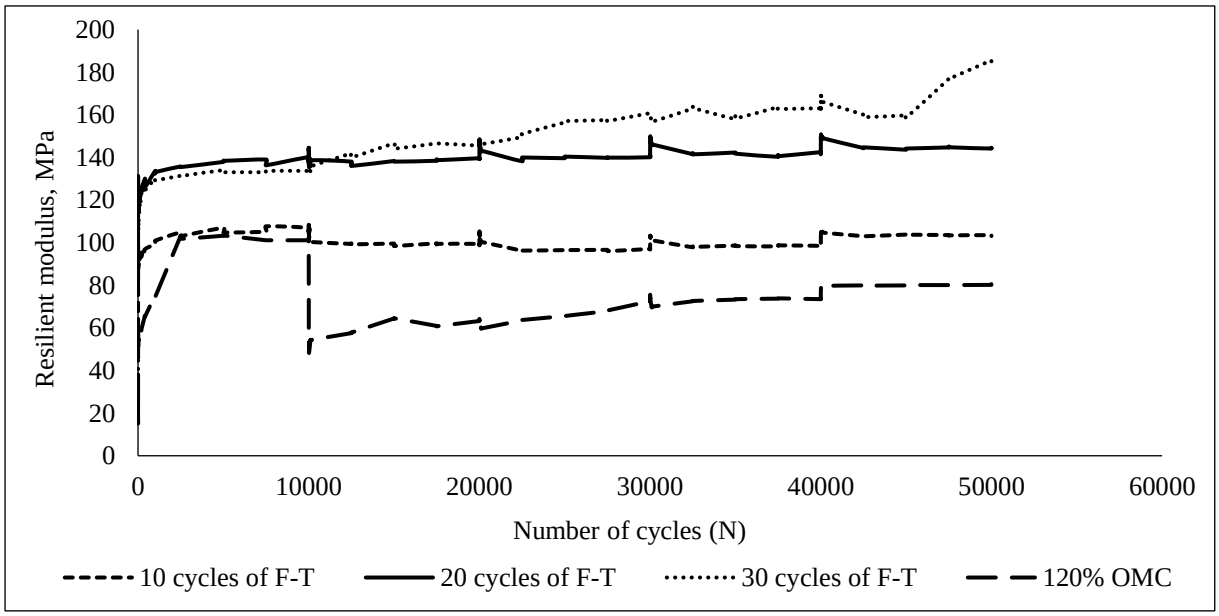

Figure 5.23 The resilient modulus of fly ash stabilized sand after 50000 cycles load, 27.6kPa, 120% OMC & Freezing-Thawing cycles.

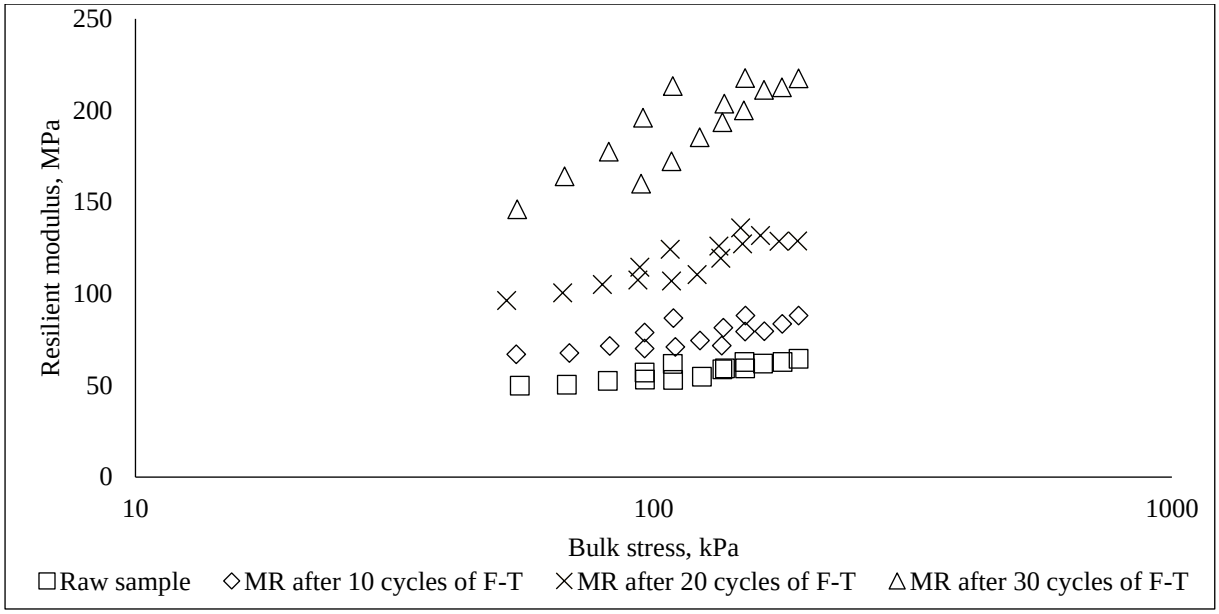

Figure 5.24 The comparison between the resilient modulus fly ash with fibre reinforced sand before and after the Freezing-Thawing cycles & OMC.

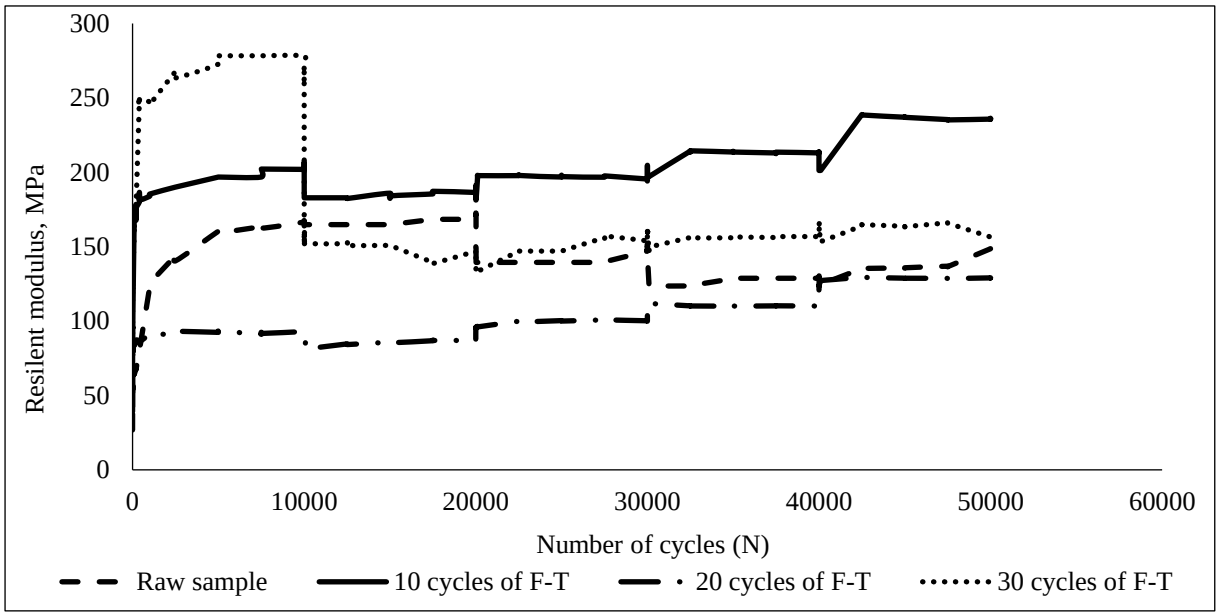

Figure 5.25 The resilient modulus fly ash with fibre reinforced sand after 50000 cycles load, 27.6kPa, and OMC & Freezing-Thawing cycles.

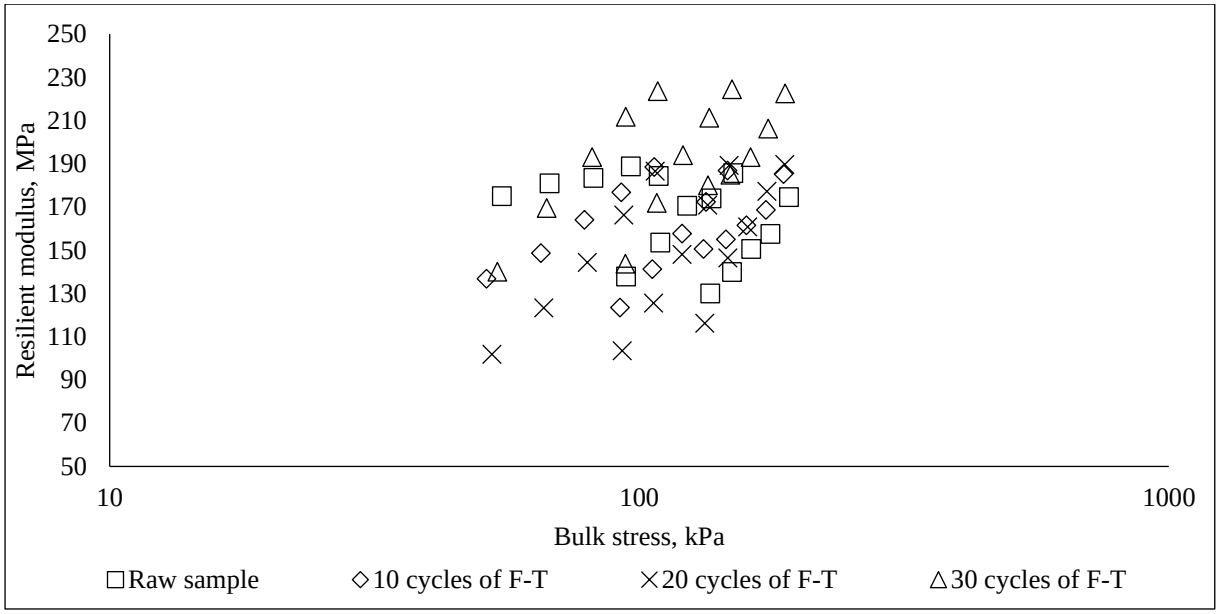

Figure 5.26 The comparison between the resilient modulus of slag stabilized sand before and after the Freezing-Thawing cycles & OMC.

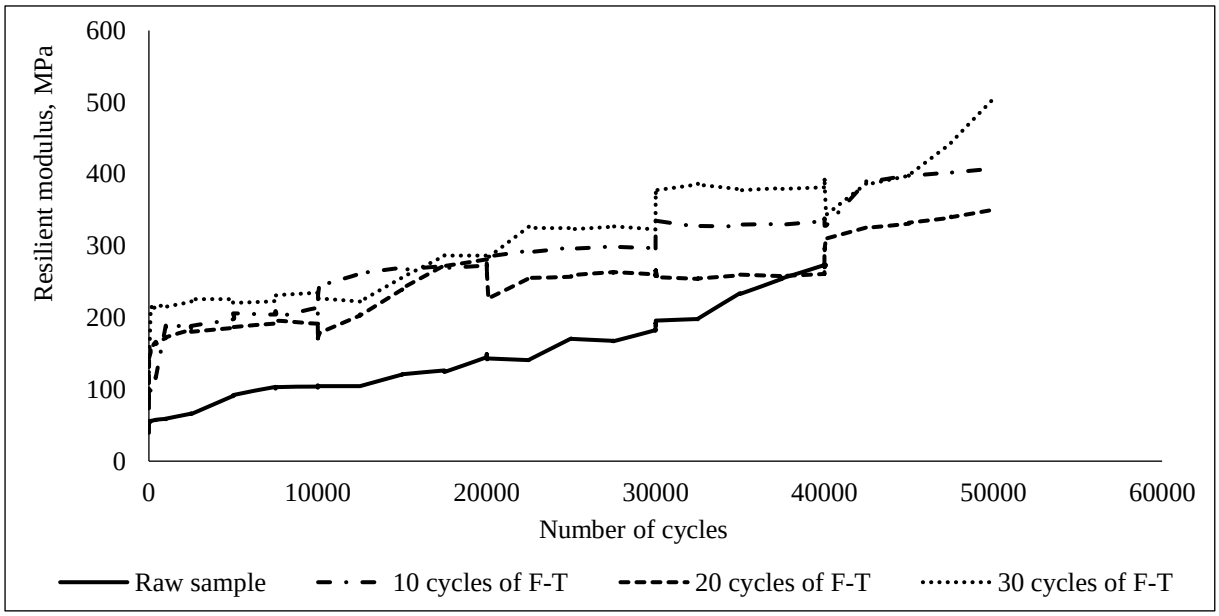

Figure 5.27 The resilient modulus of slag stabilized sand after 50000 cycles load, 27.6kPa, and OMC & Freezing-Thawing cycles.

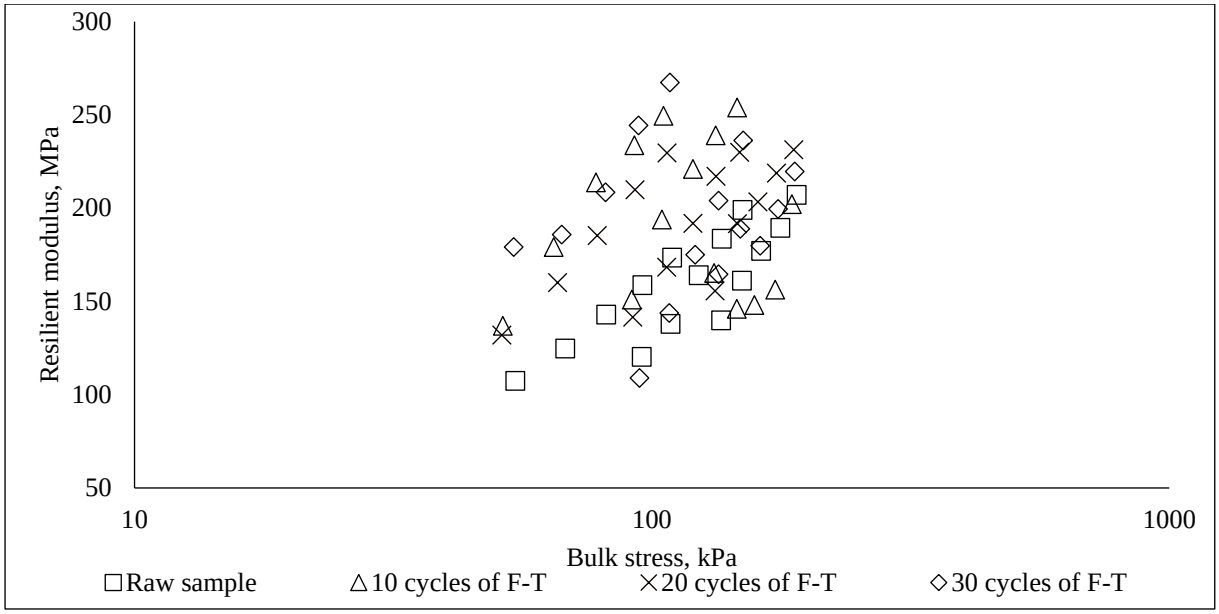

Figure 5.28 The comparison between the resilient modulus of slag with fibre stabilized sand before and after Freezing-Thawing cycles & OMC.

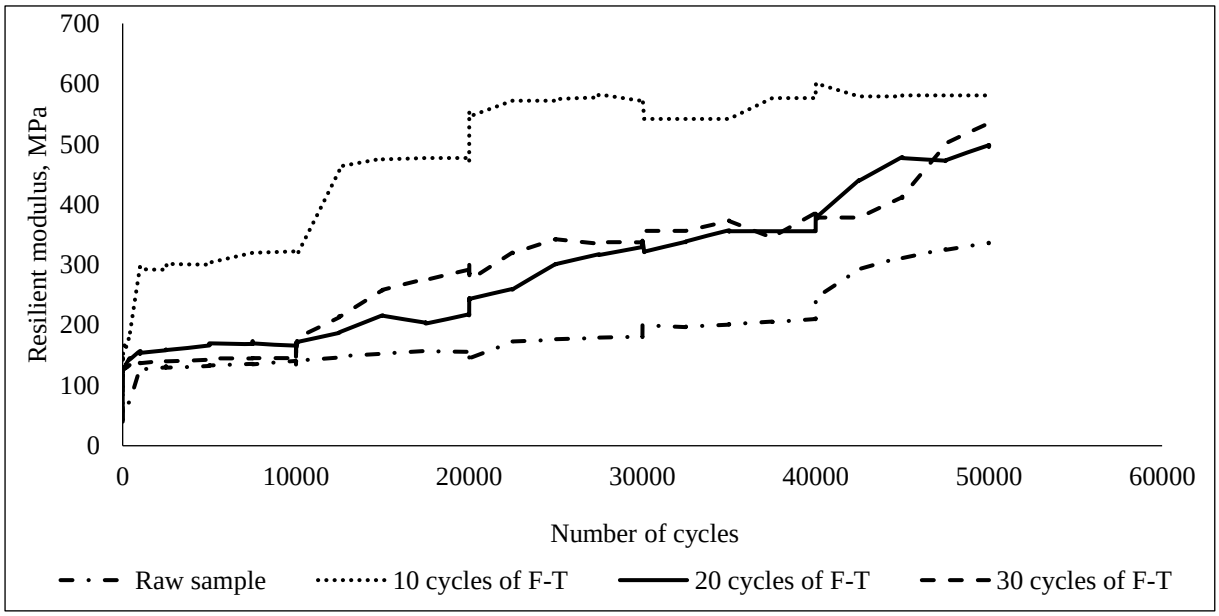

Figure 5.29 The resilient modulus of slag with fibre stabilized sand after 50000 cycles load, 27.6kPa, and OMC & Freezing-Thawing cycles.

5.3.1 Discussion

In pavement design, two types of durability tests can be conducted, wet/dry cycles and freeze/thaw cycles. In this research, wetting and drying cycles couldn't be conducted. The reason for that the sample collapsed when placed in the water, therefore, freezing-thawing

cycles were conducted to measure the durability. Also, the resilient modulus and the permeant deformation were carried out after 10, 20, and 30 cycles of F-T cycles. The test conditions included the variation of water content.

The literature review showed that in winter, the resilient modulus of unbound materials shows the highest value and smallest in spring. The ice bonding between particles in base, subbase and subgrade layers increased due to an increase in the resilient modulus. While in spring season is due to the saturated case. Therefore, the resilient modulus was obtained during the thawing stage which simulates spring season.

Most of the previous researchers conducted the unconfined compressive strength test in order to study the durability. The unconfined compressive strength test was not appropriate to simulate the field conditions due to the confining pressure zero. Therefore, the resilient modulus test is a more suitable test to measure durability.

Moreover, there was no available research to investigate the behaviour of resilient modulus of fibre reinforced sand, fly ash stabilized sand with fibre, and vitrified slag stabilized sand after F-T cycles.

To conclude the finding from the durability test

- Negligible reduction in resilient modulus of fibre reinforced sand was observed after 10 and 20 of F-T cycles at different water contents. The reason for that the equilibrium condition became predominant on the samples.
- The cementitious properties were affected by the temperature and the water content. The chemical reaction was improved with time. The result indicated that 24 hrs of thawing was sufficient to improve the pozzolanic reaction.

- Inclusion fibre with fly ash into the sand shown significant improvement in resilient modulus. The samples gained the cohesion
- Similar behaviour of sand reinforcement was observed by Multi-Stage triaxial test.

The F-T cycles improved resilient modulus. The reacted vitrified slag showed significant bonding with F-T cycles. There are two factors which expected to be the causes, the humidity during the curing time and temperature. The chemical reaction of sodium hydroxide with the slag was affected by these factors. During the gel stag of slag, it allowed the sand to be together and improve the cohesion.

5.4 Computation of Environmental Adjustment Factor

The guide for mechanistic empirical design (NCHRP, 2004) provided a procedure to obtain the resilient modulus after freezing and thawing. The evaluation of resilient modulus considers different parameters such as stress level, density, water content and freezing and thawing cycles. As mentioned in section 2.4.2, the data quality in the M-E pavement design guide was classified into three levels. In the environmental adjustment, the stress state was considered in level 1; level 2 considers the resilient modulus at the maximum dry density and optimum water content while in level 3, the resilient modulus was estimated. As stated in the guide, the variation of the resilient modulus with different stress state, resilient modulus with different environmental conditions and water content were assumed, independent. Therefore, it was not necessary to obtain the resilient modulus at optimum water content. The effect of water content as explained in section 5.2.2 is described briefly below:

All other factors are equal, while the increased water content was due to reduction in the resilient modulus of unbound granular materials. The water content has two effects, it affects the stress state (suction or pore water pressure) or the soil structure (affect the cementation

between the soil grains). Also, during the freezing, the resilient modulus increases to a large extent of about 20 to 120 times more than the resilient modulus before the freezing.

In this research, the cyclic deviator stress and water content were considered to obtain the adjustment factor F_{env}. The adjustment factor is the ratio of the resilient modulus at the optimum water content and different cyclic deviator stress to the resilient modulus after freeze-thaw conditions as expressed in Equation 5-1.

$$M_R = F_{env} * M_{Ropt} \quad \text{Equation 5-1}$$

Where

F_{env} = Adjustment factor,

M_{Ropt} = Resilient modulus at optimum condition and any stress level, and

M_R = Adjusted resilient modulus (moisture, density and freeze thaw cycles).

In this research, the reinforcement materials showed that the environmental conditions have a slight effect on the resilient modulus. Therefore, the adjusted factor was obtained based on the minimum resilient modulus value. Equation 5-1 was modified to work with the stabilized and reinforced materials as expressed in Equation 5-2.

$$M_R = F_{env} * M_{R(F-T)min} \quad \text{Equation 5-2}$$

Where

M_R = The resilient modulus for raw samples, and

$M_{R\ (F\text{-}T)\ min}$ = The minimum resilient modulus after F-T cycles.

Equation 5.2 was proposed to use in this research for fibre, fly ash, and slag. The adjusted factor of 0.95 was obtained for 135 resilient modulus values at different stresses, water content, and environmental condition. Table 5-2 shows the resilient modulus before and after applying the environmental factor. This factor was applied in the analytical pavement design in Chapter Seven.

Table 5-2 The measured resilient modulus and corresponding resilient modulus after F-T cycles.

Dev stress, kPa	Fibre		Fly ash stabilized sand		Fly ash with fibre reinforced sand		Slag stabilized sand		Slag with fibre reinforced sand	
	M_R, MPa	$M_{R\ (F\text{-}T)\ min}$	M_R, MPa	$M_{R\ (F\text{-}T)\ min}$	M_R, MPa	$M_{R\ (F\text{-}T)\ min}$	M_R, MPa	$M_{R\ (F\text{-}T)\ min}$	M_R, MPa	$M_{R\ (F\text{-}T)\ min}$
13.8	44	42	44	41	59	56	130	124	140	133
27.6	53	51	48	45	59	56	140	133	161	153
41.4	57	55	50	47	62	59	151	143	177	168
55.2	63	59	55	52	63	60	158	150	189	180
68.9	67	64	59	56	65	61	175	166	207	197
13.8	40	38	53	51	53	51	138	131	120	114
27.6	50	47	53	50	53	50	154	146	138	131
41.4	57	55	54	51	55	52	171	162	164	156
55.2	64	61	57	54	59	56	174	165	184	174
68.9	68	65	59	56	63	60	186	176	199	189
13.8	32	30	46	43	50	47	175	166	107	102
27.6	48	46	50	48	50	48	181	172	125	118
41.4	56	53	52	49	52	50	183	174	143	136
55.2	63	60	55	52	57	54	189	179	159	151
68.9	68	64	59	56	62	59	184	175	174	165

5.4.1 Discussion

As stated in the guide for mechanistic empirical design, there are three methods to measure the resilient modulus, Method 1; the resilient modulus is obtained by the laboratory testing, Method 2; correlations and other materials properties, Method 3; typical values (NCHRP, 2004). The effect of environmental conditions was used to adjust the resilient modulus in the analytical pavement design by an environmental adjustment factor.

In this research, mothed 1 was used to obtain the resilient modulus. The resilient modulus was obtained by taking the stress, optimum water content and maximum dry density into the account. Therefore, the adjusted factor will be more reliable. The environmental adjustment factor was obtained for 135 values of resilient modulus for fibre, fly ash and slag. The factor is 0.95. The corrected resilient modulus values were used to obtain the correlation models in section 5.6. In Chapter Seven, the analytical pavement design was conducted based on the corrected resilient modules values.

5.5 Nonlinear Behaviour of the Subgrade Layer

NCHRP (2004) considered the unbound base/subbase and subgrade materials nonlinear materials. Unbound Materials have been considered as nonlinear when the resilient modulus depends on the level of stress. The major categories of materials are asphalt materials, PPC materials, chemically, stabilized materials, non-stabilized granular materials, subgrade soils, and bedrock. However, the polypropylene fibre, class C fly ash, and vitrified slag materials haven't been included in the Guide.

Huang (2004) classified the soils into two types, which were fine and granular soil. Simple relationships were provided to obtain the resilient modulus of granular and fine soils as Equation 5-3, 5-6 and 5-7. The relationships were incorporated in KENLAYER software.

For the granular materials, the resilient modulus was expressed in Equation 5-3. It demonstrates the relationship between resilient modulus and the first bulk stress.

$$M_R = K_1 * \theta^{K_2} \qquad \text{Equation 5-3}$$

Bulk stress was expressed as the summation of three normal stresses or principle stress as shown in Equation 5-4. In the case of including the weight of layers, the bulk stress is determined by Equation 5.5.

$$\theta = \sigma_1 + \sigma_2 + \sigma_3 = \sigma_x + \sigma_y + \sigma_z \quad \text{Equation 5-4}$$

$$\theta = \sigma_x + \sigma_y + \sigma_z + \Upsilon z(1 + 2K_o) \quad \text{Equation 5-5}$$

For the fine materials, the resilient modulus was defined as exhibited in Equation 5-6 & 5-7. The deviator stress is defined as Equation 5.8 in the laboratory triaxial test. In the case of a layered system, the layer weight is considered as expressed in Equation 5-9. The bilinear behaviour is expressed in Equations 5-6 & 5-7.

$M_R = k_1 + k_4(k_2 - \sigma_d)$ When $\sigma_d < k_2$ Equation 5-6

$M_R = k_1 - k_4(\sigma_d - k_2)$ When $\sigma_d > k_2$ Equation 5-7

$$\sigma_d = \sigma_1 - \sigma_3 \quad \text{Equation 5-8}$$

$$\sigma_d = \sigma_1 - 0.5(\sigma_2 + \sigma_3) + \gamma z(1 - k_0) \quad \text{Equation 5-9}$$

Where:

K_1, K_2, K_3 & K_4 = Constant parameters,

Θ = Bulk stress,

σ_1, σ_2 & σ_3 = Principle stress,

σ_x, σ_y &σ_z = Normal stress,

σ_d = Deviator stress,

Υ = Dry density,

z = Depth of required resilient modulus, and

K_o = Coefficient of earth pressure at rest.

As noted from equation 5-3, the k_1 & k_2 reflect the soil behaviour in terms of bulk stress. The k_1 is the resilient modulus for granular subgrade soil when the deviator stress equal to 6.9kPa. And k_2 display the effect of deviator stress on the resilient modulus for other factors. In this research, k_2 is considered after freezing and thawing cycles and a range of water content which has a significant influence on the resilient modulus.

The pavement responses need to be determined by a finite element model. Boussinesq's solutions assumed that the existing materials in the half-space are linear elastic. It is well known that the subgrade materials are not elastic and undergo permanent deformation under loads. Linearity can apply in the superposition area but the resilient modulus must not vary with the stress level. On the other hand, the deformation of linear materials should be independent of confining stress. Indeed, this is not true for the soil. The reason for that the axial deformation is depending on the confining stress.

Iterative method was proposed to evaluate the effect of the nonlinearity of granular materials on the vertical stress and deflection by (Huang, 1968). In the iterative method, the layers were divided the half-space into seven layers. Then, Burmister's layered theory was used to obtain the stress at the midheight of each layer. The resilient modulus was determined from Equation 5-10 for each layer based on these stresses.

$$E = E_O(1 + \beta\theta) \qquad \text{Equation 5-10}$$

$$\theta = \sigma_x + \sigma_y + \sigma_z + \gamma z(1 + 2K_o)$$ Equation 5-11

Where

E = Elastic modulus under the applied stresses,

E_o = The initial elastic modulus,

θ = Sum of stresses and

β = Soil constant.

The following steps are used to analyse the nonlinear half-space:

First, an elastic modulus is assumed for each layer. And the stresses are obtained from the layered theory.

Second, from Equation 5.11 a new set of moduli is determined by the obtained stresses, and a new set of stresses is then computed.

Third, the process is repeated until the moduli between two consecutive iterations converge to a specified tolerance.

However, it was stated that the nonlinear behaviour of soils has a very small effect on vertical and shear stresses. Depending on the depth of the point, the vertical stresses based on nonlinear theory may be greater or smaller than those based on linear theory and, at a certain depth; both theories could yield the same stresses. This may explain why Boussinesq's solutions for vertical stress based on linear theory have been applied to soils with varying degrees of success, even though soils themselves are nonlinear. Linear theory of Boussinesq's

equations is used in approximate method to determine the stress at the midheight of each layer for the nonlinear behaviour.

Example is provided with 552kPa contact pressure, earth pressure at rest of 0.5. The example demonstrates both theories. Table 5-3 provides differences in stresses and moduli between Boussinesq and Burmister Solutions. Burmister Solutions proposed that the nonlinear layers are divided into sex layers. The pavement responses were obtained by KENLAYER to evaluate the difference between Boussinesq and Burmister solutions. Figure 5.30 demonstrates the layer thickness and the depth of mid-points. The results shown that the resilient modulus value shown negligible difference and little effect on the stress.

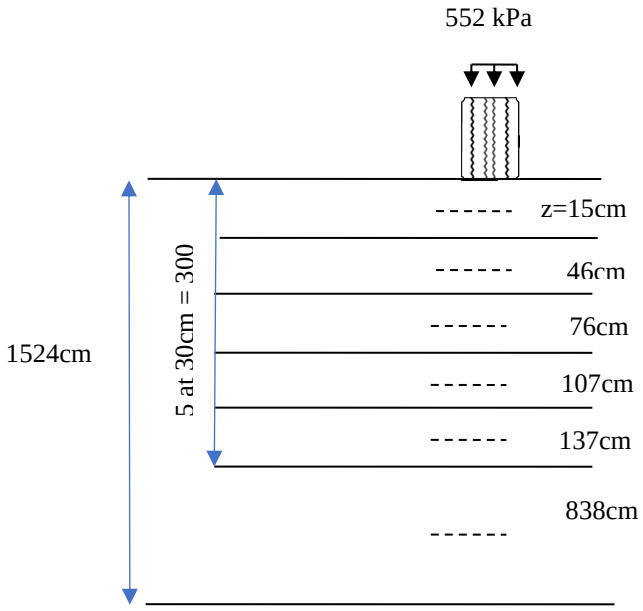

Figure 5.30 Layers layout for the pavement section.

Table 5-3 Pavement responses based on Boussinesq and Burmister Solutions for the subgrade sand soil.

No	Layer thickness, cm	z at mid-height, cm	Boussinesq			Burmister			deflection
			σ_z, kPa	σ_t, kPa	E	σ_z, kPa	σ_t, kPa	E	
1	30	15	358	32	0.21	348	31	0.21	0.044
2	30	46	81	-3.5	0.14	73	-4.5	0.14	0.018
3	30	76	31	-1.8	0.14	29.4	-1.9	0.14	0.007
4	30	107	16	-1	0.14	16	-0.76	0.14	0.0038
5	30	137	10	-0.62	0.14	10	0.07	0.14	0.0022
6	1372	838	0.27	0.00	0.18	0.27	0.00	0.18	0.0063
								Total	0.08255

Figure 5.31 demonstrates different behaviour of resilient modulus of fibre reinforced sand. The behaviour of resilient modulus can be explained k_1 and k_2. Both indicated that the reinforced sand with fibre was improved after freezing and thawing cycles. The results of k_1 reflected the effect of F-T cycles on samples at different water content. It was noted that the 10 and 20 F-T cycles shown similar trending. Both demonstrated that the compacted samples at optimum water content shown higher resilient modulus. A 30 F-T cycles shows a linear relationship which indicates that as the F-T cycles increased the resilient modulus decreases. The effect of other parameters such as confining pressure was explained by k_2. The results can be explained by k_2 value, if k_2 reduced the effect of water content and confining pressure are decreased as shown in Figure 5.32. The effect of k_2 was expressed as polynomial relationship. The compacted samples at optimum water content shows less effect by the confining pressure and F-T cycles. As mentioned in section 5.2.2, the increase in water content causes reduction in the resilient modulus by reducing the effect of confining pressure as shown in Figure 5.32

The nonlinear parameters of fly ash stabilized sand shown that the increase in water content reduces the k_1 parameter. This implies that the resilient modulus is significantly affected by water content as illustrated in Figure 5.33. Also, the compacted samples up to optimum water

content reflect that the resilient modulus increased with an increase in the number of F-T cycles. On the other hand, the effect of confining pressure was less with an increase in the number of F-T cycles as demonstrated by k_2 Figure 5.34. It can be explained that during the thawing period, cementitious properties improved the cohesion between the particles.

Either fly ash or slag with fibre stabilized samples was affected by densification due to post-compaction. The resilient modulus of fibre with fly ash reinforced sand shows that the fibre affects the behaviour of both k_1 and k_2 as illustrated in Figure 5.35 and 5.35, respectively. Also, the increase in the number of F-T cycles increases the effect of confining pressure as shown in Figure 5.36. The effect of confining pressure increases due to the increase in the number of F-T cycles as k_2 indicated. As noted from Figure 5.37 and 5.37, the resilient modulus of raw slag stabilized sand samples shown significant strength to tolerate the deviator stress as k_2 parameter reflected. The k_1 shows the initial resilient modulus. Figure 5.39 and 5.39 respectively shown the results of slag with fibre reinforced sand and it can be found that k_1 values decreases and k_2 values increases. As discussed in Chapter Four section 4.2.4, the fibre decreases the density but increase the interlock between the particles. This can be explained by the initial resilient modulus which decreases with increase in the F-T cycles while the effect of deviator stress increase with the increase in the F-T cycles. This is because the water content changes in the sample and make it weaker to tolerate the load.

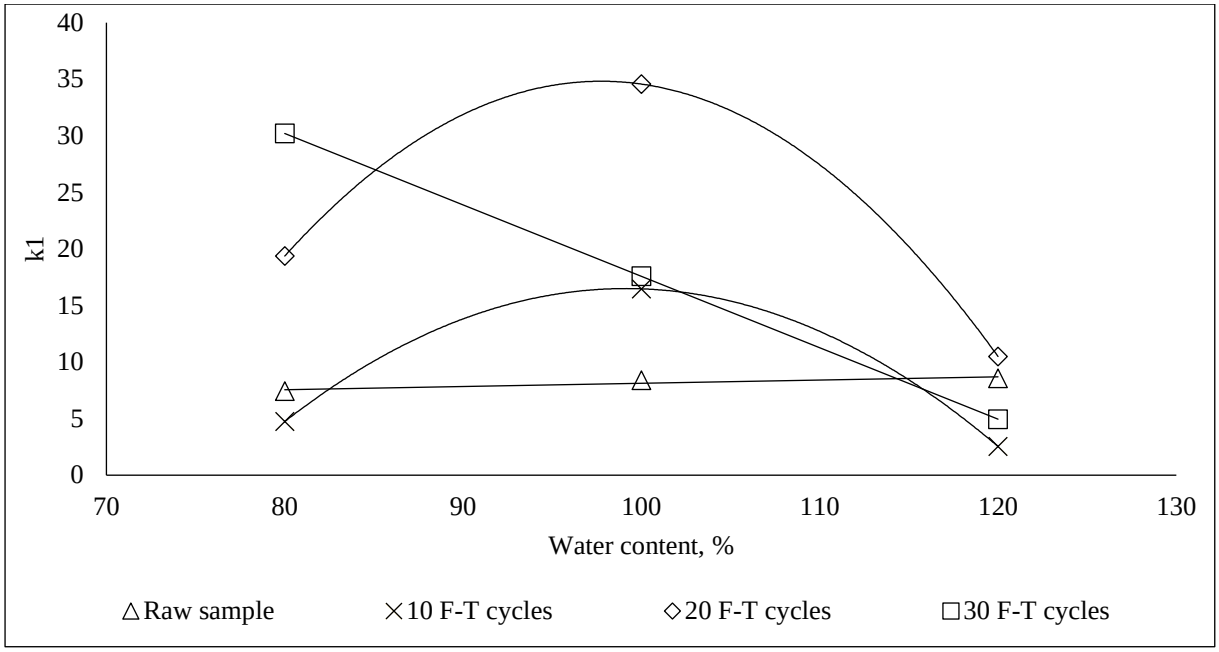

Figure 5.31 k_1 parameter for fibre reinforced sand at 80%, OMC & 120%.

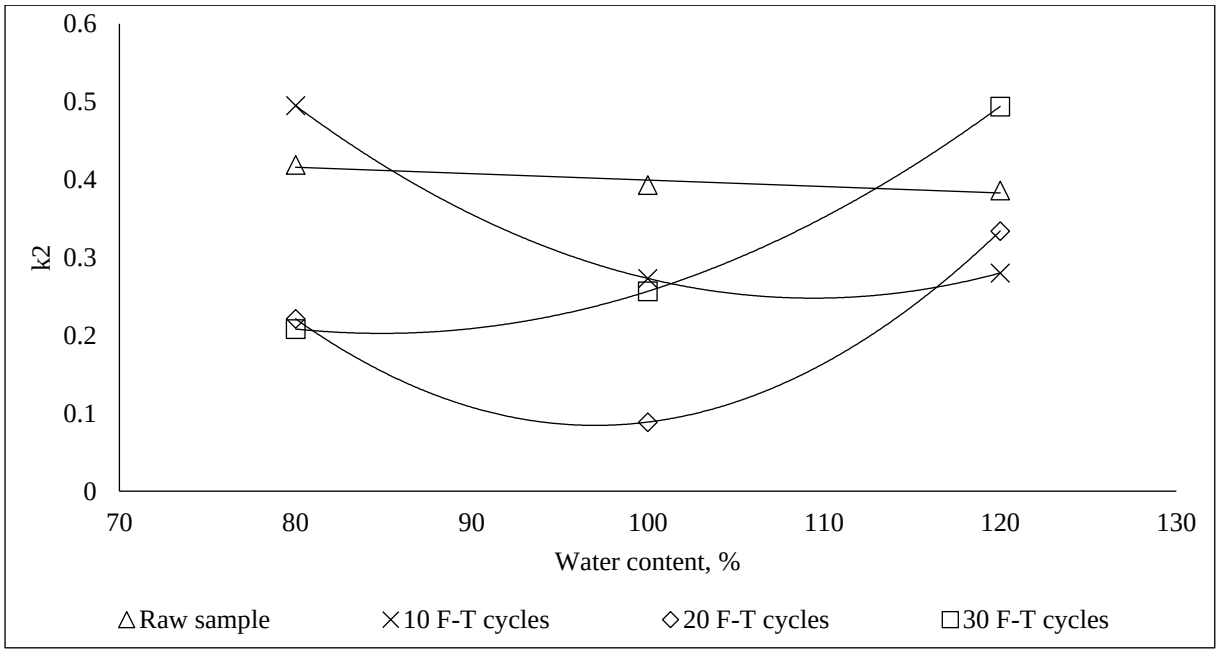

Figure 5.32 k_2 parameter for fibre reinforced sand at 80%, OMC & 120%.

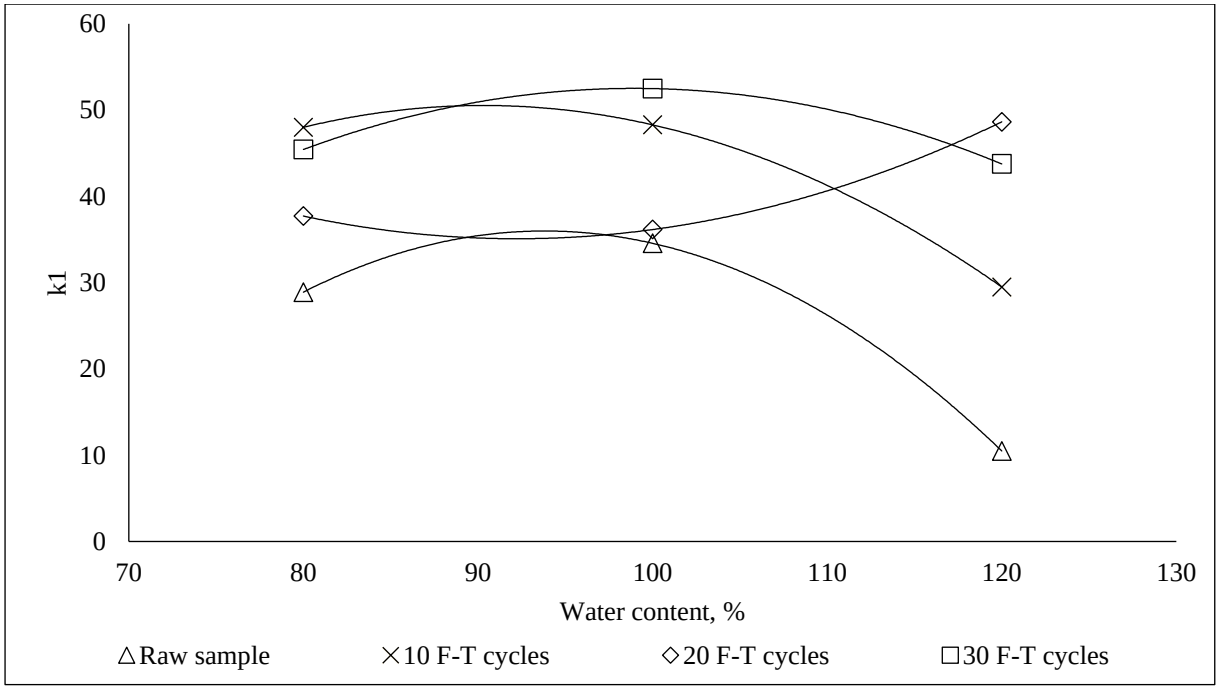

Figure 5.33 k_1 parameter for fly ash stabilized sand at 80%, OMC & 120%.

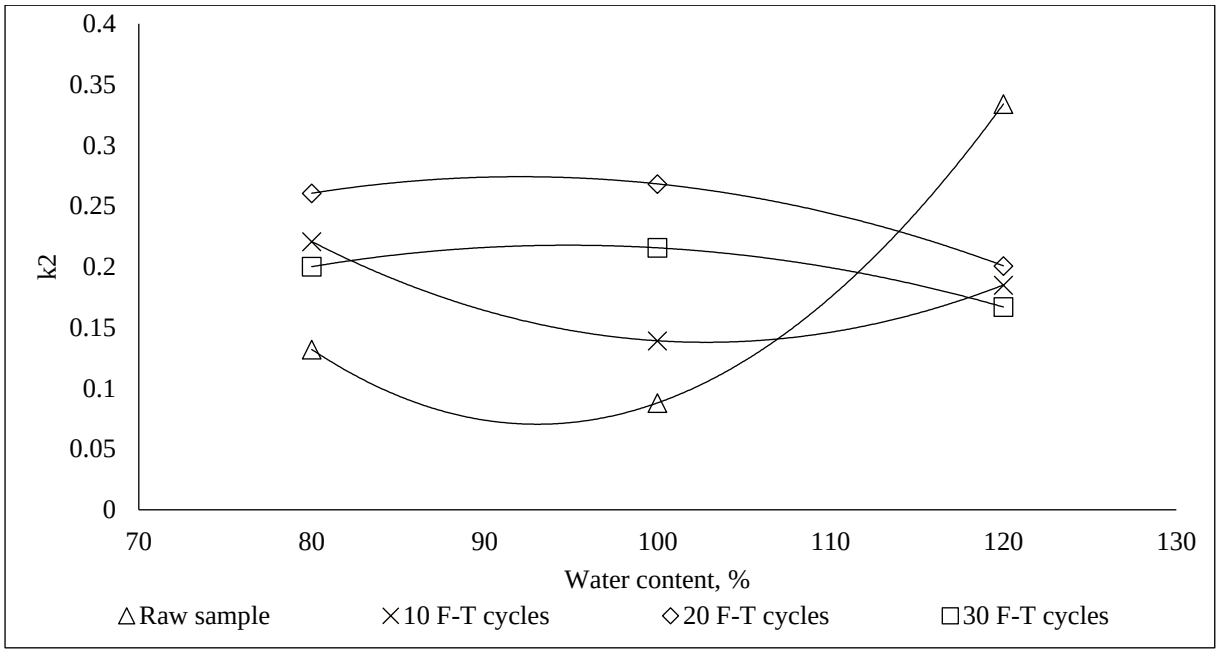

Figure 5.34 k_2 parameter for fly ash stabilized sand at 80%, OMC & 120%.

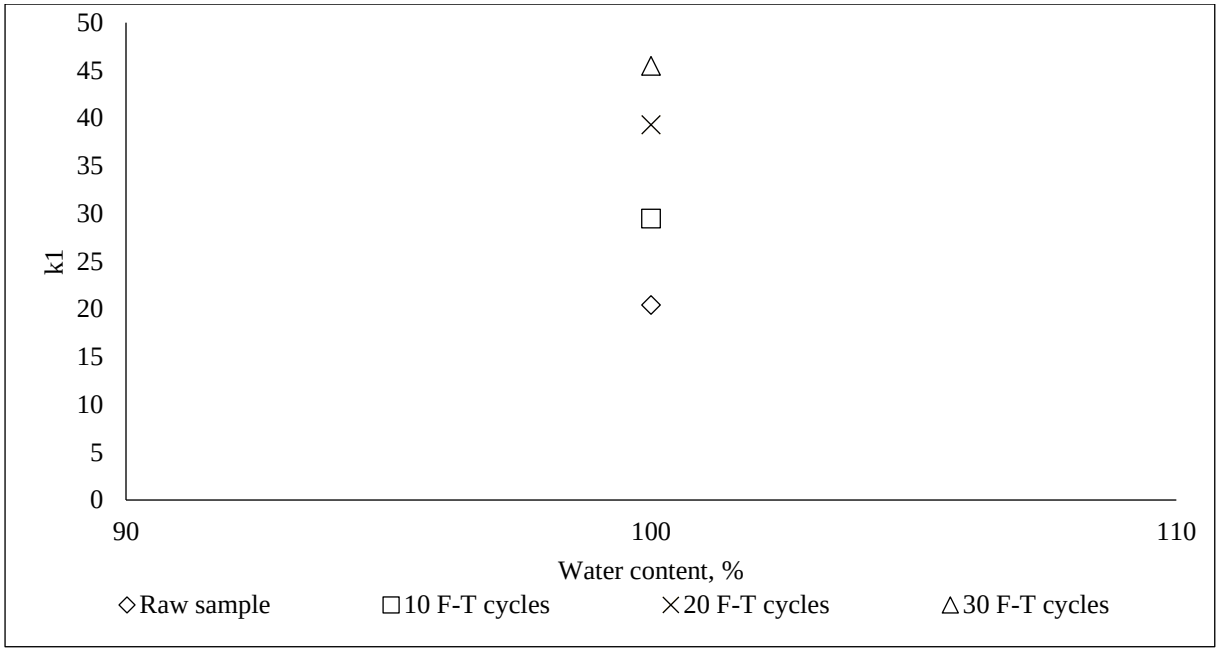

Figure 5.35 k_1 parameter for fibre with fly ash reinforced sand at OMC.

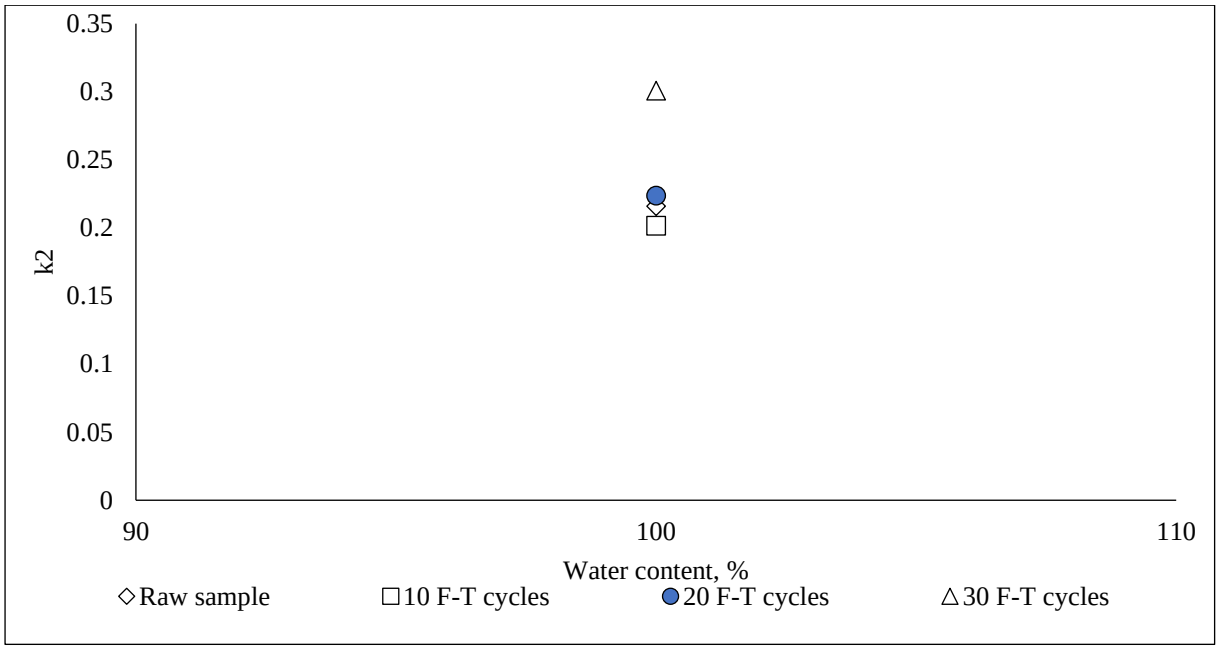

Figure 5.36 k_2 parameter for fly ash with fibre reinforced sand at OMC.

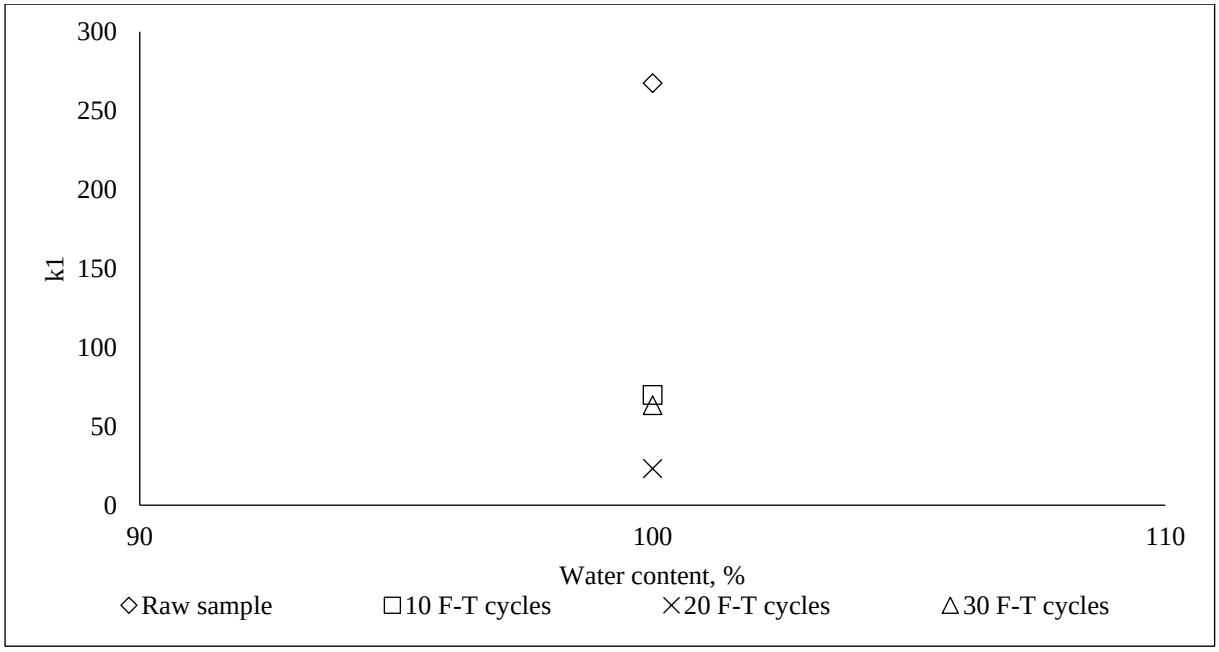

Figure 5.37 k_1 parameter for slag stabilized sand at OMC.

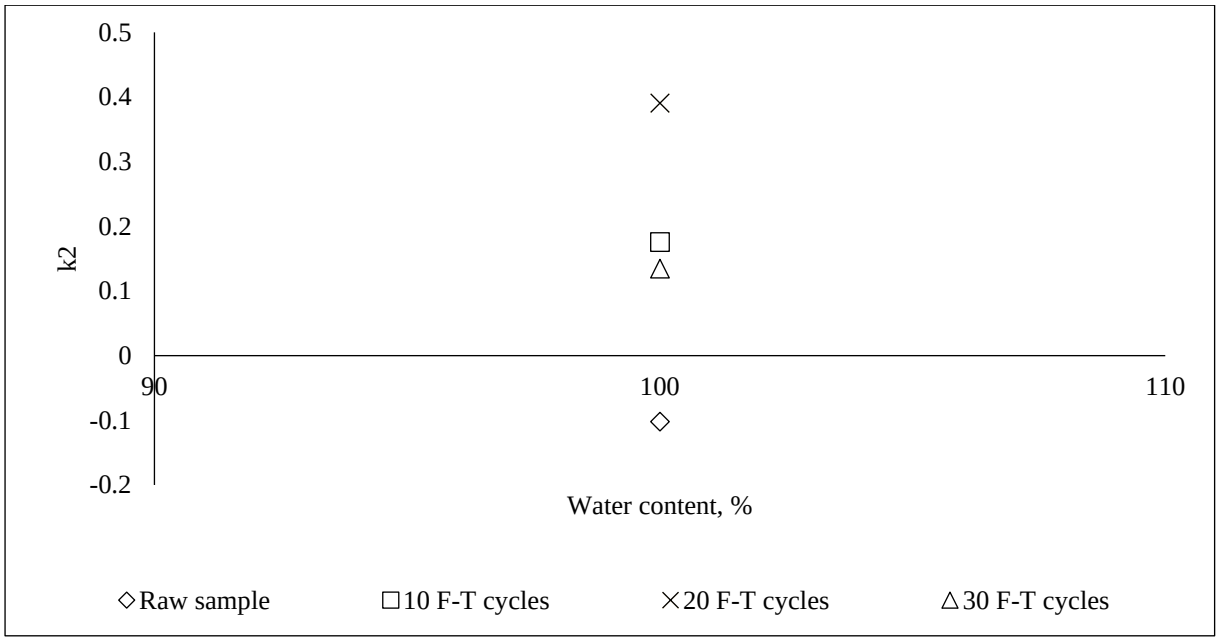

Figure 5.38 k_2 parameter for slag stabilized sand at OMC.

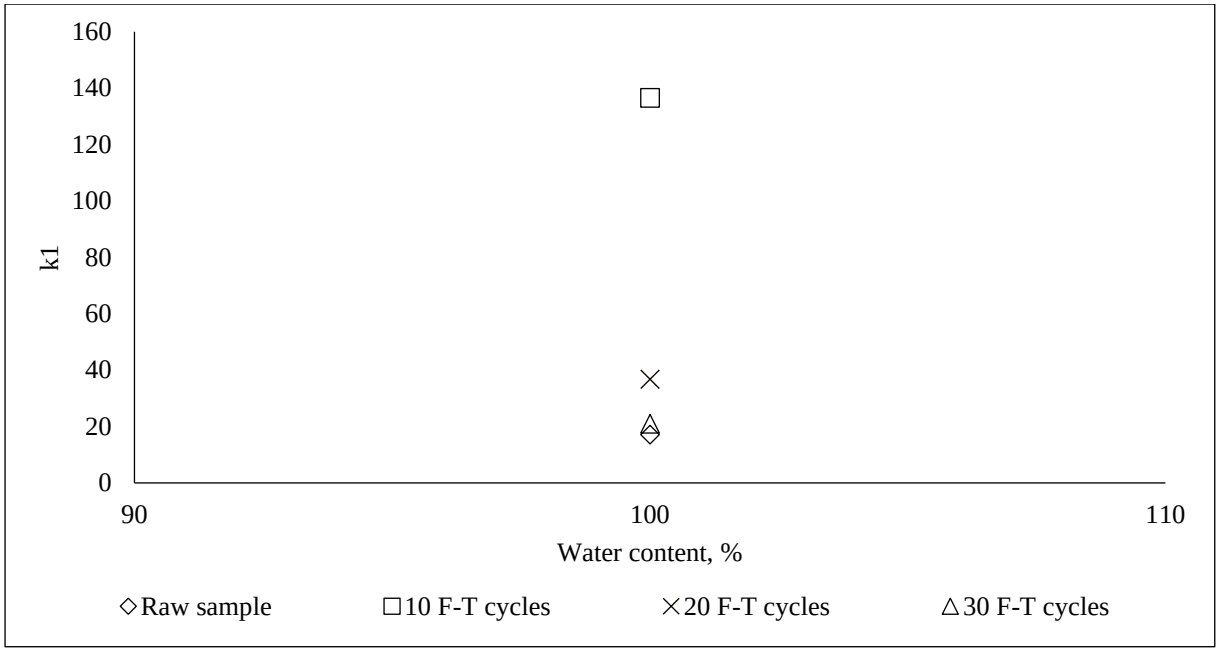

Figure 5.39 k_1 parameter for slag with fibre reinforced sand at OMC.

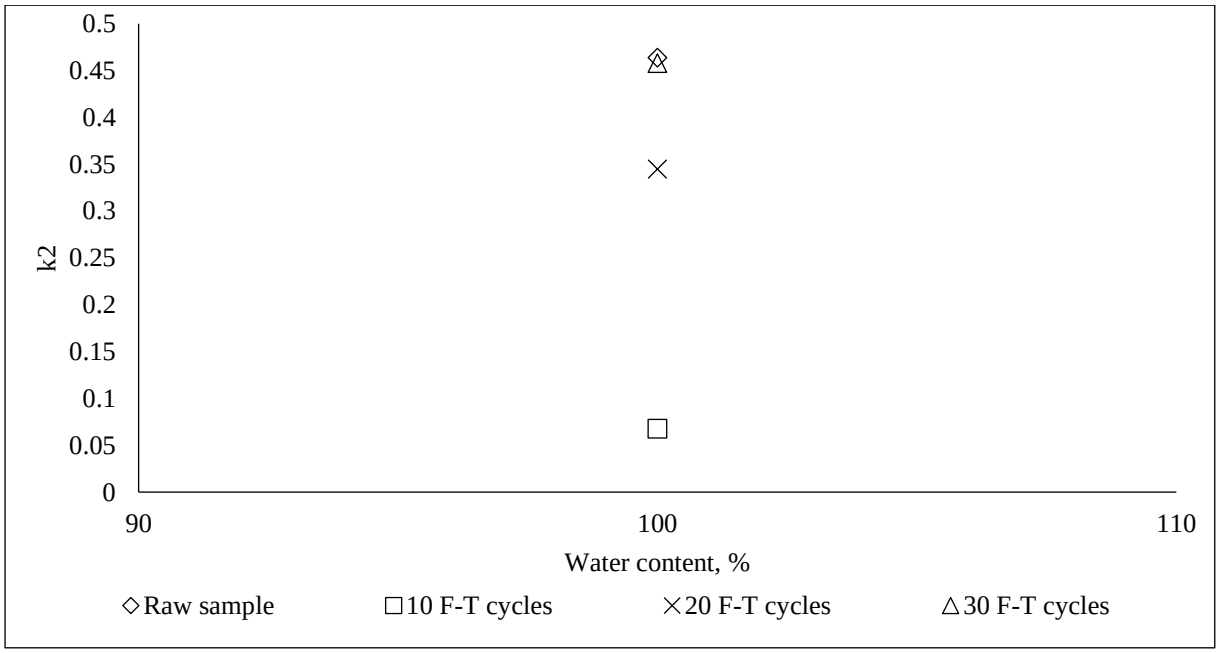

Figure 5.40 k_2 parameter for slag with fibre reinforced sand at OMC.

5.5.1 Discussion

In this section, the nonlinear behaviour of soils has a large effect on vertical and radial displacements, an intermediate effect on radial and tangential stresses, and a very small effect on vertical and shear stresses (Huang, 1969a). Also, based on the depth of the point, the

vertical stresses based on nonlinear theory may be greater or smaller than those based on linear theory and, at a certain depth; both theories could yield the same stresses. This may explain why Boussinesq's solutions for vertical stress based on linear theory have been applied to soils with varying degrees of success, even though soils themselves are nonlinear.

In section 5.2.1, the results of resilient modules shown that the confining pressures have a negligible effect on the resilient modulus values of reinforced sand. The fibre and/or fly ash reinforced sand shown that the confining pressures haven't demonstrated a notable effect on the resilient modulus values at different water content.

Therefore, Chapter Seven provides the pavement design for the sand reinforcement. The linear concept was used to provide the pavement response for different tyre load and pressure. Also, the pavement design shows how the sand reinforcement was beneficial.

5.6 Resilient Modulus Model

Guide for mechanistic-empirical design (NCHRP, 2004) provided the required resilient modulus for the chemical stabilized materials such as lean concrete, cement stabilized, soil cement, lime-cement-fly ash and lime treated materials as well as the relationships to determine the resilient modulus for these materials. These relationships correlate with the unconfined compressive strength and the resilient modulus. The only recommended relationship that was included in activated fly ash by cement is expressed in Equation 5-12. This equation is overestimated of resilient modulus of fly ash and fly ash with fibre reinforced sand.

$$E = 500 + q_u \qquad \text{Equation 5-12}$$

Where

E = The modulus of elasticity psi, and

q_u = Unconfined compressive strength psi.

In this research, other stabilized and reinforcement materials were used which are not existing in the guide. As explained previously in sections 5.2.2 and 5.5, the water content is one of the main factors that influence the pavement materials as well as the deviator stress and the confining pressure. Therefore, it was necessary to develop a correlation model to obtain the resilient modulus for different materials.

The models are based on extensive laboratory work. Huge numbers of compaction tests were conducted to determine the optimum stabilizers materials, maximum dry density, and optimum water content. The reinforced and stabilized samples were tested to evaluate the resilient modulus and unconfined compressive strength under various water contents.

The benefits of using correlation models are; the equations can be used with both cyclic load and static load test, safe the time by using the simplest test such UCST. The correlation models are correlations between the k_1 and k_2 parameters and the water content. The models are expressed as Equation 5-13 & 5-14. The parameters of k_1 and k_2 are substituted into Equation 5-3. The outcome of the relationship is given in Equation 5.15 which can be used to obtain the resilient modulus by the cycling triaxial test results while Equation 5.16 can be used with unconfined compressive strength test results. Table 5-6 compares the results of the experimental test results and the results from Equation 5-15 and 5-16.

The correlation models approached different water content of fly ash stabilized sand. Also, 80% and OMC of the water content for fibre reinforced sand were considered in the correlations. The model was not fitting at 120% OMC for fibre reinforced sand. This was because the degree of saturation at 120% OMC for fibre reinforced sand is exceeding the

degree of saturation at 120% OMC for fly ash stabilized sand as demonstrated in Figure 5.42. Figure 5.41 displays the limit of water content for the correlation model of fly ash stabilized sand.

The correlation models were validated with (Finn et al., 1986) equation which is expressed in Equations 5-3. Thereafter, the equations were subjected to statistical investigation to assess them and compare the results with (Finn et al., 1986) equations' results as summarized in Table 5-4.

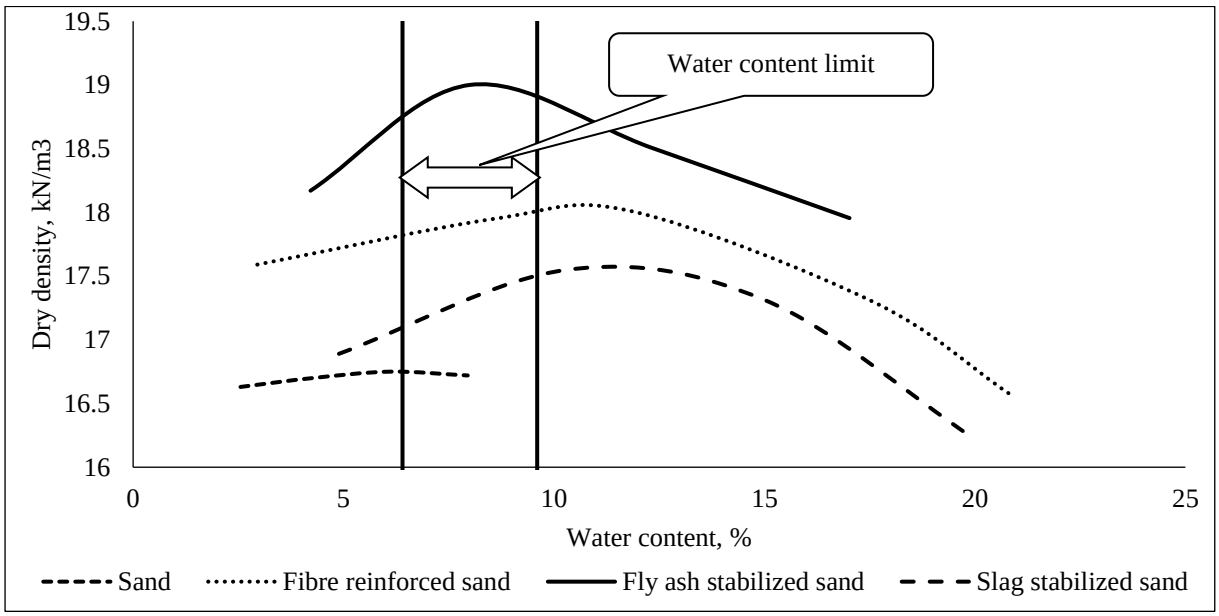

Figure 5.41Comparison of compaction test of the stabilizers and reinforced material.

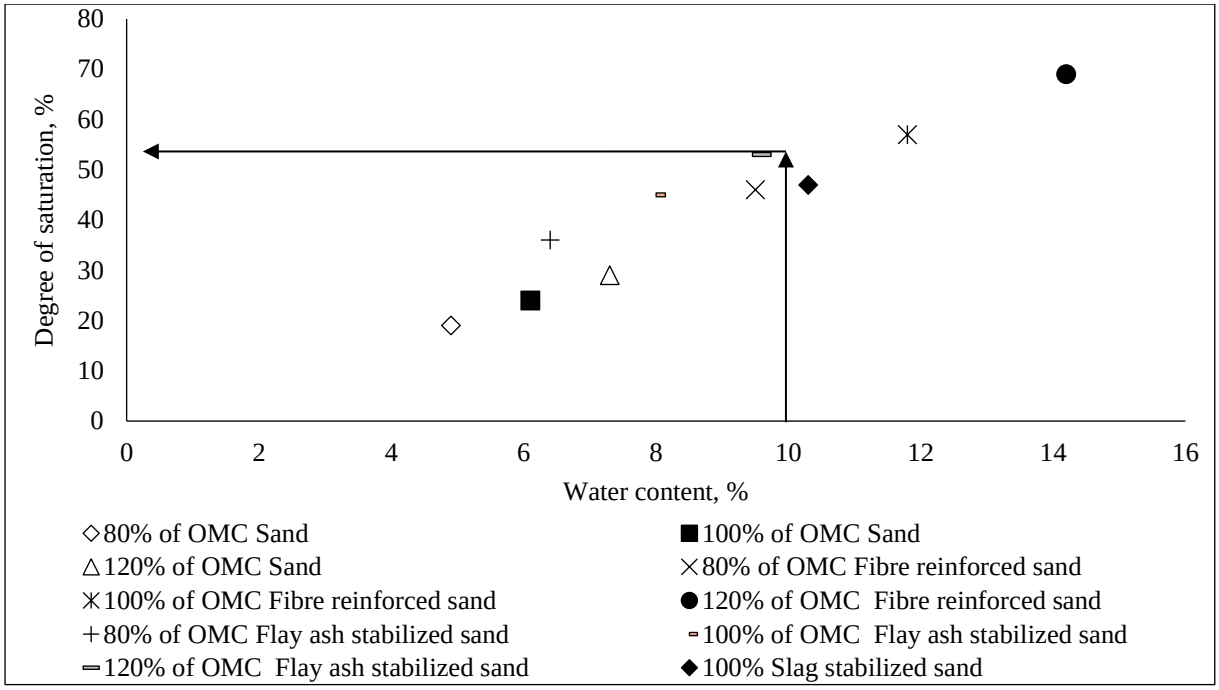

Figure 5.42 Degree of saturation against the water content.

The correlation models of the k_1 and k_2 with the water content are represented in Equation 5-13 and 5-14. Both k_1 and k_2 were substituted in Equation 5-3 to obtain the resilient modulus value as demonstrated in Equation 5-15. In the case of the confining pressure is zero, the applied stress is equal to unconfined compressive strength as Equation 5-16 shows.

$$k_1 = -3.1877w + 48.02 \qquad \text{Equation 5-13}$$

$$k_2 = 0.0387w - 0.097 \qquad \text{Equation 5-14}$$

$$M_R = (-3.1877w + 48.02) * (\sigma_d + 3\sigma_3)^{(0.0387w - 0.097)} \qquad \text{Equation 5-15}$$

$$M_R = (-3.1877w + 48.02) * (UCS)^{(0.0387w - 0.097)} \qquad \text{Equation 5-16}$$

Different tools are used to evaluate the accuracy of Equations 5-15 and 5-16. The Mean Absolute Deviation MAD was used to obtain the variability of each data and the mean. The MAD was performed for the experimental results with Equations 5-3, 5-15 and 5.16 results. The benefit of using the Mean Absolute Deviation is that both positive and negative values

can be used to obtain the distribution of the data from the mean is. Therefore, the negative values will not cancel the positive values. Also, the difference between the actual data's and the predicted results were evaluated by the Root Mean Square Error (RMSE). Mean Absolute Percentage Error (MAPE) was used also to measure the accuracy of the predicted models.

Table 5-4 describes the results of the statistic results. The mean absolute percentage error of Equation 5-16 for fibre reinforced sand and fly ash stabilized sand is 26% and 24%, respectively. For fly ash with fibre reinforced sand MAPE is 17%. The difference between the predicted and the experimental results were evaluated by the Root Mean Square Error. The RMSEs for all the reinforced sand was less than 11%. The mean absolute deviation for Equation 5-16 is the least when it was used for fly ash with fibre reinforced sand. Also, it was noted that Equation 5-15 is more accurate than Equation 5.3. Table 5-6 represents the results for different reinforced and stabilized sand and with both Equations 5-15 and 5-16. It also includes the results from Equations 5-3.

Table 5-4 The goodness of fit statistics.

Statistical tools	Fibre reinforced sand			Fly ash stabilized sand			Fly ash with fibre reinforced sand		
	Eq 5.3	Eq 5.15	Eq 5.16	Eq 5.3	Eq 5.15	Eq 5.16	Eq 5.3	Eq 5.15	Eq 5.16
MAD	7	8	14	4	4	11	2	5	9
RMSE	8	10	4	5	4	11	2	5	9
MAPE	13	17	26	9	7	24	0.9	3	17

It is well known that the definition of R-squared is fairly straight-forward; it is the percentage of the response variable variation that is explained by a linear model. Table 5-5 shows the agreement between the experimental results and the resilient modulus from Equations 5.3 & 5.15. The higher the R-squared, the better model fits the data. It can be seen that Equation 5.15 shown a good agreement with the experimental data.

Table 5-5 Comparison between R^2 of measured resilient modulus with resilient modulus of Eq 5.15 and Eq 5.3

Materials	R^2	
	Measured & Eq 5.15	Measured & Eq 5.3
Fibre	0.3613	0.3652
Fly ash + Fibre	0.798	0.7961
Fly ash	0.7365	0.1801

Table 5-6 Summary of the experimental test results, Eq 5.3, 5.15 & 5.16.

Samples condition	w, %	Measured M_R	M_R from Eq 5.3	M_R from Eq 5.15	M_R from Eq 5.16
Flay ash stabilized sand					
Raw samples	80%	55.72	54.15	55.79	53.76
	100%	52.56	52.48	62.20	56.86
	120%	48.17	51.45	64.28	54.70
Curing samples	80%	51.79	55.28	56.71	55.44
	100%	47.05	52.50	62.19	59.16
	120%	40.29	51.45	64.26	56.51
Fly ash with fibre reinforced sand					
Raw samples	100%	51.91	57.11	62.20	60.13
Curing samples	100%	57.47	57.21	62.20	67.30
Fibre reinforced sand					
Raw samples	80%	56.09	54.56	64.71	60.13
	100%	56.47	54.53	58.21	63.83
	120%	53.10	53.83	24.07	22.63

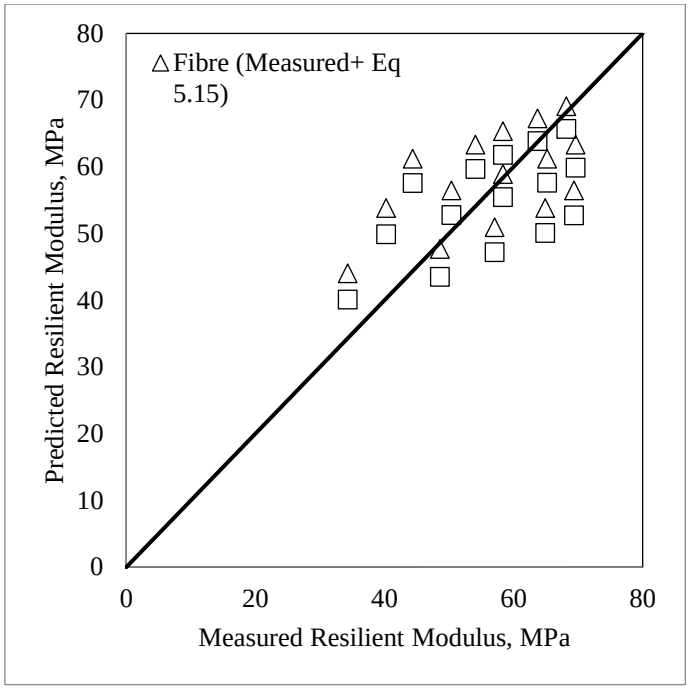

Figure 5.43 Measured resilient modulus of fibre reinforced sand from tests versus predicted resilient modulus.

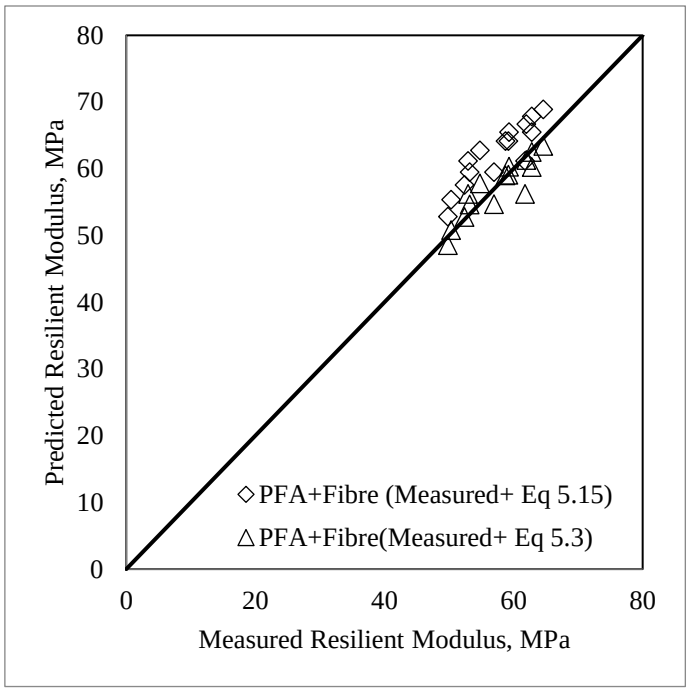

Figure 5.44 Measured resilient modulus of fly ash with fibre reinforced sand from tests versus predicted resilient modulus.

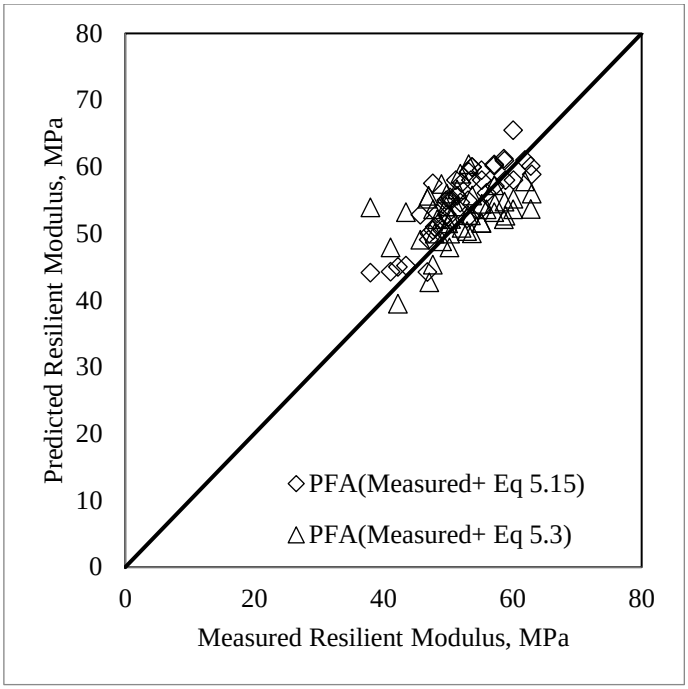

Figure 5.45 Measured resilient modulus of fly ash stabilized sand from tests versus predicted resilient modulus.

5.6.1 Discussion

In this research, the literature review explained the affecting factors on resilient modulus. The affecting factors such as deviator stress, water content and confining stress are considered in the correlation models. These factors are incorporated into the correlation models. It is well known that the minimum resilient modulus is obtained at zero confining stress. And the resilient modulus of granular soil increases with the increase in deviator stress.

New materials and correlation models need to be incorporated in the Guide for Mechanistic-Empirical Design of New and Rehabilitated Pavement Structures to obtain the resilient modulus. Therefore, two correlation equations were developed to predict the resilient modulus value, one from unconfined compressive strength results, and one from repeated load triaxial RLT results. Equation 5.15 which considers the bulk stress and water content can predict the resilient modulus from RLT. However, Equation 5.16 is simpler, which considers only the deviatoric stress (confining stress is zero) and the water content. In order to

demonstrate the results from the effect of these factors and conditions, their resilient modulus values were used in pavement analysis.

The correlation models were compared with (Finn et al., 1986) model. The results showed that there is good agreement between the correlation models with the experimental results than (Finn et al., 1986) model. The fly ash stabilized sand model shows a significant agreement with the experimental results than (Finn et al., 1986) model.

5.7 Conclusion

The resilient modulus value was obtained by two tests procedures which use AASHTO T307 and permanent deformation test in a different condition such as water content and cyclic deviator stress. The factors affecting the resilient modulus value of the subgrade layer through the design life were assessed for reinforced and stabilized sand.

Extensive and robust experimental work was carried out to investigate the affecting factors of resilient modulus. Also, the durability was conducted in this investigation and used in the analytical pavement design. Then, two correlations models were developed based on a wide range of experimental results. They were developed to predict the resilient modulus value based on the unconfined compressive strength results and repeated triaxial load test. The fitting between experimental data's and correlation models (Equations 5-15 & 5-16) was conducted in order to evaluate the goodness of them. Finn et al. (1986) equation were fitted with the experimental data's as well. The results showed significant goodness of correlation models than (Finn et al., 1986) model. Also, the vitrified slag was assessed for use in pavement construction. Finally, the resilient modulus value was used to evaluate the compression stresses on the top of the subgrade layer as explained in Chapter Two by using KENLAYER software. The pavement responses were obtained by linear theory of

Boussinesq's as explained in section 5.5. Then, analytical pavement design is represented in Chapter Seven.

CHAPTER 6 PERMANENT DEFORMATION

6.1 Introduction

Permanent deformation is one of the main factors in flexible pavement design; the challenge of permanent deformation is not only how to measure rut development but also predict the rut development. The success pavement design includes the evaluation of environmental condition as well as the traffic loading throughout the design period. As explained in Chapter 2, Section 2.3.1, it is important to understand the nature of permanent deformation behaviour in the granular materials. In this research, the effect of cyclic deviator stress, moisture content, number of cycles and environmental conditions are taken into account as described below.

6.2 Factors Affecting of Permanent Deformation

6.2.1 Effect of stress level

The British Standard BS EN 13286-7:2004 provides two procedures for determining the permanent deformation of a single-stage repeated load triaxial test (SS RLT) and Multi-Stage repeated load triaxial test (MS RLT). The difference between both of them has been discussed in Chapter Three, Section 3.4.2. In this research, MSRLT was used to assess the deformation of the reinforced and stabilized sand. Because this test allows considering the stress history, minimize both effort and time of applying different cyclic deviator stresses and it is more reliable to simulate the field conditions as reported by (Salour and Erlingssonc, 2015, Rahman, 2015, Saevarsdottir and Erlingsson, 2013).

Figure 6.1 to Figure 6.3 show the cumulative permanent deformation of stabilized and reinforced sand at different water contents, 27.6kPa confining pressure, and 50,000 load

cycles. The load cycles are divided into five sequences, and each sequence has stress level. The stress level was determined by the ratio of the applied a stress and the materials shear stress. The shear stress is obtained by static triaxial load test. Table 6-1 provides the stress ratios for the materials.

Brown (1996) stated that it was possible to apply cyclic deviator stress ratio from 20 to 60% of the static shear stress for sand soil and (Werkmeister et al., 2001) stated that the cyclic deviator stress ratio of 50% of the of static shear stress for sandy gravel.

Table 6-1 The applied stress ratios.

Materials	Cyclic deviator stress ratios, %				
Fibre reinforced sand	7	19	32	45	57
Fly ash stabilized sand	13	27	40	53	66
Fly ash & Fibre reinforced sand	6	17	28	38	66
Slag stabilized sand	6	17	28	38	66
Slag & Fibre reinforced sand	6	17	28	38	66

The reinforcement materials showed a different level of improvement of the permanent deformation. The cumulative permanent deformation of fibre reinforced sand was the highest while the lowest permanent deformation was obtained by the slag. The improvement of the bond between the sand particles leads to a decrease in permanent deformation. The cementitious properties of the slag and the fly ash materials affect both the strength and the permanent deformation of the sand. This can be seen in the below Figures for the slag, slag and fibre, fly ash and fibre and fly ash stabilized sand.

From Figure 6.1 to Figure 6.3, at 86.8kPa stress level the slag with fibre showed significant improvement and was followed by slag then fly ash with fibre and finally the fibre alone reinforced sand. At 62kPa and 50,000 cycles load, the fly ash stabilized sand provides resistance better than the fibre reinforced sand after 30,000 cycles. It was noted that the

permanent deformation of fly ash with fibre reinforced sand show a high increase when compare with slag or slag with fibre reinforced sand as shown in Figure 6.3.

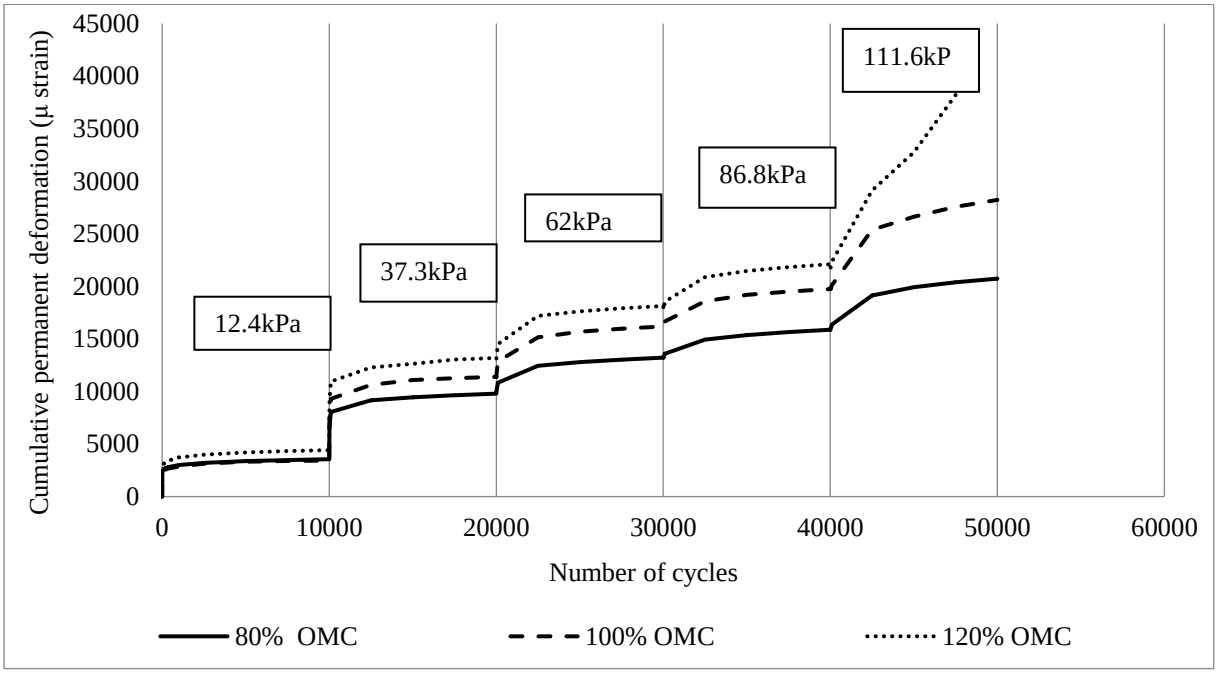

Figure 6.1 Effect of stress level on the permanent deformation development for fibre reinforced sand at 27.6kPa confining pressure.

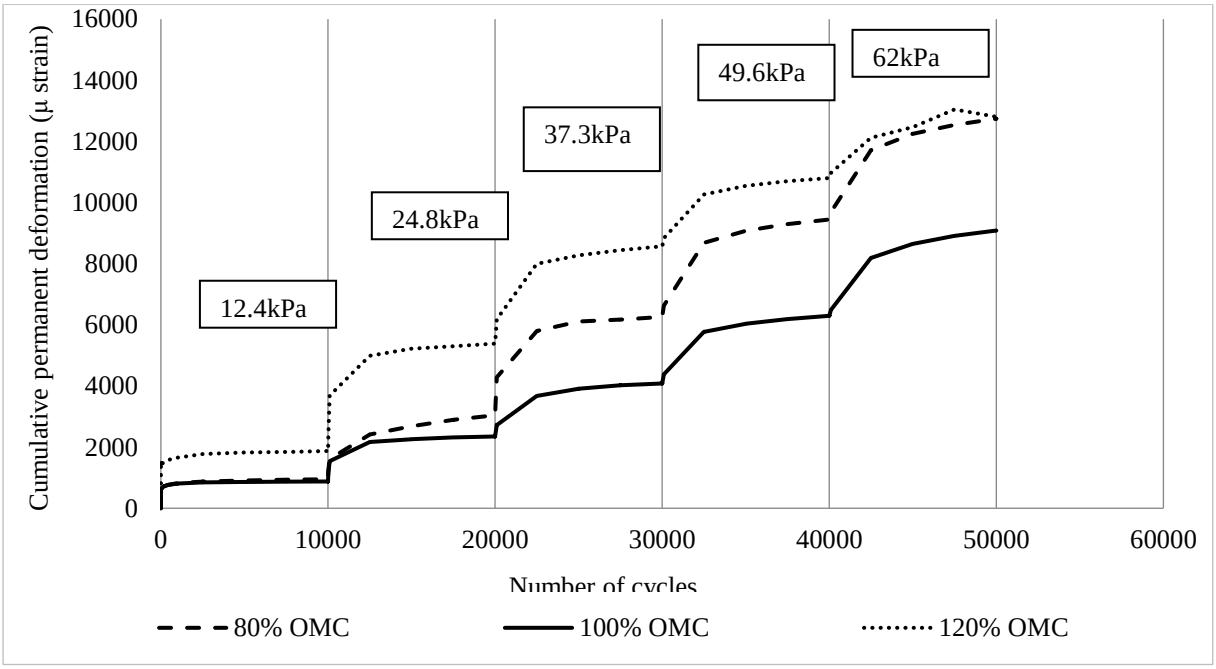

Figure 6.2 Effect of stress level on the permanent deformation development for fly ash stabilized sand at 27.6kPa confining pressure.

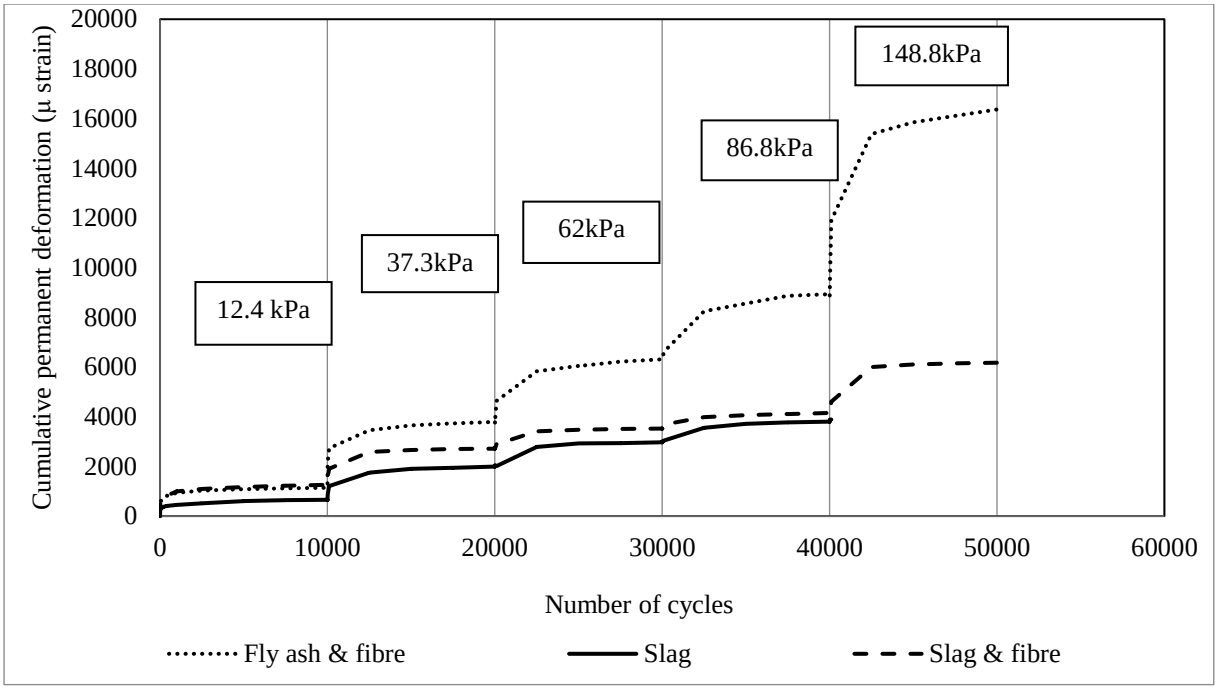

Figure 6.3 Effect of stress level on the permanent deformation development for fibre with fly ash, slag, and slag with fibre reinforced sand at 27.6kPa confining pressure & OMC.

6.2.2 Effect of moisture content

As previously discussed in section 6.2.1 and how the variation of the water content effects on the behaviour of pavement layers. The influence of water content was investigated by MS triaxial test as demonstrated in Figure 6.1, 6.2, and 6.3, respectively. Generally, the general the increase of the water content decrease the resilient modulus and increases the permanent deformation.

The highest permanent deformation occurred in fibre reinforced sand as shown in Figure 6.1. The fly ash improved the resistance of the deformation and this can be explained by the increase in the bonding and reduction in the voids between the particles. At 120% OMC, the permanent deformation is the highest while at OMC the fly ash stabilized sand show a significant reduction in permanent deformation as demonstrated in Figure 6.2. This result was confirmed by (Kim and Siddiki, 2006). The comparison of slag, fibre with slag and fly ash with fibre into the sand are provided in Figure 6.3. Three of them were compacted at OMC

and 95% of the maximum dry density. The cohesion of slag or slag with fibre show the significant effect to reduce the permanent deformation.

6.2.3 Effect of Number of Load Applications

The number of load applications was considered as one of the factors for the long-term pavement design. As mentioned earlier, MS repeated load test was conducted and the results were shown in Figure 6.1 to Figure 6.3. The permanent deformation increased with an increase in the stress level and a number of cycle's loads. The effect of stress level is decreased when the materials reach the equilibrium state by the number of load cycles. After about 1000 cycles load in each sequence, the permanent deformation gradually decreases until it reaches the equilibrium state. However, the compacted samples of the fibre reinforced sand at 120% of OMC shown that after 40,000 cycles load the permanent deformation increased with increase in the load number as shown in Figure 6.1. This behaviour was confirmed by (Lekarp et al., 2000b).

6.2.4 Effect of Stress History

In this research, the stress history was affected by the reinforced soil behaviour. When the load was applied, the effect of the stress history exhibits after a certain number of load cycles. Thus, the permanent deformation decreased gradually with an increase in the stiffness of materials. Figure 6.4 demonstrates the effect of stress history. As seen in Figure 6.4, different reinforced and stabilizations materials show similar behaviour. The behaviour is explained by the application of 12.4kPa stress level, 10000 cycles load, 27.6kPa confining pressure, and OMC. After 1000 cycles load, the permanent deformation was reduced and become stable. The behaviour was confirmed with the same test conditions but different 37.3kPa stress level and after 20000 cycles load as demonstrated in Figure 6.5. The comparison between the stress

histories was strongly clear in both Figure 6.4 and 6.5. The number of load cycles was a significant effect on the stability of the materials.

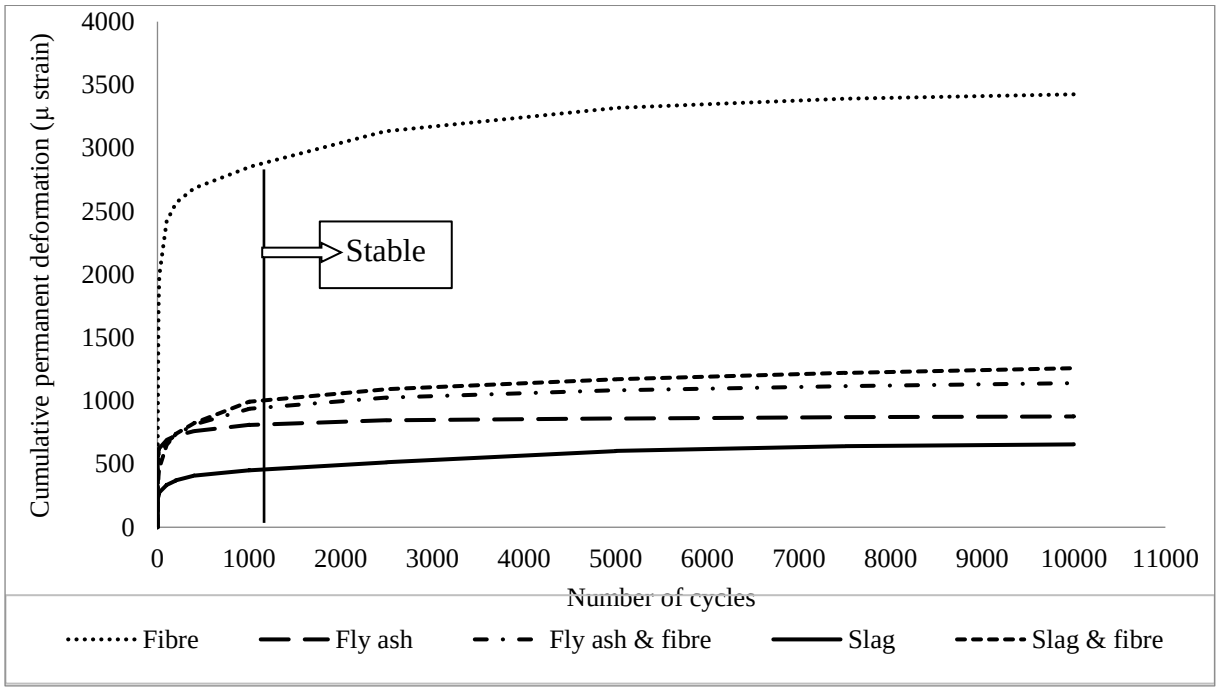

Figure 6.4 The stress history of different reinforced materials after 10000 cycles load.

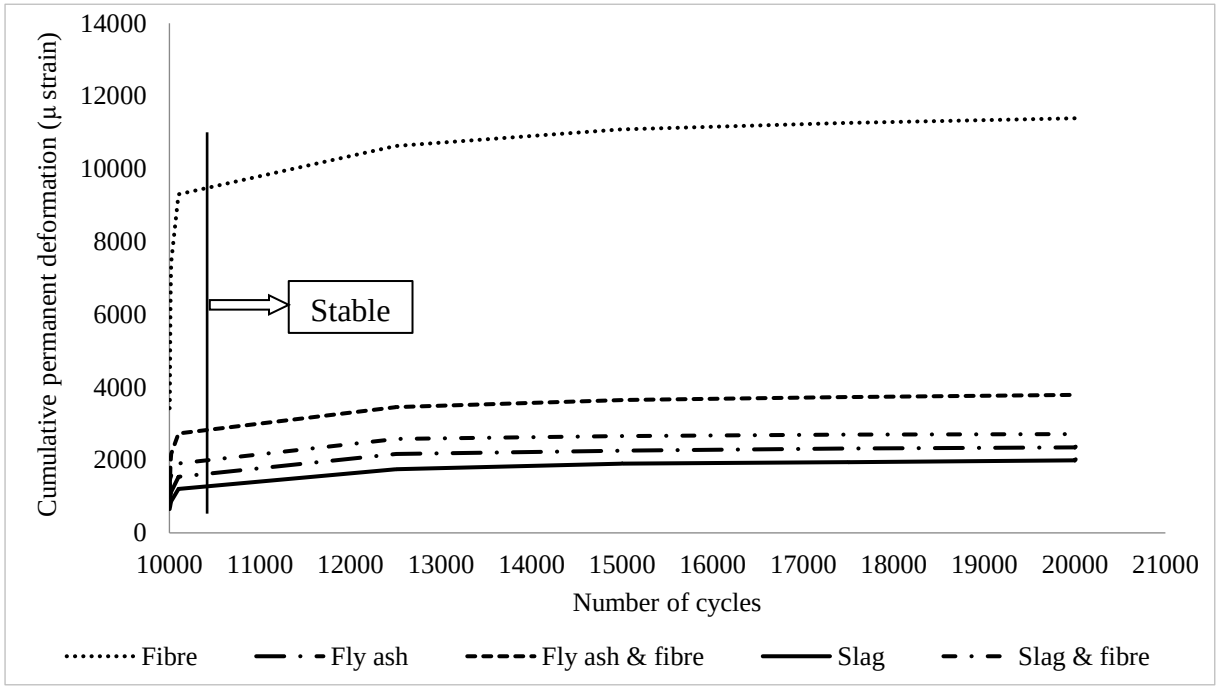

Figure 6.5 The stress history of different reinforced materials after 20000 cycles load.

6.2.5 Effect of stabilizers and reinforced materials

As explained earlier in section 4.2.4, five different mixtures were investigated in this research. Figure 6.6 shown that fibre reinforced sand has the highest permanent deformation which is caused by the low cohesion between the particles. The bonding between the particles exhibited a significant reduction in permanent deformation. It was clear that class C fly ash stabilized sand improve the resistance for permanent deformation. Moreover, the cohesion of vitrified slag stabilized sand showed more improvement of resistance to the deformation. Also, the fibre with fly ash or slag showed significant improvement to reduce the permanent deformation. The curing time also improved the strength of the material.

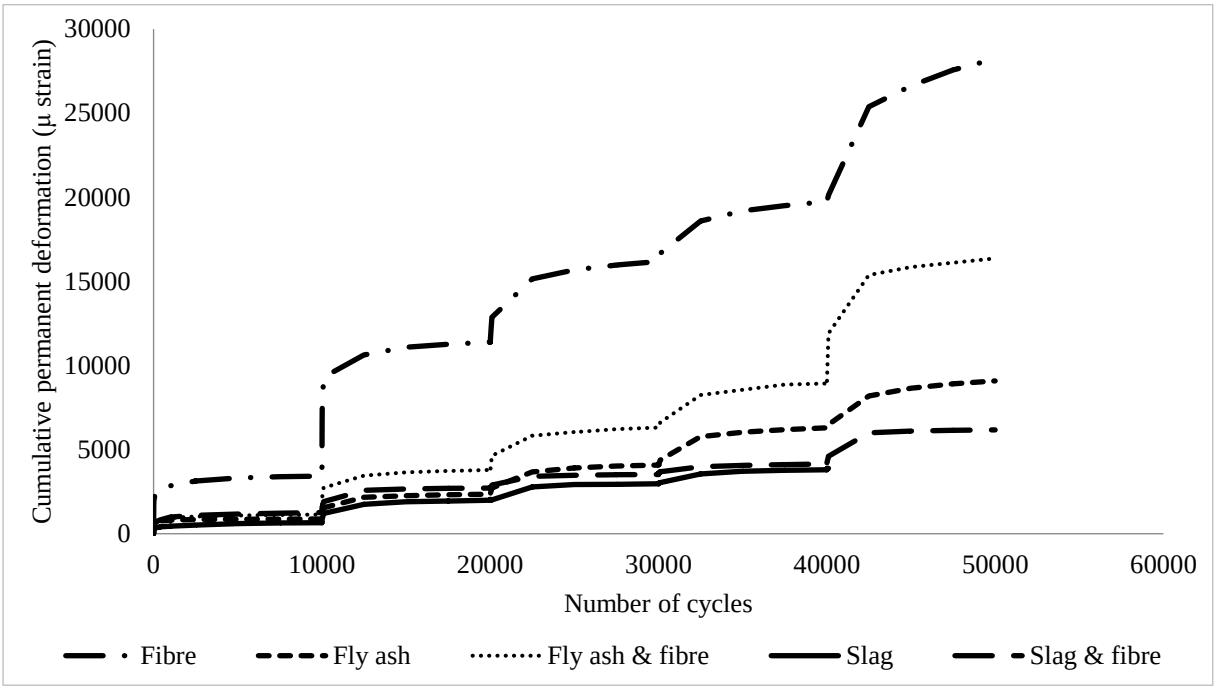

Figure 6.6 The effect the stabilizers and reinforce materials on the resilient modulus at OMC.

6.2.6 Permanent deformation after Freezing-Thawing cycles

As mentioned earlier, the resilient modulus test is the appropriate test to evaluate the effect of F-T cycles on reinforced soil. Therefore, AASHTO T307 equipment was used to assess the permanent deformation before and after the F-T cycles. In this section, the experimental work

results of permanent deformation test are presented in the below figures. Generally, the permanent deformation of granular soil increase with increase the water content.

The water content affected the behaviour of permanent deformation of fibre reinforces sand after the durability test. This can be seen in Figure 6.7, 6.8, and 6.9. As the water content increase the permeant deformation decrease when the samples subjected to cycles pf F-T. The compacted samples at the optimum water content provided the low permanent deformation. Also, it was observed that the permanent deformation after 20 cycles of F-T is the highest but after 10 or 30 cycles of F-T the permanent deformation decrease. It is worth mentioning that the effect of the water content has similar behaviour before and after the durability test.

While the fly ash stabilized sand shows significant improvement of permeant deformation after increasing the F-T cycles and the water content. As explained in section 4.3, during the thawing period the fly ash is reacting, therefore increase the bonding is due to decrease the permanent deformation. The superiority of fly ash is that the permanent deformation decreases with an increase in the number of cycles. Also, the permanent deformation does not affect much with increase the water content. Moreover, the water content of 120% of OMC did not affect the permanent deformation, and this is because the surface of particles increases and need more water content to reach saturation. Also, the hydration reaction requires water.

The inclusion fibre with fly ash showed significant improvement at high cyclic deviator stress compared with fly ash or fibre alone. The comparison of permanent deformation between the slag with/without fibre and fly ash with fibre is including the cyclic deviator stress and the number of load cycles. The test conditions of 148.8kPa cyclic deviator stress, 50,000 cycles load and OMC show that the fibre with slag reduces the permanent deformation compared

with the slag alone. While the slag exhibited about half of the permanent deformation of the fibre with fly ash. It is worth mentioning that, the permanent deformation of slag after 30 cycles is the lower than the permanent deformation after 10 and 20 cycles of F-T. The behaviour of slag with fibre showed a similar trend to the slag behaviour, an increase in the number of F-T cycle's cause's a decrease in the permanent deformation as illustrated in Figure 6.14and 6.15, respectively. This can be explained by the post compaction of the samples.

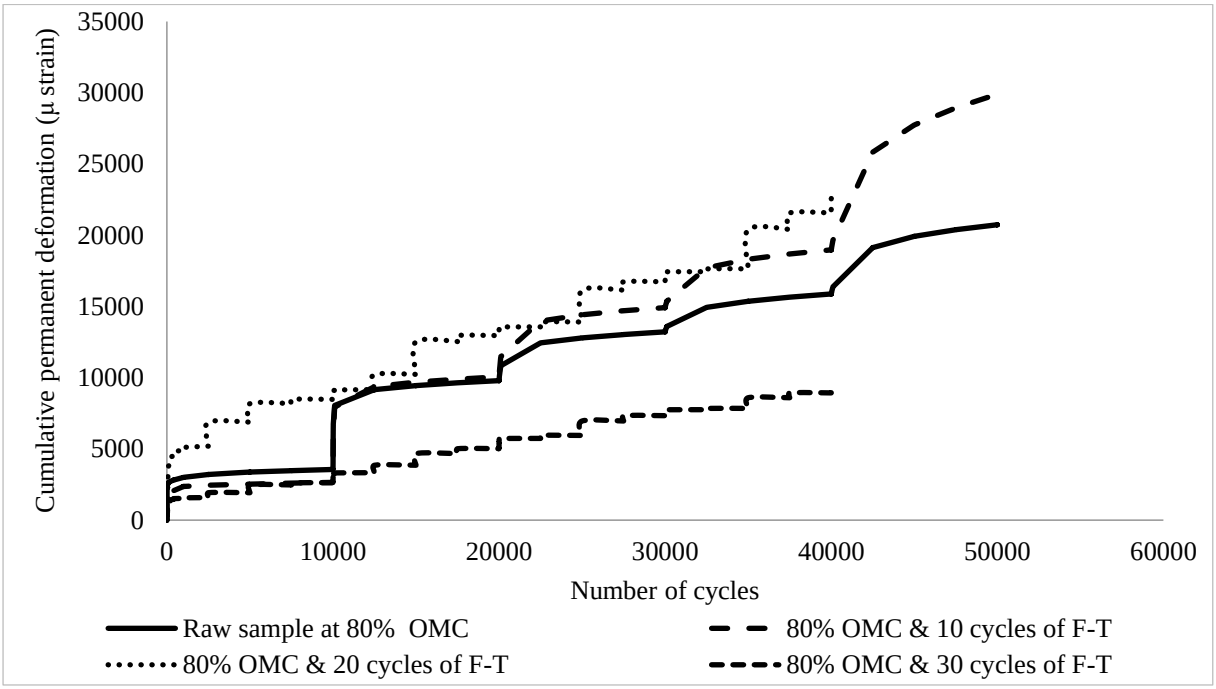

Figure 6.7 The comparison between the permanent deformations of fibre reinforced sand before and after the F-T cycles at 27.6kPa & 80% OMC

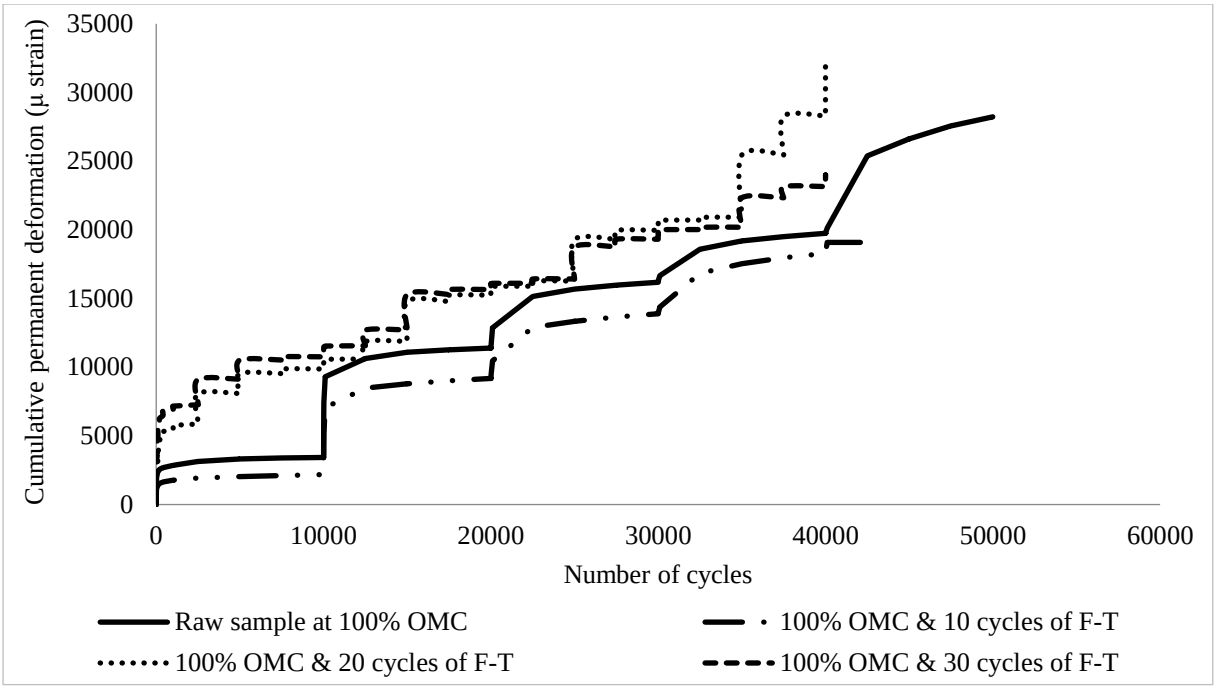

Figure 6.8 The comparison between the permanent deformations of fibre reinforced sand before and after the F-T cycles at 27.6kPa & 100% OMC

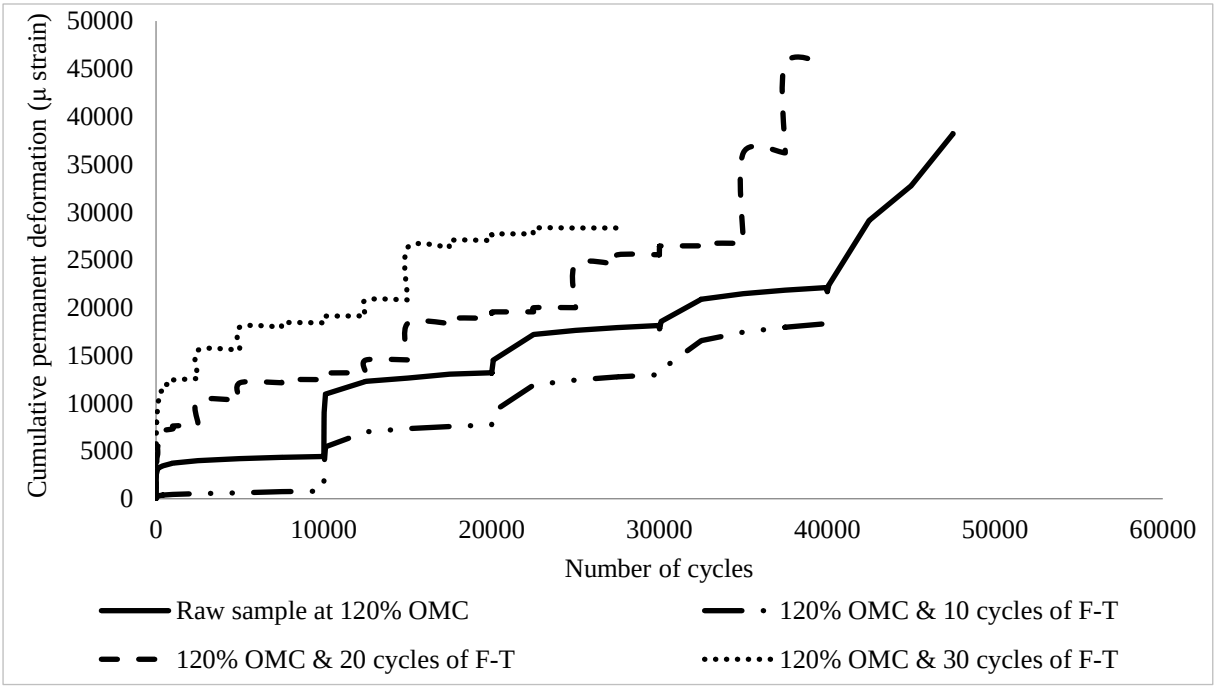

Figure 6.9 The comparison between the permanent deformations of fibre reinforced sand before and after the F-T cycles at 27.6kPa & 120% OMC

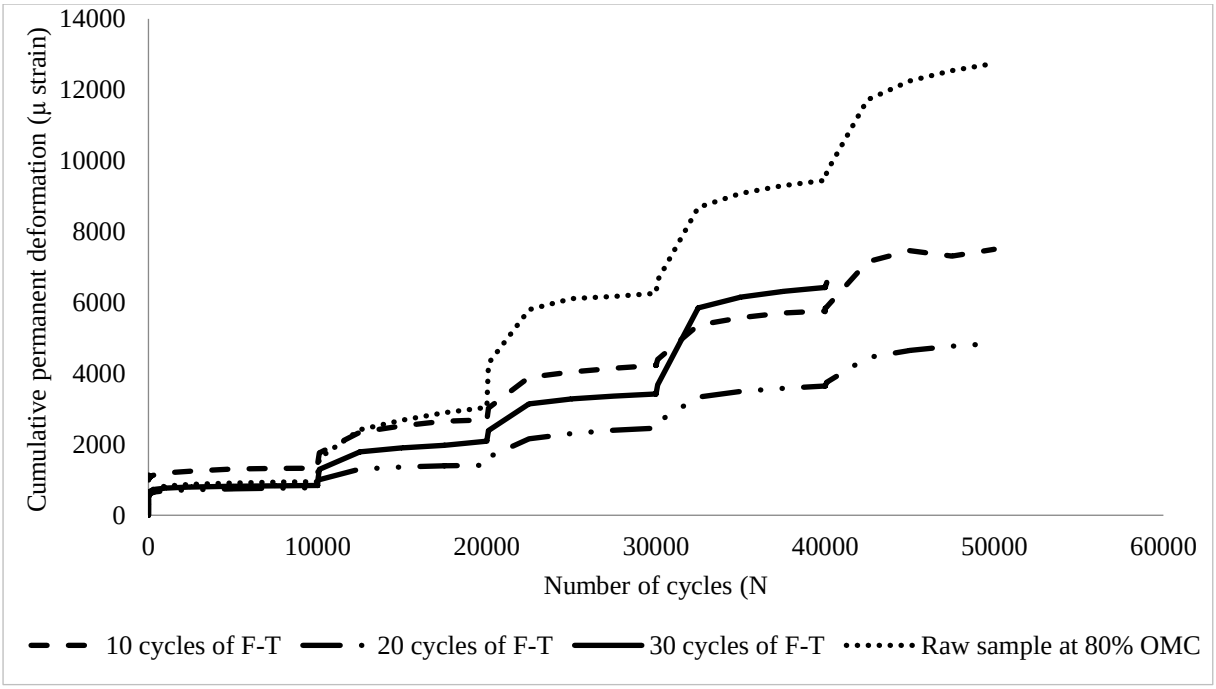

Figure 6.10 The comparison between the permanent deformations of fly ash stabilized sand before and after the F-T cycles at 27.6kPa & 80% OMC

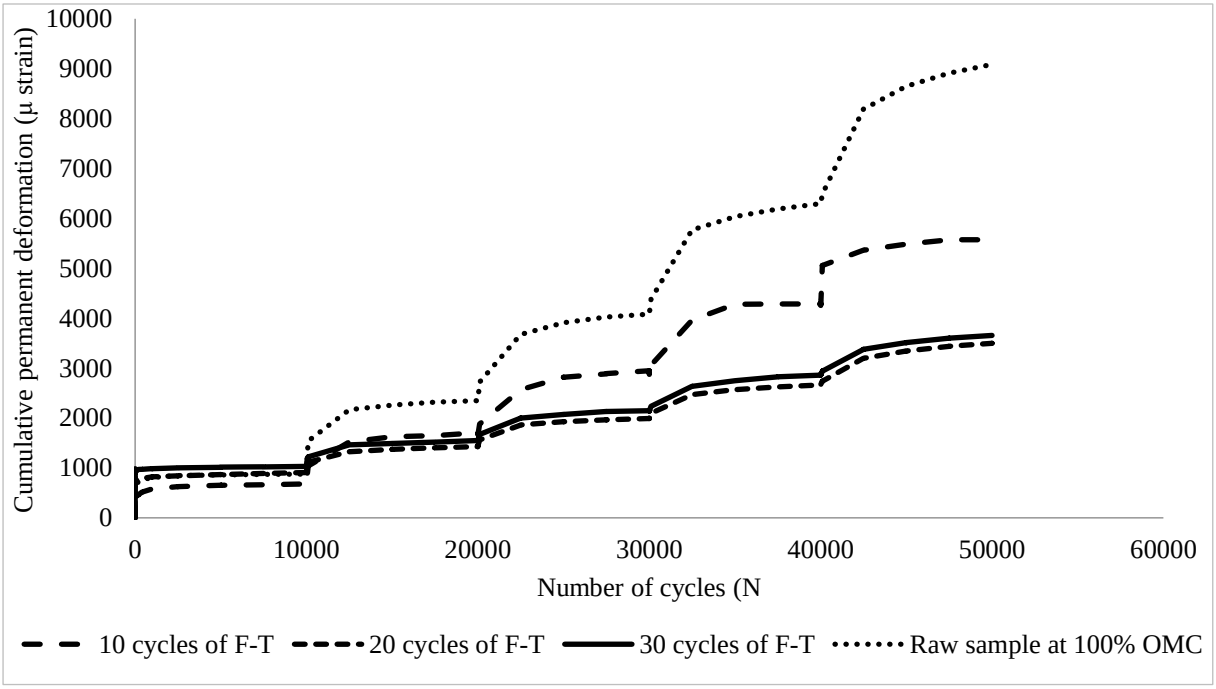

Figure 6.11 The comparison between the permanent deformations of fly ash stabilized sand before and after the F-T cycles at 27.6kPa & 100% OMC

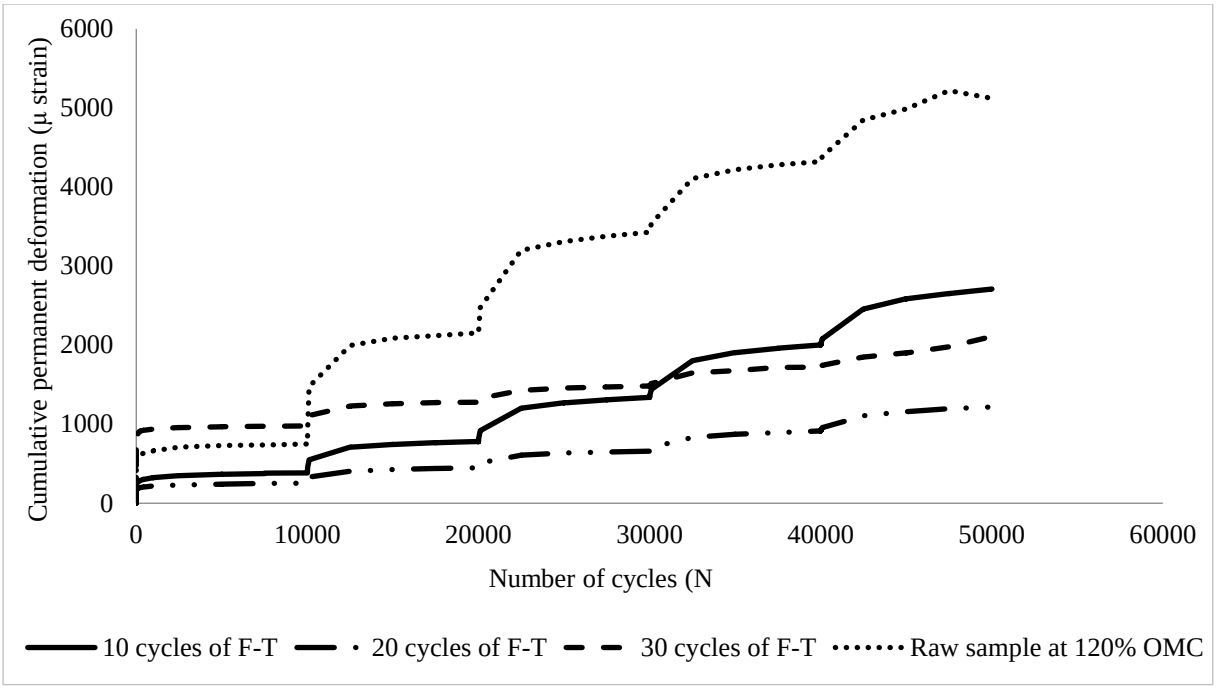

Figure 6.12 The comparison between the permanent deformations of fly ash stabilized sand before and after the F-T cycles at 27.6kPa & 120% OMC

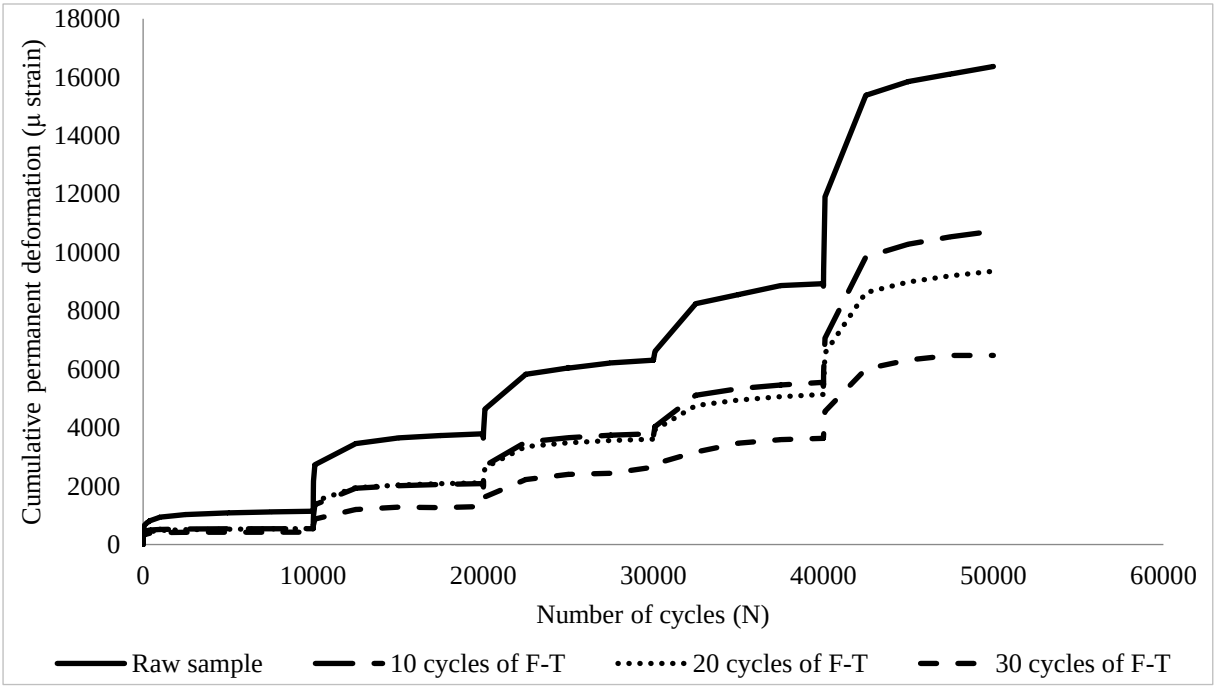

Figure 6.13 The comparison between the permanent deformations of fly ash with fibre reinforced sand before and after the F-T cycles at 27.6kPa & OMC

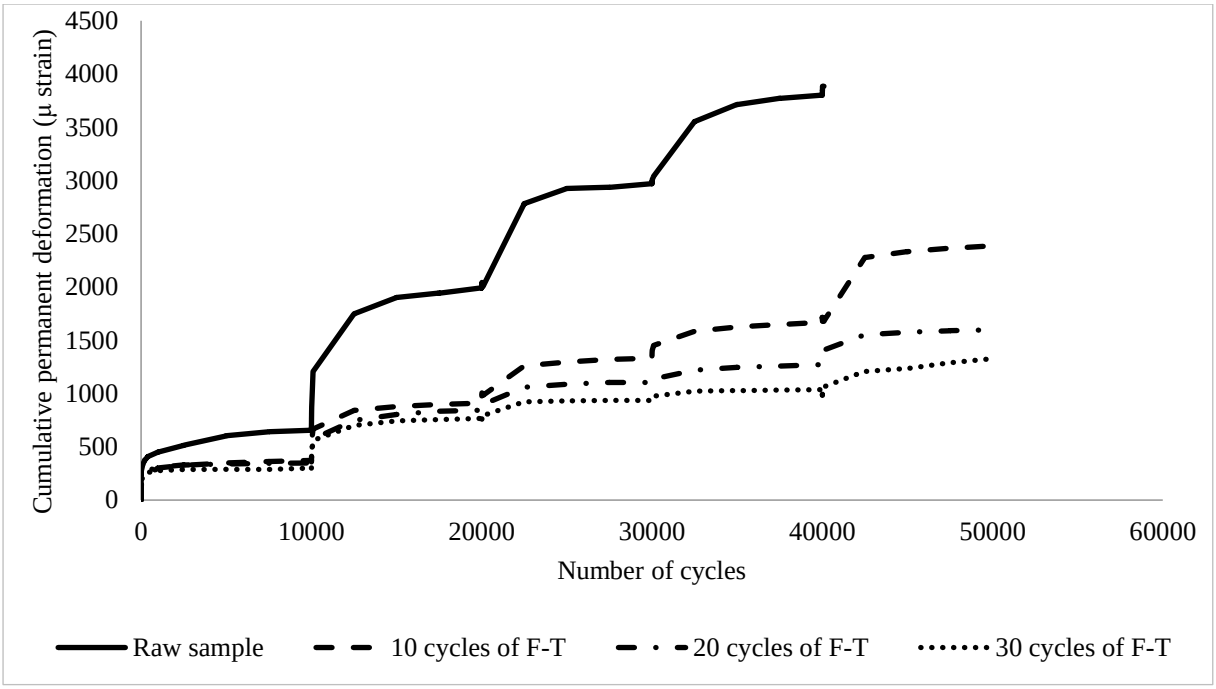

Figure 6.14 The comparison between the permanent deformations of slag stabilized sand before & after the F-T cycles at 27.6kPa & OMC

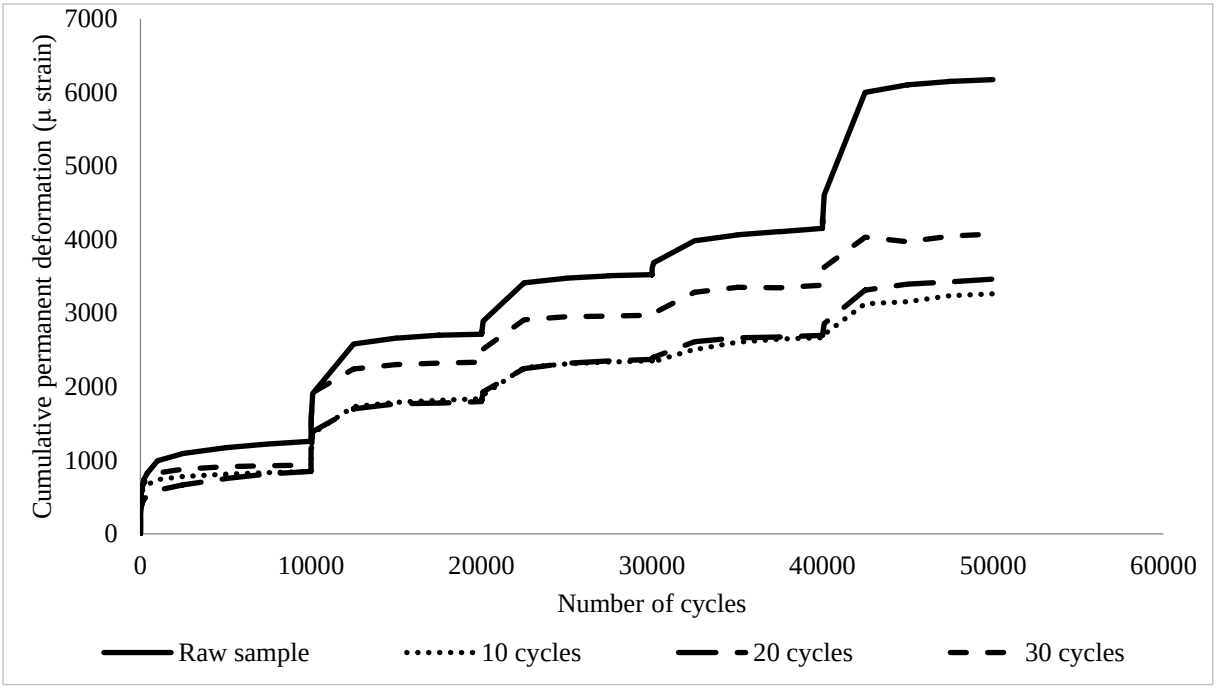

Figure 6.15 The comparison between the permanent deformations of slag with fibre reinforced sand before & after the F-T cycles at 27.6kPa & OMC

6.3 Discussion

(NCHRP, 2004) recommends undertaking the Permanent deformation test as well as the resilient modulus test for pavement design. The use of reinforcement materials in this study needed to be assessed for suitability in pavement design. The test results showed that permanent deformation for reinforced sand changed with the variation of water contents. Increase the water content of the sand reinforced with fibre resulted to increase the permanent deformation. The sand was stronger and more resistant to deformation on the dryer side of optimum. This is considered to be due to improved interlock and better friction between sand grains and fibre material. Whilst the fly ash showed different permanent deformation behaviour was observed in comparison to fibre reinforced sand. The compacted samples of fly ash stabilized sand at the optimum water content shown the lowest permanent deformation. As the number of load cycles is one of the important factors for the long-term pavement design, Lekarp et al. (2000b) reported that 1000 cycle's loads were required to reach to an equilibrium state in granular materials. In this research, the reinforcement materials are due to reach the equilibrium state before the 1000 cycle's load. Also, the permanent deformation was reduced and become stable. This why the permanent deformation test is still a necessity to be conducted for pavement design.

Brown (1996) recommended that the range of applied stress ratio is 20 to 60% for sandy soil. The reinforcement materials used in this research resulted in improvement in the shear stress ratio up to 66% of the static stress.

The durability test was verified by freeze-thaw cycles for the reinforcement materials. The observations of permanent deformation of fibre reinforced sand samples shown that the change occurred at 20 cycles. While 10 and 30 cycles, the permeant deformation was small,

since a new equilibrium condition become predominant on the samples. The permanent deformation of fly ash stabilized sand shown that there is a significant improvement in the chemical reaction of the fly ash and the slag during the thawing period due to the temperature and the humidity. The superiority of fly ash is that the permanent deformation decreases with an increase in the number of cycles. The dissolution of slag with sodium hydroxide increases due to a reduction in the polymerisation of slag binder. During the activation, the slag is dissolved, after curing the activated slag; it will hold the sand particles together. The conditions of thawing duration such temperature and humidity affected the activation. It was also noted that the particle size was one of the main factors which influence on pozzolanic activity.

The results of this chapter with the results of Chapter Five were used together to decide the appropriate reinforcement materials. Then the results were used in analytical pavement design, taking into account the pavement responses for reinforced subgrade layer calculated from the KENLAYER software.

CHAPTER 7 ANALYTICAL PAVEMENT DESIGN

7.1 Introduction

This chapter describes an analytical pavement design for flexible pavements. The design procedure here is used the required data from Chapter Four to Chapter Six. The mechanistic-empirical design procedure was followed in this chapter. Also, the procedure considered the water content, environmental condition and use stabilizations, and reinforcement materials. The traffic loading was collected from a similar location in Libya. The steps of pavement design were presented in Chapter Two in details. Also, one step of the procedure was modified in this study. (NCHRP, 2004) does not include the current waste (slag and fly ash) and recycle (Polypropylene Fibre) materials. Therefore, the correlation models were developed to be considered in the guide to obtain the resilient modulus by using a simple test such as UCST. The below sections describe the analytical pavement design process as illustrated in Figure 7.1. Figure 7.2 shows the procedure of pavement procedure for reinforced and stabilized sand.

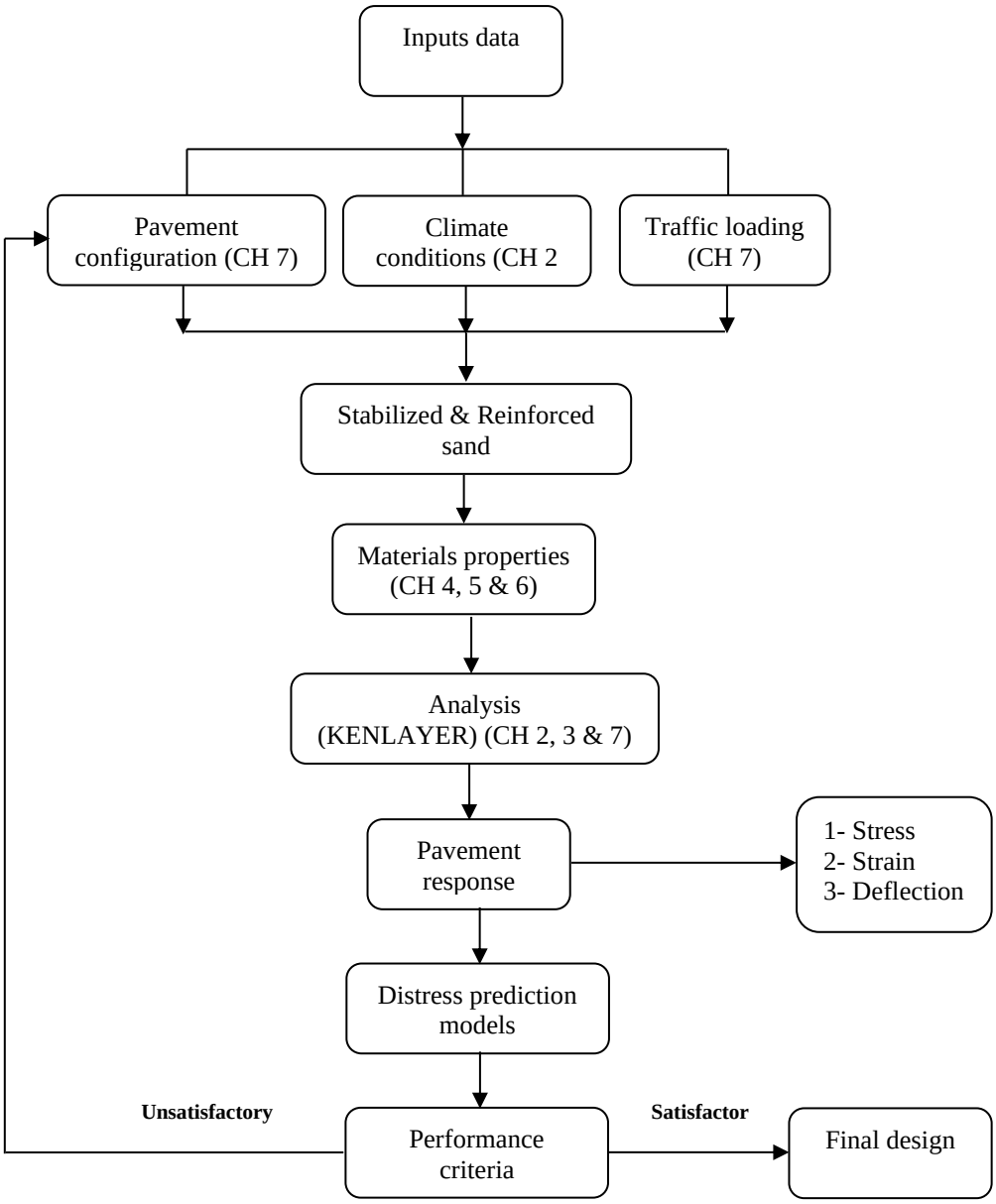

Figure 7.1 Design process for flexible pavement design

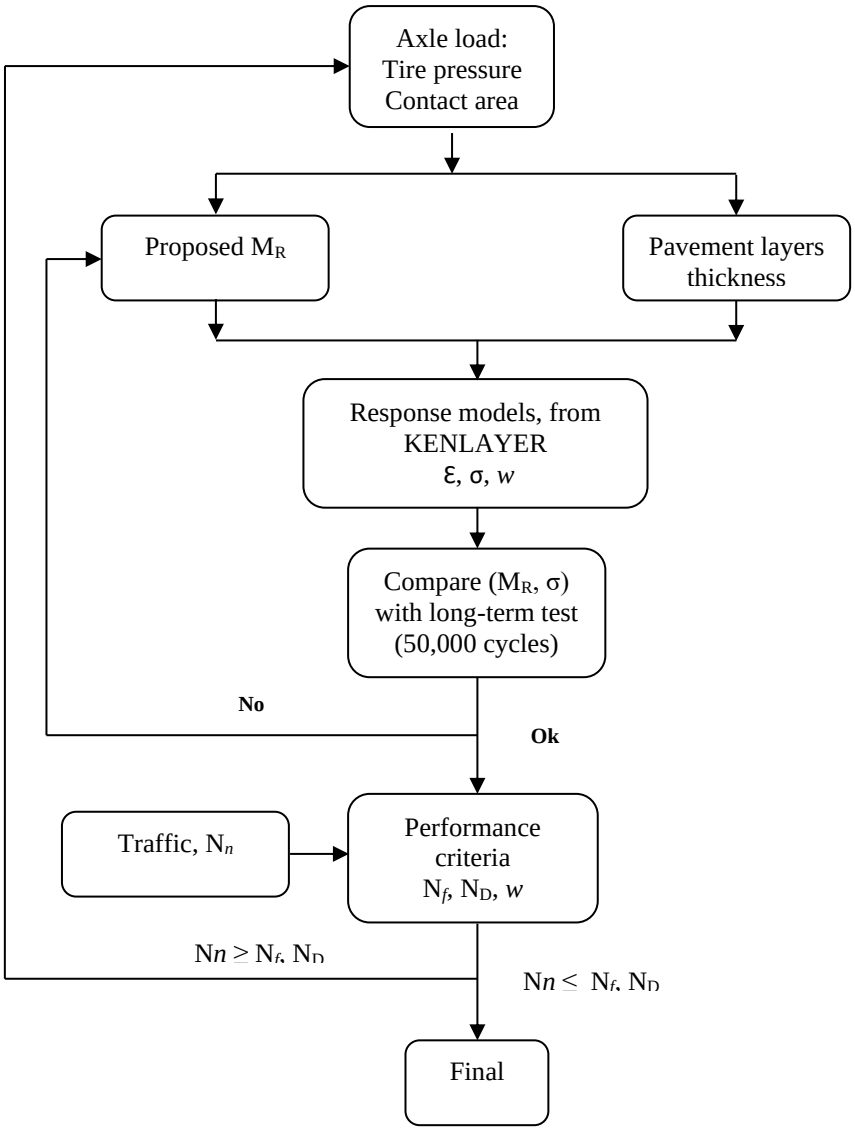

Figure 7.2 Design procedure for reinforced and stabilized sand

The explanation of Figure 7.2 is described below:

- Traffic was divided into numbers of load groups. Each one has a different load, configuration, and a number of load repetitions. The load configuration includes wheel spacing, contact radius and tire pressure.
- Pavement configuration includes the number of layers, the thickness of each layer and the type of materials.
- The proposed resilient modulus values were determined by AASHTO T307 test.
- For the design, the KENLAYER program was used to compute the pavement response.
- Based on the response models, the performance criteria would be assessed and compared with the traffic and the deflection. If it is not suitable the layers thickness and/or resilient modulus should be changed.
- If the previous step was passed, the resilient modulus will be used to obtain the stress by the results of the repeated triaxial test. The relationships between resilient modulus and deviator stress were plotted in Figure 7.6 to Figure 7.10.
- If the design was successful, then the tire pressure increased until reached to the maximum tire pressure (827kPa).
- Finally, if the pavement does not accept more load then the procedure finishes.

7.2 Design Inputs

The requirements of pavement design include traffic loading, materials properties, and geometric layers. Figure 7.2 describes the proposed procedure for pavement. The guide recommends using level 2 to evaluate the traffic loading. Level 2 uses a similar location to the design location. For the reason of use Libyan Desert sand for road construction, the traffic

loading was measured for similar road category that built-in north Libya (in the desert). The road is located between the city and villages as shown in Figure 7.3. different pavement configurations were provided in the (NCHRP, 2004) as shown in Figure 7.4.

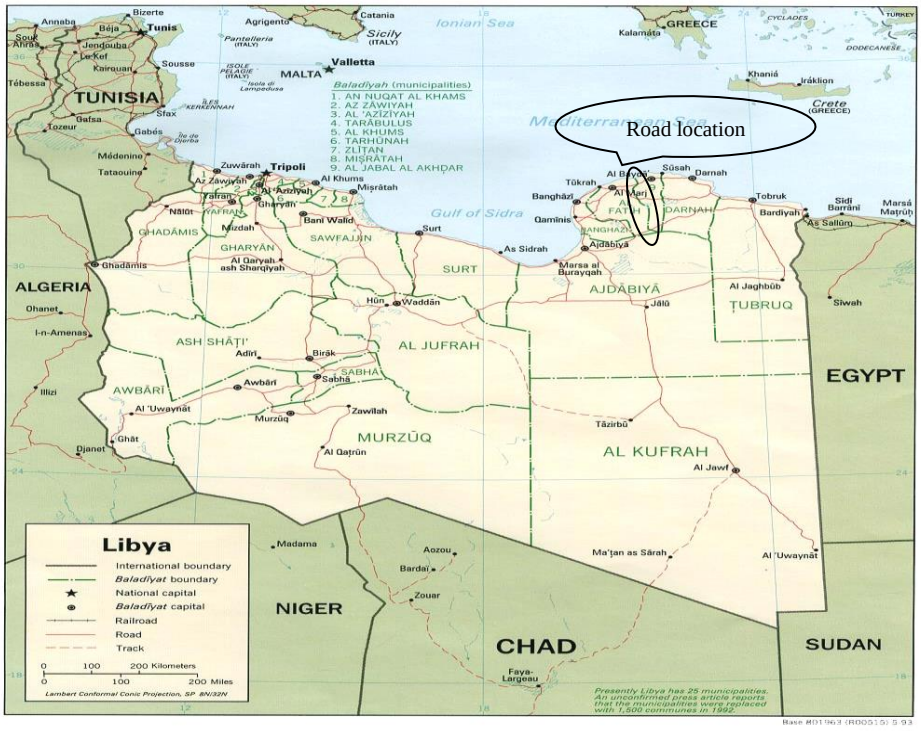

Figure 7.3 The location of road segment on Libyan map.

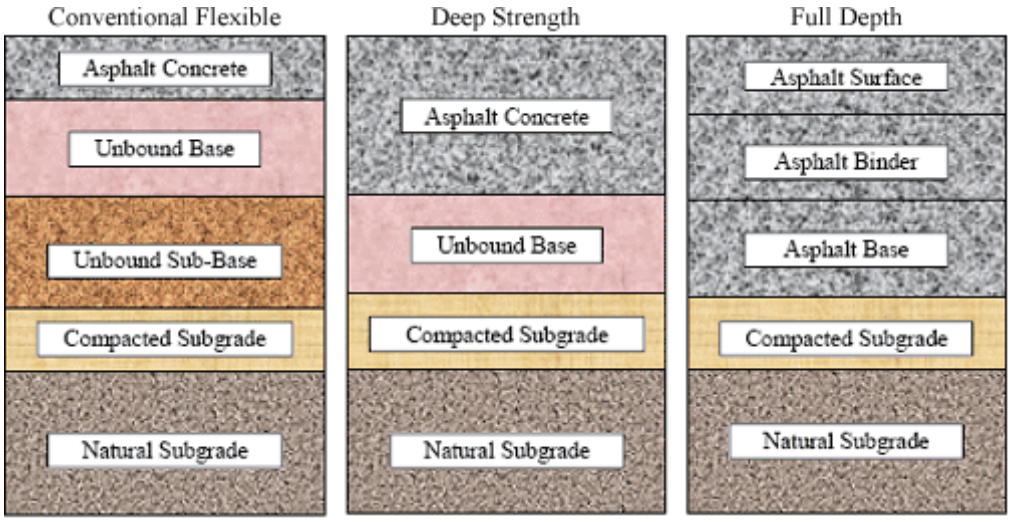

Figure 7.4 Pavement layers sections

7.2.1 Materials properties

The research was focusing on the subgrade layer. Therefore, the resilient modulus tests were conducted under subgrade layer conditions. The proposed resilient modulus was obtained by AASHTO T307. The test was conducted before and after the durability test. The AASHTO T307 conducts three sequences; each sequence has five stages at one confining pressure and five stress levels. The total cycles are 2000 cycles, the first 500 cycles were applied in the condition stage. The reset of stages is conducted with 100 cycle's interval.

The variation of water content and the freezing–thawing condition were considered in this research. The resilient modulus and the permanent deformation were evaluated under these conditions and explained in detail in Chapters Five and Six. In the analytical design, the proposed resilient modulus was used for the design purpose provided in Table 7-1.

Table 7-1 The measured resilient modulus and corresponding resilient modulus after F-T cycles by AASHTO T307.

Dev stress, kPa	Fibre		Fly ash stabilized sand		Fly ash with fibre reinforced sand		Slag stabilized sand		Slag with fibre reinforced sand	
	M_R	$M_{R\ (F\text{-}T)\ min}$	M_R	$M_{R\ (F\text{-}T)\ min}$	M_R	$M_{R\ (F\text{-}T)\ min}$	M_R	$M_{R\ (F\text{-}T)\ min}$	M_R	$M_{R\ (F\text{-}T)\ min}$
13.8	44	42	44	41	59	56	130	124	140	133
27.6	53	51	48	45	59	56	140	133	161	153
41.4	57	55	50	47	62	59	151	143	177	168
55.2	63	59	55	52	63	60	158	150	189	180
68.9	67	64	59	56	65	61	175	166	207	197
13.8	40	38	53	51	53	51	138	131	120	114
27.6	50	47	53	50	53	50	154	146	138	131
41.4	57	55	54	51	55	52	171	162	164	156
55.2	64	61	57	54	59	56	174	165	184	174
68.9	68	65	59	56	63	60	186	176	199	189
13.8	32	30	46	43	50	47	175	166	107	102
27.6	48	46	50	48	50	48	181	172	125	118
41.4	56	53	52	49	52	50	183	174	143	136
55.2	63	60	55	52	57	54	189	179	159	151
68.9	68	64	59	56	62	59	184	175	174	165

7.2.2 Traffic loading

The traffic data is very important to estimate the load and the frequency of each load during the period design. NCHRP (2004) provided the required characterizations of pavement design. The below section describes the traffic data's which are needed for the design. As recommended in (NCHRP, 2004), both Level 2 and 3 data must be from a similar location such as urban to rural or adjust land use. For this reason, an Al Bayda-Wadi El Kuf Road was used to measure the traffic volume. The road segment connects the city with the town as shown in Figure 7.3. The road is two-lane highway 80-100km/hr and 30 km length.

In this segment, the traffic survey was conducted to evaluate the traffic volume. Table 7-2 shows the traffic volume for seven hours which was between 7:00 am to 2:00 pm with a 15-minute interval. These seven hours were chosen assuming that the peak hours are expected to occur within these periods. The traffic count surveys undertaken include:

- Lane volumetric counts at the critical segment.
- Vehicle classification counts.

NCHRP (2004) reported that the annual average daily truck traffic (ADTT) is considered as class 4 to 13 (bus, lorry, and truck). The equivalent single axle load is very simple to calculate once all the data are available. Equation 7.1 was used to obtain the ESALs.

ESAL's = ADT * T *G*365*N*D * L*Y Equation 7.1

Where:

ESAL's = Equivalent Single Axel Loads

ADT = Average Daily Traffic,

T = Percentage of truck in the ADT,

GR = Growth factor,

N = Number of axle load application per truck,

D = Directional Distribution,

L = Lane factor, and

Y = Design period in year.

Huang (2004) stated that the Asphalt Institute (AI, 1981a) and the AASHTO design guide (AASHTO, 1986) recommended the simple way to obtain the growth factor over the base year using Equation 7.2.

$$GR = \frac{(1+r)^{Y}+1}{2} \qquad \text{Equation 7.2}$$

Where

GR = Total growth factor,

r = Annual growth rate (%) of vehicles, and

Y = Design period, years.

Table 7-2 Traffic volume for Al bayda - Wadi el Kuf Road

Time			PC	Van	Bus	Lorry	Truck	Total of heavy trucks	Vehs/Hr
					Class 5 single axel	Class 4, 6 tandem axels	Class 7 tridem axels		
07:00	-	07:15	12	2	1	0	1	2	15
07:15	-	07:30	19	2	1	1	2	4	15
07:30	-	07:45	18	3	1	2	2	5	14
07:45	-	08:00	27	1	0	3	1	4	13
08:00	-	08:15	23	1	0	0	2	2	12
08:15	-	08:30	22	1	0	1	2	3	11
08:30	-	08:45	23	2	1	1	2	4	11
08:45	-	09:00	15	1	0	2	1	3	10
09:00	-	09:15	19	1	0	0	1	1	12
09:15	-	09:30	12	2	1	1	1	3	17
09:30	-	09:45	18	2	1	1	1	3	16
09:45	-	10:00	18	3	2	2	1	5	17
10:00	-	10:15	20	1	0	3	3	6	13
10:15	-	10:30	23	1	0	0	2	2	9
10:30	-	10:45	20	0	1	1	2	4	8
10:45	-	11:00	16	0	0	0	1	1	6
11:00	-	11:15	15	1	0	1	1	2	7
11:15	-	11:30	9	1	1	0	0	1	7
11:30	-	11:45	18	1	0	2	0	2	8
11:45	-	12:00	12	2	1	1	0	2	7
12:00	-	12:15	18	2	1	1	0	2	6
12:15	-	12:30	12	3	2	0	0	2	6
12:30	-	12:45	10	2	1	0	0	1	5
12:45	-	13:00	12	0	0	1	0	1	5
13:00	-	13:15	10	0	1	0	1	2	4
13:15	-	13:30	5	1	0	1	0	1	2
13:30	-	13:45	9	0	0	1	0	1	1
13:45	-	14:00	9	0	0	0	0	0	0

In this research, the design period was divided into three periods 10, 20 and 30 years. Table 7-3 shown the traffic characterization which required in analytical pavement design. The traffic survey was counted on all types of vehicles. NCHRP (2004) stated that the traffic loading includes only class (4-13). Therefore, it was worth to mention that the average daily traffic was calculated only for class (4-13) and two ways.

Table 7-3 Summary of traffic loading characterization.

Total growth factor GR, %	1.24, 1.6 & 2.12
Average daily traffic ADT	816 in two ways
Percentage of Truck in the ADT: *Single axle* *Tandem axle* *Tridem axle*	 =23% of the total traffic. =38% of the total traffic. =39% of the total traffic
Number of lane in the design direction	1
Percent truck in design lane L, %	1
Truck Directional Distribution Factor D, %	50
Number of Axle Load Application Per Truck N	1, 2 & 3
Equivalent Single Axel Loads ESAL's $ESAL_{10yrs}$ $ESAL_{20yrs}$ $ESAL_{30yrs}$	 = 3,988673 = 10,293350 = 20,458034

Contact Area. In the mechanistic pavement design procedure, the contact area is important to obtain the area between the tire and the pavement. NCHRP (2004) stated that the maximum tire pressure is 827kPa. In the analytical pavement design, different tire pressures were applied which are 414, 552, 689 and 827kPa and the vehicles were classified as classes 4 to 13 and dual tires.

Huang (2004) recommended Equation 7.3 to obtain the content area. It was assumed that each tire has a circular contact area for the flexible pavement design. Also, a single circle was assumed for single tire similar to dual tire. To simplify the analysis of flexible pavements, a single circle with the same contact area as the duals is frequently used to represent a set of dual tires, instead of using two circular areas.

In this research, the tire load was constant, but the tire pressure was the variable. The tire pressure was assumed according to the minimum and maximum of the tire pressure in the guide. The contact area was obtained for different tire pressure as shown in Figure 7.4.

$$a = \sqrt{\frac{P}{p*\pi}}$$ Equation 7.3

Where

a = Contact area,

P = Tire load, and

p = Tire pressure.

Table 7-4 contact area

Tire pressure, kPa	Contact area, mm^2
414	175
552	152
689	136
827	124

7.3 Pavement responses

Different computer programs are available to compute the pavement response. In this research, the KENLAYER program was used which could be applied for single, dual, dual tandem or dual tridem. Also, it can be used for linear, nonlinear and viscoelastic layers. The pavement damage also can be obtained by the KENLAYER program. The damage occurs by fatigue and rutting over the period. The structural models were obtained at the critical location as shown in Figure 7.5. Huang (2004) stated that the most critical stress, strain, and deflection occur under the centre of the circular area on the axis of symmetry.

As explained in Chapter Five section 5.5, the vertical stresses of nonlinear could be greater or small those of linear theory at certain points. This may explain why Boussinesq's solutions for vertical stress based on linear theory have been applied to soils with varying degrees of

success, even though soils themselves are basically nonlinear. Therefore, linear theory was used to compute the stress, strain, and deflection in this research. There was a provided example in Chapter Five section 5.5, the results shown that the difference between pavement responses which were obtained by Boussinesq and Burmister solutions was not notable. For other materials, the both solutions might be showing different behaviour. However, the reinforcement materials in this research demonstrate similar pavement responses. The samples showed different behaviour such the confining pressure didn't affect the resilient modulus. These explain why the nonlinear of Boussinesq solutions couldn't simulate the behaviour.

It was assumed that when the subgrade becomes strong, the subbase layer is not needed. As explained in Chapter Two, at points 2 and 3, the tensile stress was a measure to obtain the fatigue cracking under the asphalt layer while the vertical strains were measured under the wheel load at point 1 on the asphalt layer while points 4 and 5 on the surface of the subgrade. Finally, the deflection was measured in the centre between the wheels.

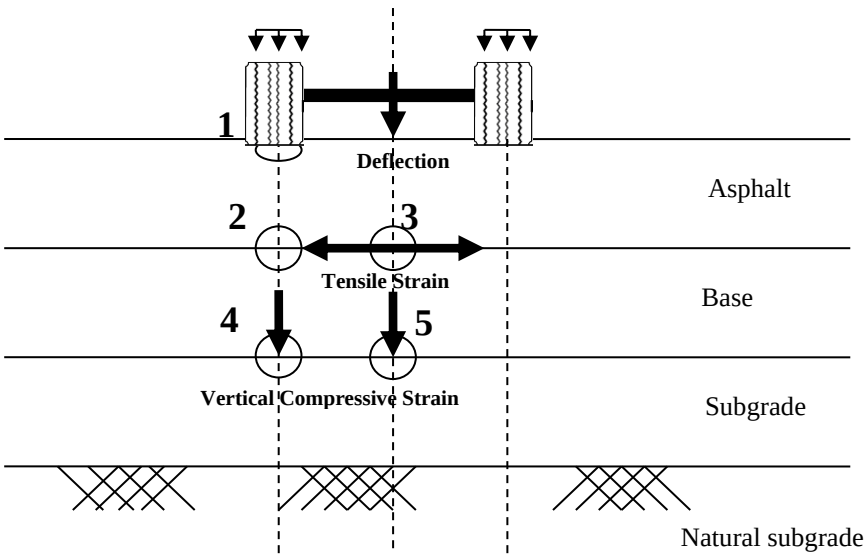

Figure 7.5 Pavement system configuration.

The structural models were obtained for five reinforced subgrade layers. Different configurations are proposed to design the thickness of layers. The tables below provide the pavement response obtained by the KENLAYER program.

In this research, the procedure was developed by add additional factor. As the vertical strain and horizontal strain are important, also the deviator stress is important. Therefore, the proposed resilient modulus which produced by the stress from the KENLAYER program, this stress was used to obtain the converged resilient modulus from Figure 7.6, 7.7, 7.8 and 7.9. Thereafter, the new resilient modulus was used in the KENLAYER program again to obtain a new set of stress, strain, and defection. This procedure would be repeated until the resilient modulus converges with the same stress from the KENLAYER. The results were adjusted by the environmental factor and plotted in Figure 7.6, 7.7, 7.8, 7.9 and 7.10 for fibre, fly ash, fibre with fly ash, slag and slag with fibre reinforced sand, respectively.

For example, the first trail of fibre reinforced sand;

Table 7-5 display the cross-section of the pavement layer which was 10cm, 15cm, and 15cm for asphalt, base, and subgrade layer, respectively. The following steps are to obtain the required resilient modulus and deviator stress for the road section:

First step, the proposed resilient modulus of 100MPa was obtained by the deviator stress of 95kPa from the KENLAYER. But when the 100MPa cross the curve in Figure 7.6, the deviator stress would be 48kPa.

Second step, use 95kPa deviator stresses to obtain the resilient modulus from the graph. Therefore, the resilient modulus was 160 MPa.

Third step, use 160MPa in the KENLAYER to obtain the deviator stress again. The deviator stress was 103kPa. If the 103kPa is applied in the graph, the resilient modulus becomes 160MPa. As a result, the resilient modulus and deviator stress from the KENLAYER was in agreement with the resilient modulus and deviator stress from the graph.

Table 7-5 Section Configuration for fibre reinforced sand at 552kPa tire pressure.

Layers	Thickness, cm		M_R		Poisson's ratio
	Trial 1	Trial 2	Trial 1	Trial 2	
Asphalt	10	10	2000	2000	0.3
Base	15	15	290	290	0.35
Reinforced Subgrade	15	15	100	160	0.35
Natural subgrade	--	--	21	21	0.35
Contact pressure, kPa	552				

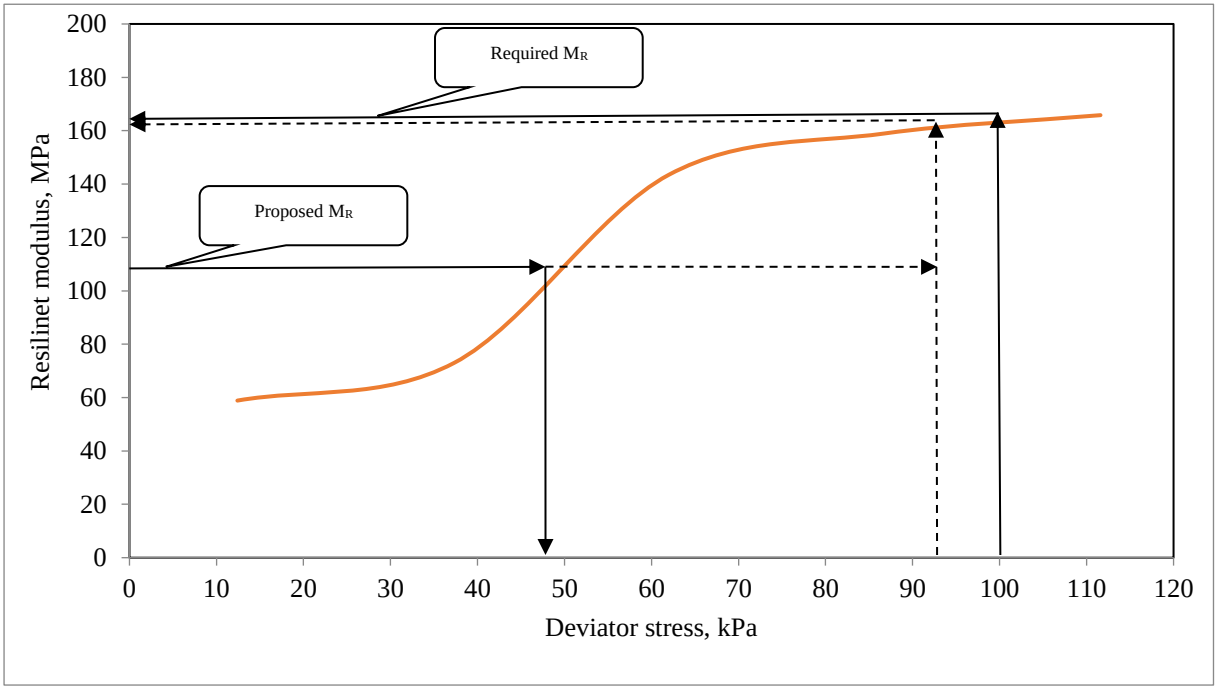

Figure 7.6 Resilient modules vs. deviator stress for fibre reinforced sand.

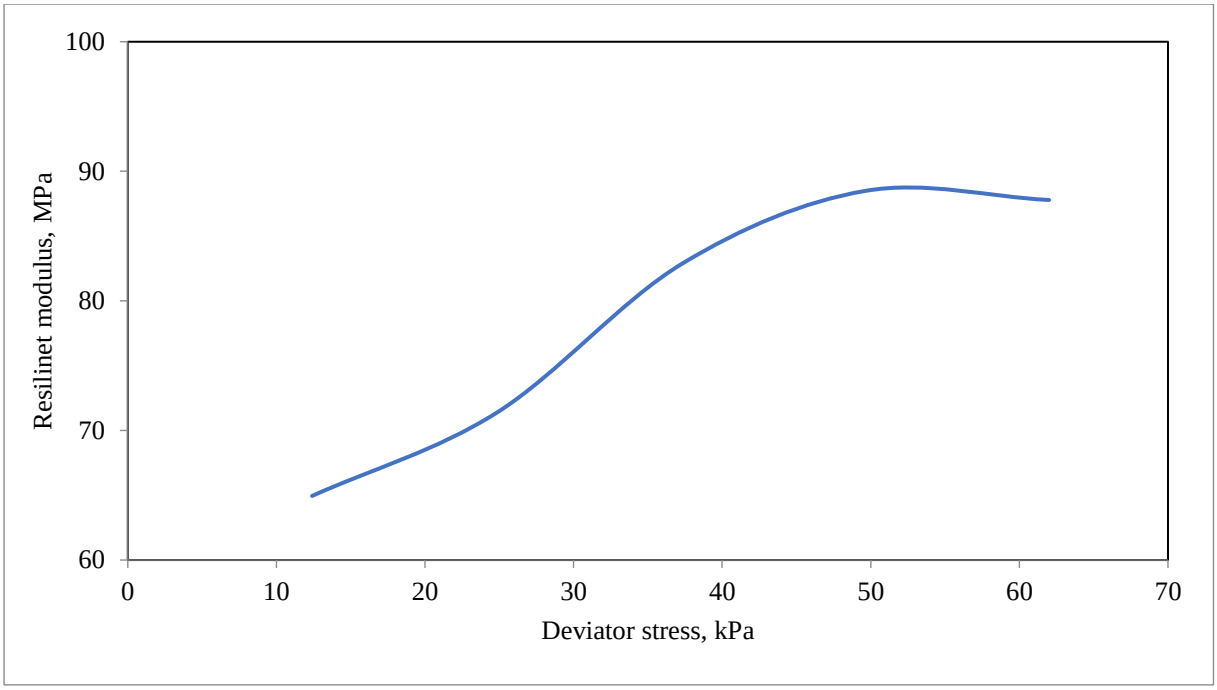

Figure 7.7 Resilient modules vs. deviator stress for fly ash stabilized sand.

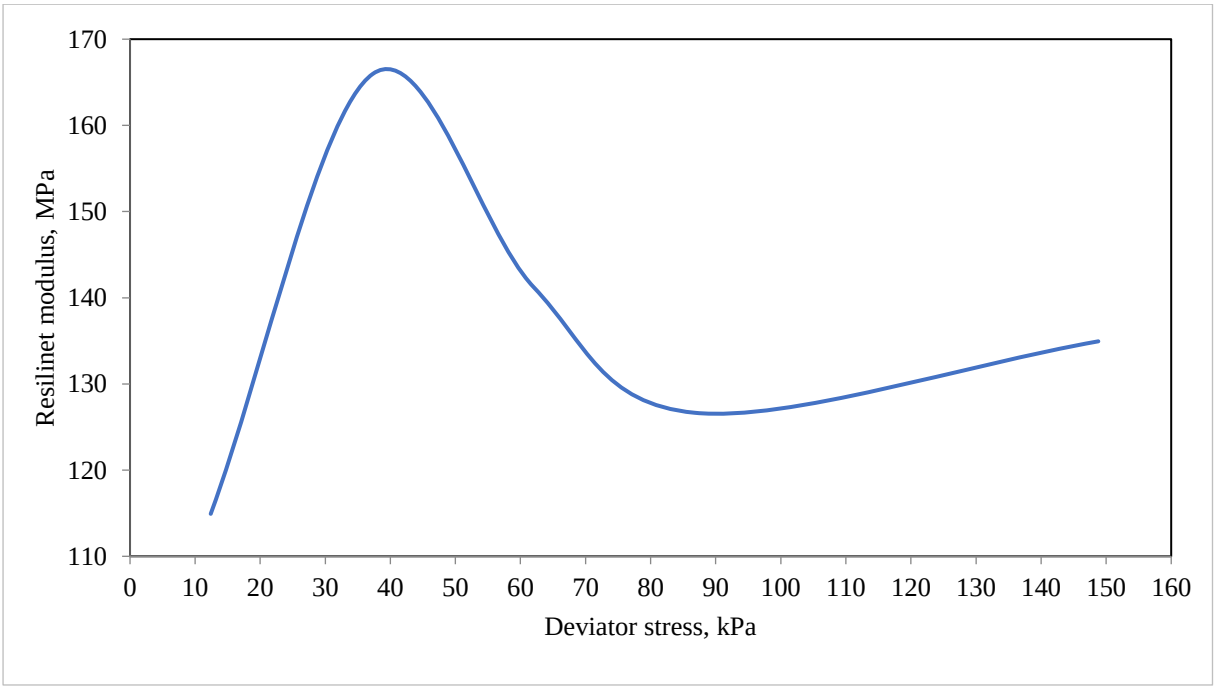

Figure 7.8 Resilient modules vs. deviator stress for fibre & fly ash reinforced sand.

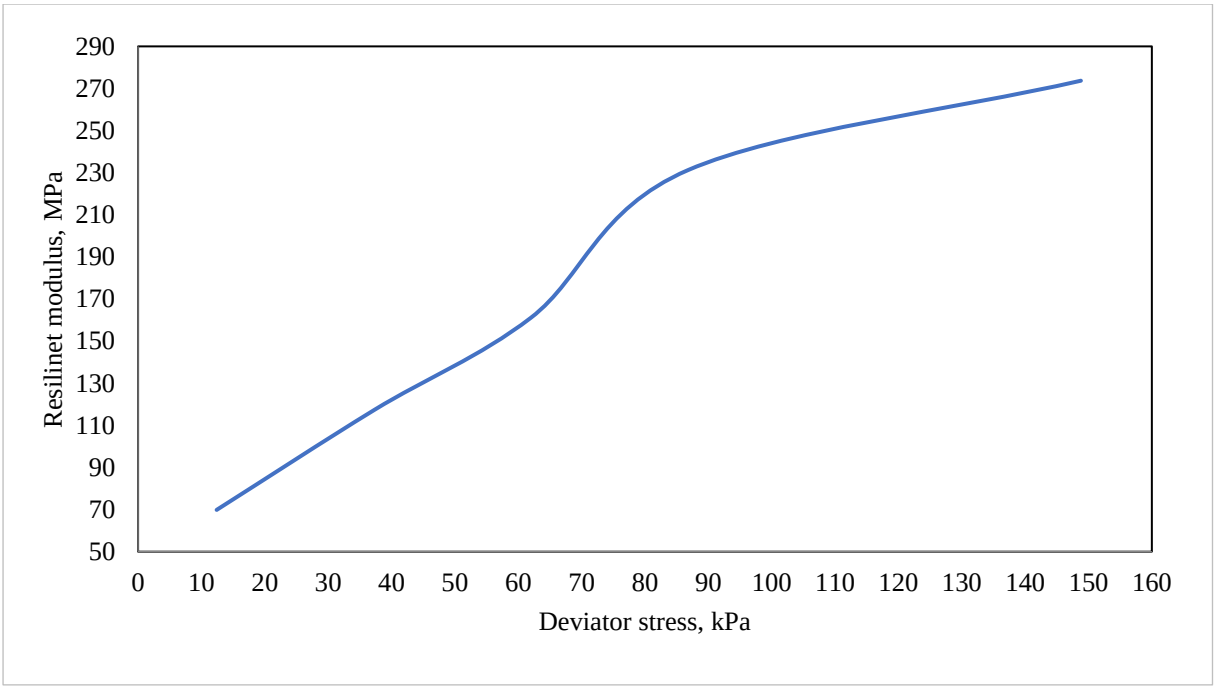

Figure 7.9 Resilient modules vs. deviator stress for slag stabilized sand.

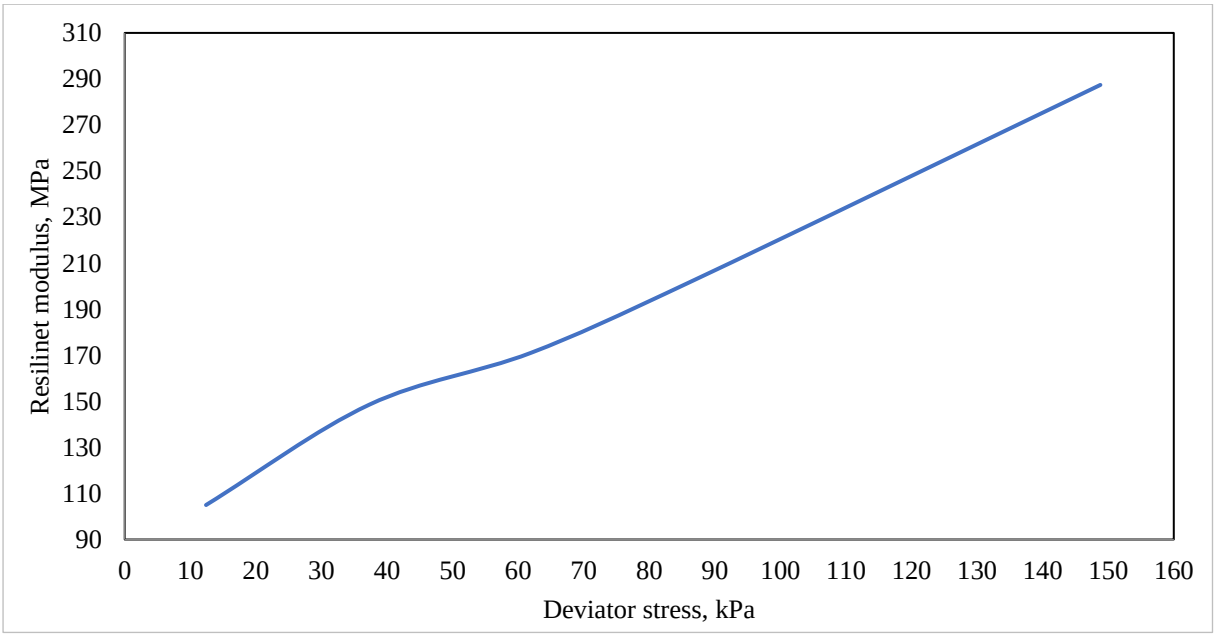

Figure 7.10 Resilient modules vs. deviator stress for fibre and slag reinforced sand.

Table 7-6 Pavement response for fibre reinforced sand at 552kPa tire pressure.

Trail (1)						
Pavement response	Vertical strain			Horizontal strain		Deflection, mm
	1	4	5	2	3	
Load Group No. 1	-2.458E-04	8.527E-04	8.991E-04	-3.928E-04	-4.324E-04	2.25
Load Group No. 2	-2.470E-04	8.478E-04	8.949E-04	-3.754E-04	-4.142E-04	3.17
Load Group No. 3	-2.464E-04	8.376E-04	8.846E-04	-3.730E-04	-4.118E-04	3.62
Deviator stress, kPa	95.14					Σ = 9.05
Trail (2)						
Pavement response	Vertical strain			Horizontal strain		Deflection, mm
	1	4	5	2	3	
Load Group No. 1	-2.199E-04	7.390E-04	7.737E-04	-3.642E-04	-4.017E-04	2.142
Load Group No. 2	-2.233E-04	7.411E-04	7.764E-04	-3.509E-04	-3.878E-04	3.05
Load Group No. 3	-2.234E-04	7.318E-04	7.671E-04	-3.496E-04	-3.866E-04	3.51
Deviator stress, kPa	103					Σ = 8.7

Table 7-7 Section Configuration for fibre reinforced sand at 689kPa tire pressure.

Layers	Thickness, cm		M_R		Poisson's ratio
	Trial 1	Trial 2	Trial 1	Trial 2	
Asphalt	10	10	2000	2000	0.3
Base	15	15	290	290	0.35
Reinforced Subgrade	15	15	100	160	0.35
Natural subgrade	--	--	21	21	0.35
Contact pressure, psi	689				

Table 7-8 Pavement response for fibre reinforced sand at 689kPa tire pressure.

Trail (1)						
Pavement response	Vertical strain			Horizontal strain		Deflection, mm
	1	4	5	2	3	
Load Group No. 1	-2.429E-04	8.888E-04	9.201E-04	-4.472E-04	4.472E-04	2.30
Load Group No. 2	-2.441E-04	8.838E-04	8.838E-04	-4.296E-04	-4.415E-04	3.23
Load Group No. 3	-2.422E-04	8.734E-04	9.053E-04	-4.272E-04	-4.392E-04	3.68
Deviator stress, kPa	97.5					Σ = 9.23
Trail (2)						
Pavement response	Vertical strain			Horizontal strain		Deflection, mm
	1	4	5	2	3	
Load Group No. 1	-2.160E-04	7.717E-04	7.917E-04	-4.178E-04	-4.284E-04	2.189
Load Group No. 2	-2.195E-04	7.737E-04	7.943E-04	-4.043E-04	-4.144E-04	3.11
Load Group No. 3	-2.196E-04	7.644E-04	7.849E-04	-4.031E-04	-4.132E-04	3.57
Deviator stress, kPa	106.1					Σ = 8.78

Table 7-9 Section Configuration for fibre reinforced sand at 827kPa tire pressure.

Layers	Thickness, cm		M_R		Poisson's ratio
	Trial 1	***Trial 2***	***Trial 1***	***Trial 2***	
Asphalt	10	10	2000	2000	0.3
Base	20	20	290	290	0.35
Reinforced subgrade	20	20	140	160	0.35
Natural subgrade		--	21	21	0.35
Contact pressure, kPa	827				

Table 7-10 Pavement response for fibre reinforced sand at 827kPa tire pressure.

Trail (1)						
Pavement response	Vertical strain			Horizontal strain		Deflection, mm
	1	4	5	2	3	
Load Group No. 1	-1.665E-04	6.792E-04	7.163E-04	-4.313E-04	-4.136E-04	2.01
Load Group No. 2	-1.835E-04	6.907E-04	7.285E-04	-4.223E-04	-4.044E-04	2.97
Load Group No. 3	-1.665E-04	6.792E-04	7.163E-04	-4.234E-04	-4.055E-04	3.45
Deviator stress, kPa	98					$\Sigma = 8.44$
Trail (2)						
Pavement response	Vertical strain			Horizontal strain		Deflection, mm
	1	4	5	2	3	
Load Group No. 1	-1.589E-04	6.461E-04	6.803E-04	-4.247E-04	-4.067E-04	1.97
Load Group No. 2	-1.813E-04	6.590E-04	6.940E-04	-4.165E-04	-3.982E-04	2.96
Load Group No. 3	-1.793E-04	6.516E-04	6.865E-04	-4.180E-04	-3.998E-04	3.44
Deviator stress, kPa	102					$\Sigma = 8.39$

Table 7-11 Section Configuration for fly ash stabilized sand at 414 & 552kPa tire pressure.

Layers	Thickness, cm			M_R			Poisson's ratio
	Trial 1	Trial 2	Trial 3	Trial 1	Trial 2	Trial 3	
Asphalt	10	10	10	2000	2000	2000	0.3
Base	20	20	20	290	290	290	0.35
Subbase	***Nil***	***Nil***	20	***Nil***	***Nil***	138	0.35
Reinforced Subgrade	20	20	20	69	90	90	0.35
Natural subgrade	--	--	--	21	21	21	0.35
Contact pressure, kPa	552		414				

Table 7-12 Pavement response for fly ash stabilized sand at 552kPa tire pressure.

Trail (1)						
Pavement response	Vertical strain			Horizontal strain		Deflection, mm
	1	4	5	2	3	
Load Group No. 1	-2.117E-04	7.772E-04	8.380E-04	-3.577E-04	-3.947E-04	2.07
Load Group No. 2	-2.198E-04	7.802E-04	8.416E-04	-3.451E-04	-3.816E-04	2.98
Load Group No. 3	-2.174E-04	7.697E-04	8.312E-04	-3.442E-04	-3.808E-04	3.43
Deviator stress, kPa	77.2					Σ =8.49
Trail (2)						
Pavement response	Vertical strain			Horizontal strain		Deflection, mm
	1	4	5	2	3	
Load Group No. 1	-1.989E-04	7.222E-04	7.779E-04	-3.472E-04	-3.836E-04	2.01
Load Group No. 2	-2.081E-04	7.285E-04	7.848E-04	-3.362E-04	-3.721E-04	2.91
Load Group No. 3	-2.058E-04	7.190E-04	7.753E-04	-3.359E-04	-3.719E-04	3.36
Deviator stress, kPa	82.7					Σ =8.28

Table 7-13Pavement response for fly ash stabilized sand at 414kPa tire pressure.

Trail (3)						
Pavement response	Vertical strain			Horizontal strain		Deflection, mm
	1	4	5	2	3	
Load Group No. 1	-1.483E-04	5.214E-04	5.673E-04	-2.589E-04	-3.142E-04	1.63
Load Group No. 2	-1.681E-04	5.597E-04	6.067E-04	-2.510E-04	-3.060E-04	2.51
Load Group No. 3	-1.680E-04	5.557E-04	6.026E-04	-2.530E-04	-3.080E-04	2.97
Deviator stress, kPa	46					Σ =7.11

Table 7-14 Section Configuration for fibre & fly ash stabilized sand at 552kPa tire pressure.

Layers	Thickness, cm		M_R		Poisson's ratio
	Trial 1	Trial 2	Trial 1	Trial 2	
Asphalt	5	10	2000	2000	0.3
Base	15	15	290	290	0.35
Reinforced Subgrade	15	15	100	100	0.35
Natural subgrade	--	--	21	21	0.35
Contact pressure, kPa	552				

Table 7-15 Pavement response for fibre & fly ash stabilized sand at 552kPa tire pressure.

Trail (1)						
Pavement response	Vertical strain			Horizontal strain		Deflection, mm
	1	4	5	2	3	
Load Group No. 1	-3.740E-04	1.191E-03	1.161E-03	-2.126E-04	-2.734E-04	2.72
Load Group No. 2	-3.721E-04	1.174E-03	1.143E-03	-2.237E-04	-2.842E-04	3.64
Load Group No. 3	-3.706E-04	1.164E-03	1.134E-03	-2.896E-04	-2.291E-04	4.08
Deviator stress, kPa	136.5					Σ =10.45
Trail (2)						
Pavement response	Vertical strain			Horizontal strain		Deflection, mm
	1	4	5	2	3	
Load Group No. 1	-2.458E-04	8.527E-04	8.991E-04	-3.928E-04	-4.324E-04	2.25
Load Group No. 2	-2.470E-04	8.478E-04	8.949E-04	-3.754E-04	-4.142E-04	3.17
Load Group No. 3	-2.464E-04	8.376E-04	8.846E-04	-3.730E-04	-4.118E-04	3.62
Deviator stress, kPa	95					Σ =9.05

Table 7-16 Section Configuration for fibre & fly ash stabilized sand at 689kPa tire pressure.

Layers	Thickness, cm		M_R		Poisson's ratio
	Trial 1	Trial 2	Trial 1	Trial 2	
Asphalt	10	10	2000	2000	0.3
Base	15	15	290	290	0.35
Reinforced Subgrade	15	15	100	125	0.35
Natural subgrade	--	--	21	21	0.35
Contact pressure, kPa	689				

Table 7-17 Pavement response for fibre & fly ash stabilized sand at 689kPa tire pressure.

Trail (1)						
Pavement response	Vertical strain			Horizontal strain		Deflection, mm
	1	4	5	2	3	
Load Group No. 1	-2.429E-04	8.888E-04	9.201E-04	-4.472E-04	-4.600E-04	2.30
Load Group No. 2	-2.441E-04	8.838E-04	9.157E-04	-4.296E-04	-4.415E-04	3.23
Load Group No. 3	-2.422E-04	8.734E-04	9.053E-04	-4.272E-04	-4.392E-04	3.68
Deviator stress, kPa	97.5					Σ =9.23
Trail (2)						
Pavement response	Vertical strain			Horizontal strain		Deflection, mm
	1	4	5	2	3	
Load Group No. 1	-2.315E-04	8.394E-04	8.660E-04	-4.349E-04	-4.468E-04	2.25
Load Group No. 2	-2.337E-04	8.375E-04	8.647E-04	-4.190E-04	-4.302E-04	3.18
Load Group No. 3	-2.341E-04	8.275E-04	8.546E-04	-4.171E-04	-4.283E-04	3.64
Deviator stress, kPa	100.6					Σ =9.08

Table 7-18 Section Configuration for fibre & fly ash stabilized sand at 827kPa tire pressure.

Layers	Thickness, cm	M_R	Poisson's ratio
	Trial 1	Trial 1	
Asphalt	10	2000	0.3
Base	15	290	0.35
Reinforced Subgrade	15	125	0.35
Natural subgrade	--	21	0.35
Contact pressure, kPa	827		

Table 7-19 Pavement response for fibre & fly ash stabilized sand at 827kPa tire pressure.

Trail (1)						
Pavement response	Vertical strain			Horizontal strain		Deflection, mm
	1	4	5	2	3	
Load Group No. 1	-2.285E-04	8.804E-04	8.964E-04	-4.867E-04	-4.729E-04	2.33
Load Group No. 2	-2.307E-04	8.783E-04	8.949E-04	-4.704E-04	-4.558E-04	3.29
Load Group No. 3	-2.312E-04	8.681E-04	8.846E-04	-4.684E-04	-4.539E-04	3.76
Deviator stress, kPa	104.7					Σ =9.39

Table 7-20 Section Configuration for slag stabilized sand at 552kPa tire pressure.

Layers	Thickness, cm		M_R		Poisson's ratio
	Trial 1	Trial 2	Trial 1	Trial 2	
Asphalt	10	10	2000	2000	0.3
Base	15	15	290	290	0.35
Reinforced Subgrade	15	15	100	240	0.35
Natural subgrade	--	--	21	21	0.35
Contact pressure, psi	552				

Table 7-21 Pavement response for slag stabilized sand at 552kPa tire pressure.

Trail (1)						
Pavement response	Vertical strain			Horizontal strain		Deflection, mm
	1	4	5	2	3	
Load Group No. 1	-3.740E-04	1.191E-03	1.161E-03	-2.126E-04	-2.734E-04	2.72
Load Group No. 2	-3.721E-04	1.174E-03	1.143E-03	-2.237E-04	-2.842E-04	3.64
Load Group No. 3	-3.706E-04	1.164E-03	1.134E-03	-2.291E-04	-2.896E-04	4.08
Deviator stress, kPa	136.5					Σ =10.45
Trail (2)						
Pavement response	Vertical strain			Horizontal strain		Deflection, mm
	1	4	5	2	3	
Load Group No. 1	-1.746E-04	6.274E-04	6.507E-04	-3.353E-04	-3.708E-04	2.03
Load Group No. 2	-1.821E-04	6.351E-04	6.591E-04	-3.258E-04	-3.609E-04	2.94
Load Group No. 3	-1.794E-04	6.273E-04	6.513E-04	-3.260E-04	-3.611E-04	3.40
Deviator stress, kPa	113					Σ =8.38

Table 7-22 Section Configuration for slag stabilized sand at 689kPa tire pressure.

Layers	Thickness, cm		M_R		Poisson's ratio
	Trial 1	Trial 2	Trial 1	Trial 2	
Asphalt	10	10	2000	2000	0.3
Base	15	15	290	290	0.35
Reinforced Subgrade	15	15	220	248	0.35
Natural subgrade	--	--	21	21	0.35
Contact pressure, kPa	689				

Table 7-23 Pavement response for slag stabilized sand at 689kPa tire pressure.

Trail (1)						
Pavement response	Vertical strain			Horizontal strain		Deflection, mm
	1	4	5	2	3	
Load Group No. 1	-1.897E-04	6.568E-04	6.658E-04	-3.882E-04	-3.966E-04	2.06
Load Group No. 2	-3.785E-04	-3.866E-04	-1.956E-04	-3.785E-04	-3.866E-04	2.98
Load Group No. 3	-1.928E-04	6.567E-04	6.663E-04	-3.788E-04	-3.869E-04	3.44
Deviator stress, kPa	116					Σ =8.5
Trail (2)						
Pavement response	Vertical strain			Horizontal strain		Deflection, mm
	1	4	5	2	3	
Load Group No. 1	-1.880E-04	6.493E-04	6.576E-04	-3.862E-04	-3.945E-04	2.06
Load Group No. 2	-1.957E-04	6.575E-04	6.663E-04	-3.768E-04	-3.847E-04	2.98
Load Group No. 3	-1.930E-04	6.497E-04	6.585E-04	-3.771E-04	-3.851E-04	3.44
Deviator stress, kPa	114.4					Σ =8.48

Table 7-24 Section Configuration for slag stabilized sand at 827kPa tire pressure.

Layers	Thickness, cm		M_R		Poisson's ratio
	Trial 1	Trial 2	Trial 1	Trial 2	
Asphalt	10	10	2000	2000	0.3
Base	15	15	290	290	0.35
Reinforced Subgrade	15	15	248	260	0.35
Natural subgrade	--	--	21	21	0.35
Contact pressure, kPa	827				

Table 7-25 Pavement response for slag stabilized sand at 827kPa tire pressure.

Trail (1)						
Pavement response	Vertical strain			Horizontal strain		Deflection, mm
	1	4	5	2	3	
Load Group No. 1	-1.831E-04	6.828E-04	6.805E-04	-4.362E-04	-4.186E-04	2.13
Load Group No. 2	-1.892E-04	6.911E-04	6.895E-04	-4.265E-04	-4.086E-04	3.078
Load Group No. 3	-1.864E-04	6.831E-04	6.815E-04	-4.269E-04	-4.090E-04	3.55
Deviator stress, kPa	120.6					Σ = 8.76
Trail (2)						
Pavement response	Vertical strain			Horizontal strain		Deflection, mm
	1	4	5	2	3	
Load Group No. 1	-1.801E-04	6.702E-04	6.668E-04	-4.328E-04	-4.150E-04	2.12
Load Group No. 2	-1.866E-04	6.790E-04	6.763E-04	-4.235E-04	-4.054E-04	3.06
Load Group No. 3	-1.838E-04	6.712E-04	6.684E-04	-4.242E-04	-4.061E-04	3.53
Deviator stress, kPa	122					Σ = 8.72

Table 7-26 Section Configuration for slag & fibre stabilized sand at 552kPa tire pressure.

Layers	Thickness, cm		M_R		Poisson's ratio
	Trial 1	Trial 2	Trial 1	Trial 2	
Asphalt	10	10	2000	2000	0.3
Base	15	15	290	290	0.35
Reinforced Subgrade	15	15	100	220	0.35
Natural subgrade	--	--	21	21	0.35
Contact pressure, kPa	552				

Table 7-27 Pavement response for slag & fibre stabilized sand at 552kPa tire pressure.

Trail (1)						
Pavement response	Vertical strain			Horizontal strain		Deflection, mm
	1	4	5	2	3	
Load Group No. 1	-3.740E-04	1.191E-03	1.161E-03	-2.126E-04	-2.734E-04	2.72
Load Group No. 2	-3.721E-04	1.174E-03	1.143E-03	-2.237E-04	-2.842E-04	3.64
Load Group No. 3	-3.706E-04	1.164E-03	1.134E-03	-2.291E-04	-2.896E-04	4.08
Deviator stress, kPa	137					Σ = 10.45
Trail (2)						
Pavement response	Vertical strain			Horizontal strain		Deflection, mm
	1	4	5	2	3	
Load Group No. 1	-1.800E-04	6.508E-04	6.764E-04	-3.415E-04	-3.773E-04	2.06
Load Group No. 2	-1.870E-04	6.574E-04	6.837E-04	-3.311E-04	-3.666E-04	2.97
Load Group No. 3	-1.843E-04	6.493E-04	6.756E-04	-3.310E-04	-3.665E-04	3.42
Deviator stress, kPa	111.3					Σ = 8.46

Table 7-28 Section Configuration for slag & fibre stabilized sand at 689kPa tire pressure.

Layers	Thickness, cm		M_R		Poisson's ratio
	Trial 1	Trial 2	Trial 1	Trial 2	
Asphalt	10	10	2000	2000	0.3
Base	15	15	290	290	0.35
Reinforced Subgrade	15	15	220	240	0.35
Natural subgrade	--	--	21	21	0.35
Contact pressure, kPa	689				

Table 7-29 Pavement response for slag & fibre stabilized sand at 689kPa tire pressure.

Trail (1)						
Pavement response	Vertical strain			Horizontal strain		Deflection, mm
	1	4	5	2	3	
Load Group No. 1	-1.952E-04	6.808E-04	6.921E-04	-3.945E-04	-4.034E-04	2.09
Load Group No. 2	-2.006E-04	6.875E-04	6.994E-04	-3.840E-04	-3.925E-04	3.01
Load Group No. 3	-1.978E-04	6.793E-04	6.911E-04	-3.839E-04	-3.925E-04	3.47
Deviator stress, kPa	113.7					Σ = 8.58
Trail (2)						
Pavement response	Vertical strain			Horizontal strain		Deflection, mm
	1	4	5	2	3	
Load Group No. 1	-1.897E-04	6.568E-04	6.658E-04	-3.882E-04	-3.966E-04	2.06
Load Group No. 2	-1.956E-04	6.646E-04	6.742E-04	-3.785E-04	-3.866E-04	2.98
Load Group No. 3	-1.928E-04	6.567E-04	6.663E-04	-3.788E-04	-3.869E-04	3.44
Deviator stress, kPa	115.8					Σ = 8.5

Table 7-30 Section Configuration for slag & fibre stabilized sand at 827kPa tire pressure.

Layers	Thickness, cm		M_R		Poisson's ratio
	Trial 1	Trial 2	Trial 1	Trial 2	
Asphalt	10	10	2000	2000	0.3
Base	15	15	290	290	0.35
Reinforced Subgrade	15	15	240	250	0.35
Natural subgrade	--	--	21	21	0.35
Contact pressure, kPa	827				

Table 7-31 Pavement response for slag & fibre stabilized sand at 827kPa tire pressure.

Trail (1)						
Pavement response	Vertical strain			Horizontal strain		Deflection, mm
	1	4	5	2	3	
Load Group No. 1	-1.849E-04	6.905E-04	6.890E-04	-4.382E-04	-4.208E-04	2.14
Load Group No. 2	-1.909E-04	6.985E-04	6.976E-04	-4.283E-04	-4.105E-04	3.08
Load Group No. 3	-1.881E-04	6.904E-04	6.895E-04	-4.286E-04	-4.109E-04	3.56
Deviator stress, kPa	120					Σ = 8.79
Trail (2)						
Pavement response	Vertical strain			Horizontal strain		Deflection, mm
	1	4	5	2	3	
Load Group No. 1	-1.831E-04	6.828E-04	6.805E-04	-4.362E-04	-4.186E-04	2.13
Load Group No. 2	-1.892E-04	6.911E-04	6.895E-04	-4.265E-04	-4.086E-04	3.07
Load Group No. 3	-1.864E-04	6.831E-04	6.815E-04	-4.269E-04	-4.090E-04	3.55
Deviator stress, kPa	120.6					Σ = 8.76

7.4 Distress Prediction Models

The cumulative distress calculations were described in this section as mentioned in Figure 7.2. The flexible pavement design includes fatigue cracking and permanent deformation. The distress was analysed at five points as shown in Figure 7.5. These include:

- Fatigue at the bottom of asphalt,
- Rutting on the asphalt surface layer, and
- Rutting on the top of subgrade layer.

Both distresses were predicted according to the pavement response which is the vertical compressive strain at points 1, 3 and 5 and horizontal or tensile strain at points 2 and 3. The results of the models simulated the allowable number of load repetitions. The traffic load repetition was obtained for three periods 10, 20 and 30 years in terms of equivalent single axle loads as shown in Table 7-3.

The fatigue and rutting models were accepted or rejected by the allowable number of load repetitions. It was believed that the allowable number of load repetition was related to the tensile strain at the bottom of the asphalt layer for the fatigue cracking. In the Asphalt Institute Method, it was recommended to use Equation 7.4.

$$N_f = f_1(\varepsilon_t)^{-f_2}(M_r)^{-f_3}$$ Equation 7.4

Where

N_f = allowable number of load repetition,

ε_t= Tensile strain at the bottom of the asphalt layer,

Mr = Resilient modules of asphalt layer, and

f_1, f_2 & f_3 = coefficients of fatigue criterion (0.0796, -3.291 & -0.854, respectively).

The rutting was limited by control two vertical compressive strains which are on the top of the asphalt layer and on the top of the subgrade layer. In the Asphalt Institute and Shell design methods recommended Equation 7.5 to determine the allowable number of load repetitions based on the vertical compressive strain.

The allowable numbers of load repetition for both fatigue and rutting were described in Table 7-32 and 7.33, respectively.

$$N_d = f_4(\varepsilon_c)^{-f_5}$$ Equation 7.5

Where

N_d = allowable number of load repetition,

ε_c= Vertical strain on the surface of the subgrade, and

f_4 & f_5 = Coefficients of permanent deformation criterion (1 .365x10^{-9} & 4.477, respectively).

Table 7-32 The allowable load repetitions of fatigue

Material	Thickness, cm	Tire Pressure, kPa	N_f			
			Single	Tandem	Tridem	Total
Fibre	10, 15, 15	552	597997	674031	681740	1953768
	10, 15, 15	689	423973	472655	477247	1373875
	10, 20, 20	827	450312	481531	475519	1407362
Fly Ash	10, 20, 20	414	1630016	1795756	1752271	5178043
Fibre & Fly Ash	10, 15, 15	552	467546	540998	552079	1560623
	10, 15, 15	689	370407	419115	425351	1214873
	10, 15, 15	827	280380	315143	319547	915070
Slag	10, 15, 15	552	782148	857762	856101	2496011
	10, 15, 15	689	552526	599688	597888	1750102
	10, 15, 15	827	410870	443750	442351	1296971
Slag & Fibre	10, 15, 15	552	737338	813919	814695	2365952
	10, 15, 15	689	543089	590471	588949	1722509
	10, 15, 15	827	410870	443750	442351	1296971

Table 7-33 The allowable load repetitions of permanent deformation or rutting

Material	Thickness, cm	Tire Pressure, kPa	N_d			
			Single	Tandem	Tridem	Total
Fibre	10, 15, 15	552	32692011	30535313	30489207	93716531
	10, 15, 15	689	35360775	32918081	32863584	101142440
	10, 20, 20	827	139366459	77390836	81331291	298088586
Fly Ash	10, 20, 20	414	190351168	108800650	109115433	408267251
Fibre & Fly Ash	10, 15, 15	552	19835861	19414168	19632723	58882752
	10, 15, 15	689	25916215	24849247	24669194	75434656
	10, 15, 15	827	27440089	26294254	26048600	79782943
Slag	10, 15, 15	552	91645243	75980556	81228835	248854634
	10, 15, 15	689	65917700	55128795	58662038	179708533
	10, 15, 15	827	74043318	63972380	68382361	206398059
Slag & Fibre	10, 15, 15	552	79947567	67446415	71979162	219373144
	10, 15, 15	689	63307751	55231064	58908506	177447321
	10, 15, 15	827	74043318	63972380	68382361	206398059

7.5 Performance criteria

The flexible pavement failures are controlled by performance criteria such as fatigue cracking and permanent deformation. Therefore, the critical pavement responses obtained were the

horizontal tensile strain at the bottom of the asphalt layer and the vertical compressive strain on the top of the subgrade layer and surface of the asphalt layer. The horizontal tensile strain causes fatigue cracking and the vertical compressive strain causes permanent deformation or rutting.

Based on the traffic data in Table 7-3, both fatigue and rutting limitations were determined by comparing the allowable number of load repetition with the equivalent single axle load. The design period was divided into three periods. The equivalent single axle load was determined for 10, 20 and 30 years as shown in Table 7-34. Therefore, it could be determined the design life based on the traffic loading.

Also, the guide limits the deflection on the surface of the road to be 7.6-12.7 mm, (0.3-0.5 in). The superiority of the reinforced and stabilized materials was that the deflection for all materials was about 0.35 in (9mm). The results of the deflections were summarized in Table 7-37 and 7.38, respectively.

To conclude, the performance criteria can be concluded in three criteria;

- The allowable load repetitions of fatigue should not increase the equivalent single axle load,
- The allowable load repetitions of rutting should not increase by the equivalent single axle load, and
- The deflection of the surface should not increase the range of 7.6-12.7mm.

Table 7-34 describes the number of the equivalent axle load for 10, 20, and 30 years. If the results in Table 7-35 and 7.36 are more than the equivalent single axle load, the pavement

section is successful. It is also possible to determine the design life based on the results in Table 7-35 and 7.36 when compared with Table 7-34.

Table 7-34 Equivalent single axle load for 10, 20, & 30

Design period	Equivalent Single Axle Load
10	3,988673
20	10,293350
30	20,458034

Table 7-35 The allowable load repetitions of fatigue

Material	Thickness, cm	Tire Pressure, kPa	N_f			
			Single	Tandem	Tridem	Total
Fibre	10, 15, 15	552	597997	674031	681740	1953768
	10, 15, 15	689	423973	472655	477247	1373875
	10, 20, 20	827	450312	481531	475519	1407362
Fly Ash	10, 20, 20	414	1630016	1795756	1752271	5178043
Fibre & Fly Ash	10, 15, 15	552	467546	540998	552079	1560623
	10, 15, 15	689	370407	419115	425351	1214873
	10, 15, 15	827	280380	315143	319547	915070
Slag	10, 15, 15	552	782148	857762	856101	2496011
	10, 15, 15	689	552526	599688	597888	1750102
	10, 15, 15	827	410870	443750	442351	1296971
Slag & Fibre	10, 15, 15	552	737338	813919	814695	2365952
	10, 15, 15	689	543089	590471	588949	1722509
	10, 15, 15	827	410870	443750	442351	1296971

Table 7-36 The allowable load repetitions of permanent deformation.

Material	Thickness, cm	Tire Pressure, kPa	N_d			
			Single	Tandem	Tridem	Total
Fibre	10, 15, 15	552	32692011	30535313	30489207	93716531
	10, 15, 15	689	35360775	32918081	32863584	101142440
	10, 20, 20	827	139366459	77390836	81331291	298088586
Fly Ash	10, 20, 20	414	190351168	108800650	109115433	408267251
Fibre & Fly Ash	10, 15, 15	552	19835861	19414168	19632723	58882752
	10, 15, 15	689	25916215	24849247	24669194	75434656
	10, 15, 15	827	27440089	26294254	26048600	79782943
Slag	10, 15, 15	552	91645243	75980556	81228835	248854634
	10, 15, 15	689	65917700	55128795	58662038	179708533
	10, 15, 15	827	74043318	63972380	68382361	206398059
Slag & Fibre	10, 15, 15	552	79947567	67446415	71979162	219373144
	10, 15, 15	689	63307751	55231064	58908506	177447321
	10, 15, 15	827	74043318	63972380	68382361	206398059

Table 7-37 The deflection for each load group

Material	Load group	Tire pressure, kPa	Deflection, mm
Fibre reinforced sand	Load Group No. 1	552	2.142
	Load Group No. 2		3.05
	Load Group No. 3		3.51
			Σ = 8.7
	Load Group No. 1	689	2.189
	Load Group No. 2		3.11
	Load Group No. 3		3.57
			Σ = 8.78
	Load Group No. 1	827	1.97
	Load Group No. 2		2.96
	Load Group No. 3		3.44
			Σ = 8.39
fly ash stabilized sand	Load Group No. 1	414	1.63
	Load Group No. 2		2.51
	Load Group No. 3		2.97
			Σ =7.11
fibre & fly ash stabilized sand	Load Group No. 1	552	2.25
	Load Group No. 2		3.17
	Load Group No. 3		3.62
			Σ =9.05
	Load Group No. 1	689	2.25
	Load Group No. 2		3.18
	Load Group No. 3		3.64
			Σ =9.08
	Load Group No. 1	827	2.33
	Load Group No. 2		3.29
	Load Group No. 3		3.76
			Σ =9.39

Table 7-38 The deflection for each load group

Material	Load group	Tire pressure, kPa	Deflection, in
slag stabilized sand	Load Group No. 1	552	2.03
	Load Group No. 2		2.94
	Load Group No. 3		3.40
			Σ =8.38
	Load Group No. 1	689	2.06
	Load Group No. 2		2.98
	Load Group No. 3		3.44
			Σ =8.48
	Load Group No. 1	827	2.12
	Load Group No. 2		3.06
	Load Group No. 3		3.53
			Σ = 8.72
slag & fibre stabilized sand	Load Group No. 1	552	2.06
	Load Group No. 2		2.97
	Load Group No. 3		3.42
			Σ = 8.46
	Load Group No. 1	689	2.06
	Load Group No. 2		2.98
	Load Group No. 3		3.44
			Σ = 8.5
	Load Group No. 1	827	2.13
	Load Group No. 2		3.07
	Load Group No. 3		3.55
			Σ = 8.76

7.6 Summary

This chapter presented the pavement analysis procedure for reinforcement desert sand. The procedure used the pavement design steps and findings to undertake the analytical design. The design inputs are the traffic load and materials properties; the traffic loading was obtained from a similar location in Libya as level 2, materials properties were evaluated by extensive laboratory work. Generally, the environmental conditions are simulated by wetting – drying or freezing-thawing durability test. In this research, the freeze-thaw cycles durability test were applied to have consistent results. The fibre reinforced sand samples were not

possible to stand them in the water, therefore, the freeze-thaw cycles test was used for all other samples.

The experimental work results were used to develop two correlation models to obtain the resilient modulus for the reinforcement desert sand. The resilient modulus of reinforcement sand was simply obtained by unconfined compressive strength test or cyclic load test. The only limitation of correlation models was that when they were used to obtain the resilient modulus values for fibre reinforced sand above the optimum water content, the variation was increasing compare with (Finn et al., 1986) model.

The reinforcement methods considered in this study showed that there is promising to build a road using reinforced desert sand without the need to replace it (sand). This conclusion is drawn from both the laboratory investigation and the analytical pavement design undertaken. The reinforced layer resists rutting and fatigue as the calculated deflection was below the limit as recommended in (NCHRP, 2004). The reinforced layer was in some cases, it was able to carry more than twice of the allowable load repetitions.

The pavement responses were obtained by KENLAYER software. The pavement configuration showed that the subbase layer was not required to build the road when reinforcing the sand with fibre, class C fly ash or vitrified slag. The pavement responses were determined by linear behaviour. The Boussinesq's solutions which based on linear theory were used to obtain the pavement responses. This solution has been incorporated in KENLAYER software. There is an example to show the results of both theories in Chapter Five section 5.5. the nonlinear behaviour is dependent on the confining pressure as a state in (Huang, 2004). But the reinforcement materials demonstrated different behaviour, the

confining pressure shown a negligible effect on the resilient modulus values of reinforced sand.

The pavement response indicated that the reinforced sand for subgrade layer resists the vertical compressive strain. On the other hand, the tensile strain at the bottom of the asphalt layer is higher than the performance criteria. It is recommended that the geogrid is powerful under the asphalt layer in order to reduce the tensile strain. Table 7-39 shows the summary of the deviator stress and resilient modulus against the tire pressure. The fibre exhibits strong resistance at different tire pressure. On the other hand, the fly ash shows different behaviour, the fly ash stabilized sand only provided strength to carry 414kPa tire pressure. Also, the limitation of deflection was controlled for all the mixtures to be in the lower range of the deflection as shown in Table 7-37 and 7-38.

Table 7-39 Summary of deviator stress and resilient modulus.

Materials	Tire pressure, kPa	Deviator stress, kPa	Resilient modulus, MPa
Fibre reinforced sand	552	103	160
	689	106	160
	827	102	160
Fly ash stabilized sand	414	46	136
Fly ash and fibre stabilized sand	552	95	100
	689	101	125
	827	105	125
Slag stabilized sand	552	113	240
	689	114	248
	827	122	260
Slag and fibre stabilized sand	552	111	220
	689	116	240
	827	121	250

CHAPTER 8 CONCLUSION AND RECOMMENDATIONS

8.1 Introduction

Using desert sand in structural layers in a road is problematic due to its uniformity in the main. It, therefore, becomes necessary to either replace it with more suitable material or to reinforce/stabilise it to improve its properties, making it more suitable for use in road construction. In this research was aimed to reinforce and stabilize the sand for road construction. Stabilization of polypropylene fibre, fly ash and vitrified slag and tested by subjecting reinforced and stabilized sand to both monotonic and cyclic loading. Variation in moisture and durability was examined. The latter through freeze-thaw cycles. Findings were used to design a section of road in Libya. Conclusions and recommendations from this research are presented in the following sections.

8.2 Conclusions

8.2.1 Experimental work

Extensive and robust experimental work was conducted to characterize the reinforcement subgrade layer. The engineering properties were identified by a series of compaction test, particles size distribution, static and cyclic triaxial tests. The static triaxial apparatus was required to investigate the shear strength parameters of reinforcement sand. The cyclic repeated tests consisted of resilient modulus and permanent deformation; they were obtained for all samples with/without freeze-thaw durability cycles.

Also, the unconfined compressive strength test was used to evaluate the strength of unreinforced and reinforced sand. The test results were required to develop correlation models with resilient modulus.

8.2.2 Stabilizers and Reinforcement Materials

The reinforcement materials were chosen to improve the sand properties such the cohesionless, shear strength, resilient modulus, and permanent deformation etc. These parameters are required for pavement design.

8.2.3 Properties of Materials

8.2.3.1 Sand

Sand, closely resembling the Libyan Desert sand was sourced from an Aggregate Industries, called Levenseat quarry in Scotland.

Numbers of compacted sand specimens were performed to evaluate the resilient modulus, but they failed before the end of the test. Therefore, only static triaxial test and unconfined compressive strength test were conducted to evaluate the strength parameters. The properties of reinforced sand were improved. Then it was possible to be subjected to cyclic repeated load on the reinforced sand.

8.2.3.2 Polypropylene Fibre

In this study, polypropylene fibre was used with three fibre lengths of 12, 19, and 50mm. the reinforced sand with fibre was compacted by the vibration table as recommended for sandy soil in according to BS 1377-4:1990. However, the vibration table separated the fibre from the sand. Therefore, the modified proctor compaction test was the proper method to determine the maximum dry density and optimum water content for sandy soil.

The fibre length of 19mm showed significant improvement in shear strength of fibre reinforced sand. The previous studies and the current study indicated that the optimum fibre

content is 0.5% of the dry weight of soil. The aspect ratio is the fibre length/fibre diameter, the literature review showed that increasing the aspect ratio increase the shear strength. But it was also observed that the fibre diameter should be less than the particles size. The performance of 19mm long fibre improved the performance of the sample during the mixing. The fibre length of 19mm at different water contents showed the highest strength and the internal friction angle. It is indicated that the inclusion of synthetic fibres significantly improved the unconfined compressive strength of all sand types evaluated. The polypropylene fibre improved the resilient modulus and decrease the permanent deformation. The durability has a negligible effect on the resilient modulus and permeant deformation of reinforced sand with fibre.

8.2.3.3 Fly Ash with/without Fibre Stabilized Sand

The literature review shown that there are few work about class C fly ash. And there is no available work for class C fly ash stabilized sand for road construction. The fly ash improved both mechanical and chemical engineering properties.

The shear strength of unstabilized sand was improved from 36kPa to 86kPa when it was stabilised with fly ash and when fibre and fly ash was added to sand, it improved to 227 kPa. The optimum fly ash content was found to be between 30 - 40 % of the dry weight of soil.

The sand stabilized with fly ash and fly ash with fibre shown improvement in unconfined compressive strength. The unconfined compressive strength was improved from 20kPa for unstabilized sand to 81kPa for fly ash stabilized sand and 368kPa for fibre with fly ash stabilized sand. Also, the fly ash improved resilient modulus, especially when incorporating the fibre with fly ash. Curing also shown significant improvement in shear strength. The

variation of water content shown that increase the water content improves the pozzolanic reaction. This is a positive point for the durability.

8.2.3.4 Slag with/without fibre stabilized sand

Alternative cementitious material was discovered in this study. The investigation was designed to carry out pilot experimental work. The results showed that the unconfined compressive strength of slag and slag with fibre reinforced sand were improved after 7 days of curing to 2000 and 4344kN/m^2, respectively. Strength of Both mixtures after 56 days of curing was improving significantly to about 9000kN/m^2.

The specimens of stabilized sand with slag were not possible to test by the unconsolidated undrained triaxial test. The strength of samples exceeded the load cell capacity. Therefore, the samples were tested by only the unconfined compressive strength test. Freeze-thaw durability has a negligible effect on the resilient modulus and permanent deformation of slag and slag with fibre stabilized sand. The temperature and humidity during the thawing affected significantly the alkali- activation.

8.2.4 Cyclic Loading

8.2.4.1 Resilient Modulus

The resilient modulus of stabilized and reinforced sand was obtained by resilient modulus AASHTO T 307 and Multi-Stage Repeated Load Tests. The Multistage Repeated Load Test is more reliable than the resilient modulus test AASHTO T307 to obtain the resilient modulus values. In accordance with EN 13286-7:2004, the resilient modulus values and the permeant strain become stable after applying 20,000cycles. This was confirmed as shown in Chapter Five and Six by apply 50,000 cycles load. Also, the results of resilient modulus values were

used to develop a correlation model between the resilient modulus and unconfined compressive strength. The effect of moisture contents on the resilient modulus of reinforced sand was evaluated as well as the number of load repetitions and the deviator stress. The variations of water content have a low effect on the reinforced sand. Increase the load cycles due to increasing resilient modulus. The fibre has a small effect on the resilient modulus when incorporating with slag.

8.2.4.2 Permanent Deformation

Multi-stage repeated load triaxial test was conducted. The effect of stress history and different stress levels were investigated. The confining pressure was determined according to the resilient modulus AASHTO T307. This allowed comparing the resilient modulus from both resilient modulus and permanent deformation tests. It was found that the reliable resilient modulus for pavement design should be obtained by the permanent deformation test. During testing, 150kPa applied on the slag stabilized samples which 66% of static deviator stresses of reinforced soil at failure. However, the slag samples are still can carry more stress but because the load cell capacity, the maximum cyclic deviator stress was 150kPa.

Generally, the increase in water content increases permanent deformation. The minimum permanent deformation was observed at 80% of OMC for the fibre reinforced sand, but at the optimum water content for the fly ash stabilized sand. This showed that the fine content affected the permanent deformation as well as the soil type. Increase the water content caused to increase the permanent deformation in the fibre reinforced sand and fly ash stabilized sand. Three stabilized sand with slag or slag with fibre significantly decreased the permanent deformation.

8.2.5 Analytical Pavement Design

Empirical pavement procedure is used in Libya that is the American Association of State Highway and Transportation Officials (AASHTO 1993). The empirical design method depends on both the experiment and experience. For this reason, the analytical pavement design was carried out in this research. The benefit of the procedure was to obtain the stress and strain at the critical point in the road structure and determine the suitable thickness.

As the traffic loading important for pavement design, the traffic loading was collected from a similar location in north Libya. The resilient modulus, deviator stress, number of equivalent axle load for both rutting and fatigue and the deflection were incorporated in new pavement design procedure in order to examine the reinforced sand for subgrade layer.

The analytical pavement designs showed that the fly ash should be used with fibre. The slag stabilized sand could be used in two layers pavement system, two layers pavement system consists of a base and reinforced subgrade layer. The reinforced subgrade layer was improved enough to catty the traffic loading without the subbase layer.

8.2.6 Durability Considerations

The reinforcement and stabilization materials showed significant improvement in the behaviour of subgrade sand under different conditions. Thus, it was important to evaluate the requirement of pavement design such as resilient modulus and permanent deformation after durability test. Then, the results were used the analytical pavement design.

8.3 Recommendations for Further Research

Use reinforcement materials to improve the properties of the subgrade layer, different materials were used throughout the study, and the extensive and robust experimental program was performed to investigate the required parameters for pavement design.

In this study, it has highlighted important aspects of the behaviour of reinforced and stabilized sand for road construction. There are still important areas requiring further investigation.

- This study has focussed on stabilising sand with a maximum amount to vitrified slag to achieve a maximum density with the expectation of highest strength and stability. This has been achieved so it is now necessary to further examine the potential use of vitrified slag as a binder for sand at lower concentrations.
- Freeze-Thaw durability test was carried out to simulate the in the desert environment, this has been confirmed. To widen the scope of using the stabilised materials described in the thesis, it is suggested that. Different durability test needs to be conducted such wetting and drying for the sample of slag that can be stand in the water bucket.
- The highest applied cyclic deviator stress was 66% of the static deviator stress. However, the reinforced samples were apple to be subjected to more than this value. But the load cell of resilient modulus apparatus AASHTO T307 was stuck due to the strength of samples. Therefore, the reinforced sample needs to be tested by repeated triaxial apparatus with high capacity of the load cell.
- In this research, the correlation models were developed for the sandy soil. Therefore, they need to be correlated with different soils.

- Further experimental works are needed to investigate the effect of water content on the resilient modulus and permanent deformation for slag with/without fibre reinforced sand and fibre with fly ash reinforced sand.

References

AASHTO 1993. AASHTO Guide for Design of Pavement Structures. Washington: American Association of State Highway and Transportation Officials, Washington, D.C.

AHMED, A. & KHALID, H. Characterizing the resilient behaviour of treated municipal solid waste bottom ash blends for use in foundations. Advances in Transportation Geotechnics: Proceedings of the International Conference held in Nottingham, UK, 25-27 August 2008, 2008. CRC Press, 59.

AHMED, A. W. & ERLINGSSON, S. 2013. Evaluation of permanent deformation models for unbound granular materials using accelerated pavement tests. *Road Materials and Pavement Design,* 14**,** 178-195.

AI-REFEAI, T. O. 1991. Behavior of Granular Soils Reinforced with Discrete Randomly Oriented Inclusions *Geotextiles and Geomembranes,* 10**,** 319-333.

AL-REFEAI, T. & AL-SUHAIBANI, A. 1998. dynamic and static characterization of polypropylene fiber reinforced dune sand. *GEOSYNTHETICS INTERNATIONAL,* 5**,** 443-458.

ALLEN, J. J. & THOMPSON, M. R. 1974. Resilient Response Of Granular Materials Subjected To Time-Dependent Lateral Stresses. *Transportation Research Board*.

ALTUN, I. A. & YILMAZ, I. 2002. Study on steel furnace slags with high MgO as additive in Portland cement. *Cement and Concrete Research,* 32**,** 1247-1249.

ANAGNOSTOPOULOS, C. A., PAPALIANGAS, T. T., KONSTANTINIDIS, D. & PATRONIS, C. 2013. Shear Strength of Sands Reinforced with Polypropylene Fibers. *Geotechnical and Geological Engineering,* 31**,** 401-423.

ARNOLD, G. K., DAWSON, A. R., HUGHES, D., WERKMEISTER, S. & ROBINSON, D. 2002. Serviceability Design of Granular Pavement Materials. *Proceedings of BCR2A***,** 957-966.

ARRIBAS, I., VEGAS, I., SAN-JOSE, J. T. & MANSO, J. M. 2014. Durability studies on steelmaking slag concretes. *Materials & Design,* 63**,** 168-176.

ASTM 2000. Standard Specification for Coal Fly Ash and Raw or Calcined Natural Pozzolan for Use as a Mineral Admixture in Concrete. *Designation: C 618 – 00.* United States: ASTM.

ATHANASOPOULOU, A. & KOLLAROS, G. 2015. Fly ash exploited in pavement layers in environmentally friendly ways. *Toxicological and Environmental Chemistry,* 97**,** 43-50.

AZIZ, M. M. A., HAININ, M. R., YAACOB, H., ALI, Z., CHANG, F. L. & ADNAN, A. M. 2014. Characterisation and utilisation of steel slag for the construction of roads and highways. *Materials Research Innovations,* 18**,** 255-259.

BARKSDALE, R. D. 1972. Laboratory evaluation of rutting in basecourse materials. 1.

BHARDWAJ, D. & MANDAL, J. 2008. Study on polypropylene fiber reinforced fly ash slopes. *International Conference of International Association for Computer Methods and Advances in Geomechanics (IACMAG)***,** 3778-3786.

BRAND, A. S. & ROESLER, J. R. 2015. Steel furnace slag aggregate expansion and hardened concrete properties. *Cement & Concrete Composites,* 60**,** 1-9.

BRANDL, H. 2008. Freezing-Thawing Behaviour Of Soils And Unbound Road Layers.

BROWN, S. F. 1996. Soil mechanics in pavement engineering. 3**,** 383-426.

BURLAND, J. B., POTTS, D. M. & WALSH, N. M. 1981. The overall stability of free and propped embedded retaining walls. *Ground Engineering,* 14**,** 28-38.

CAICEDO, B., CORONADO, O., FLEUREAU, J. M. & CORREIA, A. G. 2011. Resilient Behaviour of non Standard Unbound Granular Materials. *Road Materials and Pavement Design,* 10**,** 287-312.

CARY, C. E. & ZAPATA, C. E. 2011. Resilient Modulus for Unsaturated Unbound materials. *Road Materials and Pavement Design,* 12**,** 615-638.

CERNI, G., CARDONE, F. & BOCCI, M. 2012. Permanent deformation behaviour of unbound recycled mixtures. *Construction and Building Materials,* 37**,** 573-580.

CHAUHAN, M. S., MITTAL, S. & MOHANTY, B. 2008. Performance evaluation of silty sand subgrade reinforced with fly ash and fibre. *Geotextiles and Geomembranes,* 26**,** 429-435.

CHORE, H. S., KUMTHE, A. A., ABNAVE, S. B., SHINDE, S. S., DHOLE, S. S. & KAMERKAR, S. G. 2011. Performance evaluation of polypropylene fibers on sand-fly ash mixtures in highways. *Journal of Civil Engineering (IEB)***,** 91-102.

CHOW, L., MISHRA, D. & TUTUMLUER, E. 2014. Framework for development of an improved unbound aggregate base rutting model for mechanistic-empirical pavement design. *Transportation Research Record: Journal of the Transportation Research Board***,** 11-21.

CONSOLI, N. C., CASAGRANDE, M. D. T. & COOP, M. R. 2005. Effect of Fiber Reinforcement on the Isotropic Compression Behavior of a Sand. *Journal of Geotechnical and Geoenvironmental Engineering,* 131**,** 1434-1436.

CONSOLI, N. C., CASAGRANDE, M. D. T. & COOP, M. R. 2007a. Performance of a fibre-reinforced sand at large shear strains. *Geotechnique,* 57**,** 751-756.

CONSOLI, N. C., CASAGRANDE, M. D. T., PRIETTO, P. D. M. & THOME, A. 2003. Plate load test on fiber-reinforced soil. *Journal of Geotechnical and Geoenvironmental Engineering,* 129**,** 951-955.

CONSOLI, N. C., FESTUGATO, L. & HEINECK, K. S. 2009a. Strain-hardening behaviour of fibre-reinforced sand in view of filament geometry. *Geosynthetics International,* 16**,** 109-115.

CONSOLI, N. C., HEINECK, K. S., CASAGRANDE, M. D. T. & COOP, M. R. 2007b. Shear strength Behavior of fiber reinforced sand considering triaxial tests under distinct stress paths. *Journal of Geotechnical and Geoenvironmental Engineering,* 133**,** 1466-1469.

CONSOLI, N. C., MONTARDO, J. P., DONATO, M. & PRIETTO, P. D. M. 2004. Effect of material properties on the behaviour of sand–cement–fibre composites. 8**,** 14.

CONSOLI, N. C., RUVER, C. A., GIRARDELLO, V., FESTUGATO, L. & THOME, A. 2012. Effect of polypropylene fibers on the uplift behavior of model footings embedded in sand. *Geosynthetics International,* 19**,** 79.

CONSOLI, N. C., VENDRUSCOLO, M. A., FONINI, A. & ROSA, F. D. 2009b. Fiber reinforcement effects on sand considering a wide cementation range. *Geotextiles and Geomembranes,* 27**,** 196-203.

CORONADO, O., CAICEDO, B., TAIBI, S., GOMES CORREIA, A., SOULI, H. & FLEUREAU, J.-M. 2016. Effect of water content on the resilient behavior of non standard unbound granular materials. *Transportation Geotechnics,* 7**,** 29-39.

CRONE, D. 1952. THE MOVEMENT AND DISTRIBUTION OF WATER IN SOILS. *Geotechnique,* 5**,** 1-16.

DAS, B., PRAKASH, S., REDDY, P. S. R. & MISRA, V. N. 2007. An overview of utilization of slag and sludge from steel industries. *Resources Conservation and Recycling,* 50**,** 40-57.

DIAMBRA, A., IBRAIM, E., MUIR WOOD, D. & RUSSELL, A. R. 2010. Fibre reinforced sands: Experiments and modelling. *Geotextiles and Geomembranes,* 28**,** 238-250.

DIAMBRA, A., IBRAIM, E., RUSSELL, A. R. & MUIR WOOD, D. 2011. Modelling the Undrained Response of Fibre Reinforced Sands. *Soils & Foundations,* 51**,** 625-636.

DIAMBRA, A., IBRAIM, E., RUSSELL, A. R. & MUIR WOOD, D. 2013. Fibre reinforced sands: from experiments to modelling and beyond. *International Journal for Numerical and Analytical Methods in Geomechanics,* 37**,** 2427-2455.

DOS SANTOS, A. P. S., CONSOLI, N. C., HEINECK, K. S. & COOP, M. R. 2010. High-Pressure Isotropic Compression Tests on Fiber-Reinforced Cemented Sand. *Journal of Geotechnical and Geoenvironmental Engineering,* 136**,** 885-890.

ELDESOUKY, H. M., MORSY, M. M. & MANSOUR, M. F. 2015. Fiber-reinforced sand strength and dilation characteristics.

ELLIOTT, R. P., DENNIS, N. D. & QIU, Y. 1998. Permanent deformation of subgrade soils. Phase II: Repeated Load Testing of Four Soils. *Fayetteville, Mack-Blackwell Transportation Center Publ*.

EMERY, J. J. 1982. Slag Utilization in Pavement Construction. *American Society for Testing and Materials*.

ERLINGSSON, S. 2012. Rutting development in a flexible pavement structure. *Road Materials and Pavement Design,* 13.

FHWA-IF-03-019 2003. Fly Ash Facts for Highway Engineers.

FINN, F. N., BOARD, N. R. C. T. R., HIGHWAY, A. A. O. S., OFFICIALS, T. & ADMINISTRATION, U. S. F. H. 1986. *Development of Pavement Structural Subsystems*, Transportation Research Board, National Research Council.

FREED, W. W. 1988. *Fiber reinforced soil and method*.

GHADIMI, B., NIKRAZ, H. & LEEK, C. 2014. A Comparison of Different Approaches in Numerical Modeling of Pavement Granular Material *Journal of Civil Engineering and Architecture,* 8**,** 446-455

GHATAORA, G. S., CHAPMAN, D. N., SCHAD, M. & AST, W. Influence of Fibres on Properties of Cement Stabilised Sands and Clay. 10.

GHATAORA, G. S., FREER-HEWISH, R. J. & JESSIC, J. 2004. The Utilisation Of Recycled Aggregates Generated From Highway Arisings And Steel Slag Fines. UK.

GHAZAVI, M. & ROUSTAIE, M. 2010. The influence of freeze–thaw cycles on the unconfined compressive strength of fiber-reinforced clay. *Cold Regions Science and Technology,* 61**,** 125-131.

GIRIJA, K. M. 2013. Behaviour of Randomly Distributed Fiber-Reinforced Soil. *International Journal of Research in Engineering and Technology*.

GOMEZ, E., RANI, D. A., CHEESEMAN, C. R., DEEGAN, D., WISE, M. & BOCCACCINI, A. R. 2009. Thermal plasma technology for the treatment of wastes: a critical review. *J Hazard Mater,* 161**,** 614-26.

GRAY, D. A. O., H. 1983. Mechanics of Fiber Reinforcement in Sand. *Journal of Geotechnical Engineering,* 109**,** 335-353.

GUPTA, A. 2014. A Review of Environmental Factors on Flexible Pavement Performance Modeling. *Modern Traffic and Transportation Engineering Research (MTTER),* 3**,** 14-20.

HEAD, K. H. 1994. Manual of Soil Laboratory Testing—Volume 2: Permeability, Shear Strength and Compressibility Tests. *Quarterly Journal of Engineering Geology and Hydrogeology,* 47**,** 191-191.

HEJAZI, S. M., SHEIKHZADEH, M., ABTAHI, S. M. & ZADHOUSH, A. 2012. A simple review of soil reinforcement by using natural and synthetic fibers. *Construction and Building Materials,* 30**,** 100-116.

HO, X. N., NOWAMOOZ, H., CHAZALLON, C. & MIGAULT, B. 2014a. Effective stress concept for the effect of hydraulic hysteresis on the resilient behaviour of low traffic pavements. *International Journal of Pavement Engineering,* 16**,** 842-856.

HO, X. N., NOWAMOOZ, H., CHAZALLON, C. & MIGAULT, B. 2014b. Influence of fine content and water content on the resilient behaviour of a natural compacted sand. *Road Materials and Pavement Design,* 15**,** 606-621.

HORNYCH, P. & ABD, A. E. 2004. Selection and evaluation of models for prediction of permanent deformations of unbound granular materials in road pavements.

HUANG, Y. H. 1993. *Pavement analysis and design*, Prentice Hall.

HUANG, Y. H. 2004. *Pavement Analysis and Design*, USA.

IBRAIM, E., DIAMBRA, A., MUIR WOOD, D. & RUSSELL, A. R. 2010. Static liquefaction of fibre reinforced sand under monotonic loading. *Geotextiles and Geomembranes,* 28**,** 374-385.

IBRAIM, E., DIAMBRA, A., RUSSELL, A. R. & MUIR WOOD, D. 2012. Assessment of laboratory sample preparation for fibre reinforced sands. *Geotextiles and Geomembranes,* 34**,** 69-79.

JADHAO, P. D. & NAGARNAIK, P. B. 2008. Influence of Polypropylene Fibers on Engineering Behavior of Soil-Fly Ash Mixtures for Road Construction. *EJGE,* 13**,** 11.

JADHAO, P. D. & P.B.NAGARNAIK 2008. Performance Evaluation of Fiber Reinforced Soil- Fly Ash Mixtures. *12th International Conference of the International Association for Computer Methods and Advances in Geomechanics (IACMAG 2008).*

KANIRAJ, S. R. & GAYATHRI, V. 2003. Geotechnical behavior of fly ash mixed with randomly oriented fiber inclusions. *Geotextiles and Geomembranes,* 21**,** 123-149.

KANIRAJ, S. R. & HAVANAGI, V. G. 2001. Behavior of Cement-Stabilized Fiber-Reinforced Fly Ash-Soil Mixtures. *Journal of Geotechnical Engineering,* 127**,** 574-584.

KEELEY, P. M., ROWSON, N. A., JOHNSON, T. P. & DEEGAN, D. E. 2017. The effect of the extent of polymerisation of a slag structure on the strength of alkali-activated slag binders. *International Journal of Mineral Processing,* 164**,** 37-44.

KHEDR, S. 1985. Deformation characteristics of granular base course in flexible pavements. *Transportation Research Record,* 1043**,** 131-138.

KHOURY, N. N. & BROOKS, R. 2010. Performance of a Stabilized Aggregate Base Subject to Different Durability Procedures. *Journal Of Materials In Civil Engineering,* 22.

KHOURY, N. N., BROOKS, R. & P.E., F. 2010. Performance of a Stabilized Aggregate Base Subject to Different Durability Procedures. *Journal of Materials in Civil Engineering*, 22.

KHOURY, N. N. & ZAMAN, M. M. 2004. Correlation Between Resilient Modulus, Moisture Variation, and Soil Suction for Subgrade Soils. *Journal of the Transportation Research Board,*.

KIM, D. & KIM, J. R. 2007. Resilient behavior of compacted subgrade soils under the repeated triaxial test. *Construction and Building Materials,* 21**,** 1470-1479.

KIM, D. & SIDDIKI, N. Z. 2006. Simplification of resilient modulus testing for subgrades.

KOLISOJA, P. 1998. *Resilient deformation characteristics of granular materials.* Tampere University of Technology.

KOURTI, I., DEEGAN, D., BOCCACCINI, A. R. & CHEESEMAN, C. R. 2013. Use of DC Plasma Treated Air Pollution Control (APC) Residue Glass as Pozzolanic Additive in Portland Cement. *Waste and Biomass Valorization,* 4**,** 719-728.

KUMAR, P. & SINGH, S. P. 2008. Fiber-Reinforced Fly Ash Subbases in Rural Roads.

KUMAR, S. & PATIL, C. B. 2006. Estimation of resource savings due to fly ash utilization in road construction. *Resources Conservation and Recycling,* 48**,** 125-140.

LEE, W., BOHRA, N. C. & ALTSCHAEFFL, A. G. 1995. Resilient Characteristics of Dune Sand. *Journal of Transportation Engineering,* 121**,** 502-506.

LEKARP, F. & DAWSON, A. 1998. Modelling permanent deformation behaviour of unbound granular materials. *Construction and Building Materials,* 12**,** 9-18.

LEKARP, F., ISACSSON, U. & DAWSON, A. 2000a. State Of The Art. I:Resilient Response Of Unbound Aggregates. *JOURNAL OF TRANSPORTATION ENGINEERING,* 126**,** 66-75.

LEKARP, F., ISACSSON, U. & DAWSON, A. 2000b. State Of The Art. II: Permanent Strain Response Of Unbound Aggregates. *Journal of Transportation Engineering,* 1**,** 8.

LIU, J., WANG, G., KAMAI, T., ZHANG, F., YANG, J. & SHI, B. 2011. Static liquefaction behavior of saturated fiber-reinforced sand in undrained ring-shear tests. *Geotextiles and Geomembranes,* 29**,** 462-471.

MONISMITH, C. L., OGAWA, N. & FREEME, C. R. 1975. permanent deformation characteristics of subgrade soils due to repeated loading. *Transportation Research Board*.

MORGAN, J. 1966. The response of granular materials to repeated loading. *Australian Road Research Board Proc*.

NCHRP 2004. Mechanistic-Empirical Design of New and Rehabilitated Pavement Structures. *NCHRP Project 1-37A.* Washington, DC.: National Research Council.

OUF, M. E.-S. A. R. 2001. *Stabilisation Of Clay Subgrade Soils Using Ground Granulated Blastfurnace Slag.* Doctor of Philosophy, University of Leeds.

PAPPIN, J. W. 1979. *Characteristics of a granular material for pavement analysis.* PhD, University of Nottingham.

PAUTE, J., HORNYCH, P. & BENABEN, J. Repeated load triaxial testing of granular materials in the French Network of Laboratories des Ponts et Chaussées. FLEXIBLE PAVEMENTS. PROCEEDINGS OF THE EUROPEAN SYMPOSIUM EUROFLEX 1993 HELD IN LISBON, PORTUGAL, 20-22 SEPTEMBER 1993, 1996.

PINARD, M. I., PAIGE-GREEN, P., MUKURA, K. & MOTSWAGOLE, K. J. 2013. Guideline on the Use of Sand in Road Construction in the SADC Region AFCAP/GEN/028/C. UK.

PLAISTOW, L. C. 1994. *Non-linear behaviour of some pavement unbound aggregates.* MSC, University of Nottingham.

PUMPHREY, N. D. & LENTZ, R. W. 1986. Deformation Analyses of Florida Highway Subgrade Sand Subjectd to Repeated Load Triaxial Tests. *Pergamon Journals Ltd***,** 49-56.

PUPPALA, A. J., SARIDE, S. & CHOMTID, S. 2009. Experimental and Modeling Studies of Permanent Strains of Subgrade Soils. *JOURNAL OF GEOTECHNICAL AND GEOENVIRONMENTAL ENGINEERING,* 135**,** 11.

RAHMAN, M. S. 2015. *Characterising the Deformation Behaviour of Unbound Granular Materials in Pavement Structures.* Doctoral Thesis, KTH Royal Institute of Technology.

RAHMAN, M. S., ERLINGSSON, S. & HELLMAN, F. 2017. Stiffness and permanent deformation characteristics of open-graded unbound granular materials.

SAEVARSDOTTIR, T. & ERLINGSSON, S. 2013. Water impact on the behaviour of flexible pavement structures in an accelerated test. *Road Materials and Pavement Design,* 14**,** 256-277.

SALOUR, F. & ERLINGSSON, S. 2015. Permanent deformation characteristics of silty sand subgrades from multistage RLT tests. *International Journal of Pavement Engineering***,** 1-11.

SALOUR, F., ERLINGSSON, S. & ZAPATA, C. E. 2014. Modelling resilient modulus seasonal variation of silty sand subgrade soils with matric suction control1. *Canadian Geotechnical Journal,* 51**,** 1413-1422.

SALOUR, F. & ERLINGSSONC, S. 2015. Permanent deformation characteristics of silty sand subgrades from multistage RLT tests. *INTERNATIONAL JOURNAL OF PAVEMENT ENGINEERING,*.

SANTONI, R. L., TINGLE, J. S. & WEBSTER, S. L. 2001. Engineering Properties of Sand-Fiber Mixtures for Road Construction. *Journal of Geotechnical Engineering,* 127**,** 258-268.

SANTONI, R. L. & WEBSTER, S. L. 2001. Airfields and roads construction using fiber stabilization of sands. *Journal of Transportation Engineering-Asce,* 127**,** 96-104.

SANTOS, A. P. S. D., CONSOLI, N. C. & BAUDET, B. A. 2010. The mechanics of fibre-reinforced sand. *Geotechnique,* 60**,** 791-799.

SCOTT, C. R. 1980. *An introduction to soil mechanics and foundations,* London : Applied Science Publishers

SIMONSEN, E. & ISACSSON, U. 1999. Thaw weakening of pavement structures in cold regions. *Cold Regions Science and Technology,* 29.

SWEERE, G. T. H. 1990. *Unbound granular bases for roads.* PhD Delft University.

TAKHELMAYUM, G., SAVITHA.A.L & GUDI, K. 2013. Laboratory Study on Soil Stabilization Using Fly ash Mixtures. *International Journal of Engineering Science and Innovative Technology,* 2**,** 6.

TANG, C. S., SHI, B. & ZHAO, L. Z. 2010. Interfacial shear strength of fiber reinforced soil. *Geotextiles and Geomembranes,* 28**,** 54-62.

THOMAS, M. 2007. Optimizing the Use of Fly Ash in Concrete. University of New Brunswick.

TINGLE, J. S., SANTONI, R. L. & WEBSTER, S. L. 2002. Full-scale field tests of discrete fiber-reinforced sand. *Journal of Transportation Engineering-Asce,* 128**,** 9-16.

TIWARI, S. K. & SHARMA, J. P. 2013. Influence of Fiber-Reinforcement on CBR-Value of Sand 18**,** 9.

UD-DIN, S., MARRI, A. & WANATOWSKI1, D. 2011. Effect Of High Confining Pressure On The Behaviour Of Fibre Reinforced Sand. *Geotechnical Engineering Journal of the SEAGS & AGSSEA,* 42**,** 69-76.

UTHUS, L., HERMANSSON, Å., HORVLI, I. & HOFF, I. 2006. A study on the influence of water and fines on the deformation properties and frost heave of unbound aggregates. *Cold Regions Engineering*.

WASTI, Y. & BUTUN, M. D. 1996. Behaviour of model footings on sand reinforced with discrete inclusions. *Geotextiles and Geomembranes,* 14**,** 575-584.

WERKMEISTER, S., DAWSON, A. R. & WELLNER, F. 2001. Permanent deformation behavior of granular materials and the shakedown concept. *Transportation Research Record: Journal of the Transportation Research Board***,** 75-81.

WILLIAM B. FULLER & SANFORD E. THOMPSON 1907. The laws of proportioning concrete. *AMERICAN SOCIETY OF CIVIL ENGINEERS* 59**,** 67-143.

WOLFF, H., VISSER & H, A. T. 1994. Incorporating elasto-plasticity in granular layer pavement design. *Proceedings of the Institution of Civil Engineers: Transport,* 105**,** 259-272.

YANG YUNHUA & SHENGGUO, C. 2008. Mechanical Properties and Its Influencing Factors of Fiber Reinforced Soil. *Scientific Research Fund of Hubei Provincial Education Department***,** 5-13.

ZABIELSKA-ADAMSKA, K. 2008. Laboratory compaction of fly ash and fly ash with cement additions. *Journal of hazardous materials,* 151**,** 481-489.